Effect of nitrosative stress on ethanol production in *Saccharomyces cerevisiae*

Thesis is submitted to
The University of North Bengal for the award of the degree of Doctor of Philosophy in Microbiology

By

Swarnab Sengupta

Under the supervision of

Dr. Arindam Bhattacharjee

Department of Microbiology
University of North Bengal
INDIA

JULY, 2022

Science has no boundaries

DECLARATION

I hereby declare that the thesis entitled **"Effect of nitrosative stress on ethanol production in *Saccharomyces cerevisiae*"** has been prepared by me under the supervision of Dr. Arindam Bhattacharjee, Assistant professor, Department of Microbiology, University of North Bengal.

The work is original to the best of my knowledge. No part of this thesis has formed the basis of any previously awarded degree or fellowship.

Date: 04.07.2022

Swarnab Sengupta

Swarnab Sengupta
Department of Microbiology
University of North Bengal

UNIVERSITY OF NORTH BENGAL

Accredited by NAAC with Grade A

DEPARTMENT OF MICROBIOLOGY

समानो मन्त्र: समिति: समानी

P.O. NORTH BENGAL UNIVERSITY,
RAJA RAMMOHUNPUR, DT. DARJEELING,
WEST BENGAL, INDIA, PIN - 734 013
PHONE: 0353 2776 319
WEBSITE: www.nbu.ac.in
E-MAIL : microbiodept@nbu.ac.in

CERTIFICATE

I certify that Mr. Swarnab Sengupta has prepared the thesis entitled **"Effect of nitrosative stress on ethanol production in *Saccharomyces cerevisiae*"** for the award of ***Doctor of Philosophy*** in Microbiology from University of North Bengal under my supervision. The work is original to the best of my knowledge.

A. Bhattacharjee 9/6/2022

Dr. Arindam Bhattacharjee

(*Supervisor*)

Dr. Arindam Bhattacharjee
Assistant Professor
Department of Microbiology
University of North Bengal

Curiginal

Document Information

Analyzed document	Swarnab Sengupta_Microbiology.pdf (D138786402)
Submitted	2022-06-01T10:59:00.0000000
Submitted by	University of North Bengal
Submitter email	nbuplg@nbu.ac.in
Similarity	0%
Analysis address	nbuplg.nbu@analysis.urkund.com

Sources included in the report

W URL: https://amp.doubtnut.com/question-answer-chemistry/three-oxides-of-nitrogen-n2o-no2-and-n2o3-are-mixed-in-a-molar-ratio-of-321-find-the-vapour-density--16008423
Fetched: 2022-05-04T08:43:41.5770000 1

A. Bhattacharjee

Dr. Arindam Bhattacharjee
Assistant Professor
Department of Microbiology
University of North Bengal

Swarnab Sengupta

ACKNOWLEDGEMENT

Undertaking this PhD has been a life changing experience for me and it would not have been possible without the guidance and support of many people. So, I would like to thank all the people who have contributed in some way to this work.

First and foremost, I would like to acknowledge my indebtedness and render my warmest thanks to my supervisor, Dr. Arindam Bhattacharjee for his continuous support in this study and also for his patience, motivation. His guidance and expert advice has been very valuable and helped me in every phase of research. I am also very thankful to him for the freedom he gave me in implementing my ideas. Without his constant support this work could not be materialized.

I gratefully acknowledge Dr. Shyama Prasad Saha, Dr. Sarita Kumari, Dr. Payel Sarkar, Mrs. Khushboo Lepcha; the teachers of Microbiology Department for their assistance whenever needed. I am also thankful to Mrs. Madhumita Ghosh, Mr. Subir Sarkar, Mr. Sudipta Das, non-teaching staff of Microbiology Department for their support in all aspects.

I would like to express my gratefulness to Prof. Pranab Ghosh, Registrar (Offg.), University of North Bengal, Prof. Shilpi Ghosh, Prof. Arnab Sen, Prof. B.C. Pal, Prof. S.C. Roy for helping me to carry out my research work.

My sincere gratitude to my lab mates Aditi di, Rohan, Pratima and Madhushree for their constant support and cooperation. Their presence always gave me a very homely atmosphere.

I would like to express my thanks to some of the P.G. students namely Pema, Ankita, Debika, Minakshi, Priyanka, Akash for helping me to carry out some of the part of my research work.

I am thankful to the University of North Bengal for providing me all the infrastructural and instrumental facilities.

I would like to express my deep respect to Prof. Sanjay Ghosh, Department of Biochemistry, Calcutta University, for providing the yeast strain Y190 [ATCC 96400]. I would also like to express my thanks to Dr. Rajabrata Bhuyan, Department of Bio-Science and Biotechnology, Banasthali Vidyapith (Deemed) University, for guiding me in the bioinformatics analysis.

On a personal note, I want to convey my deepest regards to Mani and Pappa. It's because of their blessings that I could fulfill my dream. Special thanks to Dadabhai, Boudi, my loving nephew Bacillus, Kaku, Kakima, Bhai, Pisi for their endless support. Credit also goes to my wife Payel, for her unconditional love and belief in me.

Finally, I would like to thank my friends and brothers Sanat, Bibek, Sanjit, Akram, Subham, Abir, Soutrik, Bappa for their support.

With Regards

Swarnab Sengupta

Swarnab Sengupta

Abstract

Nitrosative stress is a hostile condition mediated by reactive nitrogen species (RNS). Macromolecules like DNA, proteins, lipids are very vulnerable to RNS. Protein modifications like protein tyrosine nitration (PTN) and *S*-nitrosylation are major markers of nitrosative stress. One of the best system to study nitrosative stress is *Saccharomyces cerevisiae*. Thousands of studies have been conducted by using *S. cerevisiae* to explore molecules involved in stress response, signal pathways, antioxidant system etc. but glucose metabolism and subsequent ethanol production under nitrosative stress was poorly understood. Here, metabolic response of *S. cerevisiae* has been characterized with special reference to the ethanol production under nitrosative stress mediated by acidified sodium nitrite (ac.$NaNO_2$) or *s*-nitrosoglutathione (GSNO).

Major findings of this study suggest no significant loss of cellular viability of *S. cerevisiae* in presence of 0.5 mM Ac. $NaNO_2$ or 0.25 mM GSNO as compared to the control where stress was not applied. These doses were riveted as the sub-toxic dose under experimental condition. In addition to it, growth rate of *S. cerevisiae* was found to be unaffected under these sub-toxic doses as compared to control. Redox homeostasis altered significantly, with a sharp increase in the specific activity of antioxidant enzymes i.e. glutathione reductase and catalase under sub-toxic dose of ac.$NaNO_2$ and GSNO. Confocal microscopy study revealed generation of RNS only in presence of stress inducing agents. Whereas presence of reactive oxygen species (ROS) was found in both control and treated samples without any significant differences.

Aconitase, which catalyzes the conversion of citrate to isocitrate in the tricarboxylic acid (TCA) cycle, is known to be affected under nitrosative stress. Under the specified experimental condition, it was found that enzymatic activity aconitase was strongly inhibited in the presence of 0.5 mM ac.$NaNO_2$ or 0.25 mM GSNO. Subsequent gene expression analysis also revealed that *ACO2* was affected whereas the expression level of *ACO1* was slightly higher in presence of 0.5 mM ac.$NaNO_2$. In addition to this, ethanol production increased by 1.3 fold and 1.5 fold respectively in presence of 0.5 mM ac.$NaNO_2$ or 0.25 mM GSNO as compared to the control. Volumetric productivity and yield of ethanol were also improved under the stress condition. Furthermore,

increase in alcohol dehydrogenase (ADH) enzyme activity was also observed under nitrosative stress. qPCR study revealed that gene expression of *ADH3* was significantly higher under the stress condition. Whereas western blot analysis with pure aconitase revealed that it was prone to both PTN and *S*-nitrosylation but pure ADH was not. Additionally, activity of some important enzymes of the TCA cycle, like citrate synthase, isocitrate dehydrogenase etc. were found to be negatively affected under stress. On the other hand, activity of enzymes related to malate metabolism and alcoholic fermentation were found to be increased under 0.5 mM ac.$NaNO_2$ mediated nitrosative stress. Altogether, a metabolic reprogramming towards fermentation was observed under nitrosative stress. Furthermore, ethanol production was optimized by using nitrosative stress exposed immobilized *S. cerevisiae* cells that were grown in a minimal medium containing molasses and ammonium sulfate. By performing CCRD-based RSM, optimized condition of ethanol production was determined. Overall, obtained data showed that maximum ethanol (35.24 g/L) production after 24 h of incubation. This is the first report of this kind where ethanol production by *S. cerevisiae* cells under nitrosative stress has been shown. This study has the potential to be significantly important in industrial ethanol production.

CONTENTS

LIST OF FIGURES

LIST OF TABLES

Introduction...

1. Discovery of nitric oxide:

Nitric oxide (NO) is a versatile gaseous molecule that relays some major roles in cell signaling, stress response as well as in immunity. This novel molecule was first reported by a Belgian scientist J. B. van Helmont, which was prepared in his lab in 1648. Later in 1671, one of the greatest physicists, Robert Boyle also reported nitric oxide as 'volatile nitre' in the air, which supports combustion. After a century, Sir Joseph Priestley first time characterized the chemical properties of nitric oxide in 1772. He generated the gas by the action of 'spirit of nitre' (now known as nitric acid) on copper and named as 'nitrous air' and reported its spontaneous reactivity with 'common air' to generate a soluble brown gas (now known as nitrogen dioxide).

$$3Cu + 8H^{+} + 2NO_3^{-} \rightarrow 3Cu^{2+} + 2NO + 4H_2O$$

2. Chemical and physical properties of nitric oxide:

Nitric oxide (nitrogen monoxide, NO) is a molecule of interest for physicists, chemists and biologists for over 200 years; thus, a huge database of information is already present. NO is an uncharged, small lipophilic molecule contains total odd number (8 bonding and 3 antibonding electrons, i.e. in total 11) of electrons, thus it contains an unpaired electron [1]. The oxidation state of nitrogen (N) atom in NO is +2 and it is second of the oxides in which the oxidation states of nitrogen ranges from +1 to +5 (N_2O^{+1}; NO^{+2}; $N_2O_3^{+3}$; NO_2 and $N_2O_4^{+4}$; $N_2O_5^{+5}$). The bond order of NO is around 2.5 and the bond length of N-O is 1.15 Å. Though it is one of the smallest stable molecule, but the presence of the unpaired electron helps it to react only with those molecules which contain unpaired d electron/s [2]. Thus, it can easily react with oxygen (O_2) and reactive oxygen species like O_2^{-}. It can also react with transition metals containing *d* orbital like iron (Fe) present in different proteins e.g. NO can rapidly react with oxyferrohemoglobin and ferriheme can be formed [1].

3. Biosynthesis of nitric oxide:

Biosynthesis of NO is mainly dependent on the activity of nitric oxide synthases (NOSs) [3]. But NOS-independent NO synthesis also takes place *in vivo* [4]. Hence, biosynthesis of NO is mainly classified into two groups: NOS-dependent and NOS-independent NO synthesis.

3.1. Nitric oxide synthase-dependent nitric oxide synthesis:

Nitric oxide synthases [NOSs] (EC1.14.13.39) are member of cytochrome P450 enzyme family [5]. NOSs utilize L-arginine as the substrate [3-5]. NO is formed as the byproduct, during the conversion of L-arginine to L-citrulline. It is a two-step reaction. The first step is the formation of the intermediate Nω-hydroxy-L-arginine (NHA) from L-arginine and in the next step, NHA is converted to NO and citrulline. The reaction has a 1:1 L-citrulline/NO product stoichiometry [6].

3.1.1. Structure and mechanism of action of nitric oxide synthases:

Nitric oxide synthase is a homodimeric enzyme. Each of the monomers contain two domains: reductase and oxygenase domain [3, 7]. NOSs need cofactors like flavin adenine dinucleotide (FAD), flavin mono-nucleotide (FMN), tetrahydrobiopterin (BH_4), calmodulin and haem for its activity [8, 9]. The carboxyl terminal reductase domain provides the binding sites for nicotinamide adenine dinucleotide phosphate hydrogen (NADPH) (providing reducing energy), FAD, FMN and calmodulin whereas amino terminal oxygenase domain provides binding site for BH_4 and cysteinyl thiolate-ligated haem group [3, 7]. This haem group contributes to the functional dimer formation [10]. The activity of NOS is dependent on the dimer formation. Zinc (Zn) is another factor that involves in the formation of functional dimeric NOSs [11]. The binding of calmodulin is regulated by the intracellular calcium (Ca^{2+}) ion concentration [12, 13]. Each of the monomers of NOSs, are capable of transferring electrons from reduced NADPH to FAD and FMN but has a very limited capability to reduce molecular O_2 to superoxide [14]. Electrons transfer from reductase domain to oxygenase domain only becomes possible after the formation of the dimer. Monomers of NOSs are unable to bind BH_4 and L-arginine. Hence, NO production can't be catalyzed by monomers [15]. In the functional form of NOSs, electrons are transferred from the reductase domain of the one monomer to oxygenase domain of the another monomer and consecutively two oxidation reactions take place to form NO and L-citrulline from the L-arginine via the generation of NHA as the intermediate [16,17] **[Fig. 1]**.

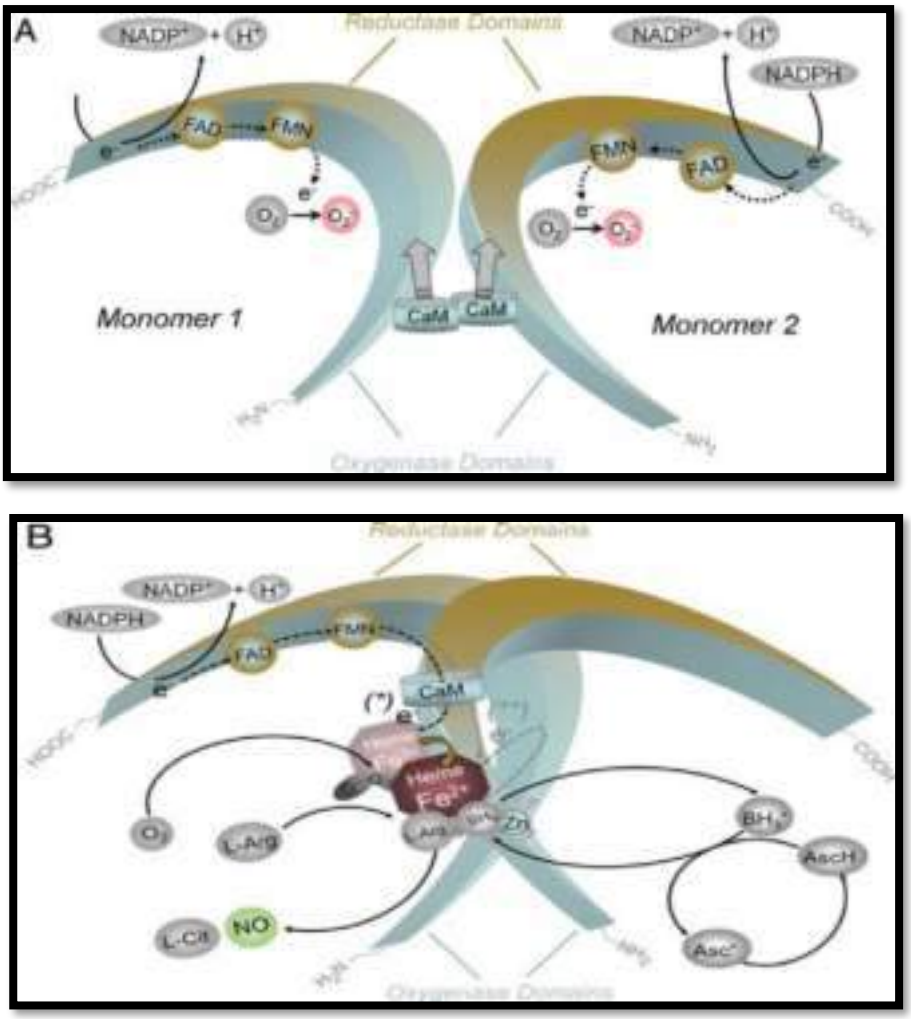

Fig. 1 Schematic representation of mechanism of action of nitric oxide synthases. (Adapted from Förstermann *et al.* 2012)

3.1.2. Mammalian nitric oxide synthases (NOSs):

Three isoforms of NOSs are present in mammals, referred to as neuronal 'n'NOS (NOS1), inducible 'i'NOS (NOS2) and endothelial 'e'NOS (NOS3). These NOSs play important roles in different pathophysiological functions. On the basis of the gene expression, isoforms of NOSs can be classified into two groups: constitutive (NOS1, NOS3) and inducible (NOS2) [7]. Localization of the isoforms is varied and isoforms have diverse roles in the regulation of different cellular processes [18-20].

3.1.2.1. Nitric oxide synthase 1 (NOS1):

nNOS is constitutively expressed in both the immature and mature neurons of the brain tissue and its activity is tightly regulated by the concentration of Ca^{2+} and calmodulin [21-26]. Immunohistochemistry analysis has revealed that nNOS is mostly present in

the spinal cord, adrenal cells, ganglia cells and vascular smooth muscle [18]. The subcellular localization of nNOS may be associated with its diverse functions. Presence of post-synaptic density protein, discs-large, zona occludens -1 (PDZ) domain is one of the significant characteristics of nNOS [27]. The PDZ domain may interact directly with the PDZ domain of another protein which results in the formation of dimer [27, 28]. Proteins containing PDZ, are believed to participate in different signal transduction pathways. The interaction of nNOS with the membrane is facilitated by the PDZ domain that may result in the alteration of NO signaling. nNOS also plays an important role in the synaptic signaling events [29, 30], like participation in the regulation of the long-term synaptic transmission [31]. NO produced by the activity of nNOS in nitrergic nerves can act as an unorthodox neurotransmitter that may stimulate NO-sensitive guanylyl cyclase in its effector cells, causing reduction in the tone of the different smooth muscles like blood vessels [18]. Inhibition in the activity of nNOS in the hypothalamus and medulla, causes systemic hypertension [32].

3.1.2.2. Nitric oxide synthase 2 (NOS2):

The expression of NOS2 is induced by the cytokines, antigens like bacterial lipopolysaccharide and other agents. Although this enzyme was first identified in macrophages, but reports suggest that iNOS has been expressed in all cell types in the presence of the appropriate agent [18, 33]. Interestingly, the expression of NOS2 is not dependent on the concentration of the intracellular Ca^{2+} [7]. The activity of this enzyme persists for a long time (many hours) after the immunological stimulation [34]. The expression of iNOS is regulated by the mitogen-activated protein kinase (MAPK) family of protein kinases [extracellular signal-regulated kinase, c-Jun N-terminal kinase (JNK), p38] and protein kinase B [35, 36]. NO, produced by the activity of iNOS in the cells, shows cytotoxic effect on the pathogens by interfering with the structure and function of the DNA and protein of the target cells [7, 37]. iNOS stimulated hepatocytes can use NO to eliminate malaria pathogens [37]. iNOS derived NO can also induce neuronal death due to inhibition of cytochrome oxidase, causing excitotoxicity [37, 38]. Large amount of NO produced by the iNOS play a significant role in the development of septic shock [39]. The fall in blood pressure is also indirectly mediated by excess production of NO by the iNOS in the vascular wall [40].

3.1.2.3. Nitric oxide Synthase 3 (NOS3):

NOS3 is mainly localized in the plasma membrane caveolae of the endothelial cells [41]. But this enzyme is also found in neurons of the brain, cardiac myocytes and platelets [18, 33]. Intracellular concentration of Ca^{2+} is very important for the activity of the eNOS. Ca^{2+} induces the binding affinity of the calmodulin (CaM) to the enzyme [42]. The bradykinin (BK) B2 receptor, a G-protein coupled receptor (GPCR), regulates the complex formation of Ca^{2+}/CaM [43]. The regulation of eNOS is also dependent on the protein-protein interactions. Heat shock protein 90 (hsp90) has a positive allosteric modulation effect on the activity of eNOS [44]. Translocation of eNOS from caveolae to other intracellular compartment like golgi bodies, is influenced by the activity of 'nitric oxide synthase interacting protein' (NOSIP) and 'nitric oxide synthase trafficking inducer' (NOSTRIN) [45]. Phosphorylation is another important factor for the stimulation of the eNOS. Specific tyrosine (Tyr), serine (Ser), threonine (Thr) residues of eNOS can be phosphorylated, activating the enzyme without depending on the concentration of Ca^{2+} [46, 47]. The best model to study such stimulation is fluid shear stress [47]. The inhibition of the activity of eNOS is mediated by the interaction of scaffolding domain of Cav-1(Caveolin-1) with the caveolin binding motif on eNOS [48]. eNOS stimulates soluble guanylyl cyclase and cyclic guanosine monophosphate (cGMP) in smooth muscle cells [49]. eNOS-derived NO decreases the expression of the genes involved in atherogenesis by inhibiting leucocyte adhesion to the vessel wall via interfering with the adhesion molecule CD11/CD18 (cluster of differentiation) [50]. NO, generated from eNOS, prevents cellular apoptosis and plays an important role in post-natal angiogenesis. Dysfunction of eNOS results in the development of cardiovascular disease [51].

3.1.3. Invertebrate nitric oxide synthase:

Like mammalians, NOS-derived NO plays an important role in bio-signaling in invertebrates [52-54]. In 1991, Radomsky *et al.* gave a clear idea about the presence of NO-mediated signaling as well as NOS activity in invertebrates like horseshoe crab (*Limulus polyphemus*) [52]. After this initial work, several studies reported the presence of NOS in invertebrates. In 1993, Eloffson *et al.* reported NADPH-diaphorase activity in osfradia, buccal ganglia, central nervous system (CNS) neurons, and in some peripheral organs [53]. In 1995, Jacklet *et al.* reported the cotransmitter activity of NO

in histaminergic synapses of *Aplysia* sp. [54]. In 1996, Moroz *et al.* reported the presence of Ca^{2+}-independent but calmodulin dependent NOS activity in mollusk species [55]. Domenech and Muñoz-Chápuli hypothesized that all the three isoforms of mammalian NOS may be derived from a single invertebrate ancestral gene through double whole genomic duplication that happened at the origin of vertebrates [56]. NOS-derived NO is an important component in defending invertebrates against pathogens. NOS from *Anopheles stephensi* (AsNOS) can be expressed inducibly in *Plasmodium*-infected mosquitoes. Inducible NOS activity is also found in *Rhodnius prolixus* when infected by *T. rangeli*, a South American Stercoraria trypanosome, pathogenic for vectors [57, 58]. NOS activity in invertebrates is also upregulated against the bacterial infection in invertebrates. It has been found that the expression of NOS is upregulated in response to systemic infection with *Escherichia coli* and *Micrococcus luteus* in *Anopheles gambiae*. Inhibition of the activity of NOS or lower NO production results in higher mortality rate of mosquito when infected by pathogenic bacteria, suggesting defensive role of NO in invertebrates [59].

3.1.4. Bacterial nitric oxide synthase (bNOS):

NOS activity is also present in prokaryotes. NOS activity in bacteria was first reported in *Nocardia* species, designated as NOS_{noc} [60] but till now none of the *Nocardia* sp. genome showed similar NOS sequence to that of the animal NOSs. Genome sequencing analysis first brought the clear evidence for the presence of NOS-like protein in bacteria which revealed that the bacterial ORFs (Open reading frames) coding for that protein with maximum sequence similarity to mammalian NOS_{ox} [61]. Key catalytic residues of NOS, are highly conserved from prokaryotes to eukaryotes. drNOS (NOS from *Deinococcus radiodurans*, a radiation-resistant bacteria) is the first NOS-like protein which was cloned, expressed and purified using *E. coli* as the host. The existence of NOS_{OX}-like proteins are mainly found in gram positive bacteria (*Bacillus* sp., *Deinococcus* sp., *Rhodococcus* sp. etc.) but gram negative bacteria like cyanobacterium also contains NOS like sequence [62]. A ~100 kD protein, found in *Rhodococcus* sp., was recognized by a human anti-iNOS antibody. In addition to it, the activity of the protein was reduced by mammalian NOS inhibitor and increased by BH_4, indicating the presence of NOS-like protein [63]. Unlike mammalian NOS, most of the bacterial NOSs only have an oxygenase domain but they can form dimer, indicating presence of different mechanism of dimerization [64, 65]. However, both the oxygenase domain

and reductase domain are present in *Sorangium cellulosum*, indicating both eukaryotes and prokaryotes may have evolved from a common ancestor [66]. NADPH-utilizing proteins like flavodoxin reductase/flavodoxin, transfers electrons to the bacterial NOS and support the production of NO [67, 68]. Bacterial NOS has essential role in cell physiology. It was found that bNOS can regulate the electron transfer to maintain membrane bioenergetics in *Staphylococcus aureus*, a human pathogen. This process is very important for the nasal colonization and resistance from membrane-targeting antibiotics like daptomycin in *Staphylococcus aureus* [69]. Thus, bNOS becomes one of the important drug target to inhibit the growth of methicillin-resistant *Staphylococcus aureus*(MRSA). It was reported that potent bNOS inhibitors like NG-nitro-L-arginine (L-NNA), can enhance MRSA killing [70]. Aminoquinolines, another compound, was found to inhibit the activity of bNOS by binding with the unique hydrophobic patch of bNOS [71].

3.1.5. Fungal nitric oxide synthase:

Orthologue of mammalian NOS is not found in fungus or yeast till today. However, some reports suggest that NOS-like proteins are present in different yeasts and fungi. In 1998, Kanadia *et al.* reported the presence of a NOS-like activity protein of 60 kD in the crude extract of yeast extract, peptone dextrose (YPD) grown *Saccharomyces cerevisiae* cells. The protein was detected by western blot using mouse monoclonal anti-neuronal NOS. That protein was activated by arginine and calmodulin whereas inhibited in the presence of NG-Nitro- L-Arginine Methyl Ester (L-NAME), a mammalian NOS inhibitor [72]. Another report suggests that the nitrite dependent-NO production can take place in mitochondria by the activity of cytochrome *c* under hypoxic condition in *S. cerevisiae* [73]. Calmodulin-dependent NOS-like activity was also found in *S. pombe*, a fission yeast [74]. In 2013, Nishimura *et al.* reported the Tah18-dependent NO production in *S. cerevisiae*. This Tah18-dependent NO production is positively regulated with generation of arginine via proline-arginine metabolic pathway, indicating NOS-like activity of Tah18. It is believed that Tah18 does not contain oxygenase domain. Tah18 may act as a reductase domain and transfer electrons from NADPH to an unknown oxygenase protein, which oxidizes arginine to citrulline and NO [75,76]. NOS-like activity has also been detected in *Blastocladiella emersonii*, an aquatic fungus. Vieira *et al.* reported that concentration of NO-derived products was increased at the sporulation stage and Ca^{2+}-NO-cGMP signaling pathway

was required for biogenesis of zoospores in *Blastocladiella emersonii* [77]. *Aspergillus oryzae* also carries a sequence which shows similarity with the arginine binding site of mammalian NOS oxygenase domain but till now there is no definite evidence of fungal NOS has been reported [78].

3.2. Nitric oxide synthase-independent nitric oxide synthesis:

Although NOS is the main catalytic enzyme for NO synthesis, but several reports suggest that NOS-independent NO synthesis also takes place *in vivo*. The main source of the NOS-independent NO generation is nitrite. In the process of denitrification, NO is produced as an intermediate product by the activity of nitrate reductase and nitrite reductase among the other enzymes. After NOS, the most important enzyme in terms of NO synthesis is nitrite reductase which catalyzes the reaction from nitrite to NO. On the basis of the requirement of co-factors, nitrite reductase is classified into two distinct unrelated groups i.e. heme containing enzyme i.e. cytochrome cd_1 and a copper containing enzyme. Soluble, dimeric Cytochrome cd_1 is widely present in the periplasmic space of the gram negative bacteria like *Pseudomonas aeruginosa*, *Thiobaccilus denitrificans* etc. While the copper containing nitrite reductases are found in both the gram positive (*Bacillus* sp.) and gram negative bacteria (*Alcaligenes* sp.). The copper containing nitrite reductase is bound tightly to the cell membrane of the gram positive bacteria [79]. Miyamoto *et al.* showed that TRPV3, a heat-activated transient receptor potential (TRP) ion channel can induce the NOS-independent NO generation from nitrite in keratinocytes [80]. Deoxyhemoglobin in erythrocytes and deoxymyoglobin in myocardial cells can convert nitrite to NO and form methemoglobin and metmyoglobin during hypoxic condition [81, 82]. Different globin proteins show nitrite reductase-like activities in neuroglobin, cytoglobin, and plant hemoglobins [83-85]. Xanthine oxidoreductase (XOR) can also act as the nitrite reductase during hypoxic conditions. XOR uses xanthine as the electron donor. The nitrite reductase-like activity of XOR is dependent on the concentration of nitrite [86, 87]. It was reported that complex III and complex IV along with cytochrome *c* of mitochondria can reduce the nitrite to NO under hypoxic condition during electron transport chain in liposome [88].

Non-enzymatic NO synthesis has also been reported in mammalian systems. The non-enzymatic NO production has been observed in the stomach under the acidic

condition. In the acidic condition nitrite is converted to nitrous acid (HNO_2). The unstable nitrous acid oxidizes to dinitrogen trioxide (N_2O_3) that subsequently decomposes to NO and nitrogen dioxide (NO_2). The conversion from HNO_2 to N_2O_3 is a second order reaction that indicates the process is comparatively slow [89, 90]. It has been also reported that ascorbate (AsA), an essential antioxidant, can induce non-enzymatic NO production by the reduction of nitrite to NO through the formation of monodehydroascorbate (MDA) radical [91, 92].

4. Beneficial role of nitric oxide:

The beneficial role of NO is associated with the regulatory activities in different biochemical processes in various organisms like mammals, plants, yeasts, bacteria [75]. In 1987, Ignarro *et al.* reported the role of NO as endothelium-derived relaxing factor (EDRF). After that researchers started to explore the NO-mediated signaling pathway and different roles of NO in complex biological processes like smooth muscle relaxation, platelet inhibition, anti-apoptosis etc. [93-96].

4.1. Nitric oxide and vascular tone:

Endothelium-derived NO stimulates soluble guanylate cyclase (sGC) that induces the formation of cGMP. cGMP is a secondary messenger and it can activate protein kinase G which inhibits the voltage-dependent calcium channel (VDCC) mediated calcium influx. Protein kinase G can also act on the SERCA (Sarco/endoplasmic reticulum calcium ATPase) to initiate reuptake of cytosolic calcium (Ca^{2+}) into the sarcoplasmic reticulum (SR), resulting in the reduction of intracellular calcium concentration. Intracellular calcium concentration is very important for the activation of calmodulin. With the reduction in the intracellular calcium concentration, the activity of calmodulin was found to have decreased. Calcium depletion inactivates myosin light chain kinase (MLCK) and upregulates the activity of myosin light chain phosphatase (MLCP). Due to the inactivation of MLCK, myosin phosphorylation is inhibited and actin-myosin cross-bridge breaks down, resulting in the relaxation of smooth muscle cells [97-99]. GPCR (G protein coupled receptors) activity is also associated with the relaxation of smooth muscle cells. Reports suggest that NO inhibits the activity of GRK2 (GPCR kinase 2), the negative regulator of GPCR signaling **[Fig. 2]**. Thus, phosphorylation of β-adrenoceptors is inhibited, that results in the inactivation of the desensitization of the

signal. This mechanism is very important for the relaxation of smooth muscle cells [100,101]. Under hypoxic condition, NO can efficiently regulate the signaling pathway for smooth muscle relaxation without activating the classical NO-sGC-cGMP pathway. The concentration of cyclic inosine monophosphate (cIMP) increases in this signaling pathway [102,103].

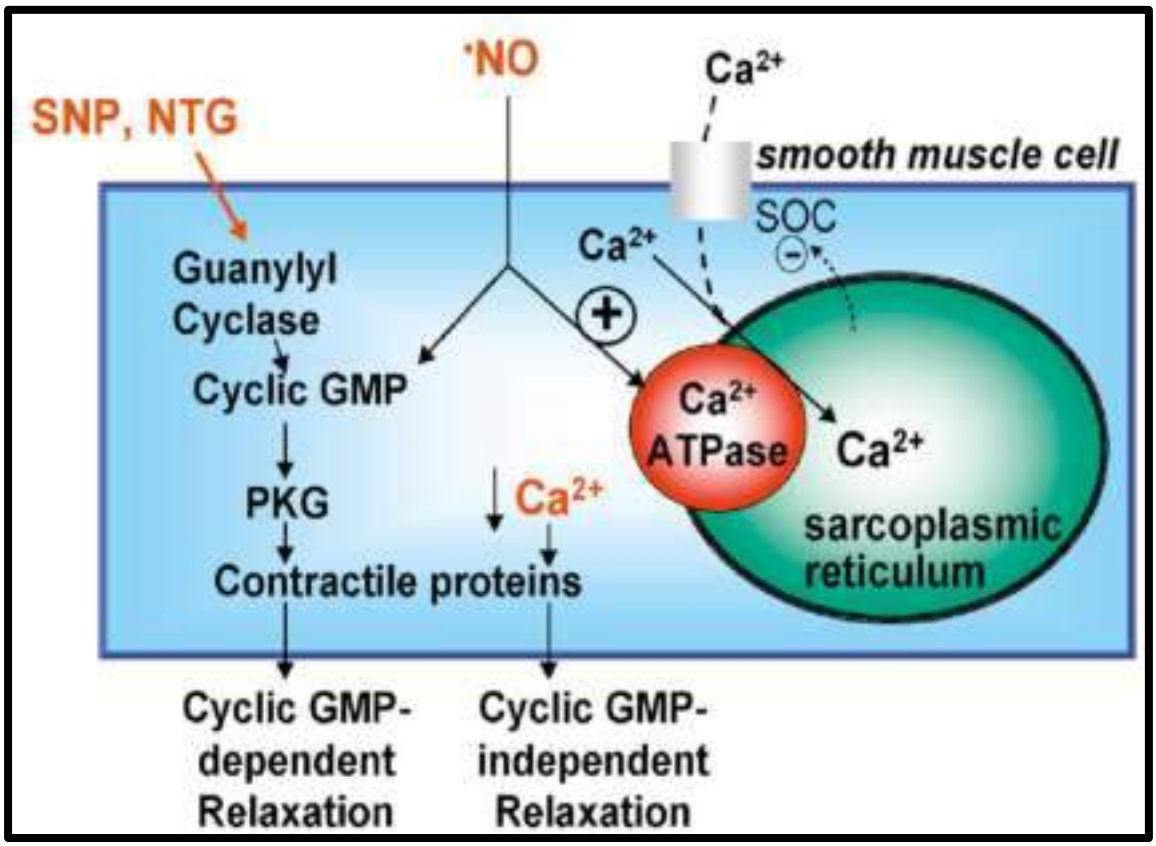

Fig. 2 Role of nitric oxide on relaxation of smooth muscle cell. (Adapted from Tong *et al.* 2010)

4.2. Nitric oxide and platelet inhibition:

Platelet inhibition is also mediated by NO-sGC-cGMP pathway. The key protein which is required for platelet inhibition is vasodilator sensitive phosphoprotein (VASP). This protein has been found in the platelets, endothelial and smooth muscle cells. Platelet activation is dependent on the interaction of the VASP with cytoskeleton proteins. The interaction leads to the polymerization of actin and the shape of the platelet changes, activating the aggregation. The interactive property of the VASP is negatively regulated by phosphorylation. Protein kinase G, the effector molecule of NO-sGC-cGMP pathway, can phosphorylate the Ser^{157} residue of the VASP that leads to the

conformational change of the protein. Due to conformational changes in VASP, the interaction of VASP with cytoskeleton proteins gets completely prevented, that result in the inhibition of platelet activation [104-106]. Report also suggest that interaction of Inositol-1,4,5-triphosphate receptor associated cGMP kinase substrate (IRAG) with inositol-1,4,5-trisphosphate receptor type I (InsP3RI) is also required for NO/cGMP-dependent inhibition of platelet aggregation [107]. Platelets have a little amount of eNOS. It has also been reported that endogenous NO may reduce the platelets response, without hampering the activation occurring at the site of blood vessel injury [104]. Dangel *et al.* showed that NO-sGC mediated cascade signaling is the only mechanism of platelet inhibition, no other mechanism is present to provoke platelet inhibition [108].

4.3. Nitric oxide as an anti-apoptotic factor:

Several reports suggest that NO can interact with the caspase and other proteins to act as an anti-apoptotic factor. NO involved anti-apoptotic event is also mediated through cGMP or cyclic adenosine monophosphate (cAMP) signaling pathway in different cells like eosinophils, PC12 cells, ovarian follicles, embryonic motor neurons and B lymphocytes etc. [109]. In general, apoptosis is initiated by the death receptor and mitochondrial signaling pathway [110]. NO can negatively regulate the activation of the both death ligand-dependent and independent apoptosis. Interaction of NO with the caspase proteins, including caspase-8, an important pro-apoptotic factor, leads to its structural alteration. Caspase-8 can upregulate the activity of Bax and cytochrome *c* in the death signaling pathway. Structural alteration of caspase-8 leads to the inhibition, preventing the death signal pathway of apoptosis [111-113]. TNF-receptor associated death domain protein (TRADD) can be inhibited in the presence of NO, preventing the stimulation of the apoptotic pathway by blocking the ceramide generation [114]. NO can also interfere with the mitochondrial function to inhibit apoptosis. Report suggests that NO can inhibit the PTP (permeability transition pore) reopening by membrane depolarization and accumulation of Ca^{2+}, that can reduce the release of cytochrome *c*, a pro-apoptotic factor [115]. Regulation of the anti-apoptotic activity of NO is concentration-dependent. In lower concentration, NO can act as an anti-apoptotic factor but in higher concentration NO can modulate the ratio of bcl-2 and Bax protein that leads to the activation of the apoptotic pathway [109].

4.4. Cytoprotective role of nitric oxide in yeast:

The cytoprotective role of NO has been reported under environmental stress conditions like high temperature, hydrostatic pressure, heat shock, redox stress etc. in yeast [75]. Nishimura *et al.* showed that the production of NO increases via Pro-Arg metabolic pathway. This elevated NO may help to overcome the stress induced by high temperature [4]. Another report suggests that NO can induce the activity of Mac1 protein by post translational modification under high temperature in *S. cerevisiae*. The higher activity of Mac1 stimulates the expression of ctr1 gene encoding high-affinity copper transporter, which in turn increases the intracellular copper concentration. This copper concentration stimulates the activity of Cu/Zn-SOD, an essential stress response enzyme [116]. NO can also activate the adaptive response by stimulating the peroxide scavenging activity and limiting the availability of iron in *S. pombe*, a fission yeast [117]. It has also been revealed that NO can act as an anti-aging agent. In yeast model, it has been observed that reduced NO production is one of the major cause of Batten disease [118]. Depletion of glucose concentration is one of the major nutrient stress for heterotrophs like yeast. Different cellular responses can be generated during glucose depletion condition by the activation of Rst2 protein in yeast. NO has been reported to induce the expression of the rst2 gene. The activity of Rst2 protein upregulates the expression of the fbp^{1+} gene, encoding a fructose-1,6-bis-phosphatase, via the STREP (stress-starvation response element of *Schizosaccharomyces pombe*) motif. This event leads to the activation of the stress response pathway to combat the hostile condition [119]. NO is also responsible for the metabolic shift in calorie restricted *S. cerevisiae* [120]. Overall, in presence of low concentration of NO, cytoprotective activities like stress resistance, fermentation, metabolism can be stimulated. In higher concentration, NO harms the cell directly or via the formation of reactive nitrogen species (RNS) [75].

5. Reactive nitrogen species (RNS) formation:

Reactive nitrogen species (RNS) is a family of reactive molecules which are derived from NO. RNS is the product of the reaction between NO with molecular oxygen (O_2) or reactive oxygen species like superoxide (O_2^-) [121]. The most common reactive nitrogen species are peroxynitrite ($ONOO^-$) and dinitrogen trioxide (N_2O_3). The reactive nitrogen species formation is dependent on the concentration of the NO. The steady-state concentration of NO is expressed by the ratio between the rate of reaction

(consumption and synthesis) and rate of diffusion [122]. Thus, the imbalance in the steady-state concentration of NO may result in the generation of reactive nitrogen species via several mechanisms like autooxidation of NO, reaction with superoxide etc. [121, 122].

5.1. Auto-oxidation of nitric oxide:

Auto-oxidation of NO is the reaction between NO with molecular oxygen (O_2) to form dinitrogen trioxide (N_2O_3). Different nitrosating agents like nitrosonium ion (NO^+), nitrous acidium ion (H_2ONO^+), can influence the reaction. The reaction is also favored under acidic condition [123]. It is a non-enzymatic, two-steps reaction.

$$2NO + O_2 \longrightarrow 2NO_2$$
$$NO + NO_2 \longrightarrow N_2O_3$$

As it is a third order reaction (second order in NO concentration and first order in O_2 concentration) [124], thus the rate equation of the reaction is expressed as

$$\text{Rate} = k[NO]^2[O_2]$$

[Where, k (rate constant) = 8.4×10^6 M^{-2} s^{-1} at 37°C]

N_2O_3 is also a reactive molecule and can react with the thiols like glutathione reduced, resulting in *S*-nitrosation ($k=1.6 \times 10^{-3}$ s^{-1}) [125]. This is an important reaction for the generation of nitrite anion.

$$RSH + N_2O_3 \longrightarrow RSNO + H^+ + NO_2^-$$

Some of the anions like bicarbonate, phosphate, and chloride have inhibitory effect on *S*-nitrosation under physiological pH. In acidic and physiological pH, nitrosyl halide is formed during the reaction between anions and N_2O_3 [126].

$$X^- + N_2O_3 \longrightarrow XNO + NO_2^-$$

[X represents bicarbonate, phosphate, and chloride]

5.2. Reaction of nitric oxide with superoxide:

At the high concentration, NO can react with the superoxide (O_2^-) to form peroxynitrite ($ONOO^-$). The rate constant of the reaction is varied from 6.6 x 10^9 to 19 x 10^9 $M^{-1}s^{-1}$, with the concentration of NO [127-129]. The rate of formation of peroxynitrite is 3-8 times greater than decomposition of superoxide by SOD [130]. Hughes and Nicklin proposed that hemolysis of peroxo bond was not a thermodynamically favorable reaction. Thus, the decaying of peroxynitrite mainly occurrs by two mechanisms: via the ion pairs or via intramolecular rearrangement, forming nitrate (NO_3^-) or nitrite (NO_2^-) respectively [131]. Proton catalyzed mediated decomposition of peroxynitrite is very rapid (k=1.3 s^{-1}) [132]. In addition to it, carbondioxide (CO_2) mediated peroxynitrite decomposition is also very rapid and end product of the reaction is NO_3^- with a half-life of ~50 ms [133-135]. Peroxynitrite is highly cytotoxic and several studies have been done with peroxynitrite [136, 137].

5.3. Formation of *s*-nitrosothiols:

S-nitrosothiols (RSNO) are the product of the reaction between NO and thiol group containing organic compounds. They are also known as thionitrites. RSNO can act as a signaling molecule in living systems. It plays a major role in platelet inhibition [138]. *S*-nitrosothiols can be formed via autooxidation of NO to N_2O_3, radical recombination between NO and a thiyl radical ($RS^{\bullet}$), and transition metal mediated pathways. It can't be formed without the presence of an electron sink. Hydrophobicity of the thiol-containing organic compound can positively influence the *s*-nitrosothiol formation [139, 140]. Activation of NOS can also contribute to the *s*-nitrosothiols generation via the formation of peroxynitrite. The most common intracellular *s*-nitrosothiol is *s*-nitrosoglutathione (GSNO), formed via the reaction of GSH (reduced glutathione) and NO [141]. The presence of oxygen is also a key factor for the formation of GSNO. The reaction of O_2, NO, and GSH is depicted below.

$$NO^{\cdot} + O_2 \longrightarrow ONOO^{\cdot} \text{ ……(i)}$$

$$ONOO^{\cdot} + NO^{\cdot} \longrightarrow 2\ {\cdot}NO_2 \text{……(ii)}$$

$$NO^{\cdot} + {\cdot}NO_2 \longrightarrow N_2O_3 \text{ ……(iii)}$$

$$GSH + N_2O \longrightarrow GSNO \text{…….....(iv)}$$

GSNO is not a stable molecule in the solution. It can be broken down to NO and GSSG. In the presence of acid, GSNO can release nitrosonium ion (NO^+). Thus, it is also referred to as a "NO donor" [141, 142]. Enzyme-dependent (GSNO reductase, Carbonyl reductase 1, Thioredoxin system) GSNO metabolism has also been found in different organisms [143].

6. Nitrosative stress:

When the ratio of nitrosants (NO and reactive nitrogen species) to antioxidants exceeds 1.0 inside the cell, in that situation, NO or reactive nitrogen species (RNS) interact with the biomolecules like DNA, lipid, proteins [109, 144]. Sometimes, this interaction is deleterious and may lead to the damage of DNA and DNA repair system, functional loss of proteins or enzymes, structural modification of lipids and also alter the redox homeostasis *in vivo* [109, 144-146]. This hostile condition is referred to as ***"nitrosative stress"***– a term first coined by Prof. Jonnathan Stamler and his co-workers in analogy with the "oxidative stress" [147]. Thus, in short, nitrosative stress can be defined as the belligerent condition, provoked by the imbalance in the concentration of NO [148].

6.1. Effect of nitrosative stress on cellular components:

Several reports suggest that NO or RNS can interact with the cellular macromolecules like DNA, lipid, protein etc. that may lead to its inactivation and structural modifications. These interactions influence the cellular homeostasis as well as its survival [109, 149] **[Fig. 3]**.

6.1.1. Nitrosative stress and DNA:

Nitrosative stress mediated DNA damage cannot be directly associated with NO but with RNS like HNO_2/acidified NO_2^-, dinitrogen trioxide (N_2O_3), and peroxynitrite ($ONOO^-$**)** [150]. The RNS mediated DNA damage can be processed through three chemical mechanisms: 1. direct interaction with DNA structure, 2. inhibition of DNA repair system and 3. via the production of genotoxic compounds like alkylating agents, and hydrogen peroxide (H_2O_2) [151]. N_2O_3 is a strong deaminating agent. It interacts with heterocyclic amines of DNA bases via the formation of diazonium ion and complete hydrolysis of diazonium ion leads to deamination. Hence, cytosine, adenine, and 5-methylcytosine are converted to uracil, inosine, and thymine respectively by the

action of N_2O_3 whereas guanine is converted to xanthine and oxanine. Deamination is the main reason for structural and characteristic alteration of the bases [152-154]. This deamination influences spontaneous depurination that leads to the break-down of DNA.

Peroxynitrite can interact with DNA during the replication and transcription process when DNA exists in the single-strand form [155]. It can damage both the sugar and bases of DNA. Guanine can be converted to 8-nitro-2′-deoxyguanosine (8-nitro-dG) and 8-Oxo-7,8-dihydro-2′-de-2 oxyguanosine by the treatment of peroxynitrite [156, 157]. These compounds are referred to as the marker of peroxynitrite mediated DNA damage [158]. Xanthine and hypoxanthine can also be formed by the treatment of peroxynitrite [159]. These changes decrease the integrity of DNA, promoting breakage of the strands. Peroxynitrite can also induce dG–dG and DNA–protein crosslinks that leads to DNA mutation [160, 150]. It can also induce fragmentation of the sugar moiety, generating strand breakage. It is believed that damage in sugar moiety involves hydrogen abstraction, generating highly reactive sugar radicals that participate in the radical mediated DNA strand breakage [158].

HNO_2/acidified NO_2^- can also induce DNA damage *in vivo* and *in vitro* [150]. It induces the DNA cross linking at G and CpG islands [161]. The indirect mechanism of DNA damage is associated with the inhibition of DNA repair system [162]. HNO_2/acidified NO_2^- can also interact with the components of DNA repair system. The Zn-finger motif of DNA repair enzymes can be affected by the NO released from acidified NO_2^-, resulting in the inhibition via losing the integrity [163]. DNA synthesis process can also be blocked by the action of NO via inhibiting ribonucleotide reductase [164, 165]. Furthermore, *in vivo* exposure of NO leads to the generation of genotoxic compounds, promoting apoptosis [109].

6.1.2. Nitrosative stress and lipid:

Nitrosative modification of lipids is associated with oxidation and nitration [166]. Lipid oxidation is a characteristic feature of inflammatory vascular diseases like atherosclerosis [167]. NO and its derivatives are usually involved in the modification of lipid and its biosynthesis [150]. But it has also been reported that at lower concentration, NO can inhibit the lipid oxidation by reacting with the lipid based radicals (L•, LO•' LOO•). LOO• mediated propagation can be blocked by the NO [168].

It was apparent that copper induced oxidation of low density lipoprotein (LDL) can be inhibited by lower concentration of NO in activated macrophages and endothelial cells [169-171]. Oxidation of liposomal cholesterol and phosphatidylcholine can be reduced in the presence of lower concentration of NO [172, 173].

In the presence of O_2 and singlet oxygen (O_2•), NO derived reactive species rigorously oxidize lipids [174]. NO_2^- mediated oxidation and nitration have been shown in unsaturated fatty acids, LDL, cholesterol etc. [175-177]. The protonated form of NO_2^- i.e. HNO_2 can react with ethyl linoleate and hydroperoxy-octadecadienoic acid and different nitrated species like nitroalcohol, nitroalkanes etc. are formed, leading to the lipid bilayer damage [178]. Peroxynitrite and its protonated form i.e. ONOOH are also involved in lipid damage [179]. Peroxynitrite mediated lipid oxidation leads to the generation of different nitrated species along with secondary oxygen species like singlet oxygen (O_2•) due to the rearrangement of unstable reactive peroxynitrite intermediates (LOONO) [180]. LOONO can form comparatively stable $LONO_2$ or breaks down to LO• and NO_2^- via hemolytic cleavage [181]. In addition to it, peroxynitrite mediated lipid oxidation also leads to the formation of lipid-protein adduct in LDL, indicating excessive breakdown of polyunsaturated acid [182].

6.1.3. Nitrosative stress and protein:

Proteins are one of the most vulnerable macromolecule in the presence of RNS including NO. Hence, the protein modifications, like, *S*-nitrosylation, protein tyrosine nitration (PTN), are referred to as the biomarkers of nitrosative stress. Both these forms are specific, inhibitory/toxic post translational modifications and can also participate in regulation of different cellular processes [183].

S-nitrosylation is a very important regulatory mechanism *in vivo* [184-186]. *S*-nitrosylation is a reversible post translational modification in which NO moiety covalently binds with specific cysteine residue(s) of a protein, yielding *S*-nitrosothiol [187, 188]. This reaction can be mediated by different chemical species like NO, metal-NO complex, nitrosonium ion (NO^+), *S*-nitrosoglutathione (GSNO) etc. *S*-nitrosylation induces the conformational changes of protein that may lead to acetylation, ubiquitylation, palmitoylation of different cellular components [189]. Proteins like hemoglobin, caspase-3, glyceraldehyde-3-phosphate dehydrogenase are involved in

transnitrosylation i.e. catalyzing the transfer of NO group to the adjacent protein [190-192]. Denitrosylation i.e. reversible reaction of *S*-nitrosylation, is also associated with the activity of proteins, protein-protein interaction, cellular signaling etc. It has been reported that caspase-3 can be activated via denitrosylation [193]. Compared to denitrosylated forms of protein, *S*-nitrosylated forms have a lower pK_a that leads to its stabilization. The presence of the bulky amino acids [e.g., phenylalanine (Phe), tyrosine (Tyr), arginine (Arg), and leucine (Leu)] near the cysteine (Cys) residue creates steric hindrance that leads to the blocking of *S*-nitrosylation [194]. However, at the higher concentration of NO or GSNO, enzymes can be inhibited. Mitochondrial proteins are the primary targets of *S*-nitrosylation mediated protein inhibition. Proteins like NADH dehydrogenase, aldehyde dehydrogenase, 2-oxoglutarate dehydrogenase can be inactivated via *S*-nitrosylation [195-197]. The activity of glyceraldehyde-3-phosphate dehydrogenase can also be inhibited via *S*-nitrosylation. The inhibition of the different proteins via *S*-nitrosylation is mainly associated with the conformational change of the active site [198, 199]. Researchers believe that *S*-nitrosylation is associated with a good number of cellular events ranging from bacteria to mammals [194]. A database (dbSNO 2.0 http://dbSNO.mbc.nctu.edu.tw) is designed to collect the *S*-nitrosylated protein from literature reviews [200]. Hence, the research is going on to uncover the *S*-nitrosothiol mediated response *in vivo*.

Protein tyrosine nitration (PTN) is another covalent post translational modification where nitro ($-NO_2$) group is added at the *meta* position of the phenolic ring of specific tyrosine residue/s of a protein [201]. Peroxynitrite, sodium nitroprusside, acidified sodium nitrite ($NaNO_2$) can form PTN via generation of $\bullet NO_2$ [202-204]. Professor Rafael Radi (Biochemist, Universidad de la República, Uruguay) and his co-workers have reported that PTN is a free radical process where not only $\bullet NO_2$ but also tyrosyl radical (•Tyr) is required [205]. Though it is not an enzymatic process but the process is still very selective and the formation of PTN is not dependent on the abundance of the tyrosine residue. PTN formation is mainly dependent on the local environment of the tyrosine residue and the secondary structure of the protein [201, 204]. Hence, PTN is considered as one of the most important biomarkers of nitrosative stress [206]. Addition of $\bullet NO_2$ radical at the tyrosine molecule, reduces the pKa value from 10.1 to 7.2 of the hydroxyl group present in the phenolic ring of the nitrotyrosine residue [207]. Nitrotyrosine residues are hydrophobic whereas tyrosine residues are mildly hydrophilic [201]. Tyrosine nitration generally contributes to the

generation of additional negative charge and are also able to add comparatively bulky substituent (due to the hydrophobicity) to the protein. This may lead to the alteration of local charge distribution as well as the configuration that results in inhibition [206]. Cellular mitochondrial matrix is the primary locus for PTN formation [208]. Reports suggest that Fe-S cluster proteins like aconitase can be inactivated by PTN [209]. Published reports suggest that peroxynitrite can form PTN in HDAC2 (Histone Deacetylase 2) at Tyr253, ascorbate peroxidase at Tyr5 and Tyr235, MnSOD at Tyr34, that results in inactivation [210-212]. The effect of protein tyrosine nitration on cellular signaling is not clear. It was hypothesized that tyrosine nitration might affect the cellular signaling due to alteration of the local environment. It has also been reported that PTN interferes with the protein phosphorylation which cannot be possible when the target Tyr residue is nitrated [213, 214]. However, previous report suggests that peroxynitrite induces both the nitration and phosphorylation of Tyr residue of protein (e.g. T-lymphocyte) [215]. Hence, the biochemistry of PTN and its functioning is not fully understood till now.

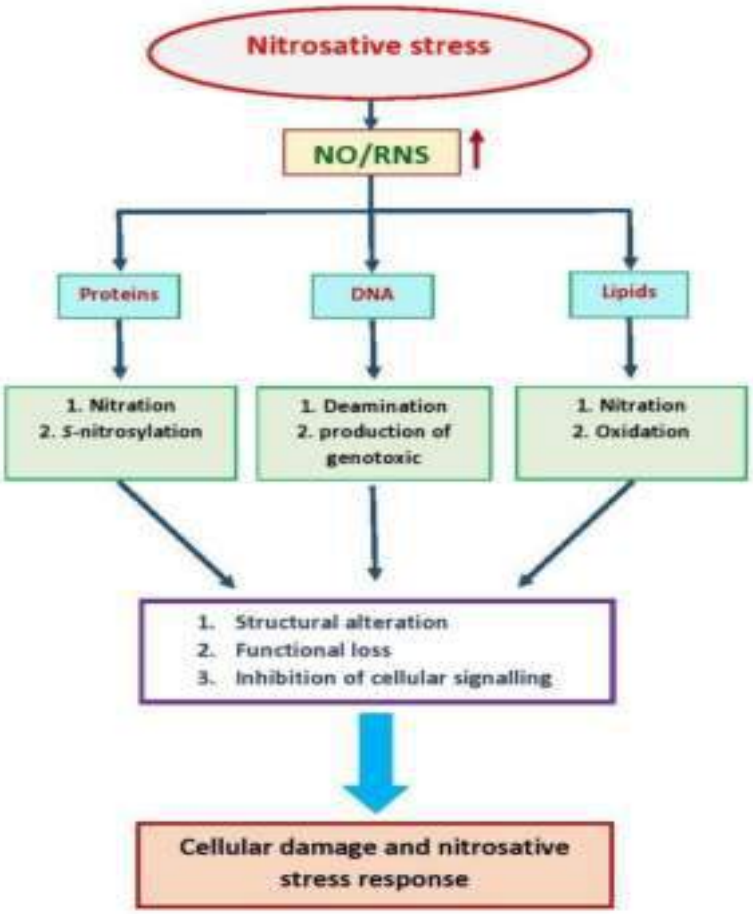

Fig. 3 Effect of nitrosative stress on protein, lipid and DNA.

6.2. Nitrosative stress and apoptosis:

At higher concentration, NO can act as a pro-apoptotic factor [109]. Intracellular higher concentration of NO can induce apoptosis in different cells like macrophage, neuroblastoma, smooth muscle cells etc. [216-219]. It has been reported that NO signaling is strongly associated with the apoptotic pathway in yeast, mammals etc. [109, 220]. It has also been mentioned that mitochondrial matrix proteins are vulnerable to nitrosative stress [201]. Higher concentration of NO can form more reactive peroxynitrite that can disrupt the mitochondrial transmembrane potential, resulting in release of cytochrome *c* due to transition in mitochondrial permeability [221-223]. The release of cytochrome *c* is the key event for the induction of apoptotic signaling pathway. This event can stimulate the downstream proteins (e.g. apaf-1, caspase-3 etc.) of the apoptotic signaling pathway [109, 224]. Caspases, a family of cysteine proteases, can induce DNase. The breakage of poly ADP-ribose polymerase (PARP), substrate of caspase-3, has been reported to increase in NO-mediated apoptosis, suggesting upregulation of caspase-3 during nitrosative stress [226]. Another important factor for apoptosis is the activity of p53, a tumor suppressor protein [224]. RNS induced DNA damage can stimulate the p53. Under nitrosative stress, induced p53 can stimulate the production of p21.

This event may lead to the blocking of cell cycle progression via inhibiting cyclin dependent kinases, an important factor for cell growth [226, 227]. In addition to it, report also suggests that activation of iNOS can induce the accumulation of p53, suggesting the role of NO as a pro-apoptotic factor [225]. NO induced p53 can also increase the expression of Bax, a pro-apoptotic protein and reduce the expression of Bcl-2, an anti-apoptotic protein [228]. The ratio of Bax to Bcl-2 is a very important factor for the induction of apoptotic pathway [109]. A recent publication by Almeida *et al.* (2020) has described the role of *S*-nitrosylation of glyceraldehyde-3-phosphate dehydrogenase (GAPDH) in NO-mediated apoptotic signaling in yeast [220] suggest that the apoptosis rate in H_2O_2-treated yeast cells is induced with the level of *S*-nitrosylation of GAPDH. It has been reported that inhibition of GAPDH via *S*-nitrosylation leads to induction of DNase and apoptotic pathway. In addition to it, NO can stimulate cGMP pathway via binding with the heme-containing protein guanylyl cyclase, resulting in the production of cGMP, a secondary messenger that leads to the apoptosis [229, 230]. The reduced activity of protein kinase C (PKC), decrease in

extracellular signal-regulated kinases (ERK) phosphorylation, are also associated with NO-induced apoptosis [231, 232]. A schematic diagram of the role of NO on apoptosis is proposed in **Fig. 4**.

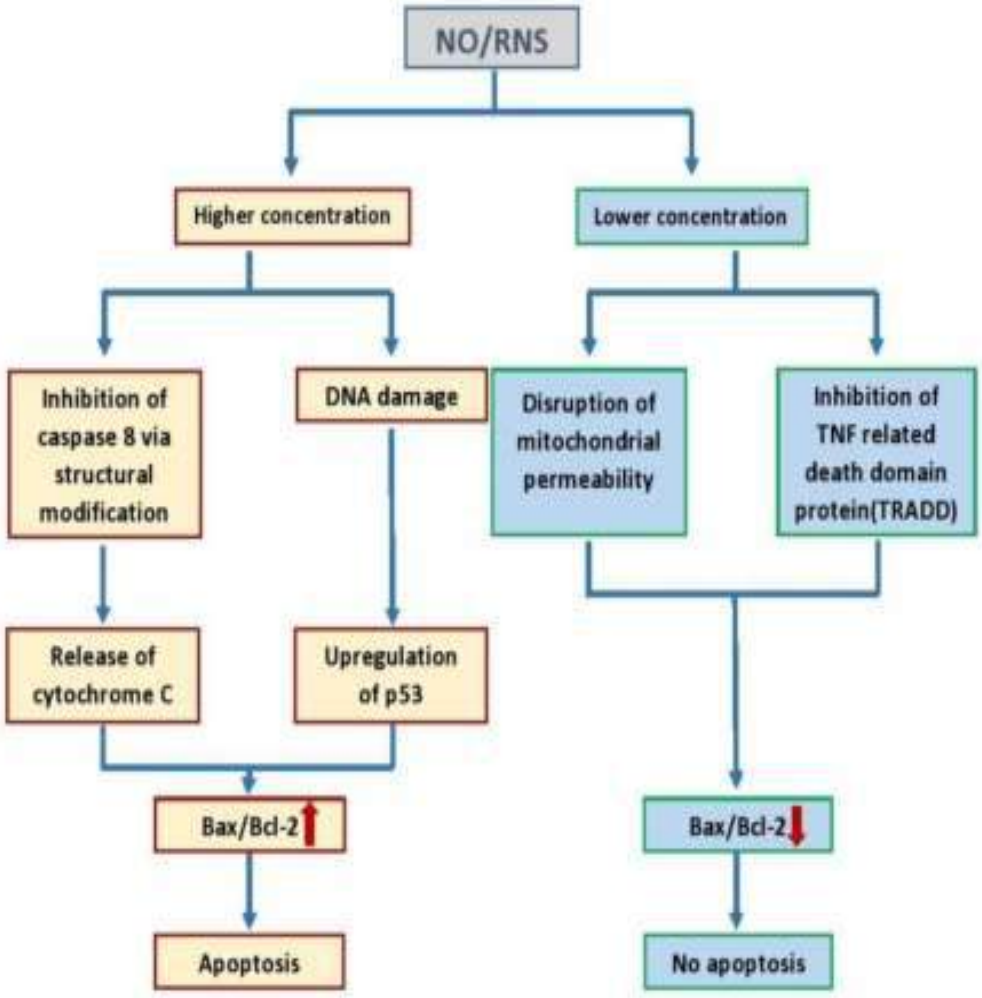

Fig. 4 Role of nitric oxide on apoptosis.

6.3. Nitrosative stress and aging:

"Aging" is a broad spectrum term, associated with chronological, replicative parameters [233, 234]. The study of aging is paradoxical, very complicated and associated with different factors like dietary restriction (DR), stress, genetic organization, environmental influences etc. [235]. To study the genetics and biochemistry of aging, *S. cerevisiae* has been the choice of organism since more than 50 years [234]. The aging of yeast, can be expressed by the two ways: replicative life span (RLS) and chronological life span (CLS). Replicative life span is defined as the number of daughter cells, generated from the mother cell before senescence, an

irreversible arrest of cell cycle. Whereas chronological life span is the length of survival time of a yeast cell in a non-dividing state [236]. These features give the opportunity to study the mechanism of aging of both the proliferating and non-proliferating cells using comparatively simple unicellular organism yeast [237]. Hence, it has become the choice of organism to characterize the underlying mechanism of aging [238].

It is well established that mitochondrial dysfunction and generation of ROS and RNS, are associated with aging [234, 239]. Though *S. cerevisiae* is petite positive (ability to survive without the mitochondrial DNA [240]) but still damaging of mtDNA, leads to aging [241]. Redox stress can lead to the accumulation of reactive species *in vivo* [236]. These reactive species can interfere with the macromolecules of the cell, resulting in the alteration of the cellular functions like metabolism, biogenesis etc. [242, 243]. The alteration in cellular metabolism (energy production, amino acid synthesis) as well as CLS is tightly associated with the TOR/Sch9 signaling and it is well established in dietary restriction mediated aging [244]. TOR/Sch9 signaling is an important factor for cell cycle progression. It also stimulates the translational process, but it represses the general stress response by restricting the localization of transcription factors Msn2 and Msn4 (important factor for redox stress response) in the cytoplasm [234, 245, 246]. Under the stress condition, the activity of TOR is reduced and cellular stress response is stimulated. It has been reported that TOR/Sch9 signaling is inhibited during redox stress due to the alteration in the localization of Sch9, increasing the CLS in yeast [247]. In addition to it, mitochondrial dysfunction also triggers retrograde signaling (a communication between mitochondria and the nucleus along with other cellular compartments [248]) which is also controlled by the TOR activity via regulating the expression of retrograde gene [249, 250]. Due to inhibition of the activity of TOR, the retrograde genes are expressed that may contribute to the extension of the chronological life span. Autophagy (recycling of the cellular macromolecules during stress condition [251]) also contributes to the extension of the CLS. It has been reported that TOR activity negatively regulates autophagy. Hence, the reduced activity of TOR increases autophagy which in turn leads to the expansion of CLS [252, 253]. The reduction in the activity of protein kinase A (PKA) is also associated with TOR/Sch9 signaling that contributes to the extension of CLS [245]. A schematic diagram of the role of NO on aging is proposed in **Fig. 5**.

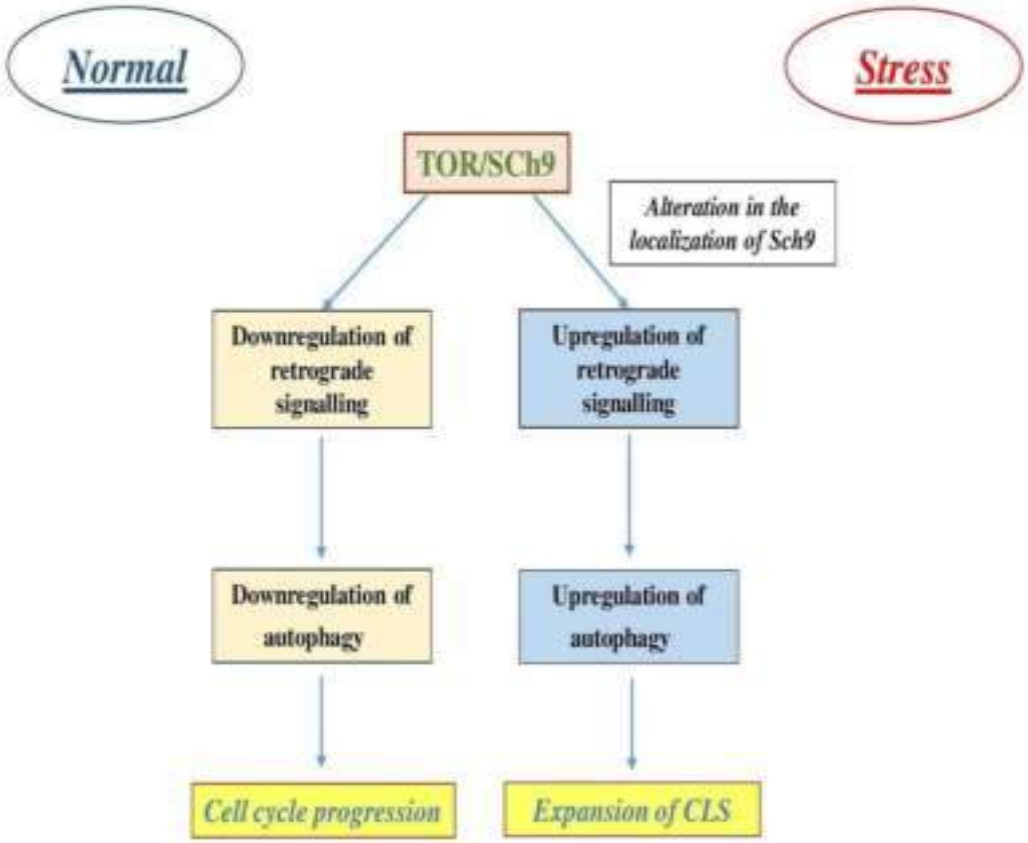

Fig. 5 Role of nitric oxide on aging.

Different studies have revealed the connection between the dysregulation of the biogenesis of ribosomes and aging. Enhanced ribosome biogenesis is one of the major characteristics feature of aging [254]. Under the stress condition, high rate of the ribosome biogenesis can promote aging through the excess translation. This event leads to the disruption of the global proteostasis, the process to maintain and regulate the proteins and their quality [255]. Loss of proteostasis is a hallmark of aging [256]. In addition to it, the accumulation of ribosomal DNA (rDNA) can also cause aging. The high rate of rDNA synthesis may lead to DNA damage that results in genetic instability, another vital cause of aging [257]. In addition to it, the inactivation of Fe-S cluster protein or the biogenesis of Fe-S may also contribute to the genetic instability [236, 258]. NO-signaling in aging is also a very complicated as well as self-contradictory subject. NO-signaling is very important for apoptosis but it can also act as an anti-aging component. Lewinska *et al.* showed that the level of NO was reduced rather than increased in dietary restriction mediated stress response. It indicates that NO-mediated pathways are involved in aging [259]. The elevated level of SOD is also associated with the extension of CLS, suggesting the hypothesis [260]. In mammalians, different

neurodegenerative diseases like alzheimer's disease (AD), parkinson's disease (PD), huntington's disease (HD), amyotrophic lateral sclerosis (ALS) etc. are related with aging [261-263].

6.3.1. Alzheimer's disease:

Alzheimer's disease (AD) is one of the most common neurodegenerative disease that is associated with nitrosative stress [264-266]. It has been observed that protein tyrosine nitration of tau protein is tightly associated with AD [267]. Tau is an axon-enriched microtubule associated brain protein, encoded by chromosome 17 in human [268, 269]. Protein tyrosine nitration in tau protein is very specific. It has been found that tyrosine residues are at the position of 18, 29, 197, 310, and 394, (using longest isoform of tau as the reference) prone to be nitrated in the presence of RNS like peroxynitrite. The sensitivity of amino terminal tyrosine resiudes (Y18, Y29) of tau proteins are more for the PTN as compared to other residues. PTN formation in Y310 is the rarest due to its localization at the hydrophobic microtubules binding repeats [270]. Nitration of tyrosine residues of tau, induces intracellular neurofibrillary tangle formation (due to polymerization) that may lead to the dysfunction of the protein as well as damage and destruction of synapses [268,271]. Another important biomarker of nitrosative stress mediated AD is the formation of extracellular senile amyloid plaques [264, 268, 272]. This event may lead to the accumulation of iron and copper inside the brain, resulting in the loss of metal homeostasis [273, 274]. In addition to it, loss of mitochondrial metabolism or dysfunction of mitochondria is also a characteristic feature of AD. Damaging of DNA and RNA, proteolysis are also associated with the nitrosative stress mediated AD [264, 275]. Overall, redox imbalance, permanent alteration cell signaling, gene expressions are also associated with AD [276, 277].

6.3.2. Parkinson's disease:

Parkinson's disease (PD) is the second most frequent neurodegenerative disorder after than AD. One of the characteristic feature of PD is the movement impairment due to the selective degeneration of dopaminergic neurons [278]. Though it is considered as a sporadic disease but evidences reveal that it can be family-linked [279]. This aging-related disease is tightly associated with nitrosative and oxidative stress [280]. Reports suggest that degeneration of dopaminergic neuron is primarily caused by the reactive oxygen species (ROS) and RNS mediated lipid peroxidation, protein modification etc

in the brain tissue [281]. Astrocytes, star-shaped glial cells in CNS, play major role in metabolism and detoxification of reactive species. One of the most important function of astrocytes is maintaining the redox homeostasis in brain [282]. Astrocytic generation of RNS involves in the dysfunction of neuronal mitochondria [283]. Characteristic features of PD includes presence of eosinophilic cytoplasmic inclusions of fibrillar, misfolded proteins known as the lewy bodies containing ubiquitinated α-synuclein, parkin, syuphilin, neurofilaments and synaptic vesicle proteins [284].

α-synuclein is very prone to tyrosine nitration and considered as one of the most important cause of protein aggregation. It has been revealed that four tyrosine residues (Y39, Y125, Y133, Y136) are susceptible for nitration [285]. α-synuclein is very sensitive to the nitrating agents like peroxynitrite. Even a very low concentration of peroxynitrite is sufficient to cause PTN in α-synuclein [286]. Nitrated α-synuclein becomes resistance to proteolysis but prone for the aggregation that leads to the reduction in both lipid binding tendency and solubility in cell, suggesting the generation of toxicity due to misfolding of this protein [287]. The nitrated α-synuclein shows more immunogenicity that may leads to the stimulation of neuroinflammation by cytokines, NF-κB and others intracellular components [278, 288, 289]. Another important protein of PD pathogenicity is parkin, an ubiquitin E3 ligase encoded by the *PARK2* gene. This protein is involved in the maintaining of mitochondrial integrity and regulates mitophagic degradation [290]. Report suggests that overproduction of NO may interfere with the structural modification as well as activity of the protein via *S*-nitrosylation. The cysteine residues of the catalytic RING domains of parkin are prone to *S*-nitrosylation. *S*-nitrosylation induces the inactivation of parkin protein that leads to the neurotoxicity [291, 292]. In addition, loss of activity of DJ-1 and PINK, have been also identified in the pathogenesis of PD. Loss of activity of these proteins under nitrosative stress which in turn causes apoptosis and neurotoxicity [278, 293].

6.3.3. Huntington's disease:

Huntington's disease (HD) is a fatal genetic neurodegenerative disorder, associated with the progressive loss of memory, mood, behavior and cognition [294]. This autosomal neurological disorder is caused by the unusual expansion of CAG repeats (>36 repeats) within IT15 gene located at chromosome 4, that code polyglutamine (polyQ) tract in N-terminal site of the huntingtin protein, a ubiquitous protein, [295-

297]. It has been established that imbalance of NO contributes to the development of HD. There are two major pathways that can link the imbalance of NO and development of HD i.e. htt/HAP-1/calmodulin/NOS link and the CREB binding protein/htt/NOS link [295]. Dysfunction of NO may contribute to the Progressive striatal damage and abnormal cerebral blood flow (CBF), important markers of HD [298, 299]. The dysfunction of nNOS may lead to the alteration in NO production, resulting in neurodegeneration [299]. RNS like peroxynitrite mediated damage has been characterized in HD. Peroxynitrite may lead to DNA damage, lipid peroxidation, induction of iNOS, depletion of NAD^+ flux, that results in neurotoxicity [300]. This neurotoxicity inversely leads to the alteration of mitochondrial membrane permeability via pore formation, resulting in the release of cytochrome *c*, a proapoptotic factor [301]. Loss of activity of respiratory chain via inhibiting complex II, III, IV, has been well characterized in HD patients [302-304]. Report suggests that reduction in NO content in platelets, interferes with the eNOS phosphorylation at ser^{1177} during the advanced stages of HD [305].

6.3.4. Amyotrophic lateral sclerosis (ALS):

One of the most dangerous neurological disorder is Amyotrophic lateral sclerosis (ALS), most patient die less than 5 years after appearing the symptoms [306]. This neurodegenerative disease (also known as Charcot's disease or Lou Gehrig's disease) is marked by the selective loss of upper motor neurons of the motor cortex, and lower motor neurons of motor neurons of spinal cord and brain stem [307]. One of the major cause of ALS is mitochondrial dysfunction that leads to the death of the neurons [308, 309]. Mitochondrial dysfunction is associated with the lipid peroxidation, DNA damage and misfolding of important proteins [307]. Loss of activity of Cu, Zn superoxide dismutase (SOD1) via reactive species mediated misfolding was reported in the patient of ALS [310, 311]. SOD1 participates in the regulation of energy metabolism, cellular respiration, stress control etc. [312-314], thus the loss of activity of SOD1 leads to the suppression of the above processes along with the generation of superoxide or ROS, causative agents of mitochondrial dysfunction [315-318]. Elevated level of ROS has been reported in CNS of the patient with ALS [319]. Peroxynitrite, an important RNS, is also generated due to higher ROS production. Peroxynitrite mediated protein modification via formation of 3-nitrotyrosine in CNS is considered as the one of the important biomarker of ALS [320-324].

RNS-mediated lipid modification has also been found in the CNS of the patient with ALS [325]. One of the most abundant product of fatty acid peroxidation by RNS is 4-hydroxy-2-nonenal (HNE), act as 'second cytotoxic messenger', has been well characterized in the ALS patients [326]. It is a very toxic product that may stimulate cellular damage and apoptosis [327, 328]. It can move across the membrane and interacts with the different cellular components, leading to the cytotoxicity, one of the major reason for loss of activity of the motor neurons [306, 327]. Overall, due to the activity of reactive species, the structure of the membrane is affected that leads to the alteration in fluidity, permeability, transport and metabolic processes [306]. These alterations severy affect the neuronal function that causes ALS.

6.4. Nitrosative stress and metabolism:

It has been reported that RNS or NO can affect the cellular metabolic processes like tricarboxylic acid (TCA) cycle, electron transport chain, fatty acid biosynthesis, β-oxidation of fatty acid etc. via interfering with the enzymes of the different metabolic pathways [329, 330]. Activities of aconitase, isocitrate dehydrogenase, α-ketoglutarate dehydrogenase have been found to be decreased under nitrosative stress due to the *S*-nitrosylation, resulting in the inhibition of TCA cycle [331-336]. RNS or NO mediated inactivation of aconitase has been characterized in chronological aging [337]. The nitration of the tyrosine residues of aconitase under nitrosative stress has also been reported [203]. Activity of glutamate dehydrogenase, catalyzes the conversion from glutamate to α-ketoglutarate has also been found to be nitrated in mice liver under nitrosative stress, that leads to the less generation of α-ketoglutarate for TCA cycle [338, 339]. Report also suggests that pyruvate dehydrogenase can be inactivated due to *S*-nitrosylation. Inactivation of pyruvate dehydrogenase directly affects the TCA cycle. Reduction in the TCA cycle via post translational modification under nitrosative stress contributes to the development of neurodegenerative disorders [301, 340-343]. In addition to it, enzymes of glycolytic pathway e.g. hexokinase, aldolase, glyceraldehyde-3-phosphate dehydrogenase, enolase etc. are also very prone to *S*-nitrosylation [301, 329, 330]. Rate limiting enzyme of fatty acid biosynthesis i.e. very long-chain acyl-CoA dehydrogenase (VLCAD) has also been found to be *S*-nitrosylated in the presence of NO that leads to the generation of more acetyl-CoA, showing beneficial effect of *S*-nitrosylation [329]. In addition to it, metabolic reprogramming in *Pseudomonas fluorescens* under nitrosative stress has also been reported by Auger *et*

al. They hypothesized that metabolic reprogramming can act as bacterial defense strategy by coupling with antioxidant system to overcome the stress [344].

7. Cellular defense strategies against nitrosative stress:

Cells always try to overcome the hostile situation mediated by the different stress agents. These defense strategies include different enzymatic and non-enzymatic pathways. Though the defense strategies are not well characterized but still some of the components are found that play a major role to overcome the nefarious activity of RNS or NO inside the cell.

7.1. Non-enzymatic defense:

To combat the RNS or NO mediated stress, a good number of non-enzymatic components have been identified, among them γ-L-glutamyl-L-cysteinyl-glycine (GSH) or reduced glutathione has been found to be a potent candidate to protect the cell from RNS-mediated damage [345]. GSH is a very important component for maintaining the redox homeostasis *in vivo* that contributes to the cellular proliferation, differentiation and apoptosis. It can directly bind with NO to form GSNO, suggesting the role of GSH as NO scavenger [347]. It was reported that NO can stimulate DNA damage and protein modifications when the intracellular GSH level declines, indicating the protective role of GSH under nitrosative stress [348]. The alteration of mitochondrial GSH level is also associated with Ca^{2+} ion distribution, pyridine nucleotide oxidation status, mtDNA damage, and induction of membrane permeability transition [349-355]. *S*-glutathionylation (reversible binding of GSH with protein) helps to mask the proteins from irreversible oxidative damage. *S*-glutathionylation of proteins also contributes to the alteration of signal transduction that is required to respond against the reactive species mediated stress [356, 345]. Reports suggest that disruption of glutathione biosynthesis also contributes to the glutathione auxotrophy in *S. cerevisiae* and *S. pombe* [357, 358]. In addition to it, NADPH and nicotinamide adenine dinucleotide hydrogen (NADH) are also two important factors that provide the non-enzymatic defense to the cell under nitrosative and oxidative stress. NADH is an important cofactor for the antioxidant [359, 360]. Vitamin C and vitamin E also provide protection against nitrosative stress. These two vitamins together contribute to increasing the intracellular flux of GSH [361]. Vitamin E also breaks the chain of lipid

peroxidation and vitamin C also gives protection against the ROS like hydrogen peroxides [362, 363]. Lipoic acid (LA), another important non-enzymatic compound which gets digested, absorbed and converted to dihydro lipoic acid (DHLA). DHLA can neutralize free radicals and contribute to the generation of vitamin C. LA also helps to stabilize lysosome under nitrosative and oxidative stress via termination of free radicals and chelating of transition metals [364, 365]. In addition to it, melatonin, β-carotenes, and flavonoids are also found to show protective roles against the free radical mediated damage [366-368]. Melatonin also induces different antioxidant enzymes like superoxide dismutase, glutathione reductase, catalase etc. [366]. It also inhibits pro-oxidant enzymes like NOS, xanthine oxidase and lipoxygenase etc. It has also been reported that melatonin helps to stabilize or protect the cellular membrane from oxidative damage and increase the rate of electron transport chain (ETC) without increasing generation of reactive species [366]. β-carotenes and flavoniods play an important role to inhibit lipid peroxidation via scavenging peroxyl radicals [367, 368].

7.2. Enzymatic defense:

To overcome the reactive species mediated stress, activities of some enzymes have been found to be upregulated and detoxify the effect of NO or RNS, known as 'stress response enzyme' e.g. flavohemoglobin, Cu/Zn superoxide dismutase (SOD), glutathione peroxidase, glutathione reductase (GR), catalase, GSNO reductase etc. [361, 369].

Flavohemoglobin (Yhb1) or nitric oxide dioxygenase (NOD) can detoxify the effect of NO by converting NO to NO_3^-, using NADPH as the reducing power [370]. Flavohemoglobin or NOD like activity is conserved from prokaryotes to higher eukaryotes [75]. In higher eukaryotes, hemoglobin shows NOD-like activity [371]. The amino acid sequence of flavohemoprotein (Hmp1) in *E. coli* shows high homological similarities with NOD of yeast [373]. In presence of NO, the overexpression of *YHB1* gene has been reported in *S. cerevisiae* and *C. albicans* [117, 372, 373]. Reduction or inhibition in the activity of Yhb1 increases the NO-mediated growth inhibition in the cells of *S. cerevisiae* and *C. albicans* [372, 374, 375]. It has also been observed that the loss of activity of Yhb1increases the intracellular RSNO production that may result in the generation of nitrosative stress condition [376]. Under the stress condition, cytochrome *c* oxidase (C*c*O) activity in mitochondrial respiratory chain complex

(MRC) can be downregulated that leads to the generation of superoxides and then it is subsequently converted to peroxynitrite, a potent nitrating agent [377, 73]. Yhb1 also helps the pathogenic yeast to resist from the macrophage-induced NO, showing its role as a virulence factor [373, 378]. The anti-nitrosative or anti-oxidative role of Yhb1 has been determined by its cytosolic and mitochondrial localization. In absence of superoxide Yhb1 is mainly present in cytosol but in the hypoxic condition, Yhb1 is mainly localized in the mitochondrial matrix, suggesting the protective role of Yhb1 under nitrosative and oxidative stress [379].

Another important anti-nitrosative enzyme is GSNO reductase (GSNOR) that breaks down toxic GSNO into oxidized glutathione (GSSG) and ammonia. GSNOR is very similar to GSH-dependent formaldehyde dehydrogenase (GS-FDH) [380], member of the formyldehyde dehydrogenase III that contains NADH binding site like alcohol dehdrogenase [381, 382]. The GSNOR activity has been reported in eukaryotes like *S. pombe*, *S. cerevisiae*, plants, and mammalians and most of bacteria [380, 381, 384, 385]. GSNOR or Fdh3 is considered as the marker of redox switch i.e. sensitive to the alteration of redox state of cell [386]. Earlier reports suggest that reduction in the activity of GSNOR can enhance nitrosative stress mediated damage [382, 387, 388]. It has also been reported that the loss of activity of GSNOR in *C. albicans* hampers the nitrosative stress response and virulent property. This suggests the role of GSNOR as the virulence factor that provides the protection from host immune response mediated by nitrosants like NO or its derivatives [382].

Catalase was the first characterized antioxidant enzyme that actively participates to combat the oxidative and nitrosative stress. Generally, the main function of catalase is the conversion of hydrogen peroxide to water and oxygen [389]. But the activity of catalase has been found to be upregulated to inhibit peroxynitrite mediated oxidation and nitration and also peroxynitrite catabolism in *S. cerevisiae* [390]. Report also suggests that catalase activity can be upregulated in *S. cerevisiae* in GSNO mediated nitrosative stress [391].

As mentioned earlier, GSH can act as the stress response component. Increase in the intracellular concentration of GSH is dependent on the activity of glutathione reductase (GR) that catalyzes the conversion from oxidized glutathione (GSSG) to reduced glutathione (GSH) using NADPH as the reducing equivalent [392]. Activity of

GR is required for mitochondrial activity. It has been reported that GR can reduce the oxidation and nitration of Fe-S cluster proteins of mitochondria [393]. In addition to it, thioredoxin system also acts as a disulfide reductase. It has been reported that thioredoxin system helps to maintain the intracellular GSH concentration in GR mutant *E. coli* [394, 395].

Superoxide dismutase also indirectly helps to overcome the nitrosative stress. SOD reduces superoxide to hydrogen peroxide and oxygen atom. In the presence of excessive NO, SOD can reduce the concentration of intracellular superoxide which in turn inhibits or reduces the production of toxic peroxynitrite [396]. Peroxynitrite mediated lipid oxidation/peroxidation can also be reduced by the activity of glutathione peroxidase (GPx). Gpx uses GSH as the reducing power [397]. It is also considered as a H_2O_2-stress response enzyme [361].

8. Yeast as a model organism to study nitrosative stress:

Budding yeast (mainly *S. cerevisiae*) is a robust model system for basic biological research [398]. This eukaryotic organism carries 6692 genes in 12 megabase pairs of DNA that is distributed in 16 linear chromosomes present in nucleus. The genomic stability of the organism makes it one of the best system to study gene manipulation. Its full genome was sequenced in 1996 as the first eukaryote [399]. The integrity of the genetic and molecular toolbox of the yeast, has placed it as the primary system to study and develop the different high-throughput technologies involved in transcriptomics, proteomics, metabolomics and so on [400-405]. Like the budding yeast, fission yeast (*S. pombe*) has also become a powerful system to study the cell growth and division [406-409]. The whole genome sequencing of *S. pombe* was also reported in 2002 [410]. *CDC2* gene, an important factor for cell division, was first discovered in *S. pombe* [409]. Different cell cycle check points have also been characterized by using *S. pombe* and *S. cerevisiae*. Spindle check point genes, DNA damage checkpoint genes *etc.* have first been characterized in *S. cerevisiae* [411, 412]. In addition to it, the growth rate of yeast is very fast (~90 min/generation) as compared to animal model and it is comparatively easy to handle.

Another important feature to use yeast as the model organism to study the genetic and biochemical characterization, is the similarity with the metabolic and

cellular pathways that occur in higher eukaryotes like humans. Thus, yeast system has become a good model to study cancer and neurodegenerative diseases like Parkinson's disease, Alzheimer's disease and Huntington's disease [413-415]. Different gene mutations related to human cancer have been characterized by using yeast as the model system [416]. Another important factor, that is associated with different physiological disorders, is nitrosative stress. Reports suggest that formation of 3-nitrotyrosine and *S*-nitrosylation are two major markers of cardiovascular disease cardiovascular disease, obesity, diabetes mellitus and so on [417, 418]. To characterize the physiochemical properties and biochemistry of 3-nitrotyrosine, *S*-nitrosylation under nitrosative stress, one of the best system is yeast.

In the last decade a good number of studies have been done to characterize the nitrosative stress response using yeast (*e.g. S. cerevisiae*, *S. pombe*, *C. albicans etc.*) as the model organism. Several critical issues have been addressed in this last decade regarding nitrosative stress response that encourages researchers to explore more mechanistic pathways of nitrosative stress response. In response to nitrosative stress transcriptional regulations mediated by different transcriptional factors (TFs) in yeast have been well characterized. Yap1, an important transcriptional factor has been reported to be upregulated under nitrosative stress. It is one of the most important factor for the higher activity of SOD and catalase. Deletion of the *YAP1* gene fails to activate SOD and catalase. In addition to it, the subcellular localization of the Yap1 protein has been found in the nucleus of *S. cerevisiae* under nitrosative stress, suggesting its role under nitrosative stress [419]. On the other hand, Yap7 plays the exact opposite role regarding nitrosative stress response. Reports suggest that Yap7 represses Yhb1, an important anti-nitrosative enzyme. Hence, the deletion of Yap7 contributes to the enhancement of NO resistance in yeast. Binding of Yap7 to the *YHB1* promoter leads to the recruitment of Tup1 repressor, resulting in the downregulation of *YHB1* [420, 421]. Cwt1p, another negative regulator of Yhb1 has been found in *C. albicans* [422]. Nitrosative stress tolerance is based on different strategies possessed by different organisms. Anam *et al.* identified a nitrosative stress tolerance gene *RIB1* which encodes GTP cyclohydrolase II that catalyzes the first step in riboflavin biosynthesis. The byproduct of the reaction of GTP cyclohydrolase II, can scavenge RNS. Thus, the author claimed that riboflavin indirectly helps to overcome nitrosative stress [423]. Kar *et al.* discovered that transcription factor Atf1 was localized in the nucleus under

nitrosative stress in *S. pombe*. Though the mechanism is not clear but authors hypothesized that Sty1-Atf1 mitogen-activated protein kinase (MAPK) pathway may be required for the nitrosative stress response [424]. Till now different proteins have been identified that are sensitive under nitrosative stress. Redox homeostasis along with the antioxidant system, has also been characterized in the presence of different RNS. Using critical molecular biology tools, different transcription factors have been recognized as the nitrosative stress response element but there is a lacony regarding metabolic strategy under nitrosative stress.

References:

1. Lancaster JR Jr. (2015) Nitric oxide: a brief overview of chemical and physical properties relevant to therapeutic applications. Future Sci. OA1:FSO59.
2. Lancaster JR Jr. (1992) Nitric Oxide in Cells. Am. Sci. 80:248–259.
3. Stuehr, D. J., &Haque, M. M. (2019). Nitric oxide synthase enzymology in the 20 years after the Nobel Prize. British journal of pharmacology, 176:177–188.
4. Nishimura A, Kawahara N, Takagi H. (2013) The flavoprotein Tah18-dependent NO synthesis confers high-temperature stress tolerance on yeast cells. BiochemBiophys Res Commun. 430:137-43.
5. Li H, Poulos TL. (2005) Structure-function studies on nitric oxide synthases. J InorgBiochem. 99:293-305.
6. Bush PA, Gonzalez NE, Griscavage JM, Ignarro LJ. (1992) Nitric oxide synthase from cerebellum catalyzes the formation of equimolar quantities of nitric oxide and citrulline from L-arginine. BiochemBiophys Res Commun. 185:960-6.
7. Förstermann U, Sessa WC. (2012) Nitric oxide synthases: regulation and function. Eur Heart J. 33:829-37.
8. Crane BR, Arvai AS, Ghosh DK, Wu C, Getzoff ED, Stuehr DJ, Tainer JA. (1998) Structure of nitric oxide synthase oxygenase dimer with pterin and substrate. Science. 279:2121-6.
9. Alderton WK, Cooper CE, Knowles RG. (2001) Nitric oxide synthases: structure, function and inhibition. Biochem J. 357:593-615.
10. Klatt P, Pfeiffer S, List BM, Lehner D, Glatter O, Bächinger HP, Werner ER, Schmidt K, Mayer B. (1996) Characterization of heme-deficient neuronal nitric-oxide synthase reveals a role for heme in subunit dimerization and binding of the amino acid substrate and tetrahydrobiopterin. J Biol Chem. 271:7336-42.
11. Hemmens B, Goessler W, Schmidt K, Mayer B. (2000) Role of bound zinc in dimer stabilization but not enzyme activity of neuronal nitric-oxide synthase. J Biol Chem. 275:35786-91.

12. Cho HJ, Xie QW, Calaycay J, Mumford RA, Swiderek KM, Lee TD, Nathan C. (1992) Calmodulin is a subunit of nitric oxide synthase from macrophages. J Exp Med. 176:599-604.

13. Hemmens B, Mayer B. (1998) Enzymology of nitric oxide synthases. Methods Mol Biol.100:1-32.

14. Stuehr D, Pou S, Rosen GM. (2001) Oxygen reduction by nitric-oxide synthases. J Biol Chem. 276:14533-6.

15. List BM, Klösch B, Völker C, Gorren AC, Sessa WC, Werner ER, Kukovetz WR, Schmidt K, Mayer B. (1997) Characterization of bovine endothelial nitric oxide synthase as a homodimer with down-regulated uncoupled NADPH oxidase activity: tetrahydrobiopterin binding kinetics and role of haem in dimerization. Biochem J. 323:159-65.

16. Nishimura JS, Martasek P, McMillan K, Salerno J, Liu Q, Gross SS, Masters BS. (1995) Modular structure of neuronal nitric oxide synthase: localization of the arginine binding site and modulation by pterin. BiochemBiophys Res Commun. 210:288-94.

17. Noble MA, Munro AW, Rivers SL, Robledo L, Daff SN, Yellowlees LJ, Shimizu T, Sagami I, Guillemette JG, Chapman SK. (1999) Potentiometric analysis of the flavin cofactors of neuronal nitric oxide synthase. Biochemistry. 38:16413-8.

18. Förstermann U, Closs EI, Pollock JS, Nakane M, Schwarz P, Gath I, Kleinert H. (1994) Nitric oxide synthase isozymes. Characterization, purification, molecular cloning, and functions. Hypertension. 23:1121-31.

19. Huang PL, Huang Z, Mashimo H, Bloch KD, Moskowitz MA, Bevan JA, Fishman MC. (1995) Hypertension in mice lacking the gene for endothelial nitric oxide synthase. Nature. 377:239-42.

20. Kanwar JR, Kanwar RK, Burrow H, Baratchi S. (2009) Recent advances on the roles of NO in cancer and chronic inflammatory disorders. Curr Med Chem.16:2373-94.

21. Jiang X, Mu D, Manabat C, Koshy AA, Christen S, Täuber MG, Vexler ZS, Ferriero DM. (2004) Differential vulnerability of immature murine neurons to oxygen-glucose deprivation. Exp Neurol. 190:224-32.

22. Chen J, Tu Y, Moon C, Matarazzo V, Palmer AM, Ronnett GV. (2004) The localization of neuronal nitric oxide synthase may influence its role in neuronal precursor proliferation and synaptic maintenance. Dev Biol. 269:165-82.

23. Matsuda H, Iyanagi T. (1999) Calmodulin activates intramolecular electron transfer between the two flavins of neuronal nitric oxide synthase flavin domain. BiochimBiophysActa. 1473:345-55.

24. Roman LJ, Masters BS. (2006) Electron transfer by neuronal nitric-oxide synthase is regulated by concerted interaction of calmodulin and two intrinsic regulatory elements. J Biol Chem. 281:23111-8.

25. Guan ZW, Iyanagi T. (2003) Electron transfer is activated by calmodulin in the flavin domain of human neuronal nitric oxide synthase. Arch BiochemBiophys. 412:65-76.

26. Nathan C, Xie QW. (1994) Nitric oxide synthases: roles, tolls, and controls. Cell. 78:915-8.

27. Cui H, Hayashi A, Sun HS, Belmares MP, Cobey C, Phan T, Schweizer J, Salter MW, Wang YT, Tasker RA, Garman D, Rabinowitz J, Lu PS, Tymianski M. (2007) PDZ protein interactions underlying NMDA receptor-mediated excitotoxicity and neuroprotection by PSD-95 inhibitors. J Neurosci. 27:9901-15.

28. Zhou L, Zhu DY. (2009) Neuronal nitric oxide synthase: structure, subcellular localization, regulation, and clinical implications. Nitric Oxide. 20:223-30.

29. Chanrion B, Mannoury la Cour C, Bertaso F, Lerner-Natoli M, Freissmuth M, Millan MJ, Bockaert J, Marin P. (2007) Physical interaction between the serotonin transporter and neuronal nitric oxide synthase underlies reciprocal modulation of their activity. Proc Natl AcadSci U S A. 104:8119-24.

30. Saitoh F, Tian QB, Okano A, Sakagami H, Kondo H, Suzuki T. NIDD, (2004) a novel DHHC-containing protein, targets neuronal nitric-oxide synthase

(nNOS) to the synaptic membrane through a PDZ-dependent interaction and regulates nNOS activity. J Biol Chem. 279:29461-8.

31. Izumi Y, Zorumski CF. (1993) Nitric oxide and long-term synaptic depression in the rat hippocampus. Neuroreport. 4:1131-4.

32. Toda N, Ayajiki K, Okamura T. (2009) Control of systemic and pulmonary blood pressure by nitric oxide formed through neuronal nitric oxide synthase. J Hypertens. 27:1929-40.

33. Förstermann U. (2000) Regulation of nitric oxide synthase expression and activity. In: Mayer B, editor. Handbook of Experimental Pharmacology—Nitric Oxide. Berlin: Springer; pp. 71–91.

34. Moncada S, Higgs EA. (2006) Nitric oxide and the vascular endothelium. HandbExp Pharmacol.176:213-54.

35. Ginnan R, Guikema BJ, Halligan KE, Singer HA, Jourd'heuil D. (2008) Regulation of smooth muscle by inducible nitric oxide synthase and NADPH oxidase in vascular proliferative diseases. Free RadicBiol Med. 44:1232-45.

36. Soskić SS, Dobutović BD, Sudar EM, Obradović MM, Nikolić DM, Djordjevic JD, Radak DJ, Mikhailidis DP, Isenović ER. (2011) Regulation of Inducible Nitric Oxide Synthase (iNOS) and its Potential Role in Insulin Resistance, Diabetes and Heart Failure. Open Cardiovasc Med J. 5:153-63.

37. Green SJ, Mellouk S, Hoffman SL, Meltzer MS, Nacy CA. (1990) Cellular mechanisms of nonspecific immunity to intracellular infection: cytokine-induced synthesis of toxic nitrogen oxides from L-arginine by macrophages and hepatocytes. Immunol Lett. 25:15-9.

38. Brown GC, Neher JJ. (2010) Inflammatory neurodegeneration and mechanisms of microglial killing of neurons. MolNeurobiol. 41:242-7.

39. Wong JM, Billiar TR. (1995) Regulation and function of inducible nitric oxide synthase during sepsis and acute inflammation. AdvPharmacol. 34:155-70.

40. Lange M, Enkhbaatar P, Nakano Y, Traber DL. (2009) Role of nitric oxide in shock: the large animal perspective. Front Biosci (Landmark Ed). 14:1979-89.

41. Lisanti MP, Scherer PE, Tang Z, Sargiacomo M. (1994) Caveolae, caveolin and caveolin-rich membrane domains: a signalling hypothesis. Trends Cell Biol. 4:231-5.

42. Hemmens B, Mayer B. (1998) Enzymology of nitric oxide synthases. Methods Mol Biol.100:1-32.

43. Fulton D, Babbitt R, Zoellner S, Fontana J, Acevedo L, McCabe TJ, Iwakiri Y, Sessa WC. (2004) Targeting of endothelial nitric-oxide synthase to the cytoplasmic face of the Golgi complex or plasma membrane regulates Akt-versus calcium-dependent mechanisms for nitric oxide release. J Biol Chem. 279:30349-57.

44. García-Cardeña G, Fan R, Shah V, Sorrentino R, Cirino G, Papapetropoulos A, Sessa WC. (1998) Dynamic activation of endothelial nitric oxide synthase by Hsp90. Nature. 392:821-4.

45. Zimmermann K, Opitz N, Dedio J, Renne C, Muller-Esterl W, Oess S. (2002) NOSTRIN: a protein modulating nitric oxide release and subcellular distribution of endothelial nitric oxide synthase. Proc Natl AcadSci U S A. 99:17167-72.

46. Fleming I, Busse R. (2003) Molecular mechanisms involved in the regulation of the endothelial nitric oxide synthase. Am J PhysiolRegulIntegr Comp Physiol. 284:R1-12.

47. McCabe TJ, Fulton D, Roman LJ, Sessa WC. (2000) Enhanced electron flux and reduced calmodulin dissociation may explain "calcium-independent" eNOS activation by phosphorylation. J Biol Chem. 275:6123-8.

48. Smart EJ, Graf GA, McNiven MA, Sessa WC, Engelman JA, Scherer PE, Okamoto T, Lisanti MP. Caveolins, (1999) liquid-ordered domains, and signal transduction. Mol Cell Biol. 19:7289-304.

49. Ignarro LJ, Harbison RG, Wood KS, Kadowitz PJ. (1986) Activation of purified soluble guanylate cyclase by endothelium-derived relaxing factor from intrapulmonary artery and vein: stimulation by acetylcholine, bradykinin and arachidonic acid. J Pharmacol Exp Ther. 237:893-900.

50. Arndt H, Smith CW, Granger DN. (1993) Leukocyte-endothelial cell adhesion in spontaneously hypertensive and normotensive rats. Hypertension. 21:667-73.

51. Dimmeler S, Zeiher AM. (1999) Nitric oxide-an endothelial cell survival factor. Cell Death Differ. 6:964-8.

52. Radomski MW, Martin JF, and Moncada S. (1991) Synthesis of nitric oxide by the haemocytes of the american horseshoe crab (*Limulus polyphemus*) Philos. Trans. R. Soc. Lond. (Biol) 334:129-133.

53. Jacklet JW. (1995) Nitric oxide is used as an orthogradecotransmitter at identified histaminergic synapses. J. Neurophysiol. 74:891-895.

54. Elofsson R, Carlberg M, Moroz L, Nezlin L, Sakharov D. (1993) Is nitric oxide (NO) produced by invertebrate neurones? Neuroreport. 4:279-282.

55. Moroz LL, and Gillette R. (1996) NADPH diaphorase localization in the CNS and peripheral tissues of the predatory sea-slug *Pleurobranchaeacalifornica*. J. Comp. Neurol. 367:607-622.

56. González-Domenech CM, Muñoz-Chápuli R. (2010) Molecular evolution of nitric oxide synthases in metazoans. Comp BiochemPhysiol Part D Genomics Proteomics. 5:295-301.

57. Ascenzi P, Gradoni L. (2002) Nitric oxide limits parasite development in vectors and in invertebrate intermediate hosts. IUBMB Life. 53:121-3.

58. Luckhart S, Li K. (2001) Transcriptional complexity of the Anopheles stephensi nitric oxide synthase gene. Insect BiochemMol Biol. 31:249-56.

59. Hillyer JF, Estévez-Lao TY. (2010) Nitric oxide is an essential component of the hemocyte-mediated mosquito immune response against bacteria. Dev Comp Immunol. 34:141-9.

60. Chen Y, Rosazza JP. (1994) A bacterial nitric oxide synthase from a Nocardia species. Biochem Biophys Res Commun. 203:1251-8.

61. White O, Eisen JA, Heidelberg JF, Hickey EK, Peterson JD, Dodson RJ, Haft DH, Gwinn ML, Nelson WC, Richardson DL, Moffat KS, Qin H, Jiang L, Pamphile W, Crosby M, Shen M, Vamathevan JJ, Lam P, McDonald L,

Utterback T, Zalewski C, Makarova KS, Aravind L, Daly MJ, Minton KW, Fleischmann RD, Ketchum KA, Nelson KE, Salzberg S, Smith HO, Venter JC, Fraser CM. (1999) Genome sequence of the radioresistant bacterium Deinococcusradiodurans R1. Science. 286:1571-7.

62. Sudhamsu J, Crane BR. (2009) Bacterial nitric oxide synthases: what are they good for? Trends Microbiol. 17:212-8.

63. Choi DW, Oh HY, Hong SY, Han JW, Lee HW. (2000) Identification and characterization of nitric oxide synthase in *Salmonella typhimurium*. Arch Pharm Res. 23:407-12.

64. Pant K, Bilwes AM, Adak S, Stuehr DJ, Crane BR. (2002) Structure of a nitric oxide synthase heme protein from *Bacillus subtilis*. Biochemistry. 41:11071-9.

65. Bird LE, Ren J, Zhang J, Foxwell N, Hawkins AR, Charles IG, Stammers DK. (2002) Crystal structure of SANOS, a bacterial nitric oxide synthase oxygenase protein from Staphylococcus aureus. Structure. 10:1687-96.

66. Agapie T, Suseno S, Woodward JJ, Stoll S, Britt RD, Marletta MA. (2009) NO formation by a catalytically self-sufficient bacterial nitric oxide synthase from *Sorangiumcellulosum*. Proc Natl AcadSci U S A. 106:16221-6.

67. Holden JK, Li H, Jing Q, Kang S, Richo J, Silverman RB, Poulos TL. (2013) Structural and biological studies on bacterial nitric oxide synthase inhibitors. Proc Natl AcadSci U S A. 110:18127-31.

68. Wang Y, Golledge J. (2013) Neuronal nitric oxide synthase and sympathetic nerve activity in neurovascular and metabolic systems. CurrNeurovasc Res. 10:81-9.

69. Kinkel TL, Ramos-Montañez S, Pando JM, Tadeo DV, Strom EN, Libby SJ, Fang FC. (2016) An essential role for bacterial nitric oxide synthase in *Staphylococcus aureus* electron transfer and colonization. Nat Microbiol. 2:16224.

70. Holden JK, Kang S, Beasley FC, Cinelli MA, Li H, Roy SG, Dejam D, Edinger AL, Nizet V, Silverman RB, Poulos TL. (2015) Nitric Oxide Synthase as a

Target for Methicillin-Resistant Staphylococcus aureus. Chem Biol. 22:785-92.

71. Holden JK, Lewis MC, Cinelli MA, Abdullatif Z, Pensa AV, Silverman RB, Poulos TL. (2016) Targeting Bacterial Nitric Oxide Synthase with Aminoquinoline-Based Inhibitors. Biochemistry. 55:5587-5594.

72. Kanadia RN, Kuo WN, Mcnabb M, Botchway A. (1998) Constitutive nitric oxide synthase in Saccharomyces cerevisiae. BiochemMolBiol Int. 45:1081-7.

73. Castello PR, David PS, McClure T, Crook Z, Poyton RO. (2006) Mitochondrial cytochrome oxidase produces nitric oxide under hypoxic conditions: implications for oxygen sensing and hypoxic signaling in eukaryotes. Cell Metab. 3:277-87.

74. Kig C, Temizkan G. (2009) Nitric oxide as a signaling molecule in the fission yeast *Schizosaccharomycespombe*. Protoplasma. 238:59-66.

75. Astuti RI, Nasuno R, Takagi H. (2016) Nitric oxide signaling in yeast. Appl Microbiol Biotechnol. 100:9483-9497.

76. Yoshikawa Y, Nasuno R, Kawahara N, Nishimura A, Watanabe D, Takagi H. (2016) Regulatory mechanism of the flavoprotein Tah18-dependent nitric oxide synthesis and cell death in yeast. Nitric Oxide. 57:85-91.

77. Vieira AL, Linares E, Augusto O, Gomes SL. (2009) Evidence of a Ca(2+)-(*)NO-cGMP signaling pathway controlling zoospore biogenesis in the aquatic fungus *Blastocladiella emersonii*. Fungal Genet Biol. 46:575-84.

78. Samalova M, Johnson J, Illes M, Kelly S, Fricker M, Gurr S. (2013) Nitric oxide generated by the rice blast fungus *Magnaporthe oryzae* drives plant infection. New Phytol. 197:207-222.

79. Zumft WG. (1993) The biological role of nitric oxide in bacteria. Arch Microbiol. 160:253-64.

80. Miyamoto T, Petrus MJ, Dubin AE, Patapoutian A. (2011) TRPV3 regulates nitric oxide synthase-independent nitric oxide synthesis in the skin. Nat Commun. 2:369.

81. Cosby K, Partovi KS, Crawford JH, Patel RP, Reiter CD, Martyr S, Yang BK, Waclawiw MA, Zalos G, Xu X, Huang KT, Shields H, Kim-Shapiro DB, Schechter AN, Cannon RO, Gladwin MT (2003) Nitrite reduction to nitric oxide by deoxyhemoglobinvasodilates the human circulation. Nat Med. 9:1498–1505,

82. Shiva S, Huang Z, Grubina R, Sun J, Ringwood LA, MacArthur PH, Xu X, Murphy E, Darley-Usmar VM, Gladwin MT (2007) Deoxymyoglobin is a nitrite reductase that generates nitric oxide and regulates mitochondrial respiration. Circ Res. 100:654–661.

83. Tiso M, Tejero J, Basu S, Azarov I, Wang X, Simplaceanu V, Frizzell S, Jayaraman T, Geary L, Shapiro C (2011) Human neuroglobin functions as a redox-regulated nitrite reductase. J Biol Chem. 286:18277–89.

84. Li H, Hemann C, Abdelghany TM, El-Mahdy MA, Zweier JL (2012) Characterization of the mechanism and magnitude of cytoglobin-mediated nitrite reduction and nitric oxide generation under anaerobic conditions. J Biol Chem. 287:36623–36633.

85. Tiso M, Tejero J, Kenney C, Frizzell S, Gladwin MT (2012) Nitrite reductase activity of nonsymbiotichemoglobins from *Arabidopsis thaliana*. Biochem. 51:5285–5292

86. Godber BLJ, Doel JJ, Sapkota GP, Blake DR, Stevens CR, Eisenthal R, Harrison R (2000) Reduction of nitrite to nitric oxide catalyzed by xanthine oxidoreductase. J Biol Chem. 275:7757–7763.

87. Millar TM, Stevens CR, Benjamin N, Eisenthal R, Harrison R, Blake DR (1998) Xanthine oxidoreductase catalyses the reduction of nitrates and nitrite to nitric oxide under hypoxic conditions. FEBS Lett. 427:225–228.

88. Shiva S (2013) Nitrite: a physiological store of nitric oxide and modulator of mitochondrial function. Redox Biol. 1:40–44.

89. L'hirondel J, L'hirondel JL (2002) Nitrate and man: toxic, harmless or beneficial? CABI Publishing, Oxon

90. Miles AM, Wink DA, Cook JC, Grisham MB (1996) Determination of nitric oxide using fluorescence spectroscopy. Methods Enzymol. 268:105–120.

91. Weitzberg E, Lundberg J (1998) Nonenzymatic nitric oxide production in humans. Nitric Oxide 2:1–7.

92. Evans HJ, McAuliffe C (1956) Identification of NO, N_2O, and N_2 as products of the nonenzymatic reduction of nitrite by ascorbate or reduced diphosphopyridine nucleotide. In: McElroy WD, Glass B (eds) Inorganic nitrogen metabolism. Johns Hopkins Press, Baltimore, pp 189–197

93. Ignarro LJ, Buga GM, Wood KS, Byrns RE, Chaudhuri G. (1987) Endothelium-derived relaxing factor produced and released from artery and vein is nitric oxide. Proc Natl AcadSci U S A. 84:9265-9.

94. Lincoln TM, Wu X, Sellak H, Dey N, Choi CS. (2006) Regulation of vascular smooth muscle cell phenotype by cyclic GMP and cyclic GMP-dependent protein kinase. Front Biosci. 11:356-67.

95. Noguchi A, Takada M, Nakayama K, Ishikawa T. (2008) cGMP-independent anti-apoptotic effect of nitric oxide on thapsigargin-induced apoptosis in the pancreatic beta-cell line INS-1. Life Sci. 83:865-70.

96. Walter U, Gambaryan S. (2009) cGMP and cGMP-dependent protein kinase in platelets and blood cells. Hand bExp Pharmacol. 191:533-48.

97. Korkmaz S, Loganathan S, Mikles B, Radovits T, Barnucz E, Hirschberg K, Li S, Hegedüs P, Páli S, Weymann A, Karck M, Szabó G. (2013) Nitric oxide- and heme-independent activation of soluble guanylate cyclase attenuates peroxynitrite-induced endothelial dysfunction in rat aorta. J Cardiovasc Pharmacol Ther. 18:70-7.

98. Carvajal JA, Germain AM, Huidobro-Toro JP, Weiner CP. (2000) Molecular mechanism of cGMP-mediated smooth muscle relaxation. J Cell Physiol. 184:409-20.

99. Word RA, Tang DC, Kamm KE. (1994) Activation properties of myosin light chain kinase during contraction/relaxation cycles of tonic and phasic smooth muscles. J Biol Chem. 269:21596-602.

100. Whalen EJ, Foster MW, Matsumoto A, Ozawa K, Violin JD, Que LG, Nelson CD, Benhar M, Keys JR, Rockman HA, Koch WJ, Daaka Y, Lefkowitz RJ,

Stamler JS. (2007) Regulation of beta-adrenergic receptor signaling by *S*-nitrosylation of G-protein-coupled receptor kinase 2. Cell. 129:511-22.

101. Whalen EJ, Johnson AK, Lewis SJ. (2000) Beta-adrenoceptor dysfunction after inhibition of NO synthesis. Hypertension. 36:376-82.

102. Chen Z, Zhang X, Ying L, Dou D, Li Y, Bai Y, Liu J, Liu L, Feng H, Yu X, Leung SW, Vanhoutte PM, Gao Y. (2014) cIMP synthesized by sGC as a mediator of hypoxic contraction of coronary arteries. Am J Physiol Heart Circ Physiol. 307:H328-36.

103. Gao Y, Chen Z, Leung SW, Vanhoutte PM. (2015) Hypoxic Vasospasm Mediated by cIMP: When Soluble Guanylyl Cyclase Turns Bad. J CardiovascPharmacol. 65:545-8.

104. Bruckdorfer R. (2005) The basics about nitric oxide. Mol Aspects Med. 26:3-31.

105. Radomski MW, Palmer RM, Moncada S. (1987) The anti-aggregating properties of vascular endothelium: interactions between prostacyclin and nitric oxide. Br J Pharmacol. 92:639-46.

106. Radomski MW, Palmer RM, Moncada S. (1990) Characterization of the L-arginine:nitric oxide pathway in human platelets. Br J Pharmacol. 101:325-8.

107. Antl M, von Brühl ML, Eiglsperger C, Werner M, Konrad I, Kocher T, Wilm M, Hofmann F, Massberg S, Schlossmann J. (2007) IRAG mediates NO/cGMP-dependent inhibition of platelet aggregation and thrombus formation. Blood. 109:552-9.

108. Dangel O, Mergia E, Karlisch K, Groneberg D, Koesling D, Friebe A. (2010) Nitric oxide-sensitive guanylyl cyclase is the only nitric oxide receptor mediating platelet inhibition. J ThrombHaemost. 8:1343-52.

109. Kim PK, Zamora R, Petrosko P, Billiar TR. (2001) The regulatory role of nitric oxide in apoptosis. Int Immunopharmacol. 1:1421-41.

110. Khan FH, Dervan E, Bhattacharyya DD, McAuliffe JD, Miranda KM, Glynn SA. (2020) The Role of Nitric Oxide in Cancer: Master Regulator or NOt? Int J Mol Sci. 21:9393.

111. Li J, Bombeck CA, Yang S, Kim YM, Billiar TR. (1999) Nitric oxide suppresses apoptosis via interrupting caspase activation and mitochondrial dysfunction in cultured hepatocytes. J Biol Chem. 274:17325-33.

112. Li J, Billiar TR, Talanian RV, Kim YM. (1997) Nitric oxide reversibly inhibits seven members of the caspase family via *S*-nitrosylation. Biochem Biophys Res Commun. 240:419-24.

113. Azad N, Vallyathan V, Wang L, Tantishaiyakul V, Stehlik C, Leonard SS, Rojanasakul Y. (2006) *S*-nitrosylation of Bcl-2 inhibits its ubiquitin-proteasomal degradation. A novel antiapoptotic mechanism that suppresses apoptosis. J Biol Chem. 281:34124-34.

114. De Nadai C, Sestili P, Cantoni O, Lièvremont JP, Sciorati C, Barsacchi R, Moncada S, Meldolesi J, Clementi E. (2000) Nitric oxide inhibits tumor necrosis factor-alpha-induced apoptosis by reducing the generation of ceramide. Proc Natl Acad Sci U S A. 97:5480-5.

115. Brookes PS, Salinas EP, Darley-Usmar K, Eiserich JP, Freeman BA, (2000) Darley-Usmar VM, Anderson PG. Concentration-dependent effects of nitric oxide on mitochondrial permeability transition and cytochrome *c* release. J Biol Chem. 275:20474-9.

116. Nasuno R, Aitoku M, Manago Y, Nishimura A, Sasano Y, Takagi H. (2014) Nitric oxide-mediated antioxidative mechanism in yeast through the activation of the transcription factor Mac1. PLoS One. 9:e113788.

117. Astuti RI, Watanabe D, Takagi H. (2016) Nitric oxide signaling and its role in oxidative stress response in *Schizosaccharomycespombe*. Nitric Oxide. 52:29-40.

118. Osório NS, Carvalho A, Almeida AJ, Padilla-Lopez S, Leão C, Laranjinha J, Ludovico P, Pearce DA, Rodrigues F. (2007) Nitric oxide signaling is disrupted in the yeast model for Batten disease. Mol Biol Cell. 18:2755-67.

119. Kato T, Zhou X, Ma Y. (2013) Possible involvement of nitric oxide and reactive oxygen species in glucose deprivation-induced activation of transcription factor rst2. PLoS One. 8:e78012.

120. Li B, Skinner C, Castello PR, Kato M, Easlon E, Xie L, Li T, Lu SP, Wang C, Tsang F, Poyton RO, Lin SJ. (2011) Identification of potential calorie restriction-mimicking yeast mutants with increased mitochondrial respiratory chain and nitric oxide levels. J Aging Res. 2011:673185.

121. Dedon PC, Tannenbaum SR. (2004) Reactive nitrogen species in the chemical biology of inflammation. Arch Biochem Biophys. 423:12-22.

122. Chen B, Deen WM. (2001) Analysis of the effects of cell spacing and liquid depth on nitric oxide and its oxidation products in cell cultures. Chem Res Toxicol. 14:135-47.

123. Caulfield JL, Singh SP, Wishnok JS, Deen WM, Tannenbaum SR. (1996) Bicarbonate inhibits N-nitrosation in oxygenated nitric oxide solutions. J Biol Chem. 271:25859-63.

124. Lewis RS, Deen WM. (1994) Kinetics of the reaction of nitric oxide with oxygen in aqueous solutions. Chem Res Toxicol. 7:568-74.

125. Licht WR, Tannenbaum SR, Deen WM. (1988) Use of ascorbic acid to inhibit nitrosation: kinetic and mass transfer considerations for an in vitro system. Carcinogenesis. 9:365-72.

126. Caulfield JL, Singh SP, Wishnok JS, Deen WM, Tannenbaum SR. (1996) Bicarbonate inhibits N-nitrosation in oxygenated nitric oxide solutions. J Biol Chem. 271:25859-63.

127. Huie RE, Padmaja S. (1993) The reaction of no with superoxide. Free Radic Res Commun. 18:195-9.

128. Kissner R, Nauser T, Bugnon P, Lye PG, Koppenol WH. (1997) Formation and properties of peroxynitrite as studied by laser flash photolysis, high-pressure stopped-flow technique, and pulse radiolysis. Chem Res Toxicol. 10:1285-92.

129. Nauser T, Koppenol WH. (2002) The Rate Constant of the Reaction of Superoxide with Nitrogen Monoxide: Approaching the Diffusion Limit. J PhysChem A.106:4084-4086.

130. Fielden EM, Roberts PB, Bray RC, Lowe DJ, Mautner GN, Rotilio G, Calabrese L. (1974) Mechanism of action of superoxide dismutase from pulse

radiolysis and electron paramagnetic resonance. Evidence that only half the active sites function in catalysis. Biochem J. 139:49-60.

131. Hughes MN, Nicklin HG. (1968) The Chemistry of Pernitrites. Part 1. Kinetics of Decomposition of Pernitrous Acid. J Chem Soc. 450–52.

132. Gerasimov OV, Lymar SV. (1999) The yield of hydroxyl radical from the decomposition of peroxynitrous acid. Inorg Chem. 38:4317-21.

133. Radi R, Cosgrove TP, Beckman JS, Freeman BA. (1993) Peroxynitrite-induced luminolchemiluminescence. Biochem J. 290:51-7.

134. Lymar SV, Jiang Q, Hurst JK. (1996) Mechanism of carbon dioxide-catalyzed oxidation of tyrosine by peroxynitrite. Biochemistry. 35:7855-61.

135. Augusto O, Bonini MG, Amanso AM, Linares E, Santos CC, De Menezes SL. (2002) Nitrogen dioxide and carbonate radical anion: two emerging radicals in biology. Free RadicBiol Med. 32:841-59.

136. Serrano R, Garrido N, Céspedes JA, González-Fernández L, García-Marín LJ, Bragado MJ. (2020) Molecular Mechanisms Involved in the Impairment of Boar Sperm Motility by Peroxynitrite-Induced Nitrosative Stress. Int J Mol Sci. 21:1208.

137. Condeles AL, Gomes F, de Oliveira MA, Soares Netto LE, Toledo Junior JC. (2020) Thiol Peroxidases as Major Regulators of Intracellular Levels of Peroxynitrite in Live *Saccharomyces cerevisiae* Cells. Antioxidants (Basel). 9:434.

138. Zhang Y, Hogg N. (2005) *S*-Nitrosothiols: cellular formation and transport. Free Radic Biol Med. 38:831-8.

139. Smith BC, Marletta MA. (2012) Mechanisms of *S*-nitrosothiol formation and selectivity in nitric oxide signaling. Curr Opin Chem Biol. 16:498-506.

140. Möller MN, Li Q, Vitturi DA, Robinson JM, Lancaster JR Jr, Denicola A. (2007) Membrane "lens" effect: focusing the formation of reactive nitrogen oxides from the $^*NO/O_2$ reaction. Chem Res Toxicol. 20:709-14.

141. Keszler A, Zhang Y, Hogg N. (2010) Reaction between nitric oxide, glutathione, and oxygen in the presence and absence of protein: How are *S*-nitrosothiols formed? Free Radic Biol Med. 48:55-64.

142. Wang PG, Xian M, Tang X, Wu X, Wen Z, Cai T, Janczuk AJ. (2002) Nitric oxide donors: chemical activities and biological applications. Chem Rev. 102:1091-134.

143. Broniowska KA, Diers AR, Hogg N. (2013) *S*-nitrosoglutathione. Biochim Biophys Acta. 1830:3173-81.

144. Klandorf H, Dyke KV (2012) Oxidative and nitrosative stresses: their role in health and disease in man and birds. J Ag & Bio Sci 3: 47-59.

145. Patra SK, Bag PK, Ghosh S. (2017) Nitrosative Stress Response in Vibrio cholerae: Role of *S*-Nitrosoglutathione Reductase. Appl Biochem Biotechnol. 182:871-884.

146. D'Autreaux B, Touati D, Bersch B, Latour JM, Michaud-Soret I. (2002) Direct inhibition by nitric oxide of the transcriptional ferric uptake regulation protein via nitrosylation of the iron. Proc Natl Acad Sci U S A. 99:16619-24.

147. Hausladen A, Privalle CT, Keng T, DeAngelo J, Stamler JS. (1996) Nitrosative stress: activation of the transcription factor OxyR. Cell. 86:719-29.

148. Corpas FJ, Leterrier M, Valderrama R, Airaki M, Chaki M, Palma JM, Barroso JB. (2011) Nitric oxide imbalance provokes a nitrosative response in plants under abiotic stress. Plant Sci. 181:604-11.

149. Patra SK, Samaddar S, Sinha N, Ghosh S. (2019) Reactive nitrogen species induced catalases promote a novel nitrosative stress tolerance mechanism in Vibrio cholerae. Nitric Oxide. 88:35-44.

150. Reiter TA. (2006) NO* chemistry: a diversity of targets in the cell. Redox Rep. 11:194-206.

151. Wink DA, Mitchell JB. (1998) Chemical biology of nitric oxide: Insights into regulatory, cytotoxic, and cytoprotective mechanisms of nitric oxide. Free Radic Biol Med.25:434-56.

152. Dong M, Wang C, Deen WM, Dedon PC. (2003) Absence of 2'-deoxyoxanosine and presence of abasic sites in DNA exposed to nitric oxide at controlled physiological concentrations. Chem Res Toxicol. 16:1044-55.

153. Dong M, Dedon PC. (2006) Relatively small increases in the steady-state levels of nucleobase deamination products in DNA from human TK6 cells exposed to toxic levels of nitric oxide. Chem Res Toxicol. 19:50-7.

154. Lim KS, Huang SH, Jenner A, Wang H, Tang SY, Halliwell B. (2006) Potential artifacts in the measurement of DNA deamination. Free Radic Biol Med. 40:1939-48.

155. Wink DA, Hanbauer I, Grisham MB, Laval F, Nims RW, Laval J, Cook J, Pacelli R, Liebmann J, Krishna M, Ford PC, Mitchell JB. (1996) Chemical biology of nitric oxide: regulation and protective and toxic mechanisms. Curr Top Cell Regul. 34:159-87.

156. Tretyakova NY, Burney S, Pamir B, Wishnok JS, Dedon PC, Wogan GN, Tannenbaum SR. (2000) Peroxynitrite-induced DNA damage in the supF gene: correlation with the mutational spectrum. Mutat Res. 447:287-303.

157. Yermilov V, Rubio J, Becchi M, Friesen MD, Pignatelli B, Ohshima H. (1995) Formation of 8-nitroguanine by the reaction of guanine with peroxynitrite in vitro. Carcinogenesis. 16:2045-50.

158. Burney S, Caulfield JL, Niles JC, Wishnok JS, Tannenbaum SR. (1999) The chemistry of DNA damage from nitric oxide and peroxynitrite. Mutat Res. 424:37-49.

159. Spencer JP, Wong J, Jenner A, Aruoma OI, Cross CE, Halliwell B. (1996) Base modification and strand breakage in isolated calf thymus DNA and in DNA from human skin epidermal keratinocytes exposed to peroxynitrite or 3-morpholinosydnonimine. Chem Res Toxicol. 9:1152-8.

160. Johansen ME, Muller JG, Xu X, Burrows CJ. (2005) Oxidatively induced DNA-protein cross-linking between single-stranded binding protein and oligodeoxynucleotides containing 8-oxo-7,8-dihydro-2'-deoxyguanosine. Biochemistry. 44:5660-71.

161. Shapiro R, Dubelman S, Feinberg AM, Crain PF, McCloskey JA. (1977) Isolation and identification of cross-linked nucleosides from nitrous acid treated deoxyribonucleic acid. J Am Chem Soc. 99:302-3.

162. Laval F, Wink DA, Laval J. (1997) A discussion of mechanisms of NO genotoxicity: implication of inhibition of DNA repair proteins. Rev Physiol Biochem Pharmacol. 131:175-91.

163. Wink DA, Laval J. (1994) The Fpg protein, a DNA repair enzyme, is inhibited by the biomediator nitric oxide in vitro and in vivo. Carcinogenesis. 15:2125-9.

164. Kwon NS, Stuehr DJ, Nathan CF. (1991) Inhibition of tumor cell ribonucleotide reductase by macrophage-derived nitric oxide. J Exp Med. 174:761-7.

165. Lepoivre M, Chenais B, Yapo A, Lemaire G, Thelander L, Tenu JP. (1990) Alterations of ribonucleotide reductase activity following induction of the nitrite-generating pathway in adenocarcinoma cells. J Biol Chem. 265:14143-9.

166. Hogg N, Kalyanaraman B. (1999) Nitric oxide and lipid peroxidation. Biochim Biophys Acta. 1411:378-84.

167. Bloodsworth A, O'Donnell VB, Freeman BA. (2000) Nitric oxide regulation of free radical- and enzyme-mediated lipid and lipoprotein oxidation. Arterioscler Thromb Vasc Biol. 20:1707-15.

168. Laskey RE, Mathews WR. (1996) Nitric oxide inhibits peroxynitrite-induced production of hydroxyeicosatetraenoic acids and F2-isoprostanes in phosphatidylcholine liposomes. Arch Biochem Biophys. 330:193-8.

169. Goss SP, Hogg N, Kalyanaraman B. (1995) The antioxidant effect of spermine NONOate in human low-density lipoprotein. Chem Res Toxicol. 8:800-6.

170. Hogg N, Struck A, Goss SP, Santanam N, Joseph J, Parthasarathy S, Kalyanaraman B. (1995) Inhibition of macrophage-dependent low density lipoprotein oxidation by nitric-oxide donors. J Lipid Res. 36:1756-62.

171. Malo-Ranta U, Ylä-Herttuala S, Metsä-Ketelä T, Jaakkola O, Moilanen E, Vuorinen P, Nikkari T. (1994) Nitric oxide donor GEA 3162 inhibits

endothelial cell-mediated oxidation of low density lipoprotein. FEBS Lett. 337:179-83.

172. Hayashi K, Noguchi N, Niki E. (1995) Action of nitric oxide as an antioxidant against oxidation of soybean phosphatidylcholine liposomal membranes. FEBS Lett. 370:37-40.

173. Korytowski W, Zareba M, Girotti AW. (2000) Nitric oxide inhibition of free radical-mediated cholesterol peroxidation in liposomal membranes. Biochemistry. 39:6918-28.

174. O'Donnell VB, Chumley PH, Hogg N, Bloodsworth A, Darley-Usmar VM, Freeman BA. (1997) Nitric oxide inhibition of lipid peroxidation: kinetics of reaction with lipid peroxyl radicals and comparison with alpha-tocopherol. Biochemistry. 36:15216-23.

175. Gallon AA, Pryor WA. (1994) The reaction of low levels of nitrogen dioxide with methyl linoleate in the presence and absence of oxygen. Lipids. 29:171-6.

176. Kamel AM, Weiner WD, Felmeister A. (1971) Identification of cholesteryl nitrate as a product of the reaction between NO 2 and cholesterol monomolecular films. Chem Phys Lipids. 6:225-34.

177. Kikugawa K, Beppu M, Okamoto Y. (1995) Uptake by macrophages of low-density lipoprotein damaged by nitrogen dioxide in air. Lipids. 30:313-20.

178. Napolitano A, Camera E, Picardo M, d'Ischia M. (2000) Acid-promoted reactions of ethyl linoleate with nitrite ions: formation and structural characterization of isomeric nitroalkene, nitrohydroxy, and novel 3-nitro-1,5-hexadiene and 1,5-dinitro-1, 3-pentadiene products. J Org Chem. 65:4853-60.

179. Khairutdinov RF, Coddington JW, Hurst JK. (2000) Permeation of phospholipid membranes by peroxynitrite. Biochemistry. 39:14238-49.

180. Khairutdinov RF, Coddington JW, Hurst JK. (2000) Permeation of phospholipid membranes by peroxynitrite. Biochemistry. 39:14238-49.

181. O'Donnell VB, Taylor KB, Parthasarathy S, Kühn H, Koesling D, Friebe A, Bloodsworth A, Darley-Usmar VM, Freeman BA. (1999) 15-Lipoxygenase

catalytically consumes nitric oxide and impairs activation of guanylate cyclase. J Biol Chem. 274:20083-91.

182. Trostchansky A, Batthyány C, Botti H, Radi R, Denicola A, Rubbo H. (2001) Formation of lipid-protein adducts in low-density lipoprotein by fluxes of peroxynitrite and its inhibition by nitric oxide. Arch Biochem Biophys. 395:225-32.

183. Xie Y, Luo X, Li Y, Chen L, Ma W, Huang J, Cui J, Zhao Y, Xue Y, Zuo Z, Ren J. (2018) DeepNitro: Prediction of Protein Nitration and Nitrosylation Sites by Deep Learning. Genomics Proteomics Bioinformatics. 16:294-306.

184. Hess DT, Matsumoto A, Kim SO, Marshall HE, Stamler JS. (2005) Protein *S*-nitrosylation: purview and parameters. Nat Rev Mol Cell Biol. 6:150-66.

185. Hill BG, Dranka BP, Bailey SM, Lancaster JR Jr, Darley-Usmar VM. (2010) What part of NO don't you understand? Some answers to the cardinal questions in nitric oxide biology. J Biol Chem. 285:19699-704.

186. Smith BC, Marletta MA. (2012) Mechanisms of *S*-nitrosothiol formation and selectivity in nitric oxide signaling. Curr Opin Chem Biol. 16:498-506.

187. Martínez-Ruiz A, Cadenas S, Lamas S. (2011) Nitric oxide signaling: classical, less classical, and nonclassical mechanisms. Free Radic Biol Med. 51:17-29.

188. Gould N, Doulias PT, Tenopoulou M, Raju K, Ischiropoulos H. (2013) Regulation of protein function and signaling by reversible cysteine *S*-nitrosylation. J Biol Chem. 288:26473-9.

189. Hess DT, Stamler JS. (2012) Regulation by *S*-nitrosylation of protein post-translational modification. J Biol Chem. 287:4411-8.

190. Kornberg MD, Sen N, Hara MR, Juluri KR, Nguyen JV, Snowman AM, Law L, Hester LD, Snyder SH. (2010) GAPDH mediates nitrosylation of nuclear proteins. Nat Cell Biol. 12:1094-100.

191. Nakamura T, Lipton SA. (2013) Emerging role of protein-protein transnitrosylation in cell signaling pathways. Antioxid Redox Signal. 18:239-49.

192. Sengupta R, Holmgren A. (2013) Thioredoxin and thioredoxin reductase in relation to reversible *S*-nitrosylation. Antioxid Redox Signal. 18:259-69.

193. Martínez-Ruiz A, Araújo IM, Izquierdo-Álvarez A, Hernansanz-Agustín P, Lamas S, Serrador JM. (2013) Specificity in *S*-nitrosylation: a short-range mechanism for NO signaling? Antioxid Redox Signal. 19:1220-35.

194. Lamotte O, Bertoldo JB, Besson-Bard A, Rosnoblet C, Aimé S, Hichami S, Terenzi H, Wendehenne D. (2015) Protein *S*-nitrosylation: specificity and identification strategies in plants. Front Chem. 2:114.

195. Prime TA, Blaikie FH, Evans C, Nadtochiy SM, James AM, Dahm CC, Vitturi DA, Patel RP, Hiley CR, Abakumova I, Requejo R, Chouchani ET, Hurd TR, Garvey JF, Taylor CT, Brookes PS, Smith RA, Murphy MP. (2009) A mitochondria-targeted *S*-nitrosothiol modulates respiration, nitrosates thiols, and protects against ischemia-reperfusion injury. Proc Natl Acad Sci U S A. 106:10764-9.

196. Di Virgilio F, Azzone GF. (1982) Activation of site I redox-driven H+ pump by exogenous quinones in intact mitochondria. J Biol Chem. 257:4106-13.

197. Vinogradov AD. (1998) Catalytic properties of the mitochondrial NADH-ubiquinone oxidoreductase (complex I) and the pseudo-reversible active/inactive enzyme transition. Biochim Biophys Acta. 1364:169-85.

198. Mohr S, Hallak H, de Boitte A, Lapetina EG, Brüne B. (1999) Nitric oxide-induced S-glutathionylation and inactivation of glyceraldehyde-3-phosphate dehydrogenase. J Biol Chem. 274:9427-30.

199. Piantadosi CA. (2012) Regulation of mitochondrial processes by protein *S*-nitrosylation. Biochim Biophys Acta. 1820:712-21.

200. Chen YJ, Lu CT, Su MG, Huang KY, Ching WC, Yang HH, Liao YC, Chen YJ, Lee TY. (2015) dbSNO 2.0: a resource for exploring structural environment, functional and disease association and regulatory network of protein *S*-nitrosylation. Nucleic Acids Res. 43:D503-11.

201. Abello N, Kerstjens HA, Postma DS, Bischoff R. (2009) Protein tyrosine nitration: selectivity, physicochemical and biological consequences,

denitration, and proteomics methods for the identification of tyrosine-nitrated proteins. J Proteome Res. 8:3222-38.

202. Bian K, Gao Z, Weisbrodt N, Murad F. (2003) The nature of heme/iron-induced protein tyrosine nitration. Proc Natl Acad Sci U S A. 100:5712-7.

203. Bhattacharjee A, Majumdar U, Maity D, Sarkar TS, Goswami AM, Sahoo R, Ghosh S. (2009) In vivo protein tyrosine nitration in S. cerevisiae: identification of tyrosine-nitrated proteins in mitochondria. Biochem Biophys Res Commun. 388:612-7.

204. Souza JM, Daikhin E, Yudkoff M, Raman CS, Ischiropoulos H. (1999) Factors determining the selectivity of protein tyrosine nitration. Arch Biochem Biophys. 371:169-78.

205. Radi R. (2013) Protein tyrosine nitration: biochemical mechanisms and structural basis of functional effects. Acc Chem Res. 46:550-9.

206. Radi R. (2018) Oxygen radicals, nitric oxide, and peroxynitrite: Redox pathways in molecular medicine. Proc Natl Acad Sci U S A. 5:5839-5848.

207. Sokolovsky M, Riordan JF, Vallee BL. (1967) Conversion of 3-nitrotyrosine to 3-aminotyrosine in peptides and proteins. Biochem Biophys Res Commun. 27:20-5.

208. Heijnen HF, van Donselaar E, Slot JW, Fries DM, Blachard-Fillion B, Hodara R, Lightfoot R, Polydoro M, Spielberg D, Thomson L, Regan EA, Crapo J, Ischiropoulos H. (2006) Subcellular localization of tyrosine-nitrated proteins is dictated by reactive oxygen species generating enzymes and by proximity to nitric oxide synthase. Free Radic Biol Med. 40:1903-13.

209. Ferrer-Sueta G, Campolo N, Trujillo M, Bartesaghi S, Carballal S, Romero N, Alvarez B, Radi R. (2018) Biochemistry of Peroxynitrite and Protein Tyrosine Nitration. Chem Rev. 118:1338-1408.

210. Osoata GO, Yamamura S, Ito M, Vuppusetty C, Adcock IM, Barnes PJ, Ito K. (2009) Nitration of distinct tyrosine residues causes inactivation of histone deacetylase 2. Biochem Biophys Res Commun. 384:366-71.

211. Begara-Morales JC, Sánchez-Calvo B, Chaki M, Valderrama R, Mata-Pérez C, López-Jaramillo J, Padilla MN, Carreras A, Corpas FJ, Barroso JB. (2014)

Dual regulation of cytosolic ascorbate peroxidase (APX) by tyrosine nitration and *S*-nitrosylation. J Exp Bot. 65:527-38.

212. Moreno DM, Martí MA, De Biase PM, Estrin DA, Demicheli V, Radi R, Boechi L. (2011) Exploring the molecular basis of human manganese superoxide dismutase inactivation mediated by tyrosine 34 nitration. Arch Biochem Biophys. 507:304-9.

213. Monteiro HP, Arai RJ, Travassos LR. (2008) Protein tyrosine phosphorylation and protein tyrosine nitration in redox signaling. Antioxid Redox Signal. 10:843-89.

214. Kong SK, Yim MB, Stadtman ER, Chock PB. (1996) Peroxynitrite disables the tyrosine phosphorylation regulatory mechanism: Lymphocyte-specific tyrosine kinase fails to phosphorylate nitrated cdc2(6-20)NH2 peptide. Proc Natl Acad Sci U S A. 93:3377-82.

215. Brito C, Naviliat M, Tiscornia AC, Vuillier F, Gualco G, Dighiero G, Radi R, Cayota AM. (1999) Peroxynitrite inhibits T lymphocyte activation and proliferation by promoting impairment of tyrosine phosphorylation and peroxynitrite-driven apoptotic death. J Immunol. 162:3356-66.

216. Brockhaus F, Brüne B. (1999) p53 accumulation in apoptotic macrophages is an energy demanding process that precedes cytochrome *c* release in response to nitric oxide. Oncogene. 18:6403-10.

217. Nishio E, Watanabe Y. (1997) Nitric oxide donor-induced apoptosis in smooth muscle cells is modulated by protein kinase C and protein kinase A. Eur J Pharmacol. 339:245-51.

218. Estévez AG, Crow JP, Sampson JB, Reiter C, Zhuang Y, Richardson GJ, Tarpey MM, Barbeito L, Beckman JS. (1999) Induction of nitric oxide-dependent apoptosis in motor neurons by zinc-deficient superoxide dismutase. Science. 286:2498-500.

219. Hortelano S, Alvarez AM, Boscá L. (1999) Nitric oxide induces tyrosine nitration and release of cytochrome *c* preceding an increase of mitochondrial transmembrane potential in macrophages. FASEB J. 13:2311-7.

220. Almeida B, Buttner S, Ohlmeier S, Silva A, Mesquita A, Sampaio-Marques B, Osório NS, Kollau A, Mayer B, Leão C, Laranjinha J, Rodrigues F, Madeo F, Ludovico P. (2007) NO-mediated apoptosis in yeast. J Cell Sci. 120:3279-88.

221. Hortelano S, Dallaporta B, Zamzami N, Hirsch T, Susin SA, Marzo I, Boscá L, Kroemer G. (1997) Nitric oxide induces apoptosis via triggering mitochondrial permeability transition. FEBS Lett. 410:373-7.

222. Erusalimsky JD, Moncada S. (2007) Nitric oxide and mitochondrial signaling: from physiology to pathophysiology. Arterioscler Thromb Vasc Biol. 27:2524-31.

223. Kwun MS, Lee DG. (2020) An Insight on the Role of Nitric Oxide in Yeast Apoptosis of Curcumin-Treated *Candida albicans*. Curr Microbiol. 77:3104-3113.

224. Brüne B, von Knethen A, Sandau KB. (1998) Nitric oxide and its role in apoptosis. Eur J Pharmacol. 351:261-72.

225. Messmer UK, Brüne B. (1996) Nitric oxide (NO) in apoptotic versus necrotic RAW 264.7 macrophage cell death: the role of NO-donor exposure, NAD+ content, and p53 accumulation. Arch Biochem Biophys. 327:1-10.

226. Liebermann DA, Hoffman B, Steinman RA. (1995) Molecular controls of growth arrest and apoptosis: p53-dependent and independent pathways. Oncogene. 11:199-210.

227. Shankland SJ. (1997) Cell-cycle control and renal disease. Kidney Int. 52:294-308.

228. Ambs S, Hussain SP, Marrogi AJ, Harris CC. (1999) Cancer-prone oxyradical overload disease. IARC Sci Publ. 150:295-302.

229. Moncada S, Higgs A. (1993) The L-arginine-nitric oxide pathway. N Engl J Med. 329:2002-12.

230. Ignarro LJ. (1990) Biosynthesis and metabolism of endothelium-derived nitric oxide. Annu Rev Pharmacol Toxicol 30:535-60.

231. Jun CD, Oh CD, Kwak HJ, Pae HO, Yoo JC, Choi BM, Chun JS, Park RK, Chung HT. (1999) Overexpression of protein kinase C isoforms protects RAW

264.7 macrophages from nitric oxide-induced apoptosis: involvement of c-Jun N-terminal kinase/stress-activated protein kinase, p38 kinase, and CPP-32 protease pathways. J Immunol. 162:3395-401.

232. Oh-hashi K, Maruyama W, Yi H, Takahashi T, Naoi M, Isobe K. (1999) Mitogen-activated protein kinase pathway mediates peroxynitrite-induced apoptosis in human dopaminergic neuroblastoma SH-SY5Y cells. Biochem Biophys Res Commun. 263:504-9.

233. Steptoe A, Zaninotto P. (2020) Lower socioeconomic status and the acceleration of aging: An outcome-wide analysis. Proc Natl Acad Sci U S A. 117:14911-7.

234. Kaeberlein M, Burtner CR, Kennedy BK. (2007) Recent developments in yeast aging. PLoS Genet. 3:e84.

235. Steinkraus KA, Kaeberlein M, Kennedy BK. (2008) Replicative aging in yeast: the means to the end. Annu Rev Cell Dev Biol. 24:29-54.

236. Dawes IW, Perrone GG. (2020) Stress and ageing in yeast. FEMS Yeast Res. 20:foz085.

237. Fabrizio P, Longo VD. (2003) The chronological life span of *Saccharomyces cerevisiae*. Aging Cell. 2:73-81.

238. Kaeberlein M. (2006) Longevity and aging in the budding yeast. In: Conn PM, editor. Handbook of models for human aging. Boston: Elvesier Press. pp. 109–120

239. Breitenbach M, Laun P, Dickinson JR, Klocker A, Rinnerthaler M, Dawes IW, Aung-Htut MT, Breitenbach-Koller L, Caballero A, Nyström T, Büttner S, Eisenberg T, Madeo F, Ralser M. (2012) The role of mitochondria in the aging processes of yeast. Subcell Biochem. 57:55-78.

240. Kominsky DJ, Thorsness PE. (2000) Expression of the Saccharomyces cerevisiae gene YME1 in the petite-negative yeast Schizosaccharomyces pombe converts it to petite-positive. Genetics. 154:147-54.

241. Mandavilli BS, Santos JH, Van Houten B. (2002) Mitochondrial DNA repair and aging. Mutat Res. 509:127-51.

242. Lin SJ, Kaeberlein M, Andalis AA, Sturtz LA, Defossez PA, Culotta VC, Fink GR, Guarente L. (2002) Calorie restriction extends Saccharomyces cerevisiae lifespan by increasing respiration. Nature. 418:344-8.

243. Powers T, Walter P. (1999) Regulation of ribosome biogenesis by the rapamycin-sensitive TOR-signaling pathway in *Saccharomyces cerevisiae*. Mol Biol Cell. 10:987-1000.

244. Kaeberlein M, Powers RW 3rd, Steffen KK, Westman EA, Hu D, Dang N, Kerr EO, Kirkland KT, Fields S, Kennedy BK. (2005) Regulation of yeast replicative life span by TOR and Sch9 in response to nutrients. Science. 310:1193-6.

245. Smith A, Ward MP, Garrett S. (1998) Yeast PKA represses Msn2p/Msn4p-dependent gene expression to regulate growth, stress response and glycogen accumulation. EMBO J. 17:3556-64.

246. Longo VD. (2003) The Ras and Sch9 pathways regulate stress resistance and longevity. Exp Gerontol. 38:807-11.

247. Takeda E, Jin N, Itakura E, Kira S, Kamada Y, Weisman LS, Noda T, Matsuura A. (2018) Vacuole-mediated selective regulation of TORC1-Sch9 signaling following oxidative stress. Mol Biol Cell. 29:510-522.

248. Trendeleva TA, Zvyagilskaya RA. (2018) Retrograde Signaling as a Mechanism of Yeast Adaptation to Unfavorable Factors. Biochemistry (Mosc). 83:98-106.

249. Dilova I, Chen CY, Powers T. (2002) Mks1 in concert with TOR signaling negatively regulates RTG target gene expression in *S. cerevisiae*. Curr Biol. 12:389-95.

250. Powers T, Dilova I, Chen CY, Wedaman K. (2004) Yeast TOR signaling: a mechanism for metabolic regulation. Curr Top Microbiol Immunol. 279:39-51.

251. Yorimitsu T, Klionsky DJ. (2005) Autophagy: molecular machinery for self-eating. Cell Death Differ. 12:1542-52.

252. Noda T, Ohsumi Y. (1998) Tor, a phosphatidylinositol kinase homologue, controls autophagy in yeast. J Biol Chem. 273:3963-6.

253. Kamada Y, Sekito T, Ohsumi Y. (2004) Autophagy in yeast: a TOR-mediated response to nutrient starvation. Curr Top Microbiol Immunol. 279:73-84.

254. Turi Z, Lacey M, Mistrik M, Moudry P. (2019) Impaired ribosome biogenesis: mechanisms and relevance to cancer and aging. Aging (Albany NY). 11:2512-2540.

255. Buchwalter A, Hetzer MW. (2017) Nucleolar expansion and elevated protein translation in premature aging. Nat Commun. 8:328.

256. Tiku V, Antebi A. (2018) Nucleolar Function in Lifespan Regulation. Trends Cell Biol. Aug;28:662-672.

257. Helmrich A, Ballarino M, Tora L. (2011) Collisions between replication and transcription complexes cause common fragile site instability at the longest human genes. Mol Cell. 44:966-77.

258. Lill R. (2009) Function and biogenesis of iron-sulphur proteins. Nature. 460:831-8.

259. Lewinska A, Macierzynska E, Grzelak A, Bartosz G. (2011) A genetic analysis of nitric oxide-mediated signaling during chronological aging in the yeast. Biogerontology. 12:309-20.

260. Fabrizio P, Liou LL, Moy VN, Diaspro A, Valentine JS, Gralla EB, Longo VD. (2003) SOD2 functions downstream of Sch9 to extend longevity in yeast. Genetics. 163:35-46.

261. Hou Y, Dan X, Babbar M, Wei Y, Hasselbalch SG, Croteau DL, Bohr VA. (2019) Ageing as a risk factor for neurodegenerative disease. Nat Rev Neurol. 15:565-581.

262. Patel A, Lee HO, Jawerth L, Maharana S, Jahnel M, Hein MY, Stoynov S, Mahamid J, Saha S, Franzmann TM, Pozniakovski A, Poser I, Maghelli N, Royer LA, Weigert M, Myers EW, Grill S, Drechsel D, Hyman AA, Alberti S. (2015) A Liquid-to-Solid Phase Transition of the ALS Protein FUS Accelerated by Disease Mutation. Cell. 162:1066-77.

263. Maiuri T, Suart CE, Hung CLK, Graham KJ, Barba Bazan CA, Truant R. (2019) DNA Damage Repair in Huntington's Disease and Other Neurodegenerative Diseases. Neurotherapeutics. 16:948-956.

264. Mangialasche F, Polidori MC, Monastero R, Ercolani S, Camarda C, Cecchetti R, Mecocci P. (2009) Biomarkers of oxidative and nitrosative damage in Alzheimer's disease and mild cognitive impairment. Ageing Res Rev. 8:285-305.

265. Price DL, Cork LC, Struble RG, Kitt CA, Walker LC, Powers RE, Whitehouse PJ, Griffin JW. (1987) Dysfunction and death of neurons in human degenerative neurological diseases and in animal models. Ciba Found Symp. 126:30-48.

266. Dalle-Donne I, Rossi R, Colombo R, Giustarini D, Milzani A. (2006) Biomarkers of oxidative damage in human disease. Clin Chem. 52:601-23.

267. Shishehbor MH, Aviles RJ, Brennan ML, Fu X, Goormastic M, Pearce GL, Gokce N, Keaney JF Jr, Penn MS, Sprecher DL, Vita JA, Hazen SL. (2003) Association of nitrotyrosine levels with cardiovascular disease and modulation by statin therapy. JAMA. 289:1675-80.

268. Bloom GS. (2014) Amyloid-β and tau: the trigger and bullet in Alzheimer disease pathogenesis. JAMA Neurol. 71:505-8.

269. Goedert M, Spillantini MG, Jakes R, Rutherford D, Crowther RA. (1989) Multiple isoforms of human microtubule-associated protein tau: sequences and localization in neurofibrillary tangles of Alzheimer's disease. Neuron. 3:519-26.

270. Reynolds MR, Berry RW, Binder LI. (2005)Site-specific nitration differentially influences tau assembly in vitro. Biochemistry. 44:13997-4009.

271. Gamblin TC, Chen F, Zambrano A, Abraha A, Lagalwar S, Guillozet AL, Lu M, Fu Y, Garcia-Sierra F, LaPointe N, Miller R, Berry RW, Binder LI, Cryns VL. (2003) Caspase cleavage of tau: linking amyloid and neurofibrillary tangles in Alzheimer's disease. Proc Natl Acad Sci U S A. 100:10032-7.

272. Chen X, Yan SD. (2006) Mitochondrial Abeta: a potential cause of metabolic dysfunction in Alzheimer's disease. IUBMB Life 58:686-94.

273. Crouch PJ, White AR, Bush AI. (2007) The modulation of metal bio-availability as a therapeutic strategy for the treatment of Alzheimer's disease. FEBS J. 274:3775-83.

274. Lovell MA, Robertson JD, Teesdale WJ, Campbell JL, Markesbery WR. (1998) Copper, iron and zinc in Alzheimer's disease senile plaques. J Neurol Sci. 158:47-52.

275. Moreira PI, Nunomura A, Nakamura M, Takeda A, Shenk JC, Aliev G, Smith MA, Perry G. (2008) Nucleic acid oxidation in Alzheimer disease. Free Radic Biol Med. 44:1493-505.

276. Dröge W. (2002) Free radicals in the physiological control of cell function. Physiol Rev. 82:47-95.

277. Schopfer FJ, Baker PR, Freeman BA. (2003) NO-dependent protein nitration: a cell signaling event or an oxidative inflammatory response? Trends Biochem Sci. 28:646-54.

278. Rizor A, Pajarillo E, Johnson J, Aschner M, Lee E. (2019) Astrocytic Oxidative/Nitrosative Stress Contributes to Parkinson's Disease Pathogenesis: The Dual Role of Reactive Astrocytes. Antioxidants (Basel). 8:265.

279. Muñoz E, Oliva R, Obach V, Martí MJ, Pastor P, Ballesta F, Tolosa E. (1997) Identification of Spanish familial Parkinson's disease and screening for the Ala53Thr mutation of the alpha-synuclein gene in early onset patients. Neurosci Lett. 235:57-60.

280. Tsang AH, Chung KK. (2009) Oxidative and nitrosative stress in Parkinson's disease. Biochim Biophys Acta. 1792:643-50.

281. Chinta SJ, Andersen JK. (2008) Redox imbalance in Parkinson's disease. Biochim Biophys Acta. 1780:1362-7.

282. McBean GJ. (2017) Cysteine, Glutathione, and Thiol Redox Balance in Astrocytes. Antioxidants (Basel). 6:62.

283. Beal MF. (1998) Excitotoxicity and nitric oxide in Parkinson's disease pathogenesis. Ann Neurol. 44:S110-4.

284. Giasson BI, Duda JE, Murray IV, Chen Q, Souza JM, Hurtig HI, Ischiropoulos H, Trojanowski JQ, Lee VM. (2000) Oxidative damage linked to neurodegeneration by selective alpha-synuclein nitration in synucleinopathy lesions. Science. Nov 290:985-9.

285. Chavarría C, Souza JM. (2013) Oxidation and nitration of α-synuclein and their implications in neurodegenerative diseases. Arch Biochem Biophys. 533:25-32.

286. Souza JM, Giasson BI, Chen Q, Lee VM, Ischiropoulos H. (2000) Dityrosine cross-linking promotes formation of stable alpha -synuclein polymers. Implication of nitrative and oxidative stress in the pathogenesis of neurodegenerative synucleinopathies. J Biol Chem. 275:18344-9.

287. Hodara R, Norris EH, Giasson BI, Mishizen-Eberz AJ, Lynch DR, Lee VM, Ischiropoulos H. (2004) Functional consequences of alpha-synuclein tyrosine nitration: diminished binding to lipid vesicles and increased fibril formation. J Biol Chem. 279:47746-53.

288. Benner EJ, Banerjee R, Reynolds AD, Sherman S, Pisarev VM, Tsiperson V, Nemachek C, Ciborowski P, Przedborski S, Mosley RL, Gendelman HE. (2008) Nitrated alpha-synuclein immunity accelerates degeneration of nigral dopaminergic neurons. PLoS One. 3:e1376.

289. Bassani TB, Vital MA, Rauh LK. (2015) Neuroinflammation in the pathophysiology of Parkinson's disease and therapeutic evidence of anti-inflammatory drugs. Arq Neuropsiquiatr. 73:616-23.

290. Dawson TM, Dawson VL. (2010) The role of parkin in familial and sporadic Parkinson's disease. Mov Disord. 1:S32-9.

291. Chung KK, Thomas B, Li X, Pletnikova O, Troncoso JC, Marsh L, Dawson VL, Dawson TM. (2004) *S*-nitrosylation of parkin regulates ubiquitination and compromises parkin's protective function. Science. 304:1328-31.

292. Yao D, Gu Z, Nakamura T, Shi ZQ, Ma Y, Gaston B, Palmer LA, Rockenstein EM, Zhang Z, Masliah E, Uehara T, Lipton SA. (2004) Nitrosative stress linked to sporadic Parkinson's disease: *S*-nitrosylation of parkin regulates its E3 ubiquitin ligase activity. Proc Natl Acad Sci U S A. 101:10810-4.

293. Waak J, Weber SS, Waldenmaier A, Görner K, Alunni-Fabbroni M, Schell H, Vogt-Weisenhorn D, Pham TT, Reumers V, Baekelandt V, Wurst W, Kahle PJ. (2009) Regulation of astrocyte inflammatory responses by the Parkinson's disease-associated gene DJ-1. FASEB J. 23:2478-89.

294. Boje KM. (2004) Nitric oxide neurotoxicity in neurodegenerative diseases. Front Biosci. 9:763-76.

295. Deckel AW. (2001) Nitric oxide and nitric oxide synthase in Huntington's disease. J Neurosci Res. 64:99-107.

296. Sugars KL, Rubinsztein DC. (2003) Transcriptional abnormalities in Huntington disease. Trends Genet. 19:233-8.

297. (1993) A novel gene containing a trinucleotide repeat that is expanded and unstable on Huntington's disease chromosomes. The Huntington's Disease Collaborative Research Group. Cell. 72:971-83.

298. Deckel AW, Gordinier A, Nuttal D, Tang V, Kuwada C, Freitas R, Gary KA. (2001) Reduced activity and protein expression of NOS in R6/2 HD transgenic mice: effects of L-NAME on symptom progression. Brain Res. 919:70-81.

299. Pérez-Severiano F, Escalante B, Vergara P, Ríos C, Segovia J. (2002) Age-dependent changes in nitric oxide synthase activity and protein expression in striata of mice transgenic for the Huntington's disease mutation. Brain Res. 951:36-42.

300. Deckel AW, Cohen D. (2000) Increased CBF velocity during word fluency in Huntington's disease patients. Prog Neuropsychopharmacol Biol Psychiatry. 24:193-206.

301. Ghasemi M, Mayasi Y, Hannoun A, Eslami SM, Carandang R. (2018) Nitric Oxide and Mitochondrial Function in Neurological Diseases. Neuroscience. 376:48-71.

302. Browne SE, Bowling AC, MacGarvey U, Baik MJ, Berger SC, Muqit MM, Bird ED, Beal MF. (1997) Oxidative damage and metabolic dysfunction in Huntington's disease: selective vulnerability of the basal ganglia. Ann Neurol. 41:646-53.

303. Gu M, Gash MT, Mann VM, Javoy-Agid F, Cooper JM, Schapira AH. (1996) Mitochondrial defect in Huntington's disease caudate nucleus. Ann Neurol. 39:385-9.

304. Mann VM, Cooper JM, Javoy-Agid F, Agid Y, Jenner P, Schapira AH. (1990) Mitochondrial function and parental sex effect in Huntington's disease. Lancet. 336:749.

305. Carrizzo A, Di Pardo A, Maglione V, Damato A, Amico E, Formisano L, Vecchione C, Squitieri F. (2014) Nitric oxide dysregulation in platelets from patients with advanced Huntington disease. PLoS One. 9:e89745.

306. D'Amico E, Factor-Litvak P, Santella RM, Mitsumoto H. (2013) Clinical perspective on oxidative stress in sporadic amyotrophic lateral sclerosis. Free Radic Biol Med. 65:509-527.

307. Carrera-Juliá S, Moreno ML, Barrios C, de la Rubia Ortí JE, Drehmer E. (2020) Antioxidant Alternatives in the Treatment of Amyotrophic Lateral Sclerosis: A Comprehensive Review. Front Physiol. 11:63.

308. Schon EA, Manfredi G. (2003) Neuronal degeneration and mitochondrial dysfunction. J Clin Invest. 111:303-12.

309. Federico A, Cardaioli E, Da Pozzo P, Formichi P, Gallus GN, Radi E. (2012) Mitochondria, oxidative stress and neurodegeneration. J Neurol Sci. 1322:254-62.

310. Bosco DA, Morfini G, Karabacak NM, Song Y, Gros-Louis F, Pasinelli P, Goolsby H, Fontaine BA, Lemay N, McKenna-Yasek D, Frosch MP, Agar JN, Julien JP, Brady ST, Brown RH Jr. (2010) Wild-type and mutant SOD1 share an aberrant conformation and a common pathogenic pathway in ALS. Nat Neurosci. 13:1396-403.

311. Forsberg K, Jonsson PA, Andersen PM, Bergemalm D, Graffmo KS, Hultdin M, Jacobsson J, Rosquist R, Marklund SL, Brännström T. (2010) Novel antibodies reveal inclusions containing non-native SOD1 in sporadic ALS patients. PLoS One. 5:e11552.

312. Li Q, Spencer NY, Pantazis NJ, Engelhardt JF. (2011) Alsin and SOD1(G93A) proteins regulate endosomal reactive oxygen species production by glial cells and proinflammatory pathways responsible for neurotoxicity. J Biol Chem. 286:40151-62.

313. Mattiazzi M, D'Aurelio M, Gajewski CD, Martushova K, Kiaei M, Beal MF, Manfredi G. (2002) Mutated human SOD1 causes dysfunction of oxidative phosphorylation in mitochondria of transgenic mice. J Biol Chem. 277:29626-33.

314. Pehar M, Beeson G, Beeson CC, Johnson JA, Vargas MR. (2014) Mitochondria-targeted catalase reverts the neurotoxicity of hSOD1G^{93}A astrocytes without extending the survival of ALS-linked mutant hSOD1 mice. PLoS One. 9:e103438.

315. Israelson A, Arbel N, Da Cruz S, Ilieva H, Yamanaka K, Shoshan-Barmatz V, Cleveland DW. (2010) Misfolded mutant SOD1 directly inhibits VDAC1 conductance in a mouse model of inherited ALS. Neuron. 67:575-87.

316. Pickles S, Destroismaisons L, Peyrard SL, Cadot S, Rouleau GA, Brown RH Jr, Julien JP, Arbour N, Vande Velde C. (2013) Mitochondrial damage revealed by immunoselection for ALS-linked misfolded SOD1. Hum Mol Genet. 22:3947-59.

317. Pickles S, Semmler S, Broom HR, Destroismaisons L, Legroux L, Arbour N, Meiering E, Cashman NR, Vande Velde C. (2016) ALS-linked misfolded SOD1 species have divergent impacts on mitochondria. Acta Neuropathol Commun. 4:43.

318. Richardson K, Allen SP, Mortiboys H, Grierson AJ, Wharton SB, Ince PG, Shaw PJ, Heath PR. (2013) The effect of SOD1 mutation on cellular bioenergetic profile and viability in response to oxidative stress and influence of mutation-type. PLoS One. 8:e68256.

319. Golenia A, Leśkiewicz M, Regulska M, Budziszewska B, Szczęsny E, Jagiełła J, Wnuk M, Ostrowska M, Lasoń W, Basta-Kaim A, Słowik A. (2014) Catalase activity in blood fractions of patients with sporadic ALS. Pharmacol Rep. 66:704-7.

320. Abe K, Pan LH, Watanabe M, Konno H, Kato T, Itoyama Y. (1997) Upregulation of protein-tyrosine nitration in the anterior horn cells of amyotrophic lateral sclerosis. Neurol Res. 19:124-8.

321. Casoni F, Basso M, Massignan T, Gianazza E, Cheroni C, Salmona M, Bendotti C, Bonetto V. (2005) Protein nitration in a mouse model of familial amyotrophic lateral sclerosis: possible multifunctional role in the pathogenesis. J Biol Chem. 280:16295-304.

322. Bruijn LI, Beal MF, Becher MW, Schulz JB, Wong PC, Price DL, Cleveland DW. (1997) Elevated free nitrotyrosine levels, but not protein-bound nitrotyrosine or hydroxyl radicals, throughout amyotrophic lateral sclerosis (ALS)-like disease implicate tyrosine nitration as an aberrant in vivo property of one familial ALS-linked superoxide dismutase 1 mutant. Proc Natl Acad Sci U S A. 94:7606-11.

323. Yoshino H, Kimura A. (2006) Investigation of the therapeutic effects of edaravone, a free radical scavenger, on amyotrophic lateral sclerosis (Phase II study). Amyotroph Lateral Scler. 7:241-5.

324. Nardo G, Pozzi S, Pignataro M, Lauranzano E, Spano G, Garbelli S, Mantovani S, Marinou K, Papetti L, Monteforte M, Torri V, Paris L, Bazzoni G, Lunetta C, Corbo M, Mora G, Bendotti C, Bonetto V. (2011) Amyotrophic lateral sclerosis multiprotein biomarkers in peripheral blood mononuclear cells. PLoS One. 6:e25545.

325. Radak Z, Zhao Z, Goto S, Koltai E. (2011) Age-associated neurodegeneration and oxidative damage to lipids, proteins and DNA. Mol Aspects Med. 32:305-15.

326. Catalá A. (2006) An overview of lipid peroxidation with emphasis in outer segments of photoreceptors and the chemiluminescence assay. Int J Biochem Cell Biol. 38:1482-95.

327. Farooqui AA, Horrocks LA. (2006) Phospholipase A2-generated lipid mediators in the brain: the good, the bad, and the ugly. Neuroscientist. 12:245-60.

328. Eckl PM. (2003) Genotoxicity of HNE. Mol Aspects Med. 24:161-5.

329. Doulias PT, Tenopoulou M, Greene JL, Raju K, Ischiropoulos H. (2013) Nitric oxide regulates mitochondrial fatty acid metabolism through reversible protein *S*-nitrosylation. Sci Signal. 6:rs1.

330. Lee YI, Giovinazzo D, Kang HC, Lee Y, Jeong JS, Doulias PT, Xie Z, Hu J, Ghasemi M, Ischiropoulos H, Qian J, Zhu H, Blackshaw S, Dawson VL, Dawson TM. (2014) Protein microarray characterization of the *S*-nitrosoproteome. Mol Cell Proteomics. 13:63-72.

331. Tórtora V, Quijano C, Freeman B, Radi R, Castro L. (2007) Mitochondrial aconitase reaction with nitric oxide, *S*-nitrosoglutathione, and peroxynitrite: mechanisms and relative contributions to aconitase inactivation. Free Radic Biol Med. 42:1075-88.

332. Gupta KJ, Shah JK, Brotman Y, Jahnke K, Willmitzer L, Kaiser WM, Bauwe H, (2012) Igamberdiev AU. Inhibition of aconitase by nitric oxide leads to induction of the alternative oxidase and to a shift of metabolism towards biosynthesis of amino acids. J Exp Bot. 63:1773-84.

333. Yang ES, Richter C, Chun JS, Huh TL, Kang SS, Park JW. (2002) Inactivation of NADP(+)-dependent isocitrate dehydrogenase by nitric oxide. Free Radic Biol Med. 33:927-37.

334. Lee JH, Yang ES, Park JW. (2003) Inactivation of NADP+-dependent isocitrate dehydrogenase by peroxynitrite. Implications for cytotoxicity and alcohol-induced liver injury. J Biol Chem. 278:51360-71.

335. Sun J, Morgan M, Shen RF, Steenbergen C, Murphy E. (2007) Preconditioning results in *S*-nitrosylation of proteins involved in regulation of mitochondrial energetics and calcium transport. Circ Res. 101:1155-63.

336. Chouchani ET, Hurd TR, Nadtochiy SM, Brookes PS, Fearnley IM, Lilley KS, Smith RA, Murphy MP. (2010) Identification of *S*-nitrosated mitochondrial proteins by *S*-nitrosothiol difference in gel electrophoresis (SNO-DIGE): implications for the regulation of mitochondrial function by reversible *S*-nitrosation. Biochem J. 430:49-59.

337. Yarian CS, Rebrin I, Sohal RS. (2005) Aconitase and ATP synthase are targets of malondialdehyde modification and undergo an age-related decrease in activity in mouse heart mitochondria. Biochem Biophys Res Commun. 330:151-6.

338. Elfering SL, Haynes VL, Traaseth NJ, Ettl A, Giulivi C. (2004) Aspects, mechanism, and biological relevance of mitochondrial protein nitration sustained by mitochondrial nitric oxide synthase. Am J Physiol Heart Circ Physiol. 286:H22-9.

339. Zhang Y, Lu N, Gao Z. (2009) Hemin-H2O2-NO2(-) induced protein oxidation and tyrosine nitration are different from those of SIN-1: a study on glutamate dehydrogenase nitrative/oxidative modification. Int J Biochem Cell Biol. 41:907-15.

340. Chen Z, Zhong C. (2013) Decoding Alzheimer's disease from perturbed cerebral glucose metabolism: implications for diagnostic and therapeutic strategies. Prog Neurobiol. 108:21-43.

341. Gibson GE, Kingsbury AE, Xu H, Lindsay JG, Daniel S, Foster OJ, Lees AJ, Blass JP. (2003) Deficits in a tricarboxylic acid cycle enzyme in brains from patients with Parkinson's disease. Neurochem Int. 43:129-35.

342. Naseri NN, Xu H, Bonica J, Vonsattel JP, Cortes EP, Park LC, Arjomand J, Gibson GE. (2015) Abnormalities in the tricarboxylic Acid cycle in Huntington disease and in a Huntington disease mouse model. J Neuropathol Exp Neurol. 74:527-37.

343. Veyrat-Durebex C, Corcia P, Piver E, Devos D, Dangoumau A, Gouel F, Vourc'h P, Emond P, Laumonnier F, Nadal-Desbarats L, Gordon PH, Andres CR, Blasco H. (2016) Disruption of TCA Cycle and Glutamate Metabolism Identified by Metabolomics in an In Vitro Model of Amyotrophic Lateral Sclerosis. Mol Neurobiol. 53:6910-6924.

344. Auger C, Lemire J, Cecchini D, Bignucolo A, Appanna VD. (2011) The metabolic reprogramming evoked by nitrosative stress triggers the anaerobic utilization of citrate in Pseudomonas fluorescens. PLoS One. 6:e28469.

345. Aquilano K, Baldelli S, Ciriolo MR. (2014) Glutathione: new roles in redox signaling for an old antioxidant. Front Pharmacol. 5:196.

346. Dickinson DA, Forman HJ. (2002) Cellular glutathione and thiols metabolism. Biochem Pharmacol. 64:1019-26.

347. Atakisi O, Erdogan HM, Atakisi E, Citil M, Kanici A, Merhan O, Uzun M. (2010) Effects of reduced glutathione on nitric oxide level, total antioxidant and oxidant capacity and adenosine deaminase activity. Eur Rev Med Pharmacol Sci. 14:19-23.

348. Sies H, Sharov VS, Klotz LO, Briviba K. (1997) Glutathione peroxidase protects against peroxynitrite-mediated oxidations. A new function for selenoproteins as peroxynitrite reductase. J Biol Chem. 272:27812-7.

349. Beatrice MC, Stiers DL, Pfeiffer DR. (1984) The role of glutathione in the retention of Ca2+ by liver mitochondria. J Biol Chem. 259:1279-87.

350. Savage MK, Jones DP, Reed DJ. (1991) Calcium- and phosphate-dependent release and loading of glutathione by liver mitochondria. Arch Biochem Biophys. 290:51-6.

351. Savage MK, Reed DJ. (1994) Release of mitochondrial glutathione and calcium by a cyclosporin A-sensitive mechanism occurs without large amplitude swelling. Arch Biochem Biophys. 315:142-52.

352. de la Asuncion JG, Millan A, Pla R, Bruseghini L, Esteras A, Pallardo FV, Sastre J, Viña J. (1996) Mitochondrial glutathione oxidation correlates with age-associated oxidative damage to mitochondrial DNA. FASEB J. 10:333-8.

353. Esteve JM, Mompo J, Garcia de la Asuncion J, Sastre J, Asensi M, Boix J, Vina JR, Vina J, Pallardo FV. (1999) Oxidative damage to mitochondrial DNA and glutathione oxidation in apoptosis: studies in vivo and in vitro. FASEB J. 13:1055-64.

354. Chernyak BV, Bernardi P. (1996) The mitochondrial permeability transition pore is modulated by oxidative agents through both pyridine nucleotides and glutathione at two separate sites. Eur J Biochem. 238:623-30.

355. Scarlett JL, Packer MA, Porteous CM, Murphy MP. (1996) Alterations to glutathione and nicotinamide nucleotides during the mitochondrial permeability transition induced by peroxynitrite. Biochem Pharmacol. 52:1047-55.

356. Klatt P, Molina EP, De Lacoba MG, Padilla CA, Martinez-Galesteo E, Barcena JA, Lamas S. (1999) Redox regulation of c-Jun DNA binding by reversible S-glutathiolation. FASEB J. 13:1481-90.

357. Wu AL, Moye-Rowley WS. (1994) GSH1, which encodes gamma-glutamylcysteine synthetase, is a target gene for yAP-1 transcriptional regulation. Mol Cell Biol. 14:5832-9.

358. Chaudhuri B, Ingavale S, Bachhawat AK. (1997) apd1+, a gene required for red pigment formation in ade6 mutants of Schizosaccharomyces pombe, encodes an enzyme required for glutathione biosynthesis: a role for glutathione and a glutathione-conjugate pump. Genetics. 145:75-83.

359. Miyagi H, Kawai S, Murata K. (2009) Two sources of mitochondrial NADPH in the yeast Saccharomyces cerevisiae. J Biol Chem. 284:7553-60.

360. Xiao W, Wang RS, Handy DE, Loscalzo J. (2018) NAD(H) and NADP(H) Redox Couples and Cellular Energy Metabolism. Antioxid Redox Signal. 28:251-272.

361. Kurutas EB. (2016) The importance of antioxidants which play the role in cellular response against oxidative/nitrosative stress: current state. Nutr J. 15:71.

362. Wang X, Quinn PJ. (2000) The location and function of vitamin E in membranes (review). Mol Membr Biol. 17:143-56.

363. Kojo S. (2004) Vitamin C: basic metabolism and its function as an index of oxidative stress. Curr Med Chem. 11:1041-64.

364. Packer L, Roy S, Sen CK. (1997) Alpha-lipoic acid: a metabolic antioxidant and potential redox modulator of transcription. Adv Pharmacol. 38:79-101.

365. Senoglu M, Nacitarhan V, Kurutas EB, Senoglu N, Altun I, Atli Y, Ozbag D. (2009) Intraperitoneal Alpha-Lipoic Acid to prevent neural damage after crush injury to the rat sciatic nerve. J Brachial Plex Peripher Nerve Inj. 4:22.

366. Reiter RJ, Acuña-Castroviejo D, Tan DX, Burkhardt S. (2001) Free radical-mediated molecular damage. Mechanisms for the protective actions of melatonin in the central nervous system. Ann N Y Acad Sci. 939:200-15.

367. Fiedor J, Burda K. (2014) Potential role of carotenoids as antioxidants in human health and disease. Nutrients. 6:466-88.

368. Rice-Evans CA, Miller NJ, Paganga G. (1996) Structure-antioxidant activity relationships of flavonoids and phenolic acids. Free Radic Biol Med. 20:933-56.

369. Lindemann C, Lupilova N, Müller A, Warscheid B, Meyer HE, Kuhlmann K, Eisenacher M, Leichert LI. (2013) Redox proteomics uncovers peroxynitrite-sensitive proteins that help Escherichia coli to overcome nitrosative stress. J Biol Chem. 288:19698-714.

370. Gardner PR. (2005) Nitric oxide dioxygenase function and mechanism of flavohemoglobin, hemoglobin, myoglobin and their associated reductases. J Inorg Biochem. 99:247-66.

371. Gardner PR. (2012) Hemoglobin: a nitric-oxide dioxygenase. Scientifica (Cairo).; 2012:683729.

372. Ullmann BD, Myers H, Chiranand W, Lazzell AL, Zhao Q, Vega LA, Lopez-Ribot JL, Gardner PR, Gustin MC. (2004) Inducible defense mechanism against nitric oxide in Candida albicans. Eukaryot Cell. 3:715-23.

373. Hromatka BS, Noble SM, Johnson AD. (2005) Transcriptional response of Candida albicans to nitric oxide and the role of the YHB1 gene in nitrosative stress and virulence. Mol Biol Cell. 16:4814-26.

374. Gardner PR, Gardner AM, Martin LA, Dou Y, Li T, Olson JS, Zhu H, Riggs AF. (2000) Nitric-oxide dioxygenase activity and function of flavohemoglobins. sensitivity to nitric oxide and carbon monoxide inhibition. J Biol Chem. 275:31581-7.

375. Helmick RA, Fletcher AE, Gardner AM, Gessner CR, Hvitved AN, Gustin MC, Gardner PR. (2005) Imidazole antibiotics inhibit the nitric oxide dioxygenase function of microbial flavohemoglobin. Antimicrob Agents Chemother. 49:1837-43.

376. Lewinska A, Bartosz G. (2006) Yeast flavohemoglobin protects against nitrosative stress and controls ferric reductase activity. Redox Rep. 11:231-9.

377. Brown GC. (2007) Nitric oxide and mitochondria. Front Biosci. 12:1024-33.

378. Rocco NM, Carmen JC, Klein BS. (2011) Blastomyces dermatitidis yeast cells inhibit nitric oxide production by alveolar macrophage inducible nitric oxide synthase. Infect Immun. 79:2385-95.

379. Cassanova N, O'Brien KM, Stahl BT, McClure T, Poyton RO. (2005) Yeast flavohemoglobin, a nitric oxide oxidoreductase, is located in both the cytosol and the mitochondrial matrix: effects of respiration, anoxia, and the mitochondrial genome on its intracellular level and distribution. J Biol Chem. 280:7645-53.

380. Liu L, Hausladen A, Zeng M, Que L, Heitman J, Stamler JS. (2001) A metabolic enzyme for *S*-nitrosothiol conserved from bacteria to humans. Nature. 410:490-4.

381. Xu S, Guerra D, Lee U, Vierling E. (2013) *S*-nitrosoglutathione reductases are low-copy number, cysteine-rich proteins in plants that control multiple developmental and defense responses in Arabidopsis. Front Plant Sci. 4:430.

382. Tillmann AT, Strijbis K, Cameron G, Radmaneshfar E, Thiel M, Munro CA, MacCallum DM, Distel B, Gow NA, Brown AJ. (2015) Contribution of Fdh3 and Glr1 to Glutathione Redox State, Stress Adaptation and Virulence in Candida albicans. PLoS One. 10:e0126940.

383. Guerra D, Ballard K, Truebridge I, Vierling E. (2016) *S*-Nitrosation of Conserved Cysteines Modulates Activity and Stability of *S*-Nitrosoglutathione Reductase (GSNOR). Biochemistry. 55:2452-64.

384. Jensen DE, Belka GK, Du Bois GC. (1998) *S*-Nitrosoglutathione is a substrate for rat alcohol dehydrogenase class III isoenzyme. Biochem J. 331:659-68.

385. Lee U, Wie C, Fernandez BO, Feelisch M, Vierling E. (2008) Modulation of nitrosative stress by *S*-nitrosoglutathione reductase is critical for thermotolerance and plant growth in Arabidopsis. Plant Cell. 20:786-802.

386. Luebke JL, Giedroc DP. (2015) Cysteine sulfur chemistry in transcriptional regulators at the host-bacterial pathogen interface. Biochemistry. 54:3235-49.

387. Li B, Skinner C, Castello PR, Kato M, Easlon E, Xie L, Li T, Lu SP, Wang C, Tsang F, Poyton RO, Lin SJ. (2011) Identification of potential calorie

restriction-mimicking yeast mutants with increased mitochondrial respiratory chain and nitric oxide levels. J Aging Res. 2011:673185.

388. Sahoo R, Dutta T, Das A, Sinha Ray S, Sengupta R, Ghosh S. (2006) Effect of nitrosative stress on Schizosaccharomyces pombe: inactivation of glutathione reductase by peroxynitrite. Free Radic Biol Med. 40:625-31.

389. Sies H. (2015) Oxidative stress: a concept in redox biology and medicine. Redox Biol. 4:180-3.

390. Sahoo R, Bhattacharjee A, Majumdar U, Ray SS, Dutta T, Ghosh S. (2009) A novel role of catalase in detoxification of peroxynitrite in S. cerevisiae. Biochem Biophys Res Commun. 385:507-11.

391. Lushchak OV, Lushchak VI. (2008) Catalase modifies yeast Saccharomyces cerevisiae response towards *S*-nitrosoglutathione-induced stress. Redox Rep. 13:283-91.

392. Carlberg I, Mannervik B. (1975) Purification and characterization of the flavoenzyme glutathione reductase from rat liver. J Biol Chem. 250:5475-80.

393. Song JY, Cha J, Lee J, Roe JH. (2006) Glutathione reductase and a mitochondrial thioredoxin play overlapping roles in maintaining iron-sulfur enzymes in fission yeast. Eukaryot Cell. 5:1857-65.

394. Tuggle CK, Fuchs JA. (1985) Glutathione reductase is not required for maintenance of reduced glutathione in *Escherichia coli* K-12. J Bacteriol. 162:448-50.

395. Russel M, Holmgren A. (1988) Construction and characterization of glutaredoxin-negative mutants of *Escherichia coli*. Proc Natl Acad Sci U S A. 85:990-4.

396. Sheng Y, Abreu IA, Cabelli DE, Maroney MJ, Miller AF, Teixeira M, Valentine JS. (2014) Superoxide dismutases and superoxide reductases. Chem Rev. Apr 9;114(7):3854-918.

397. Molavian H, Madani Tonekaboni A, Kohandel M, Sivaloganathan S. (2015) The Synergetic Coupling among the Cellular Antioxidants Glutathione Peroxidase/Peroxiredoxin and Other Antioxidants and its Effect on the Concentration of H_2O_2. Sci Rep. 5:13620.

398. Mohammadi S, Saberidokht B, Subramaniam S, Grama A. (2015) Scope and limitations of yeast as a model organism for studying human tissue-specific pathways. BMC Syst Biol. 9:96.

399. Goffeau A, Barrell BG, Bussey H, Davis RW, Dujon B, Feldmann H, Galibert F, Hoheisel JD, Jacq C, Johnston M, Louis EJ, Mewes HW, Murakami Y, Philippsen P, Tettelin H, Oliver SG. (1996) Life with 6000 genes. Science. 274:563-7.

400. Lashkari DA, DeRisi JL, McCusker JH, Namath AF, Gentile C, Hwang SY, Brown PO, Davis RW. (1997) Yeast microarrays for genome wide parallel genetic and gene expression analysis. Proc Natl Acad Sci U S A. 94:13057-62.

401. DeRisi JL, Iyer VR, Brown PO. (1997) Exploring the metabolic and genetic control of gene expression on a genomic scale. Science. 278:680-6.

402. Cho RJ, Campbell MJ, Winzeler EA, Steinmetz L, Conway A, Wodicka L, Wolfsberg TG, Gabrielian AE, Landsman D, Lockhart DJ, Davis RW. (1998) A genome-wide transcriptional analysis of the mitotic cell cycle. Mol Cell. 2:65-73.

403. Zhu H, Bilgin M, Bangham R, Hall D, Casamayor A, Bertone P, Lan N, Jansen R, Bidlingmaier S, Houfek T, Mitchell T, Miller P, Dean RA, Gerstein M, Snyder M. Global analysis of protein activities using proteome chips. (2001) Science. 293:2101-5.

404. Villas-Bôas SG, Moxley JF, Akesson M, Stephanopoulos G, Nielsen J. (2005) High-throughput metabolic state analysis: the missing link in integrated functional genomics of yeasts. Biochem J. 388:669-77.

405. Jewett MC, Hofmann G, Nielsen J. (2006) Fungal metabolite analysis in genomics and phenomics. Curr Opin Biotechnol. 17:191-7.

406. Mitchison JM. (1990) The fission yeast, Schizosaccharomyces pombe. Bioessays. 12:189-91. doi: 10.1002/bies.950120409.

407. Mitchison JM, Nurse P. (1985) Growth in cell length in the fission yeast Schizosaccharomyces pombe. J Cell Sci. 75:357-76.

408. Mitchison JM. (1957) The growth of single cells. I. *Schizosaccharomyces pombe.* Exp Cell Res. 13:244-62.

409. Fantes PA. (1977) Control of cell size and cycle time in Schizosaccharomyces pombe. J Cell Sci. 24:51-67.

410. Wood V, *et al*. (2002) The genome sequence of Schizosaccharomyces pombe. Nature. 415:871-80.

411. Hoyt MA, Totis L, Roberts BT. (1991) *S. cerevisiae* genes required for cell cycle arrest in response to loss of microtubule function. Cell. 66:507-17.

412. al-Khodairy F, Carr AM. (1992) DNA repair mutants defining G2 checkpoint pathways in *Schizosaccharomyces pombe*. EMBO J. 11:1343-50.

413. Guaragnella N, Palermo V, Galli A, Moro L, Mazzoni C, Giannattasio S. (2014) The expanding role of yeast in cancer research and diagnosis: insights into the function of the oncosuppressors p53 and BRCA1/2. FEMS Yeast Res.14:2-16.

414. Ferreira R, Limeta A, Nielsen J. (2019) Tackling Cancer with Yeast-Based Technologies. Trends Biotechnol. 37:592-603.

415. Miller-Fleming L, Giorgini F, Outeiro TF. (2008) Yeast as a model for studying human neurodegenerative disorders. Biotechnol J. 3:325-38.

416. Cervelli T, Lodovichi S, Bellè F, Galli A. (2020) Yeast-based assays for the functional characterization of cancer-associated variants of human DNA repair genes. Microb Cell. 7:162-174.

417. Pérez-Torres I, Manzano-Pech L, Rubio-Ruíz ME, Soto ME, Guarner-Lans V. (2020) Nitrosative Stress and Its Association with Cardiometabolic Disorders. Molecules. 25:2555.

418. Chatterji A, Banerjee D, Billiar TR, Sengupta R. (2021) Understanding the role of *S*-nitrosylation/nitrosative stress in inflammation and the role of cellular denitrosylases in inflammation modulation: Implications in health and diseases. Free Radic Biol Med. 172:604-621.

419. Lushchak OV, Inoue Y, Lushchak VI. (2010) Regulatory protein Yap1 is involved in response of yeast Saccharomyces cerevisiae to nitrosative stress. Biochemistry (Mosc). 75:629-64.

420. Merhej J, Delaveau T, Guitard J, Palancade B, Hennequin C, Garcia M, Lelandais G, Devaux F. (2015) Yap7 is a transcriptional repressor of nitric oxide oxidase in yeasts, which arose from neofunctionalization after whole genome duplication. Mol Microbiol. 96:951-72.

421. Merhej J, Thiebaut A, Blugeon C, Pouch J, Ali Chaouche Mel A, Camadro JM, Le Crom S, Lelandais G, Devaux F. (2016) A Network of Paralogous Stress Response Transcription Factors in the Human Pathogen Candida glabrata. Front Microbiol. 7:645.

422. Sellam A, Tebbji F, Whiteway M, Nantel A. (2012) A novel role for the transcription factor Cwt1p as a negative regulator of nitrosative stress in Candida albicans. PLoS One. 7:e43956.

423. Anam K, Nasuno R, Takagi H. (2020) A Novel Mechanism for Nitrosative Stress Tolerance Dependent on GTP Cyclohydrolase II Activity Involved in Riboflavin Synthesis of Yeast. Sci Rep. 10:6015.

424. Kar P, Biswas P, Patra SK, Ghosh S. (2018) Transcription factors Atf1 and Sty1 promote stress tolerance under nitrosative stress in *Schizosaccharomyces pombe*. Microbiol Res. 206:82-90.

Objectives of the study...

Objectives of the study:

Reactive oxygen species (ROS) can be generated in the yeast cells due to the physiochemical activities of it and subsequently reactive nitrogen species (RNS) are formed. Nitric oxide (NO) reacts with ROS or molecular oxygen (O_2) and RNS like peroxynitrite ($ONOO^-$), nitrogen trioxide (N_2O_3), nitrite (NO_2^-) and nitrate (NO_3^-) are formed. Accumulation of such RNS, may lead to damage of the important macromolecules like enzymes, proteins, lipids, DNA etc., this hostile condition is known as nitrosative stress, in analogy with the 'oxidative stress'. Due to the alteration of the structure of important macromolecules and redox homeostasis, electron transport chain as well as metabolism may be affected. Thus, the work was planned to characterize the effect of nitrosative stress on ethanol production using *Saccharomyces cerevisiae*, one of the best system to study the effect of nitrosative stress as its genome sequence has been well characterized and an excellent background on nitrosative stress studies. Hence, the work was performed with the following objectives:

- Determination of the cell viability and growth of *Saccharomyces cerevisiae* under nitrosative stress.
- Characterization of physiochemical properties of *Saccharomyces cerevisiae* under nitrosative stress.
- Quantification and analysis of the ethanol production by *Saccharomyces cerevisiae* under nitrosative stress.
- Optimization of ethanol production using immobilized stressed *Saccharomyces* cells.

Materials and methods...

1. Strain and media:

Sachharomyces cerevisiae Y190 (ATCC 96400) was used in this study. The strain was grown in YPD medium (2% W\V Yeast extract [HiMedia], 2% W\V peptone [HiMedia] and 2% W\V dextrose [Merck]), YPG medium (2% W\V yeast extract, 2% W\V peptone, and 3% V/V glycerol) and minimal media containing different concentration of molasses and ammonium sulphate was used for the experiment based on CCRD-RSM. Strains were grown at 30˚C under shaking condition (80 RPM). The strain was preserved in 50% glycerol stocks at -20°C freezer. The glycerol stock was used for the preparation of preinoculum. 200 µL from the glycerol stock was inoculated in a fresh YPD broth and incubated overnight at 30°C. Then, streak plating was performed on YPD agar plate using the overnight grown culture and incubated overnight at 30°C to isolate single colonies. After that, the culture was checked for contamination by phase contrast microscopy. Following that, pre-inoculum was prepared by inoculating single isolated colony in YPD broth and again incubated overnight at 30°C. The overnight grown *S. cerevisiae* cells were then used as inoculum for further experiments and initial $O.D._{600}$~0.05 was maintained for each of the samples.

2. Preparation of acidified sodium nitrite:

100 mM acidified sodium nitrite (ac. $NaNO_2$) stock solution was prepared by mixing dissolved $NaNO_2$ (Sigma-Aldrich) in double distilled (DdH_2O) with concentrated HCl in a 1:1 ratio (V/V) [1]. Effective concentrations (0.5 mM, 1 mM, and 3 mM) of acidified sodium nitrite was prepared from the stock solution for the experiments.

3. Preparation of *S*-nitrosoglutathione:

GSNO was prepared as per the method of Hart with slight modifications [2]. In brief, 0.5 M GSNO was obtained by mixing 1 M of $NaNO_2$ (Sigma-Aldrich) in DdH_2O and 1 M GSH (Himedia) in 1 N HCl in cold (1:1 V/V). The concentration of GSNO was determined spectrophotometrically (ThermoScientific MultiskanGO) at 335 nm (ε = 922 $M^{-1}cm^{-1}$).

4. Cell viability assay:

S. cerevisiae cells were grown in YPD medium and treated with different concentrations of ac. $NaNO_2$ (0.5 mM, 1 mM, 3 mM)) and GSNO (0.25 mM, 0.5 mM, 1 mM) at the early log phase ($O.D._{600}$~0.3). Following an overnight incubation, 1 ml of culture from each sample was serially diluted and plated on YPD agar medium for viable cell count. As a control, a culture without GSNO or ac. $NaNO_2$ treatment was used. The growth curve was created by recording the O.D. at 600 nm for 11 hours at 60-min intervals [3]. The growth curve was used to calculate the specific growth rate using $\mathbf{Y=Ae^{BX}}$ formula where Y= Final cell count, A= Initial cell count, B=growth rate, X= O.D. value.

5. Preparation of cell-free extracts (CFE) and estimation of total protein:

Cell-free extract (CFE) of treated and control or untreated cultures were prepared for different enzymatic assays. Overnight grown cultures of treated and untreated samples were centrifuged, and the supernatants were discarded. The cell pellets were lysed by using glass beads, 425-600 μM diameter (Sigma) and lysis buffer containing 100 mM Tris-HCl (pH 7.6), 150 mM NaCl, 1 mM SDS, 2 mM EDTA, 0.1% protease inhibitor cocktail (Sigma-Aldrich), and 1 mM PMSF [4]. CFEs were used for all the enzymatic assays. The concentration of protein was estimated as per the Bradford protocol. The standard curve for estimation of protein concentration was prepared by using BSA [5].

6. Estimation of reduced and oxidized glutathione:

The concentrations of GSH (reduced glutathione) and GSSG (oxidized glutathione) were determined using the method described by Akerboom *et al.* [6]. CFEs (from both treated and untreated samples) were first deproteinized with 2 M $HCLO_4$ (Merck), 2 M EDTA (Himedia), and then neutralized with 2 M KOH (Himedia), 0.3 M HEPES (Himedia) to pH 7. After centrifuging one portion of the neutralized samples at 5000 *g* for 5 min, the supernatants were collected to determine the total *in vivo* thiol concentration (GSH+GSSG) using Glutathione Reductase (GR) dependent DTNB (Himedia) reduction. Another portion of the sample was treated with 2-vinylpyridine (50:1 V/V) for 60 min and used to mask GSH and determine the concentration of

GSSG. Time scan was done at 412 nm for 3 min using spectrophotometer. Both GSH and GSSG concentrations were expressed in nmol/mg of protein.

7. Detection of reactive nitrogen species (RNS) and reactive oxygen species (ROS):

Reactive nitrogen species (RNS) and reactive oxygen species (ROS) were detected by using confocal microscopy and FACS.

7.1. *Confocal microscopy:*

Confocal microscopy (Leica TCS SP8) was used to detect reactive nitrogen species (RNS) and reactive oxygen species (ROS). RNS and ROS were detected using the Invitrogen protocol, with some modifications. In brief, $2x10^6$ cells were washed and resuspended in PBS pH 7.4 before being fixed with absolute ethanol. The dyes (H_2DCFDA [Invitrogen] specific for ROS and DAF-FM [Invitrogen] specific for RNS) were then added at a final concentration of 1.5 μM and incubated in the dark for 20 minutes. Excitation was set to 495 nm and emission to 515 nm for confocal microscopy. Experiments for RNS and ROS were repeated independently at least three times, and micrographs (45X) were taken. The intensity of fluorescence was measured using the Leica LAS X software.

7.2. *FACS*:

FACS (BD LSRFortessa) analysis for ROS and RNS was done from IICB, Kolkata. Samples were prepared as mentioned for the confocal microscopy. Dye free cell preparation was used as the blank for FACS analysis. The photomultiplier tube voltage was kept at 190 mV for FITC channel and flow rate was set at12 μl/min for all the experiments.10^4 events were recorded for each sample and histograms were prepared by plotting the cell count against fluorescence in the FITC channel. For the FACS analysis excitation was fixed at 495 nm and emission at 515 nm (as per the protocol of Invitrogen).

8. Estimation of ethanol production:

Ethanol was estimated by the modified potassium dichromate method [7] and potassium permanganate method [8] with slight modifications. In case of potassium

dichromate method, overnight grown untreated and treated *S. cerevisiae* broth cultures were centrifuged at 5000 *g*, and supernatants were collected. 1 ml supernatant of each sample was then mixed with a reaction mixture containing 0.25 M potassium dichromate ($K_2Cr_2O_7$) [Himedia], 0.1 M silver nitrate ($AgNO_3$) [Himedia], and 6 N sulfuric acid (H_2SO_4) [Himedia] and incubated for 10 min. The samples were then diluted, and the O.D. was recorded at 560 nm. Reaction mixture without supernatant was taken as blank.

In case of potassium permanganate method, supernatants of overnight grown untreated and treated *S. cerevisiae* broth cultures were mixed with equal volume of 20% TCA at room temperature for 5 min and then centrifuged at 10000 *g*. The supernatants were then treated with 1/5 volume of 20% CTAB at 65°C for 10 min and again centrifuged at 10000 *g*. These pretreated samples were then diluted 100-fold for ethanol estimation. Pretreated samples were mixed with 10 mM $KMnO_4$ solution and incubated at 40°C for 90 min. Initial and final O.D. were recorded at 526 nm. The 10-fold diluted pretreated sample was mixed with DNS solution for the estimation of sugar concentration. The final ethanol concentration of the pretreated sample was determined by subtracting the concentration of reducing sugar contributing in A526 from the concentration of the ethanol determined by using $KMnO_4$ method. Standard curves for the estimation of ethanol and reducing sugar concentration were prepared by using EMSURE absolute ethanol (Merck) and glucose (Merck) respectively. Further, ethanol yield and productivity were determined as mentioned by Mithra *et al.* with slight modification [9]. The volumetric productivity and yield were expressed as g/L/h and g/g of glucose. Percentage of the theoretical ethanol yield was calculated as follows:

Ethanol concentration X 100/ (Theoretical maximum ethanol yield/g of sugar i.e. 0.511 X concentration of consumed reducing sugar).

9. Enzymatic assay:

Enzymatic assays were done with the CFE or pure protein. 1 enzymatic unit (1 U) is defined as the 1 mg of protein that catalyzes the conversion of one micromole of substrate per minute under the specified conditions of the assay method.

9.1. *Glutathione reductase assay:*

The glutathione reductase assay was performed according to the protocol of Carlberg and Mannervik with slight modification [10]. In brief, 2 mM GSSG (Himedia), 3 mM DTNB, and 2 mM NADPH (Himedia) were mixed with an assay buffer containing 1 mM EDTA and CFE. Time scan was done at 412 nm for 3 min using spectrophotometer. Reaction mixture without CFE was taken as a blank. Specific activity was expressed in mU/mg of protein.

9.2. *Catalase assay:*

Catalase activity was assayed according to the method of Aebi with slight modification [11]. In brief, H_2O_2 degradation was measured at 240 nm for 2 min using spectrophotometer. The reaction mixture contained 0.1 M potassium phosphate buffer at pH 7.5, 50 mM EDTA, H_2O_2 (Sigma-Aldrich), and CFE. Reaction mixture without CFE was taken as a blank. Specific activity was expressed in mU/mg of protein.

9.3. S-*nitrosoglutathione reductase (GSNOR) assay:*

GSNO Reductase assay was performed according to the protocol of Sahoo *et al.* with slight modifications [12]. In brief, 100 mM GSNO, 0.2 mM NADH (Himedia), and 0.5 mM EDTA were mixed in 20 mM Tris-Cl pH 8.0 with CFE. The conversion of NADH to NAD was recorded at 340 nm for 5 min. Reaction mixture without CFE was taken as a blank. Specific activity was expressed in mU/mg of protein.

9.4. *Alcohol dehydrogenase assay:*

Alcohol dehydrogenase activity was determined as per the protocol of Walker with some modifications [13]. In brief, the reaction mixture contained 50 mM sodium phosphate buffer at pH 8.8, 95% V/V acetaldehyde (Sigma-Aldrich), 50 mM β-NADH, and diluted CFE. The O.D. was recorded at 340 nm for 6 min to determine the formation of β-NAD from β-NADH. Reaction mixture without CFE was taken as a blank. Specific activity was expressed in mU/mg of protein.

In a different set, the effect of GSNO or Ac. $NaNO_2$ was studied by directly adding the nitrosative stress agent to CFE. Cells were first grown under the previously mentioned conditions, and CFE was prepared. The CFE was then treated directly with

0.25 mM GSNO or ac. $NaNO_2$ for 60 min. Following that, the ADH activity of treated and untreated samples was determined, as previously stated [13]. The experiment was repeated with pure ADH (Sigma-Aldrich).

9.5. *Aconitase assay:*

Aconitase assay was performed according to the protocol of Castro *et al.* [14] with slight modifications. In brief, the formation of isocitrate (Sigma-Aldrich) from cis-aconitate was determined spectrophotometrically at 240 nm for 3 min. The reaction mixture contained 500 mM cis-aconitate, 100 mM Tris-Cl pH 8 with CFE. Reaction mixture without CFE was taken as a blank. Specific activity was expressed in mU/mg of protein.

9.6. *Aldehyde dehydrogenase assay:*

Aldehyde dehydrogenase (ALDH) activity was assayed spectrophotometrically by measuring the increase in NADH concentration at 340 nm for 3 min [15]. Reaction mixture contained final concentration of 1 M Tris-Cl buffer pH 8, 20 mM ß-Nicotinamide adenine dinucleotide (ß-NAD), 0.1 M acetaldehyde, 3 M potassium Chloride, 1 M 2-Mercaptoethanol and CFE was added to start the reaction. Specific activity was expressed in mU/mg of protein.

9.7. *Pyruvate dehydrogenase assay:*

Pyruvate dehydrogenase activity was assayed spectrophotometrically by measuring the decrease in NADH concentration at 340 nm for 5 min [16]. In short, reaction mixture contained 150 mM MOPS pH 7.4, 12 mM magnesium chloride, 0.6 mM calcium chloride, 18 mM TPP, 0.75 mM coenzyme A, 20 mM NAD^+, 15.6 mM L-cysteine, 75 mM pyruvic acid as the final concentration along with CFE. Reaction mixture without CFE was taken as blank. Specific activity was expressed in mU/mg of protein.

9.8. *Isocitare dehydrogenase assay:*

Isocitrate dehydrogenase assay was performed as per the protocol of Bergmeyer *et al.* with slight modification [16]. In short, the reaction mixture contained 70 mM glycylglycine pH 7.4, 0.5 mM isocitric acid, 1 mM β-nicotinamide adenine dinucleotide phosphate 0.5 mM manganese chloride as the final concentration. Assay reaction was

started with CFE. The conversion of NAD to NADH was measured spectrophotometrically at 340 nm for 3 min. Specific activity was expressed in mU/mg of protein.

9.9. *Pyruvate carboxylase assay:*

Pyruvate carboxylase activity was assayed spectrophotometrically by measuring the decrease in NADH concentration at 340 nm for 3 min as per the protocol of Payne and Morris with slight modification [17]. The reaction mixture contained 1 M Tris-Cl pH 8, 1 M magnesium sulfate, 0.1 M pyruvic acid, 0.1mM acetyl coenzyme A (Sigma), 0.1 M adenosine 5'-triphosphate, 0.5 M potassium bicarbonate as the final concentration. Assay reaction was started with CFE. Specific activity was expressed in mU/mg of protein.

9.10. *Pyruvate decarboxylase assay:*

Pyruvate decarboxylase assay was performed as per the protocol of Gounaris *et al.* with some modifications [18]. The reaction mixture contained 187 mM citric acid, 33 mM sodium pyruvate, 0.11 mM ß-nicotinamide adenine dinucleotide, reduced form, 10 unit of alcohol dehydrogenase (Sigma-Aldrich) as the final concentration. Reaction was started with CFE. The conversion of NADH to NAD was measured spectrophotometrically at 340 nm for 3 min. Specific activity was expressed in mU/mg of protein.

9.11. *Malate dehydrogenase assay:*

Malate dehydrogenase activity was assayed spectrophotometrically by measuring the decrease in NADH concentration at 340 nm for 3 min [16]. The reaction mixture contained 100 mM potassium phosphate, 0.13 mM β-nicotinamide adenine dinucleotide, 0.25 mM oxaloacetic acid as the final concentration. Assay reaction was started with CFE. Specific activity was expressed in mU/mg of protein.

9.12. *Citrate synthase assay:*

Citrate synthase assay was performed as per the protocol of Srere [19]. The final concentrations of the reagents were 100 mM Tris-Cl pH 8, 0.3 mM 5,5'-dithiobis-(2-nitrobenzoate), 0.2 mM acetyl coenzyme A, and 0.2 mM oxaloacetate. Assay reaction

was started with CFE and O.D. was recorded for 2 min at 412 nm. Specific activity was expressed in mU/mg of protein.

9.13. *Malate dehydrogenase (Decarboxylating) assay:*

Malate dehydrogenase (Decarboxylating) assay was performed as per the protocol of Geer *et al.* with some modifications [20]. The final concentrations of the reagents were 65 mM triethanolamine buffer (HiMedia), 3.3 mM L-malic acid, 0.3 mM β-nicotinamide adenine dinucleotide phosphate, 5 mM manganese chloride. Assay reaction was started with CFE. The conversion of NADP to NADPH was measured spectrophotometrically at 340 nm for 3 min. Specific activity was expressed in mU/mg of protein.

9.14. *Malate synthase assay:*

Malate synthase assay was performed as per the protocol of Chell *et al.* with some modifications [21]. The reaction mixture contained 30 mM imidazole Buffer, pH 8.0, 10 mM magnesium chloride, 0.25 mM acetyl-CoA, 1 mM glyoxylic acid, 0.2 mM DTNB. Assay reaction was started with CFE and O.D. was recorded for 2 min at 412 nm. Specific activity was expressed in mU/mg of protein.

10. Estimation of the concentration of citrate:

Intracellular and extracellular citrate concentration was determined by using citrate assay kit (Sigma-Aldrich). concentration of citrate was expressed in ng/µL.

11. Gene expression analysis quantitative Real Time PCR:

11.1. *RNA isolation:*

RNA was isolated as per the protocol of Dr. KPC Life Sciences, India, using their developed RNA isolation kit. In brief, treated and untreated *S. cerevisiae* cells were centrifuged at 5000 *g*, and then pellets were washed with 1X PBS. Following the addition of buffers, the entire solution containing cell pellets were transferred to prelim column and centrifuged at 10000 *g*. After that, isopropanol was added with cell pellet and then entire solution was transferred to a Chrome Column and centrifuged at 10000 *g*. Following a wash, RNA was extracted finally in nuclease-free water and then quantified using 1% agarose TAE gel.

11.2. *cDNA preparation*:

cDNA was prepared as per the protocol of Dr. KPC Life Sciences, India, using their developed cDNA synthesis kit. In brief, 500 ng of RNA was used as the template for cDNA synthesis for each sample. At first, RNA sample was mixed with 10 mM dNTP and 10 mM random hexamer and denatured at 65°C for 5 min, followed by chilling on ice. Then, diluted reverse transcriptase (RT) enzyme (Thermo Scientific) was then mixed with the chilled reaction mixture and incubated at 42°C for 60 min to synthesize cDNA. The reaction was inactivated by heating at 65°C for 15 min.

11.3. *quantitative Real Time PCR set up:*

SUPERZym qPCR mastermix, manufactured by Dr. KPC Life sciences, India was used to perform Quantitative Real-time PCR (Biorad CFX-96) Synthesized cDNA was used as the template for one reaction (+RT). To set up the (-RT) negative reaction, diluted RNA sample was used as the template. This set up was very important to check any DNA contamination. Negative control (NTC) reaction was set up without adding template. The qPCR set up was a two steps process including denaturation at 95°C for 15 sec, annealing and extension at 60°C for 30 sec. The number of cycle was repeated for 40 times and melt curve was created. All these reactions were performed in triplicate. The primers for the experimental and housekeeping genes were designed from NCBI and enlisted in **Table 1**.

Table 1: List of primers along with their sequences

Primers	Sequences (5′▼ 3′)	~Amplicon lengths (bp)
*ADH3*F	GTTGCCATCTCTGGTGCTGC	
*ADH3*R	ACACCATGAGGGCCACCTTT	300
*ADH1*F	GTTACACCCACGACGGTTCT	
*ADH1*R	ACGGTGGTACCGTTAGCTCT	445
*ADH2*F	CTGTCCTCACGCTGACTTGT	
*ADH2*R	CAACAGTACCGTTCGCCCTA	440
*ACO1*F	AGACCGTAGCACCGTTGAAG	
*ACO1*R	ATGATAGCGAAACCGCCCAA	400
*ACO2*F	TCGCATCTTTGCGATCCTGA	
*ACO2*R	CGCCTGCATTTGGTGTATGG	400
*GAPDH*F1	CGGTAGATTGGTCATGAGAAT	
*GAPDH*R1	TGGTACAAGAAGCGTTGGAAA	400
*GAPDH*F2	AACTGTTTGGCTCCATTGGC	
*GAPDH*R2	CGTTGTCGTACCAGGAAACC	200

12. Functional annotation and network analysis:

The enzymes, with the altered activity in the presence of 0.5 mM acidified sodium nitrite, were subjected for functional enrichment analysis. Initially, the STRING database was used to screen out the interactions among those enzymes in yeast system followed by creating a functionally interacting network [22]. Few closely associated enzymes were added to the network to make more stable for reliable predictions. The networks were analyzed and visualized using Cytoscape (Version 3.7) [23]. Annotation of functionally activated and deactivated enzymes were analyzed using Gene Ontology (GO) analysis by DAVID (Database for Annotation, Visualization and Integrated Discovery) [24]. Gene sets were taken from respective networks, and their annotations classified into biological process (BP), cellular component (CC) and molecular function (MF). For the GO analyses, Bonferroni correction method was used to find out the significant terms associated with the genes and decrease the error rates by removing the false discovery outcomes from any prediction.

13. Condition of stress and assays with pure aconitase and alcohol dehydrogenase:

Pure proteins were subjected to treatment by different concentrations (0.1 mM, 0.3 mM, 0.5 mM) of acidified sodium nitrite and 0.1 mM peroxynitrite (positive control). 200 µg of pure proteins were exposed to acidified sodium nitrite or peroxynitrite treatment for 30 min at room temperature. 80 µg of these treated proteins were used for determining PTN by western blotting. The rest portion of the proteins were used for specific activity determination as mentioned earlier.

14. Western blotting for Protein tyrosine nitration (PTN):

Treated and untreated pure enzymes (Aconitase [Sigma-Aldrich], Alcohol dehydrogenase [Sigma-Aldrich]) were run in 10% SDS-PAGE as per the protocol of Laemmli [25] and then transferred to PVDF membranes using wet transfer apparatus (Biorad) and transfer buffer pH 8.3 containing 25 mM Tris, 190 mM glycine and 20% methanol at 50 V for 60 min in a cold condition. To observe the successful transfer of proteins, PVDF membrane was stained with ponceau-S (HiMedia). After that, PVDF membrane was blocked overnight by using blocking buffer (HiMedia) at 4°C. Then, membranes were washed by TBST buffer (0.019 M Tris, 0.136 M, 0.1% V/V Tween 20) and probed with anti 3-nitrotyrosine monoclonal antibody (Sigma-Aldrich) at 1:1000 dilution in TBST, for 60 min at room temperature. The membranes were then washed in TBST. Following that, membranes were probed with a HRP conjugated goat anti-mouse IgG secondary antibody (Sigma-Aldrich) at 1:10000 dilution in TBST, for 30 min at room temperature. After that membranes were again washed in TBST [26]. Then the immunopositive spots were visualized by using chemilluminiscent reagent (Abcam) as per the direction of the manufacturer. Photographic plates were captured by using DNR bio-imaging system miniBIS Pro (USA) with GelQuant Express Analysis Software.

15. Western blotting analysis for *S*-nitrosylation:

S-nitrosylation was detected using Pierce™ *S*-nitrosylation western blot kit (Thermo-Fisher). At first, pure proteins were subjected to treatment by different concentrations (0.1 mM and 0.25 mM) of GSNO. 200 µg of pure proteins were exposed to GSNO

treatment for 30 min at room temperature. 100 µg of these treated and untreated proteins were used for sample preparation as mentioned in the manual of Pierce™ *S*-nitrosylation western blot kit. In short, GSNO treated proteins were treated with MMTS to block free sulfhydryl group. Following that sodium ascorbate and iodoTMT were added to modify S-NO to S-TMT. After that, proteins were run in 10% SDS-PAGE and anti-TMT monoclonal antibody was used as the primary antibody at 1:1000 ratio. Remaining protocol was same as mentioned earlier. Rest of the proteins were used for specific activity determination as mentioned earlier.

16. Estimation of ethanol production by immobilization of nitrated yeast cells:

16.1. *Immobilization of nitrated yeast cells*:

For the immobilization assay *S. cerevisiae* cells were first grown overnight in specified media in presence of 0.5 mM sodium nitrite. Next, the culture was centrifuged and the cell pellet was resuspended in PBS buffer pH 7.0. Resuspended cells were then added slowly with 1% sodium alginate. After that cells were transferred to 0.5 M $CaCl_2$ solution drop wise with the help of a syringe with the formation of Ca-alginate beads having immobilized yeast cells [27].

16.2. *Estimation of ethanol production*:

To quantify the ethanol concentration produced by immobilized nitrated yeast cells, 20 such beads were inoculated in a broth medium. Ethanol concentration was determined as stated earlier [10].

17. Optimization of ethanol production by central composite rotatable design based (CCRD) response surface methodology (RSM):

Optimization of ethanol production was carried out using central composite rotatable design based (CCRD) response surface methodology (RSM) in order to study the interaction effect between three independent variables viz., molasses concentration (C-source) (A), ammonium sulphate concentration (N-source) (B) and incubation time of yeast (C) in the fermentation broth. Due to the presence of "axial points" around the centre point in the CCRD design curvature of the model is allowed. As suggested by Saha *et al.* [26]. Three independent variables molasses concentration (A), ammonium

sulphate concentration (B) and incubation time of yeast (C) were used in five different coded levels (-α,-1,0,+1,+α). **Table 2** represents the relationship between the coded level and actual values of each variable used in this study to optimize ethanol production. The relation between the coded level of variables and actual values of the variables were explained by the following equation [28].

$$X_\alpha=(Z_\alpha-Z_0)/\Delta Z$$

Where, X_α is the coded value, Z_α is the actual value, Z_o is the actual value at the centre point and ΔZ is the step change of the variables. Total 20 experimental runs were conducted and the ethanol produced by the yeast was analyzed by the second order polynomial regression equation.

$$Y=a_0+a_1x_1+a_2x_2+a_3x_3+a_{11}x_1^2+a_{22}x_2^2+a_{33}x_3^2+a_{12}x_1x_2+a_{13}x_1x_3+a_{23}x_2x_3$$

Table 2: Coded and actual levels of variables used to construct the model

Factor	Unit	Coded levels				
		-α	**-1**	**0**	**+1**	**+ α**
A(Carbon source)	%W/V	0	5	12.5	20	25.11
B(Nitrogen source)	%W/V	0	0.05	1.02	2	2.66
C(Incubation time)	Hours	0	6	15	24	30.14

18. Statistical analysis:

All individual results are expressed as mean ± SD (Standard deviation) of at least three independent experiments for each biological sample, whereever applicable. To analyze the significant difference between control and treated samples, Student T-test, F-test were performed at 0.05 level of significance (p).

References:

1. Heaselgrave W, Andrew PW, Kilvington S. (2010) Acidified nitrite enhances hydrogen peroxide disinfection of Acanthamoeba, bacteria and fungi. J Antimicrob Chemother. 65:1207-14.

2. Hart TW. (1985) Some observations concerning the S-nitroso and S-phenylsulphonyl derivatives of Lcysteine and glutathione. Tetrahedron Lett. 26:2013-16.

3. Stevenson K, McVey AF, Clark IBN, Swain PS, Pilizota T. (2016) General calibration of microbial growth in microplate readers. Sci Rep. 6:38828.

4. Sahoo R, Sengupta R, Ghosh S. (2003) Nitrosative stress on yeast: inhibition of glyoxalase-I and glyceraldehyde-3-phosphate dehydrogenase in the presence of GSNO. Biochem Biophys Res Commun. 302:665-70.

5. Bradford MM. (1976) A rapid and sensitive method for the quantitation of microgram quantities of protein utilizing the principle of protein-dye binding. Anal Biochem. 72: 248–54.

6. Akerboom TP, Sies H. (1981) Assay of glutathione, glutathione disulfide, and glutathione mixed disulfides in biological samples. Methods Enzymol. 77:373-82.

7. Seo HB, Kim HJ, Lee OK, Ha JH, Lee HY, Jung KH. (2009) Measurement of ethanol concentration using solvent extraction and dichromate oxidation and its application to bioethanol production process. J Ind Microbiol Biotechnol. 36:285-92.

8. Zhang P, Hai H, Sun D, Yuan W, Liu W, Ding R, Teng M, Ma L, Tian J, Chen C. (2019) A high throughput method for total alcohol determination in fermentation broths. BMC Biotechnol. 19:30.

9. Mithra MG, Jeeva ML, Sajeev MS, Padmaja G. (2018) Comparison of ethanol yield from pretreated lignocellulo-starch biomass under fed-batch SHF or SSF modes. Heliyon. 4:e00885.

10. Carlberg I, Mannervik B. (1975) Purification and characterization of the flavoenzyme glutathione reductase from rat liver. J Biol Chem. 250: 5475-80.

11. Aebi H. (1984) Catalase in vitro. Methods Enzymol. 105; 121-26.

12. Sahoo R, Sengupta R, Ghosh S. (2003) Nitrosative stress on yeast: inhibition of glyoxalase-I and glyceraldehyde-3-phosphate dehydrogenase in the presence of GSNO. Biochem Biophys Res Commun. 302:665-70.

13. Walker JRL. (1992) Spectrophotometric determination of enzyme activity: alcohol dehydrogenase (ADH). Biochem. Edu. 20:42-43.

14. Castro L, Rodriguez M, Radi R. (1994) Aconitase is readily inactivated by peroxynitrite, but not by its precursor, nitric oxide. J Biol Chem. 269:29409-15.

15. Bostian KA, Betts GF. (1978) Kinetics and reaction mechanism of potassium-activated aldehyde dehydrogenase from *Saccharomyces cerevisiae*. Biochem J. 173: 787-98.

16. Bergmeyer HU, Gawehn K, Grassl M. (1974) Methods of enzymatic analysis. 2nd edn. Weinheim : Verlag Chemie, Academic Press, NY.

17. Payne J, Morris JG. (1969) Pyruvate carboxylase in *Rhodopseudomonas spheroides*. J Gen Microbiol. 59: 97-101.

18. Gounaris AD, Turkenkopf I, Buckwald S, Young A. (1971) Pyruvate decarboxylase. I. Protein dissociation into subunits under conditions in which thiamine pyrophosphate is released. J Biol Chem. 246: 1302-9.

19. Srere, PA. (1969) Citrate synthase: [EC 4.1.3.7. Citrate oxaloacetate-lyase (CoA-acetylating)]. Methods Enzymol. 13:3-11.

20. Geer, BW, Krochko D, Oliver MJ, Walker VK, Williamson JH. (1980) A comparative study of the NADP-malic enzymes from Drosophila and chick liver. Comp Biochem Physiol. 65:25-34.

21. Chell RM, Sundaram TK, Wilkinson AE. (1978) Isolation and characterization of isocitratelyase from a thermophilic *Bacillus* sp. Biochem J. 173:165-77.

22. Szklarczyk D, Gable AL, Lyon D, Junge A, Wyder S, Huerta-Cepas J, Simonovic M, Doncheva NT, Morris JH, Bork P, Jensen LJ, Mering CV. (2019) STRING v11: protein-protein association networks with increased coverage, supporting

functional discovery in genome-wide experimental datasets. Nucleic Acids Res. 47: D607-D613.

23. Shannon P, Markiel A, Ozier O, Baliga NS, Wang JT, Ramage D, Amin N, Schwikowski B, Ideker T. (2003) Cytoscape: a software environment for integrated models of biomolecular interaction networks. Genome Res. 13: 2498-504.

24. Dennis G Jr, Sherman BT, Hosack DA, Yang J, Gao W, Lane HC, Lempicki RA. (2003) DAVID: database for annotation, visualization, and integrated discovery. Genome Biol. 4:P3.

25. Laemmli UK. (1970) Cleavage of structural proteins during the assembly of the head of bacteriophage T4. Nature 227:680-5.

26. Bhattacharjee A, Majumdar U, Maity D, Sarkar TS, Goswami AM, Sahoo R, Ghosh S. (2009) In vivo protein tyrosine nitration in S. cerevisiae: identification of tyrosine-nitrated proteins in mitochondria. Biochem Biophys Res Commun. 388:612-7.

27. Agashima M, Azuma M, Noguchi S, Inuzuka K, Samejima H. (1984) Continuous ethanol fermentation using immobilized yeast cells. Biotechnol Bioeng. 26:992-7.

28. Saha SP & Ghosh S. (2014) Optimization of xylanase production by *Penicillium citrinum* xym2 and application in saccharification of agro-residues. Biocatal. Agric. Biotechnol. 3:188–196.

Results and Discussion...

Chapter 1

Determination of the cell viability and growth of *Saccharomyces cerevisiae* under nitrosative stress

Introduction:

Reactive nitrogen species (RNS) including NO can effect on physiological and physicochemical properties of the cell [1]. These may create a hostile condition generated inside the cell, known as nitrosative stress [2]. RNS is generated inside the cell by the reaction of ROS with NO [3]. Within the solution, NO can be donated by some of the chemical species, known as NO donors e.g. acidified sodium nitrite, *S*-nitrosoglutathione, DetaNONOate, peroxynitrite etc. Each of the NO donors is different from another in respect to chemical reactivity, stability etc. [4]. Some of the compounds need enzymatic action to release NO while some other compounds produce NO non-enzymatically like through the reaction of metals, thiols etc. [5]. The percentage of NO production varies with the chemical species due to their chemical organizations like presence of non-ionic bond, covalent bond etc. Solubility, half-life, pH, light can also affect the stability and the kinetics or production of NO from NO donors [6]. NO donors like acidified sodium nitrite (ac.$NaNO_2$) and *S*-nitrosoglutathione (GSNO) have different properties from each other. In presence of oxygen, ac.$NaNO_2$ can generate nitrogen dioxide (NO_2), dinitrogen trioxide (N_2O_3), and nitric oxide (NO^+) [7]. The decomposition of ac.$NaNO_2$ is dependent on the acidity of the medium [8]. The formation of NO is also proportional with the formation of N_2O_3, a highly efficient nitrosating agent [7]. On the other hand, the decomposition of GSNO is dependent on light, thiols, metal etc [9]. GSNO can be decomposed through both homolytic and heterolytic fission. Homolytic fission of GSNO depends on the metals like Cu^{2+} but heterolytic decomposition is mainly predominated in the biological system. The effect of thiols on the decomposition of GSNO is also very complex. It has been reported that excess cysteine can contribute to increase the half-life of *S*-nitrosoglutathiones [10, 11]. On the other hand, thiols can increase the rate of the decomposition of *S*-nitrosoglutathiones. Thus, depending on the redox conditions, *S*-nitrosoglutathiones can be decomposed heterolytically and NO, NO^-, NO^+ reactive chemical species are formed [9]. NO derivatives, produced *in vivo*, can either be beneficial or deleterious to the organisms [1]. The toxicity of these compounds depends on the concentration of the dose along with the duration of the treatment. Choice of cell/organism also influences the effect of these compounds. These NO derivatives including peroxynitrite, *S*-nitrosothiols, nitrogen oxides etc. can influence the *in vivo* redox homeostasis, resulting in nitrosative stress [2, 3].

Thus, at the initial phase of the work, the effect of nitrosative stress agents upon the growth of *Saccharomyces cerevisiae* were evaluated under the specified experimental condition. *Saccharomyces cerevisiae* is a budding yeast and one of the best model to study the effect of nitrosative stress. Acidified sodium nitrite (inorganic) **[Fig. 6A]** and *S*-nitrosoglutathione (organic) **[Fig. 6B]** were chosen as the 'NO donor' in this study. This study was performed to determine the sub-toxic dose (the concentration of the respective agents where growth was almost similar to the control) of these two compounds on the growth of *Saccharomyces cerevisiae* strain Y190 (ATCC 96400).

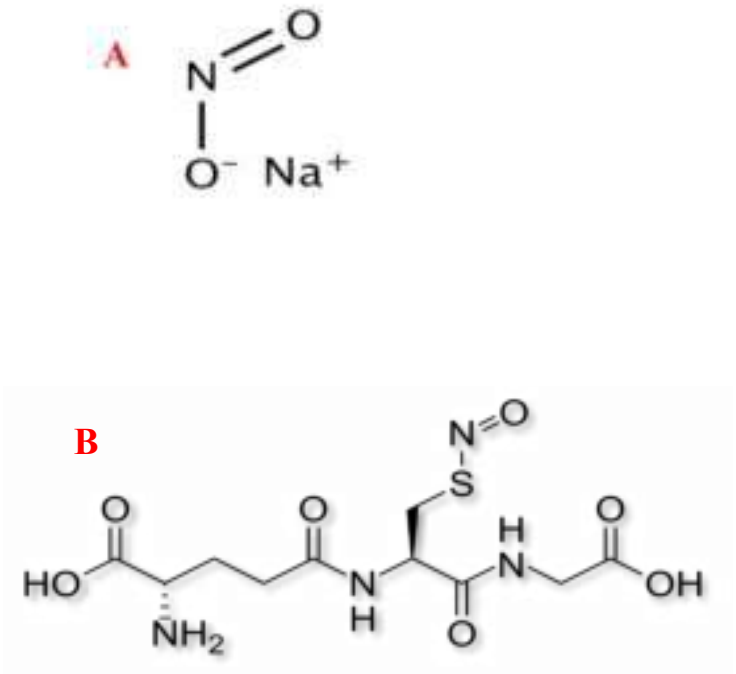

Fig. 6 Chemical formula of the reactive nitrogen species. **(A)** Sodium nitrite and **(B)** *S*-nitrosoglutathione (GSNO).

Results:

To observe the effect of ac. $NaNO_2$ and GSNO on the cell growth, *Saccharomyces cerevisiae* cells were grown in YPD medium and after 3 h, different concentrations of nitrosative stress agents were added and incubated overnight Under shaking condition. Following an overnight incubation, cell viability was determined. For the growth curve analysis, cell growth was monitored for atleast 12 h by measuring the optical density at 600 nm with one hour intervals.

It was observed that the cell viability of *Saccharomyces cerevisiae* cells were not altered in the presence of 0.5 mM ac.$NaNO_2$ as compared to the control (0 mM ac.$NaNO_2$). In presence of 1 mM and 3 mM ac.$NaNO_2$, under the same experimental conditions, cellular viability was significantly affected by nearly 25% and 50%, respectively **[Fig. 7A]**. Observed result indicated that 0.5 mM ac.$NaNO_2$ had no effect on the cell viability. Furthermore, specific growth rate was determined from growth curves. 0.5 mM ac.$NaNO_2$ treated cells showed no difference in specific growth rate (0.22 h^{-1}) as compared to the control **[Fig. 7B]**.

When a similar experiment was conducted with the treatment of various concentrations (0, 0.25, 0.5, 1 mM) of GSNO, cell viability of *Saccharomyces cerevisiae* cells were almost unaffected at 0.25 mM concentration of GSNO as compared to the control. Whereas, in presence of 0.5 and 1 mM GSNO, cell viability was significantly decreased by 30% and 60% respectively **[Fig. 8A]**. After that specific growth rates of control and 0.25 mM GSNO treated *Saccharomyces cerevisiae* cells were also determined in that condition. Observed result showed no significant difference in the specific growth rate (0.22 h^{-1}) of *S. cerevisiae* in presence of 0.25 mM GSNO as compared to the control **[Fig. 8B]**.

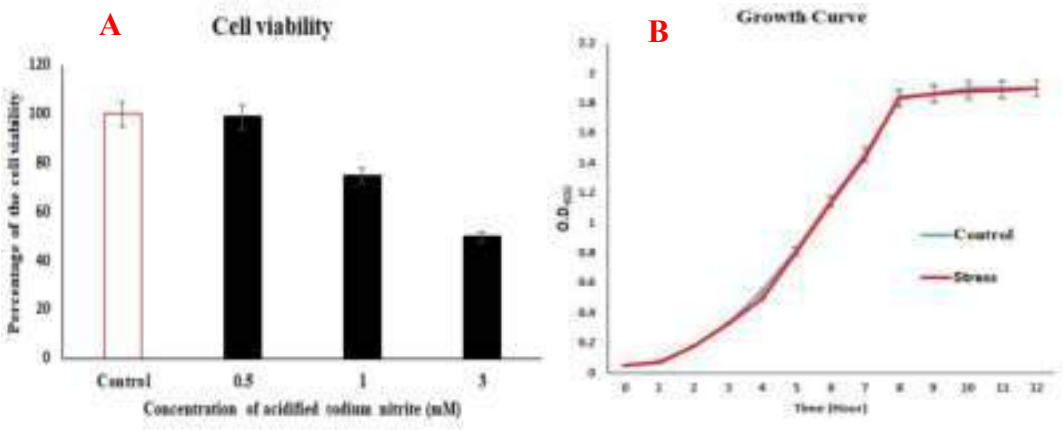

Fig. 7 Effect of acidified sodium nitrite on growth of *Saccharomyces cerevisiae* in YPD medium. (A) Cell viability assay of control (untreated) and treated (0.5 mM, 1 mM and 3 mM acidified sodium nitrite) *S. cerevisiae*. **(B)** Comparison of growth curves between control (untreated) and treated (0.5 mM) *S. cerevisiae*.

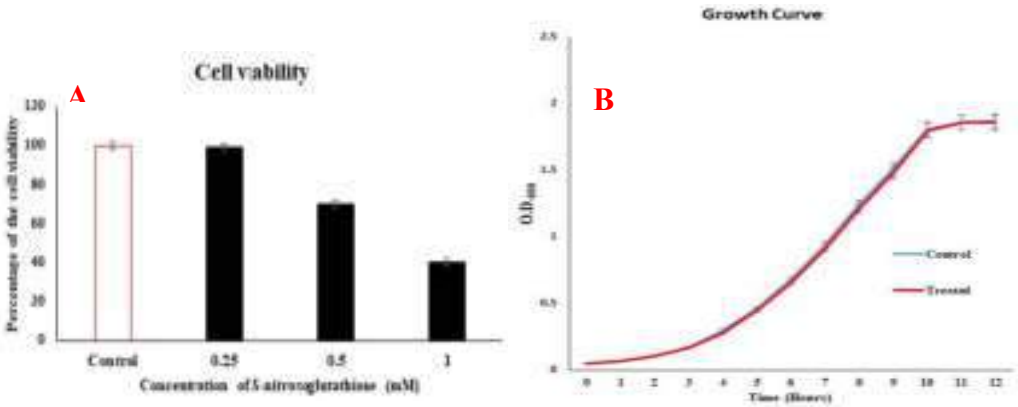

Fig. 8 Effect of *S*-nitrosoglutathione on growth of *Saccharomyces cerevisiae* in YPD medium. (A) Cell viability assay of control (untreated) and treated (0.25 mM, 0.5 mM and 1 mM acidified sodium nitrite) *S. cerevisiae*. **(B)** Comparison of growth curves between control (untreated) and treated (0.25 mM) *S. cerevisiae*.

Discussion:

The obtained results reveal some interesting insights regarding the effect of ac.$NaNO_2$ and GSNO, on the growth of *S. cerevisiae*. In the presence of higher concentrations of ac.$NaNO_2$ and GSNO, cell viability of *S. cerevisiae* was significantly decreased, indicating ac.$NaNO_2$ and GSNO has toxic effect on the cellular growth depending on their concentration. Acidified $NaNO_2$ and GSNO are well-known NO donor [4, 6, 7]. Thus, it can be assumed that nitrosative stress, generated by the action of ac.$NaNO_2$ and GSNO, was lethal for the cells. In addition to it, *S. cerevisiae* cells clearly showed more sensitivity to GSNO as compared to ac.$NaNO_2$.

Determination of the sub-toxic dose of these two agents was very important for all further experiments. The above mentioned experiments also gave insights for choosing the sub toxic doses of ac. $NaNO_2$ and GSNO. When the cells were treated with different concentration of ac.$NaNO_2$, It was found that the cell viability and specific growth rate was not altered in the presence of 0.5 mM ac.$NaNO_2$ as compared to the control whereas *S. cerevisiae* cells tolerated upto 0.25 mM GSNO and beyond this concentration the cell viability was drastically decreased. Thus, the sub-toxic doses were set to 0.5 mM and 0.25 mM for the treatment with ac.$NaNO_2$ and GSNO respectively.

References:

1. Di Meo S, Reed TT, Venditti P, Victor VM. (2016) Role of ROS and RNS Sources in Physiological and Pathological Conditions. Oxid Med Cell Longev. 2016:1245049.
2. Patra SK, Samaddar S, Sinha N, Ghosh S. (2019) Reactive nitrogen species induced catalases promote a novel nitrosative stress tolerance mechanism in Vibrio cholerae. Nitric Oxide. 88:35-44.
3. Ridnour LA, Thomas DD, Mancardi D, Espey MG, Miranda KM, Paolocci N, Feelisch M, Fukuto J, Wink DA (2004) The chemistry of nitrosative stress induced by nitric oxide and reactive nitrogen oxide species. Putting perspective on stressful biological situations. Biol Chem. 385: 1-10.
4. Howland JL. (1996) Methods in nitric oxide research: Edited by M Feelisch and J S Stamler. John Wiley and Sons, New York. pp 712.
5. Huerta S, Chilka S, Bonavida B. (2008) Nitric oxide donors: novel cancer therapeutics (review). Int J Oncol. 33:909-27.
6. Mooradian DL, Hutsell TC, Keefer LK. (1995) Nitric oxide (NO) donor molecules: effect of NO release rate on vascular smooth muscle cell proliferation in vitro. J Cardiovasc Pharmacol. 25:674-8.
7. Regev-Shoshani G, Crowe A, Miller CC. (2013) A nitric oxide-releasing solution as a potential treatment for fungi associated with tinea pedis. J Appl Microbiol. 114:536-44.
8. Kono Y, Shibata H, Adachi K, Tanaka K. (1994) Lactate-dependent killing of Escherichia coli by nitrite plus hydrogen peroxide: a possible role of nitrogen dioxide. Arch Biochem Biophys. 311:153-9.
9. Broniowska KA, Diers AR, Hogg N. (2013) *S*-nitrosoglutathione. Biochim Biophys Acta. 1830:3173-81.
10. Dicks A, Swift HR, Williams, DL, Butler A, Al-Sa'doni H, Cox B. (1996). Identification of Cu^{+} as the effective reagent in nitric oxide formation from S-nitrosothiols (RSNO). J Chem Soc perkin Trans. 2:481-487.
11. Noble DR, Swift HR, Williams DLH. (1999) Nitric oxide release from S-nitrosoglutathione (GSNO). Chem Commun. 1999:2317-18.

Chapter 2

Characterization of physiochemical properties of *Saccharomyces cerevisiae* under nitrosative stress

Introduction:

Redox homeostasis is one of the most important factor to maintain the cellular integrity. ROS and RNS including NO interfere with redox homeostasis, resulting in oxidative or nitrosative stress. Hence, alteration of redox homeostasis is a key marker of oxidative or nitrosative stress [1]. Thiol is one of the most important component to maintain the redox homeostasis *in vivo* [2]. The most abundant thiol that is present in almost all form of life, is glutathione [3]. It is a tripeptide containing glycine, glutamate and cysteine residue. Generally, two forms of glutathione exist in the cellular environment i.e. reduced glutathione (GSH) and oxidized glutathione (GSSG). Intracellularly, GSH is synthesized via the activity of two enzymes: γ-glutamylcysteine ligase (GCL) and GSH synthetase (GS). At first glutamate reacts with the cysteine by the action of GCL to form dipeptide γ-glutamylcysteine and then glycine reacts with the dipeptide by the action of GS and GSH is formed [4]. It acts as the redox buffer of the cell due to the generation of a huge amount of reducing equivalent [5]. GSH can be oxidized to GSSG by the action of GSH peroxidase (GPx). GPx uses GSH as the substrate to detoxify the effect of H_2O_2, lipid peroxides etc. that can interfere with the redox homeostasis. Again, GSSG can be reduced to GSH by the activity of NADPH dependent glutathione reductase (GR) [3, 6]. Thus, the activities of GPx and GR are very crucial for maintaining the redox status. In addition to it, intracellular thiol status is determined as the ratio of reduced to oxidized forms, i.e., GSH/GSSG. Change in the ratio of GSH/GSSG is considered as an important hallmark of nitrosative stress [7]. GSH has a protective role against NO mediated stress. The intracellular GSH can bind efficiently with NO which in turn reduces the activity of NO mediated destruction. Hence, it is very important to determine the GSH/GSSG ratio to investigate the redox status *in vivo* [8].

Saccharomyces cerevisiae also counteracts the stress by inducing different enzymes known as stress responsive enzymes e.g. catalase, Glutathione reductase (GR), superoxide dismutase (SOD), GSNOR etc. which in turn can also maintain the redox homeostasis. Thus it became imperative to determine the activities in these enzymes in the presence of ac. $NaNO_2$ and GSNO. In addition to it, *in vivo* generation of ROS and RNS is associated with the alteration of redox homeostasis. Thus, it became very important to investigate and quantify the amount of ROS and RNS in the context of this study.

Results:

To examine the effect of ac. $NaNO_2$ and GSNO at their respective sub-toxic doses (0.5 mM for ac. $NaNO_2$ and 0.25 mM for GSNO) on the cellular glutathione status, *S. cerevisiae* cells were first grown in YPD medium and then treated with either 0.5 mM ac. $NaNO_2$ or 0.25 mM GSNO. Following the treatment, cells were harvested, lysed and different parameters were determined using cell-free extract. The change in the glutathione status, GR and catalase activity were compared with the control. Treated and control cells were also checked for ROS and RNS including NO generation by performing FACS and Confocal microscopy.

Effect of acidified sodium nitrite on the redox homeostasis of *S. cerevisiae*:

To characterize the glutathione status of treated and untreated *S. cerevisiae* cells, reduced glutathione concentration (GSH), oxidized glutathione concentration (GSSG), total thiol concentration (GSH+GSSG) and GSH/GSSG ratio were measured. It was found that total glutathione concentration was not significantly altered in the presence of 0.5 mM ac. $NaNO_2$ as compared to the control. Whereas the concentration of GSSG was found to be decreased by ~2.3 fold and the concentration of GSH was increased by ~1.8 fold in the presence of 0.5 mM ac. $NaNO_2$ as compared to the control. overall, a sharp increase in GSH/GSSG ratio (4.2 fold higher) was found in the 0.5 mM ac. $NaNO_2$ treated cells as compared to the control under the specified experimental condition **[Table 3]**. In addition to it, GR activity was also found to be increased by 4 fold in the presence of 0.5 mM ac. $NaNO_2$ in comparison to the control **[Table 3]**. It was also observed that the activity of catalase was increased by approximately 2.4 fold in the 0.5 mM ac. $NaNO_2$ treated sample as compared to the control **[Table 3]**. Altogether these findings suggested that the redox homeostasis of the cells were significantly altered in the presence of 0.5 mM ac. $NaNO_2$ and the cells were trying to thwart it out.

To study the alteration of redox homeostasis, it was very important to investigate the *in vivo* generation and accumulation of ROS and RNS including NO [16]. Thus, confocal microscopy **[Fig. 9&10]** and FACS **[Fig. 11]** were performed. It was observed that the ROS was generated in both the treated and control cells with no significant change. On the contradictory, the generation of RNS was only observed in

the 0.5 mM ac. $NaNO_2$ treated cells (79%), clearly suggesting that the changes observed in the treated cells were solely due to the generation of RNS including NO.

Table 3: Estimation of total glutathione (GSH+GSSG), GSH/GSSG and activity of glutathione reductase (GR), and catalase in both treated and untreated (control) samples of *S. cerevisiae*

Sample	(GSH+GSSG) nmol/mg of protein	GSH nmol/mg of protein	GSSG nmol/mg of protein	GSH/GSSG	GR activity (mU/mg protein)	Catalase activity (mU/mg protein)
Control	77.6±2.4	33.9±1	43.7±2	0.78	4.3±NA	4.1±NA
0.5 mM ac.$NaNO_2$ treated	78.27±1.9	59.9±1.1	18.27±1.7	3.28	17.2±1.5	10±0.6

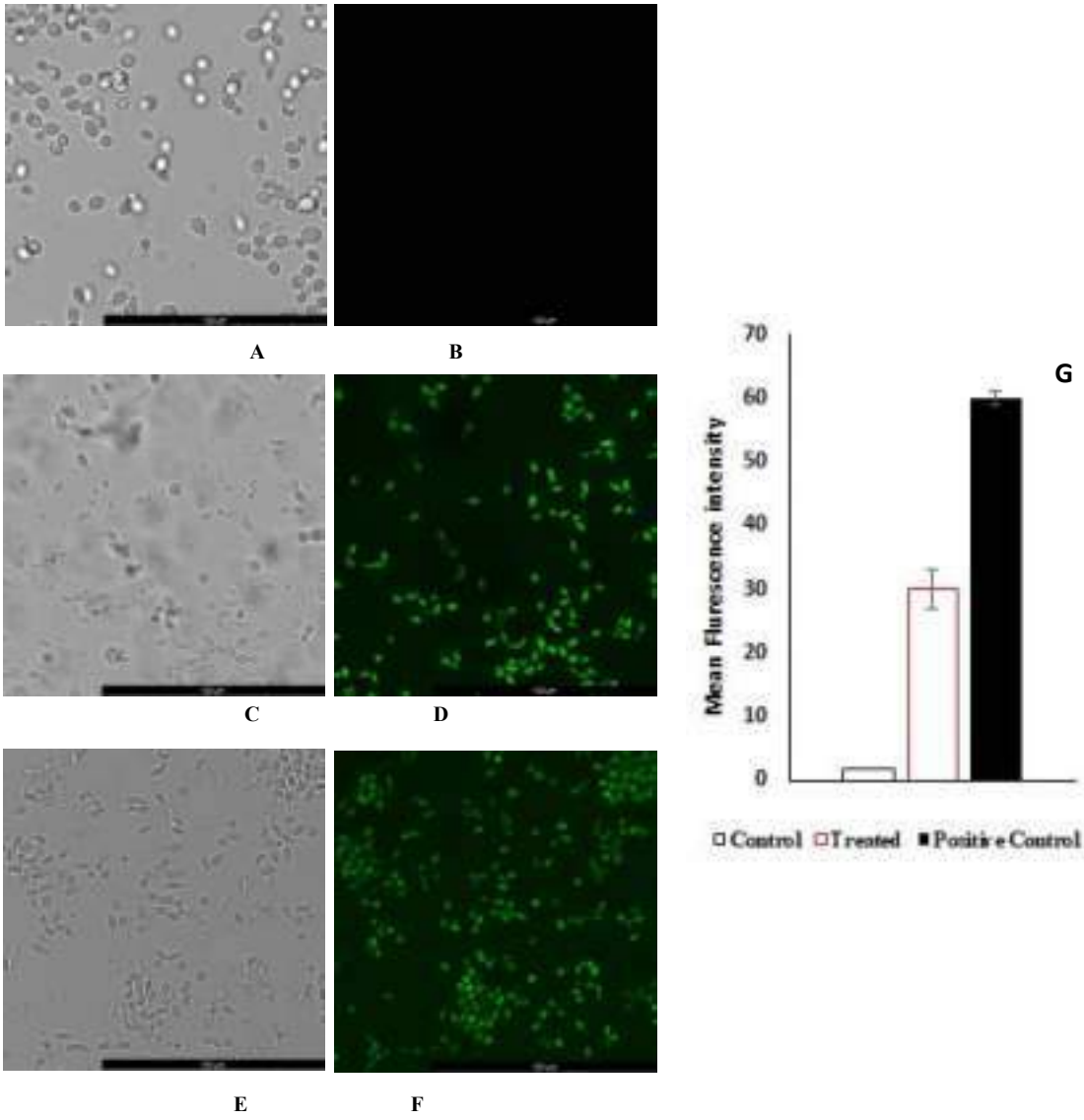

Fig. 9 Effect of acidified sodium nitrite on Reactive nitrogen species (RNS) including nitric oxide (NO) generation: The presence of NO was visualized as green colour using DAF-FM (excitation at 495 nm and emission at 515 nm). Phase contrast and corresponding fluorescence images of *S. cerevisiae* control (A and B), 0.5 mM acidified sodium nitrite treated (C and D) and positive control [peroxynitrite treated] (E and F). Micrographs were recorded at 45X. Bar=100 µm. The mean fluorescent intensity (G) was determined by using Leica LAS X software and represented as Mean±SD.

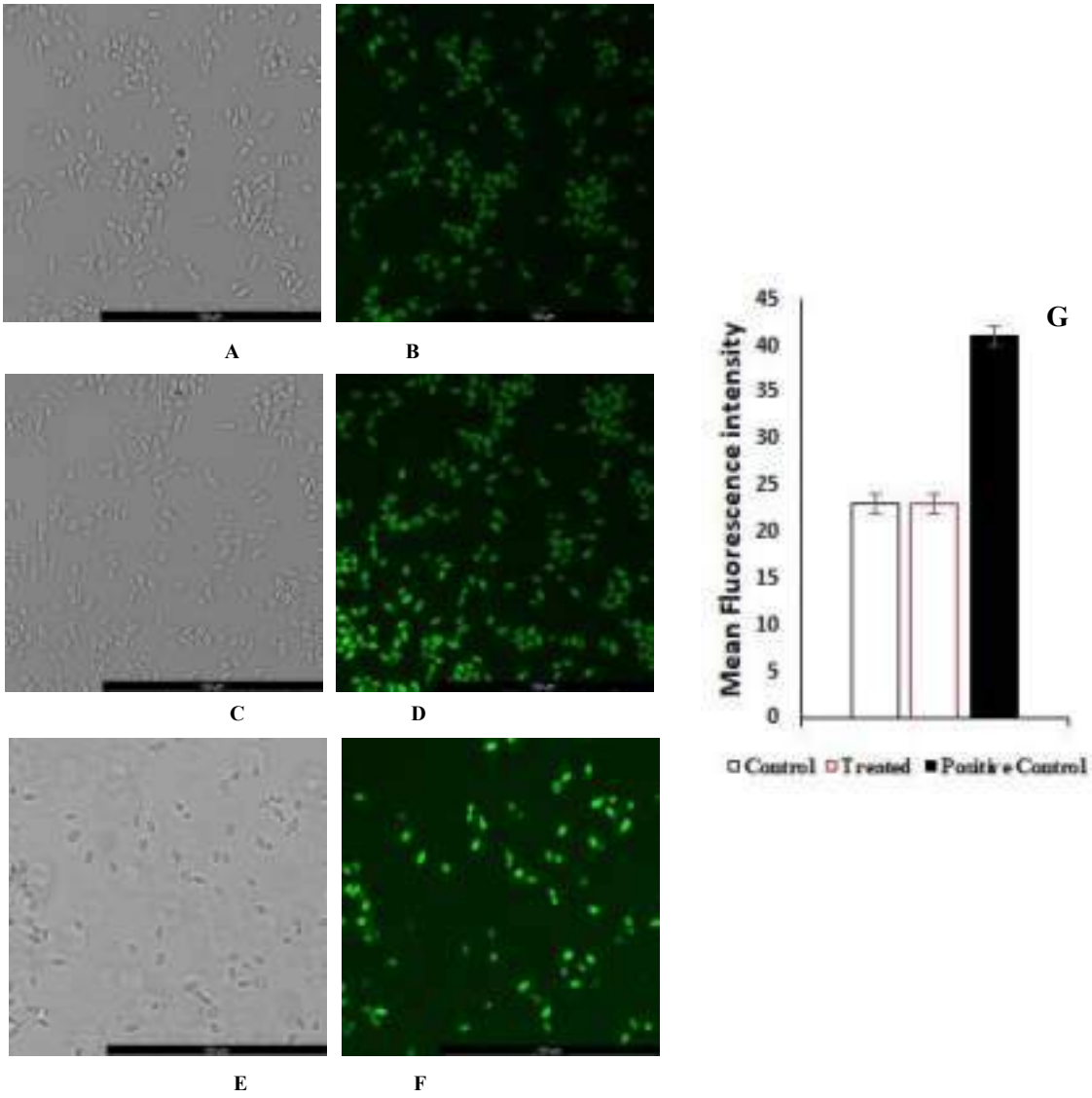

Fig. 10 Effect of acidified sodium nitrite on reactive oxygen species (ROS) generation: The presence of ROS was visualized as green colour using H_2DCFDA (excitation at 495 nm and emission at 515 nm). Phase contrast and corresponding fluorescence images of *S. cerevisiae* control or untreated (A and B), 0.5 mM acidified sodium nitrite treated (C and D) and positive control [H_2O_2 treated] (E and F). Micrographs were recorded at 45X. Bar=100 µm. The mean fluorescent intensity (G) was determined by using Leica LAS X software and represented as Mean±SD.

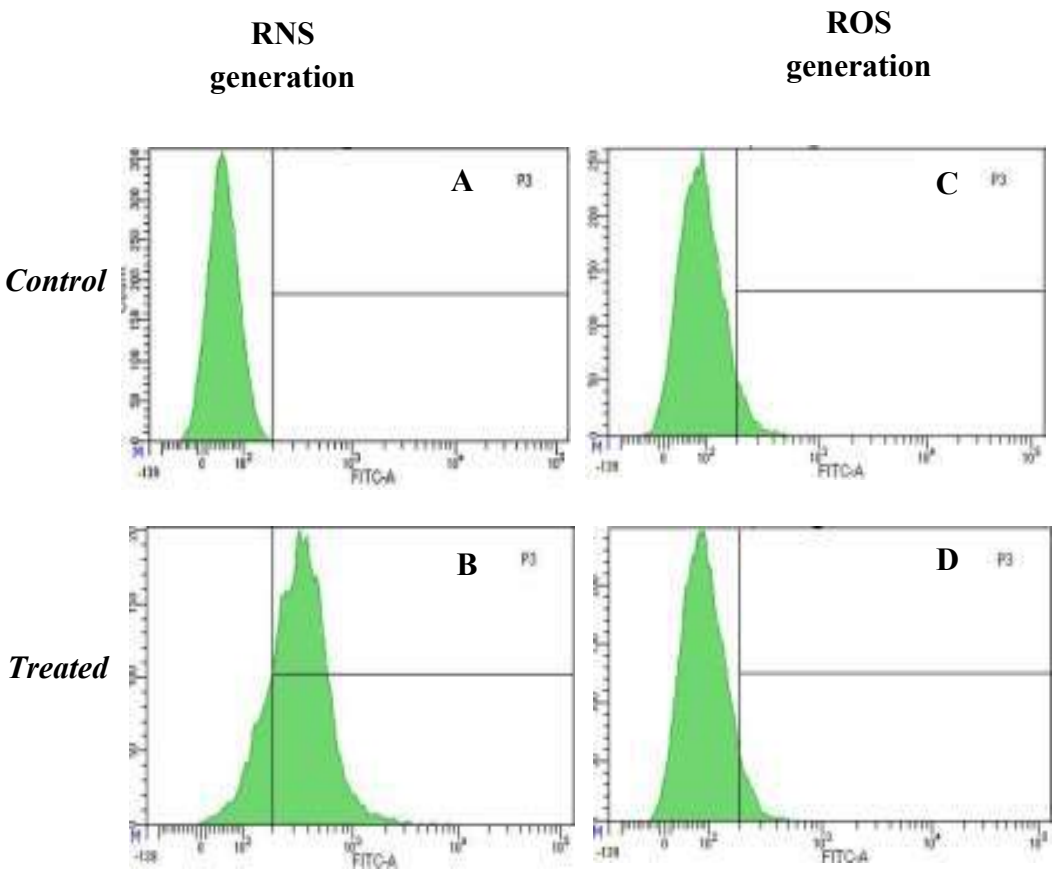

Fig. 11 Effect of 0.5 mM acidified sodium nitrite on reactive nitrogen species and reactive oxygen species generation: FACS analysis for the reactive nitrogen species (A, B) and reactive oxygen species (C, D). FACS analysis was done by using FACS Diva software. Excitation and emission were set at 495 nm and 515 nm respectively (for both the reactive nitrogen and oxygen species)

Effect of *S*-nitrosoglutathione on the redox homeostasis of *S. cerevisiae*:

To investigate the alteration in redox homeostasis *in vivo* in the presence of 0.25 mM GSNO, GSSG/GSH ratio, GR, GSNOR, and catalase activity, were assessed. Under the specified experimental condition, it was observed that the concentration of oxidized glutathione (GSSG) was decreased by 2.4 fold and reduced glutathione (GSH) was increased by 1.6 fold in the 0.25 mM GSNO treated cells as compared to the control. This resulted in a 3.9 fold increase in the GSH/GSSG ratio in treated cells in comparison to the control **[Table 4]**. A sharp 3.3 fold increase in GR activity was observed in the treated cells **[Table 4]**. Furthermore, treated cells also showed 4.3 fold higher activity of GSNOR (GSNO reductase) as compared to control, indicating that cells were expressing these enzymes to counteract the deleterious effect of GSNO **[Table 4]**. The activity of catalase was also found to be increased by 2.6 fold in presence of 0.25 mM GSNO as compared to control **[Table 4]**, implying that any ROS produced during the process was detoxified.

The presence of reactive species (ROS and RNS including NO) were detected and quantified under specified experimental conditions using confocal microscopy and mean fluorescence intensity. RNS was only detected in GSNO-treated cells **[Fig. 12]**. Whereas ROS was found in both the treated and untreated samples, there was no significant difference in ROS generation **[Fig. 13]**. Hence, it can be assumed that the effect observed under the specified experimental condition is solely due to the generation of RNS including NO by 0.25 mM GSNO.

Table 4: Estimation of total glutathione (GSH+GSSG), GSH/GSSG and activity of glutathione reductase (GR), catalase and *S*-nitrosoglutathione reductase (GSNOR) in both treated and untreated (control) samples of *S. cerevisiae*

Sample	(GSH+GSSG) nmol/mg of protein	GSH nmol/mg of protein	GSSG nmol/mg of protein	GSH/ GSSG	GR Activity (mU/mg protein)	Catalase Activity (mU/mg protein)	GSNOR Activity (mU/mg protein)
Control	81.92±2	34.2±0.5	47.72±1.2	0.7	3.95±0.5	3.88±0.4	1±0.02
0.25 mM GSNO treated	75.4±2	55.3±0.4	20.1±1.1	2.75	13.82±0.7	9.97±0.5	4±0.46

*Data has been rounded off to the nearest whole number for the publication

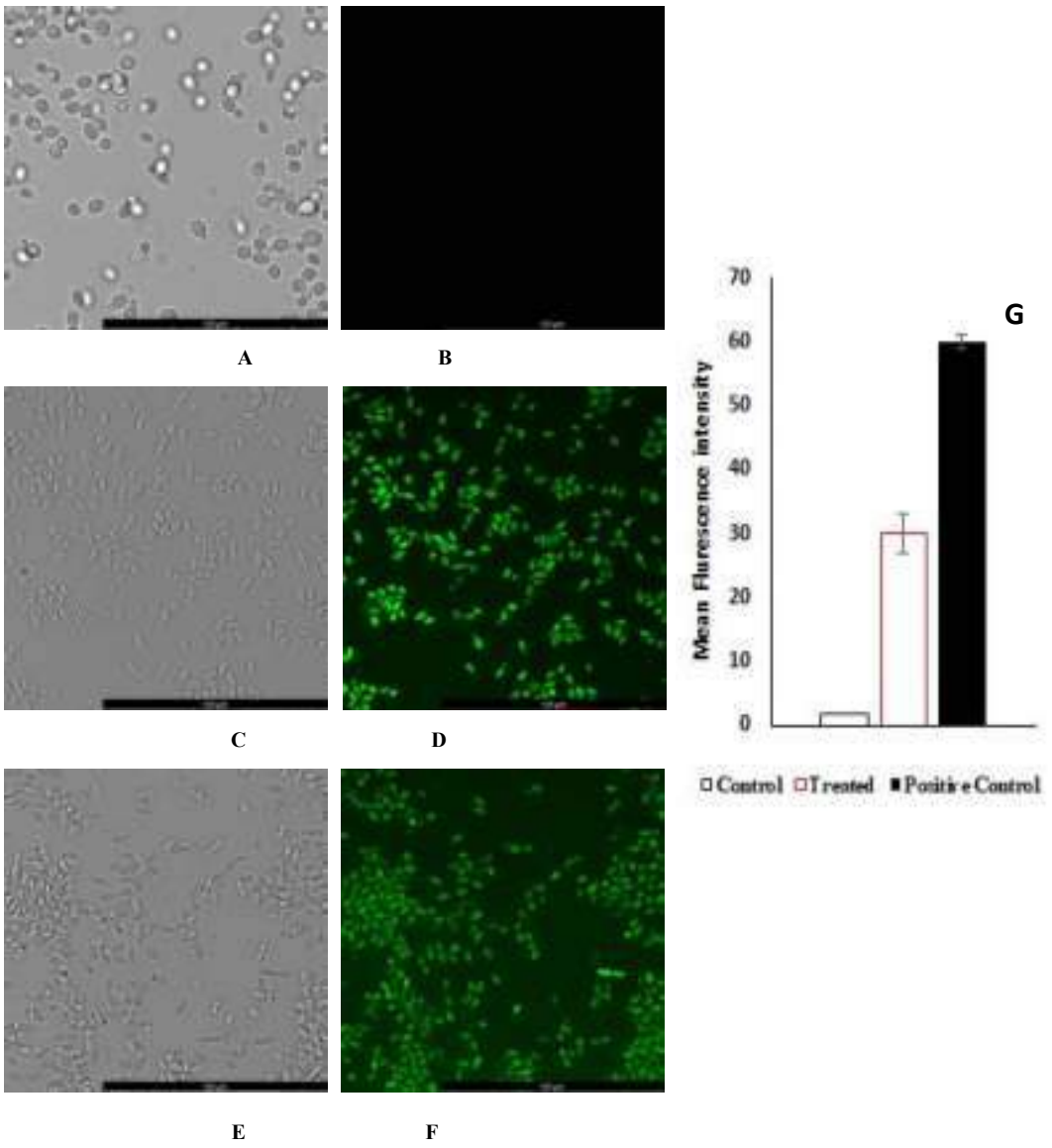

Fig. 12 Effect of *S*-nitrosoglutathione on Reactive nitrogen species (RNS) including nitric oxide (NO) generation: The presence of NO was visualized as green colour using DAF-FM (excitation at 495 nm and emission at 515 nm). Phase contrast and corresponding fluorescence images of *S. cerevisiae* control (A and B), 0.25 mM GSNO treated (C and D) and and positive control [peroxynitrite treated] (E and F) Micrographs were recorded at 45X. Bar=100 µm. The mean fluorescent (G) was determined by using Leica LAS X software and represented as Mean±SD.

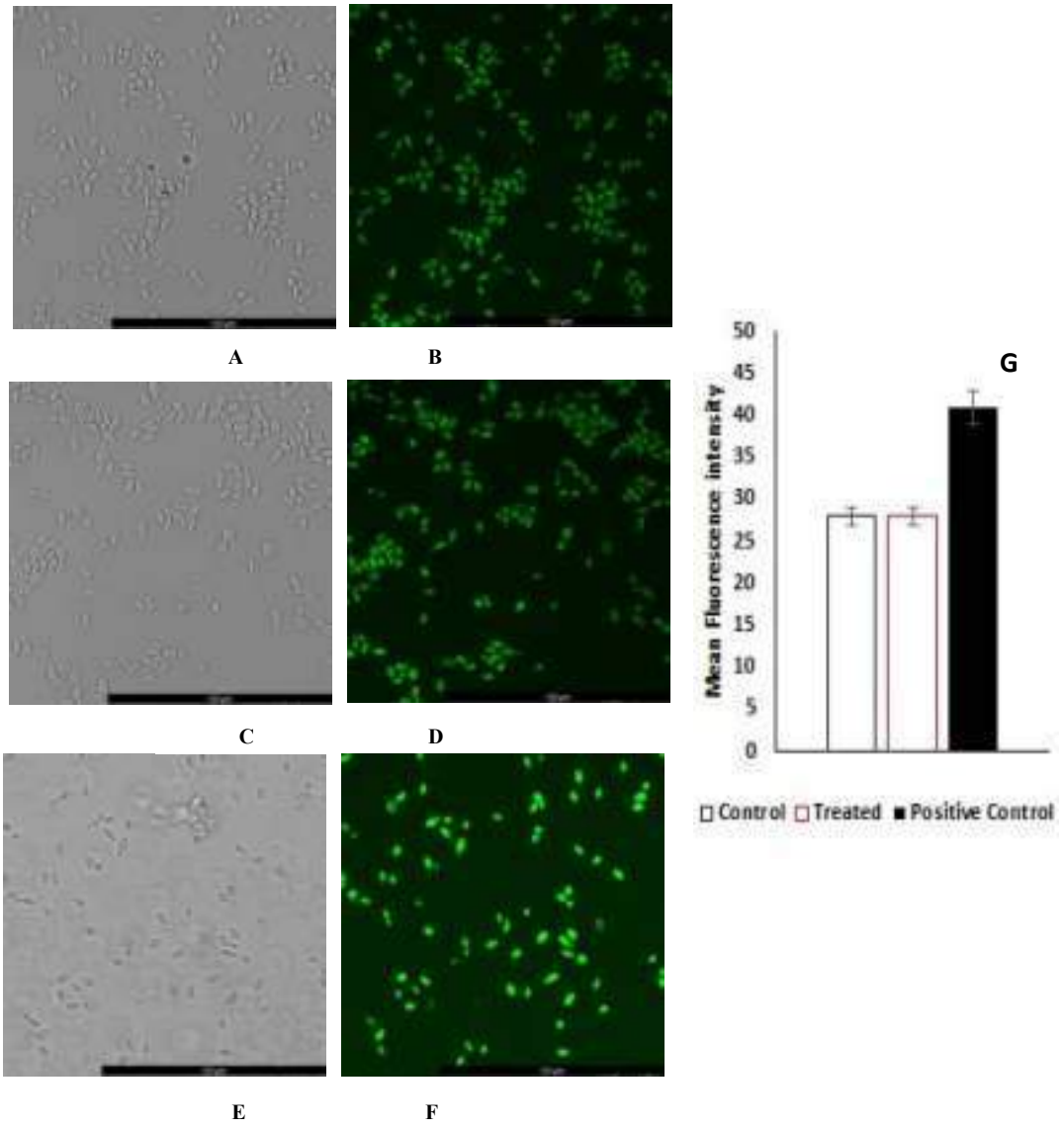

Fig. 13 Effect of *S*-nitrosoglutathione on reactive oxygen species (ROS) generation: The presence of ROS was visualized as green colour using H_2DCFDA (excitation at 495 nm and emission at 515 nm). Phase contrast and corresponding fluorescence images of *S. cerevisiae* control or untreated (A and B), 0.25 mM GSNO treated (C and D) and positive control [H_2O_2 treated] (E and F). Micrographs were recorded at 45X. Bar=100 µm. The mean fluorescent intensity (G) was determined by using Leica LAS X software and represented as Mean±SD.

Discussion:

Under sub-toxic dose of GSNO and ac. $NaNO_2$, some significant changes in physicochemical properties as well as redox homeostasis of *S. cerevisiae* were found in comparison to control, indicating that the cells were trying to overcome the stress for survival. GSH is regarded as a stress response component that plays an important role in the inhibition of NO activity, metal toxicity and so on [10, 12, 13]. When the GSH level decreases, NO activity induces DNA damage as well as protein modifications such as protein tyrosine nitration, *S*-nitrosylation [14, 15]. This study showed an increase in GSH/GSSG ratio under GSNO and ac. $NaNO_2$ stress, suggesting that the treated cells were trying to increase the reduced equivalent inside the cell in the form of GSH [16]. GSH acts as the redox buffer under the stress conditions and maintains the redox homeostasis as per the requirement of the cell [17]. Higher activity of GR under sub toxic dose of GSNO and ac. $NaNO_2$ also supported the finding. Thus, it can be concluded that the higher activity of GR under stress condition might contribute to the higher GSH/GSSG ratio. In addition to this, activity of catalase was also found to be increased in treated cells that might be involved to detoxify any reactive species that were generated by the action of ac. $NaNO_2$ and GSNO [10, 18-20]. Though it is well-known for its oxidative stress response activity, but the activity of catalase may also get stimulated under nitrosative stress to overcome the hostile situation [20].

GSNOR activity was induced in GSNO treated cells. GSNOR activity was very important to reduce GSNO. It cleaves GSNO into GSSG and NH_3. Hence, the possible outcome under GSNO stress is increase in the concentration of GSSG due to the action of GSNOR and subsequent reduction of GSSG to GSH by GR. This implies that an elevated level of reduced equivalents was required to maintain redox homeostasis *in vivo*.

Results from FACS and confocal microscopy confirmed that there was no such significant difference in ROS generation in the acidified sodium nitrite treated cells as compared to the control whereas formation of was observed only in the treated cells. Therefore, it can be concluded that the observed phenomena were only due to acidified sodium nitrite mediated nitrosative stress.

Similarly, generation of RNS was also found in GSNO treated cells. There was no such significant difference in ROS generation in GSNO treated cells as compared to the control. Therefore, it can be concluded that the observed phenomena were only due to GSNO mediated nitrosative stress.

References:

1. Maciejczyk M, Zalewska A, Gryciuk M, Hodun K, Czuba M, Płoszczyca K, Charmas M, Sadowski J, Baranowski M. (2022) Effect of Normobaric Hypoxia on Alterations in Redox Homeostasis, Nitrosative Stress, Inflammation, and Lysosomal Function following Acute Physical Exercise. Oxid Med Cell Longev. 2022:4048543.

2. Deponte M. (2017) The Incomplete Glutathione Puzzle: Just Guessing at Numbers and Figures? Antioxid Redox Signal. 27:1130-1161.

3. Forman HJ, Zhang H, Rinna A. (2009) Glutathione: overview of its protective roles, measurement, and biosynthesis. Mol Aspects Med. 30:1-12.

4. Huang CS, Chang LS, Anderson ME, Meister A. (1993) Catalytic and regulatory properties of the heavy subunit of rat kidney gamma-glutamylcysteine synthetase. J Biol Chem. 268:19675-80.

5. Sies H. (1999) Glutathione and its role in cellular functions. Free Radic Biol Med. 27:916-21.

6. Ralat LA, Manevich Y, Fisher AB, Colman RF. (2006) Direct evidence for the formation of a complex between 1-cysteine peroxiredoxin and glutathione S-transferase pi with activity changes in both enzymes. Biochemistry. 45:360-72.

7. Xiong Y, Uys JD, Tew KD, Townsend DM. (2011) S-glutathionylation: from molecular mechanisms to health outcomes. Antioxid Redox Signal. 15:233-70.

8. Lushchak VI. (2012) Glutathione homeostasis and functions: potential targets for medical interventions. J Amino Acids. 2012:736837.

9. Patra SK, Samaddar S, Sinha N, Ghosh S. (2019) Reactive nitrogen species induced catalases promote a novel nitrosative stress tolerance mechanism in *Vibrio cholerae*. Nitric Oxide. 88:35-44.

10. Navarro MV, Chaves AFA, Castilho DG, Casula I, Calado JCP, Conceição PM, Iwai LK, de Castro BF, Batista WL. (2020) Effect of Nitrosative Stress on the *S*-Nitroso-Proteome of *Paracoccidioides brasiliensis*. Front Microbiol. 11:1184.

11. Lindemann C, Lupilova N, Müller A, Warscheid B, Meyer HE, Kuhlmann K, Eisenacher M, Leichert LI. (2013) Redox proteomics uncovers peroxynitrite-sensitive proteins that help Escherichia coli to overcome nitrosative stress. J Biol Chem. 288:19698-714.

12. Aquilano K, Baldelli S, Ciriolo MR. (2014) Glutathione: new roles in redox signaling for an old antioxidant. Front Pharmacol. 5:196.

13. Kalinina E, Novichkova M. (2021) Glutathione in Protein Redox Modulation through S-Glutathionylation and S-Nitrosylation. Molecules. 26:435.

14. Lei XG, Zhu JH, Cheng WH, Bao Y, Ho YS, Reddi AR, Holmgren A, Arnér ES. (2016) Paradoxical Roles of Antioxidant Enzymes: Basic Mechanisms and Health Implications. Physiol Rev. 96:307-64.

15. Sies H, Sharov VS, Klotz LO, Briviba K. (1997) Glutathione peroxidase protects against peroxynitrite-mediated oxidations. A new function for selenoproteins as peroxynitrite reductase. J Biol Chem. 272:27812-7.

16. Astuti RI, Nasuno R, Takagi H. (2016) Nitric oxide signaling in yeast. Appl Microbiol Biotechnol. 100:9483-9497.

17. Ghosh D, Levault KR, Brewer GJ. (2014) Relative importance of redox buffers GSH and NAD(P)H in age-related neurodegeneration and Alzheimer disease-like mouse neurons. Aging Cell. 13:631-40.

18. Bhattacharjee A, Majumdar U, Maity D, Sarkar TS, Goswami AM, Sahoo R, Ghosh S (2010) Characterizing the effect of nitrosative stress in *Saccharomyces cerevisiae*. Arch Biochem Biophys 496:109-16.

19. Gebicka L, Didik J (2009) Catalytic scavenging of peroxynitrite by catalase. J Inorg Biochem 103:1375-79.

20. Sahoo R, Bhattacharjee A, Majumdar U, Ray SS, Dutta T, Ghosh S (2009) A novel role of catalase in detoxification of peroxynitrite in *S. cerevisiae*. Biochem Biophys Res Commun 385:507-11.

Chapter 3

Quantification and analysis of the ethanol production by *Saccharomyces cerevisiae* under nitrosative stress

Introduction:

Excessive production of reactive nitrogen species including NO interferes with the structure as well as function of different macromolecules like DNA, proteins, enzymes, lipids etc. *in vivo* [1-3]. Protein modifications like protein tyrosine nitration (PTN) and *S*-nitrosylation are considered as the biomarkers of nitrosative stress [2, 3]. It has been reported that mitochondrial matrix proteins are the primary target of RNS [4]. Reports also suggest that the function of respiratory chain in *S. cerevisiae* may get hampered under nitrosative stress due to inactivation of several TCA cycle enzymes [5, 6]. Aconitase (catalyzes the reaction from citrate to isocitrate), one of the important enzyme of TCA cycle, has been reported to get affected under nitrosative insult [5, -8]. It is also a well-known marker of redox stress [9]. On the other hand, alcohol dehydrogenase (ADH), an important fermentative enzyme, may act as a Thus, higher activity of ADH may affect the metabolism via modulating fermentation (i.e. ethanol formation) [10, 11]. Hence, it was very important to investigate the status of ADH and aconitase under nitrosative stress.

Therefore, in this study the activity of ADH and aconitase along with the gene expression in the presence of sub-toxic dose of acidified sodium nitrite in *S. cerevisiae* were investigated under the specified experimental condition. To establish the phenomena as the effect of nitrosative stress, some of the key experiments were also repeated using *S*-nitrosoglutathione as a nitrosative stress agent.

Results:

To determine the status of ADH and aconitase under nitrosative stress, *S. cerevisiae* cells were first grown in YPD medium and then treated with either 0.5 mM ac. $NaNO_2$ or 0.25 mM GSNO. Then, the cells were harvested, lysed and cell free-extract were prepared to investigate aconitase and ADH activity. The supernatants were used to quantify the ethanol and the concentration of reducing sugar as per the protocol of Zhange *et al.* (Mentioned in materials and methods). For the gene expression analysis, RNA was isolated from *S. cerevisiae* cells and cDNA was prepared for the experiments. All these parameters were compared with the control.

Effect of acidified sodium nitrite and *S*-nitrosoglutathione on the activity of aconitase:

Under the specified experimental condition, it was observed that the specific activity of aconitase was approximately dropped by 50% in the 0.5 mM ac. $NaNO_2$ treated cells as compared to the control **[Fig. 14]**.

Whereas, aconitase activity was not detected in the presence of 0.25 mM GSNO. These data clearly suggest that aconitase activity was suppressed in the presence of stress agent under the specified experimental condition **[Fig. 14]**.

Effect of acidified sodium nitrite on *ACO* genes expression:

As it was observed that aconitase activity was only present in acidified sodium nitrite treated sample, thus, the gene expression level of *ACO* genes were only determined in presence of ac. $NaNO_2$ and compared with the control. In the presence of 0.5 mM ac. $NaNO_2$, gene expression of *ACO1* was found to be increased by 1.2 fold **[Fig. 15A]** whereas gene expression of *ACO2* was dropped by 50% as compared to the control **[Fig. 15B]** which may be the cause of the reduction in the activity of aconitase.

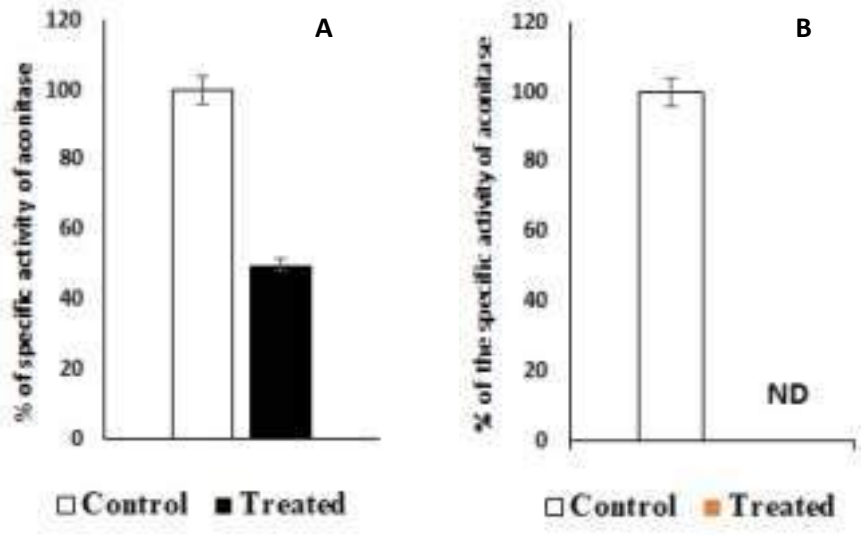

Fig. 14 (A) Effect of 0.5 mM acidified sodium nitrite and **(B)** Effect of 0.25 mM *S*-nitrosoglutathione on the specific activity of aconitase. Data is represented as the change in the percentage of specific activity as compared to the control. The enzyme assay was repeated for three times for each experimental set up and expressed as mean±SD. 100% specific activity equals to 7 mU/mg.

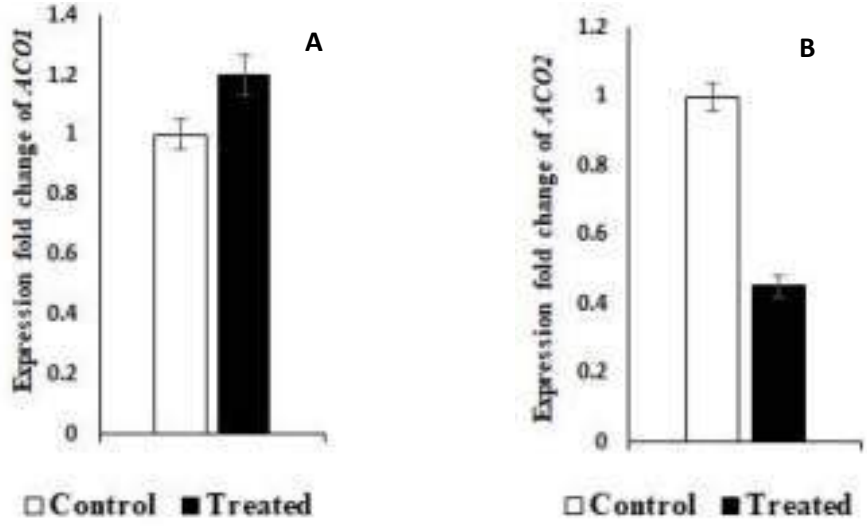

Fig. 15. (**A)** Effect of 0.5 mM acidified sodium nitrite on relative gene expression of *ACO1* and **(B)** relative gene expression of *ACO2*. The expression levels of *ACO1* and *ACO2* were normalized with that of *GAPDH* (glyceraldehyde-3-phosphate dehydrogenase) in each set and expressed as relative fold change as compared to the control. Supporting information are mentioned in Table S1 and S2.

Effect of acidified sodium nitrite and on *S*-nitrosoglutathione ethanol production:

Initially, ethanol quantification was done by potassium dichromate method (Mentioned in materials and methods) and a sharp 1.3 fold increase in ethanol production was found in 0.5 mM ac. $NaNO_2$ treated cells as compared to control under the specified experimental condition. Later on, the kinetics of ethanol production was determined by a more clarified method of Zhang *et al.* (Mentioned in materials and methods). By performing this new method, the similar result was found i.e. when 0.5 mM ac. $NaNO_2$ was present, ethanol production increased significantly (~1.3 fold) in comparison to the control. The ethanol yield was increased by approximately 1.3 fold and consumption of sugar was also ~14% higher under the stress condition. The volumetric productivity was also increased by approximately 1.5 fold in the presence of 0.5 mM ac. $NaNO_2$. 66% of the theoretical ethanol yield was achieved in the presence of 0.5 mM ac. $NaNO_2$ **[Table 5]**.

In the presence of 0.25 mM GSNO, ~1.5 fold increase in ethanol production was discovered as compared to the control under the specified experimental condition. In this condition, ethanol yield was increased by approximately 1.3 fold and consumption of sugar was also 15% higher under the stress condition. The volumetric productivity was also increased by approximately 1.5 fold in the presence of 0.25 mM GSNO. 76% of the theoretical ethanol yield was achieved in the presence of 0.25 mM GSNO **[Table 5]**.

Effect of acidified sodium nitrite and *S*-nitrosoglutathione on the activity of ADH:

By performing spectrophotometric assay at 340 nm, it was found that alcohol dehydrogenase activity was increased by 1.3 fold in the presence of 0.5 mM ac. $NaNO_2$, as compared to the control **[Fig. 16A]**.

Similarly, alcohol dehydrogenase activity was increased by 3.5 fold in the presence of 0.25 mM GSNO as compared to the control **[Fig. 16B]**.

Table 5: Estimation of ethanol concentration, glucose consumption, ethanol yield, percentage of theoretical yield and volumetric productivity of 0.5 mM ac. $NaNO_2$ treated, 0.25 mM GSNO treated and untreated (control) samples of *S. cerevisiae*

Sample	Ethanol concentration (g/L)	Glucose consumed (g/L)	Ethanol yield (g/g of glucose)	% of theoretical yield	Volumetric Productivity (g/L/h)
Control	4.5±0.3	15±0.3	0.30	59	0.38
0.5 mM ac. $NaNO_2$ Treated	6±0.5	17±0.4	0.35	69	0.50
0.25 mM GSNO Treated	7±0.5	18±0.4	0.39	76	0.58

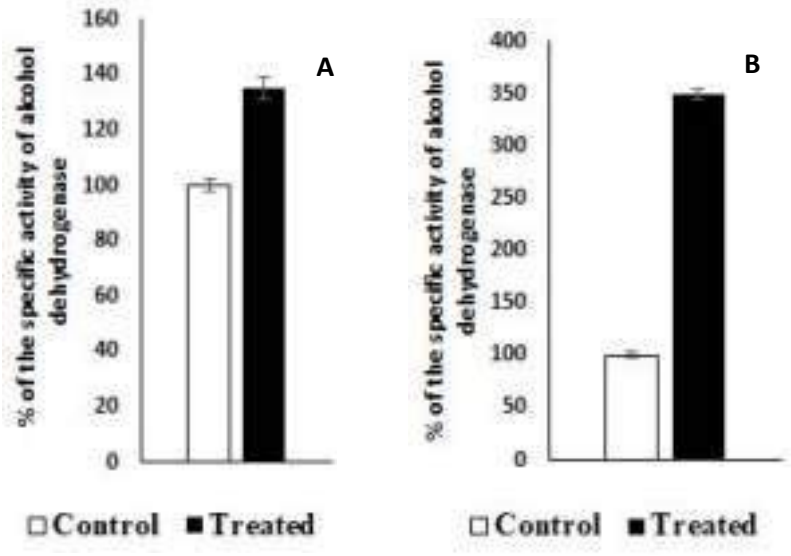

Fig. 16 (A) Effect of 0.5 mM acidified sodium nitrite and **(B)** Effect of 0.25 mM *S*-nitrosoglutathione on the specific activity of alcohol dehydrogenase. Data is represented as the change in the percentage of specific activity as compared to the control. The enzyme assay was repeated for three times for each experimental set up and expressed as mean±SD. 100% specific activity equals to 10 mU/mg.

In another set, CFE from *S. cerevisiae* was directly treated with 0.25 mM GSNO or 0.5 mM ac. $NaNO_2$ and ADH assay was performed. Interestingly, no change in ADH activity was observed in the treated CFE as compared to the untreated CFE **[Table 6]**, implying that GSNO and ac. $NaNO_2$ may not be involved in ADH protein modification. The inhibition assay of ADH was also studied using 0.1 mM 2,2,2-trifluoroethanol.

Table 6: Estimation of alcohol dehydrogenase activity of cell free extract (CFE) and treated CFE

Conditions	ADH activity (mU/mg)
CFE	4±NA
0.5 mM ac. $NaNO_2$ treated CFE	4±NA
0.25 mM GSNO treated CFE	4±NA
CFE + 2,2,2- trifluoroethanol	Not found
0.5 mM ac. $NaNO_2$ treated CFE + 2,2,2-trifluoroethanol	Not found
0.25 mM GSNO treated CFE + 2,2,2-trifluoroethanol	Not found

Effect of acidified sodium nitrite and *S*-nitrosoglutathione on *ADH* genes expression:

As ethanol production and ADH activity were significantly increased in the presence of 0.5 mM ac. $NaNO_2$ and 0.25 mM GSNO, hence, the gene expression level of *ADH1, ADH2* and *ADH3* genes under the same condition were investigated.

When 0.5 mM ac. $NaNO_2$ was present, the expression of *ADH1*, *ADH2* and *ADH3* genes were found to be increased by ~2.1 fold **[Fig. 17A]** ~2.4 fold **[Fig. 17B]** and ~3.5 fold **[Fig. 17C]** respectively as compared to the control.

Unlike 0.5 mM ac. $NaNO_2$, the expression level of *ADH1* **[Fig. 18A]** and *ADH2* **[Fig. 18B]**, were not significantly increased but the gene expression of *ADH3* **[Fig. 18C]** was increased by ~4 fold in the presence of 0.25 mM GSNO.

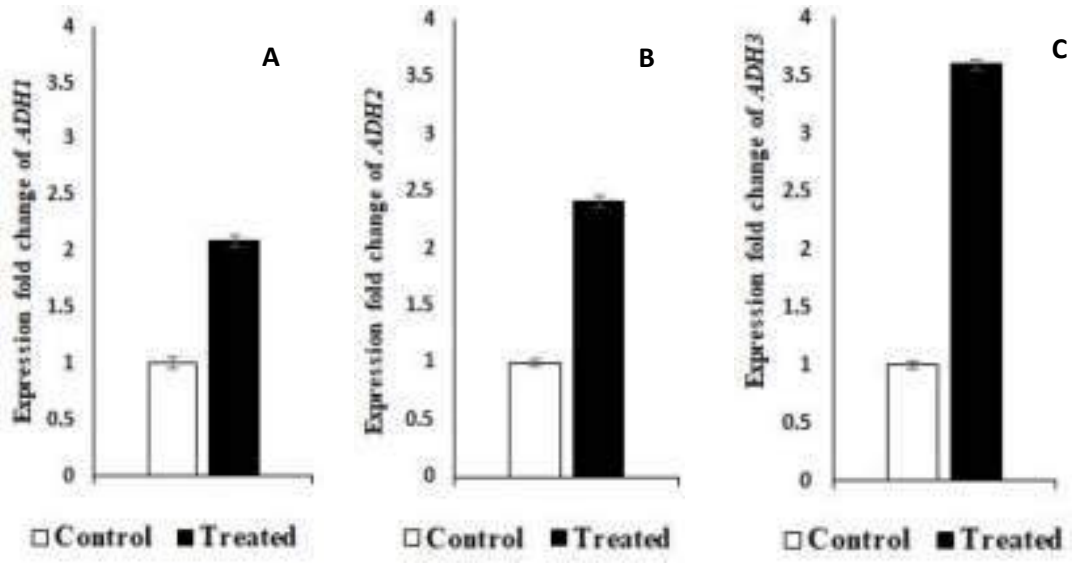

Fig. 17 (A) Effect of 0.5 mM acidified sodium nitrite on relative gene expression of *ADH1*, **(B)** relative gene expression of *ADH2*, **(C)** relative gene expression of *ADH3*. The expression level of *ADH1*, *ADH2* and *ADH3* genes were normalized with that of *GAPDH* (glyceraldehyde-3-phosphate dehydrogenase) in each set and expressed as the change in relative fold change as compared to the control. Supporting information are mentioned in Table S3, S4 and S5.

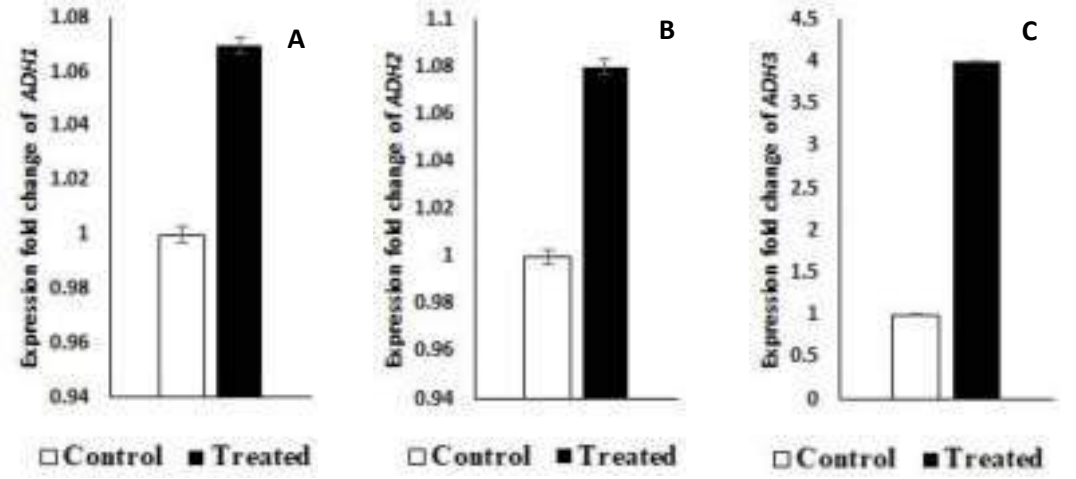

Fig. 18 (A) Effect of *S*-nitrosoglutathione on relative gene expression of *ADH1* **(B)** relative gene expression of *ADH2* and **(C)** relative gene expression of *ADH3*. The expression levels of *ADH* genes (*ADH1, ADH2* and *ADH3*) were normalized with that of *GAPDH* (glyceraldehyde-3-phosphate dehydrogenase) in each set and expressed as relative fold change taking the normalized expression level in respective untreated control as unity. Supporting information are mentioned in Table S6, S7 and S8.

***In vitro* Protein tyrosine nitration (PTN) study and activity of pure aconitase and ADH in presence of acidified sodium nitrite:**

To see protein level modification in case of ac. $NaNO_2$ mediated nitrosative stress, formation of PTN, a key marker of redox stress [12, 13] was checked.

Depending on the concentration of ac. $NaNO_2$, PTN was assessed. By performing western blot analysis using 3-nitrotyrosine monoclonal antibody, PTN formation was observed in 0.3 and 0.5 mM ac. $NaNO_2$ treated aconitase but no impression of PTN formation was detected in untreated and 0.1 mM ac. $NaNO_2$ treated aconitase **[Fig. 19A]**. Here, 0.1 mM peroxynitrite treated aconitase was used as the positive control for this study. PTN study with pure ADH showed different result. The impression of PTN formation was only found in 0.1 mM peroxynitrite treated ADH. There was no impression of PTN formation in ac. $NaNO_2$ treated and untreated ADH **[Fig. 19B]**.

The specific activity of aconitase was also reduced with the treatment of higher concentration of acidified sodium nitrite. The reduction in the activity of aconitase was found to be the highest in 0.1 mM peroxynitrite treated sample **[Fig. 19A]**. The specific activity of ADH was found to be unaltered in acidified sodium nitrite treated samples as compared to untreated ADH but the specific activity of 0.1 mM peroxynitrite treated ADH was drastically decreased as compared to the untreated ADH **[Fig. 19B]**.

***In vitro S*-nitrosylation study and activity of pure aconitase and ADH in presence of acidified sodium nitrite:**

As GSNO is a nitrosylating agent thus *in vitro* formation of *S*-nitrosylation, an important biomarker of nitrosative stress, was checked in pure aconitase and ADH using *S*-nitrosylation western blot kit (Thermo-fisher). Here, strong signal of *S*-nitrosylation in 0.1 mM and 0.25 mM GSNO-treated aconitase was found **[Fig. 20]** but no impression of *S*-nitrosylation was recorded in GSNO-treated ADH samples (data not shown). In addition to it, the specific activity of GSNO-treated samples was drastically dropped. Whereas no significant decrease in activity was found in GSNO-treated ADH samples.

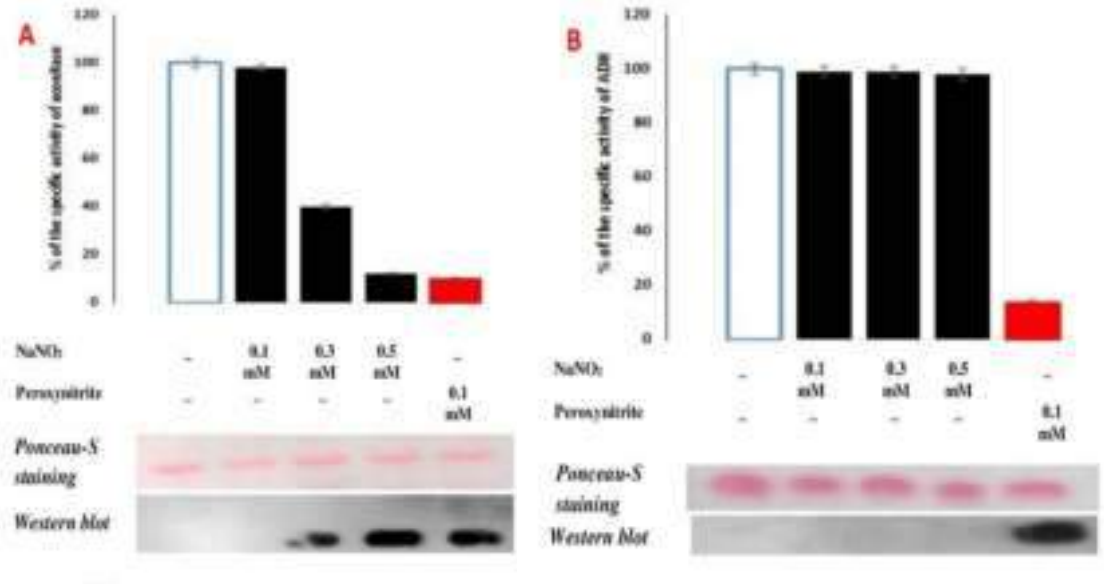

Fig. 19 Effect of different concentrations of acidified sodium nitrite (0.1, 0.3, 0.5 mM) and 0.1 mM peroxynitrite on the specific activity of pure proteins (aconitase and alcohol dehydrogenase) along with the protein tyrosine nitration (PTN) formation: **(A)** Western blotting for PTN and specific activity of aconitase. **(B)** Western blotting for PTN and specific activity of alcohol dehydrogenase. Data are expressed as the change in the percentage of specific activity as compared to the control. The assays were performed in triplicate and expressed as mean±SD. Western blot analysis for PTN was done by using anti 3-nitrotyrosine as the primary antibody and HRP conjugated goat anti-mouse IgG as the secondary antibody.

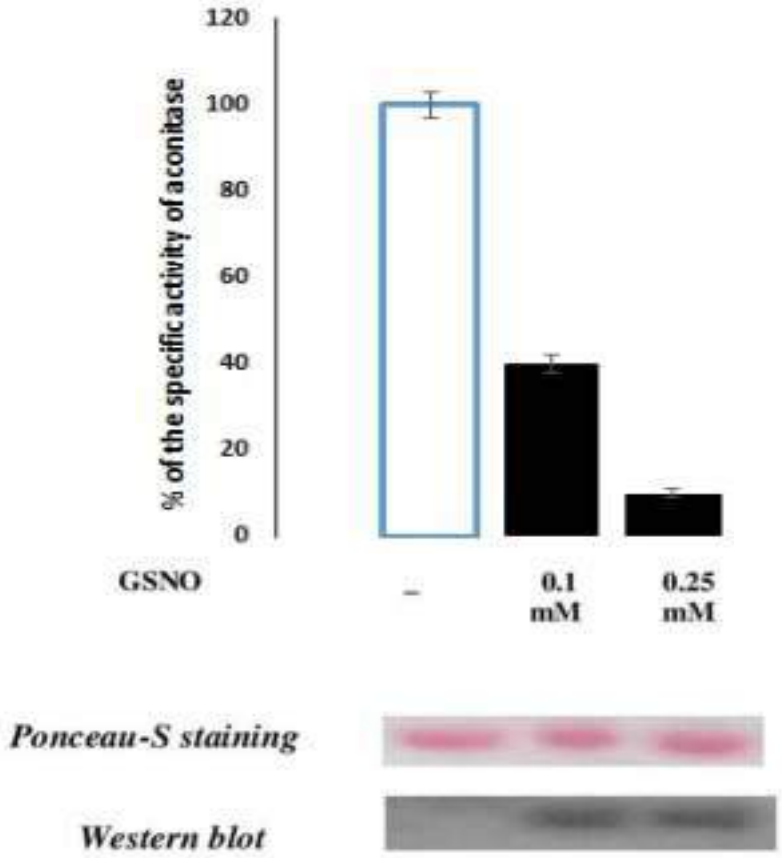

Fig. 20 Effect of different concentrations of *S*-nitrosoglutathione (0.1, 0.25 mM) on the specific activity of aconitase along with *S*-initrosylation formation: Data are expressed as the change in the percentage of specific activity as compared to the control. The assays were performed in triplicate and expressed as mean±SD. Western blot analysis for *S*-initrosylation was done by using anti-TMT as the primary antibody and HRP conjugated goat anti-mouse IgG as the secondary antibody.

Discussion:

Under the sub-toxic dose of GSNO or ac. $NaNO_2$, aconitase activity dropped significantly. As mentioned earlier, aconitase is a well-known redox stress marker [9]. This enzyme contains a Fe-S cluster in its active site. According to the evidences, oxidation of the active $[4Fe\text{-}4S]^{2+}$ can take place in presence of GSNO and paramagnetic cluster $[3Fe\text{-}4S]^{1+}$, is formed, resulting in the complete inactivation of the enzyme [14, 15]. *In vitro S*-nitrosylation formation in GSNO-treated aconitase samples also supports our findings. Whereas, western blot analysis with pure aconitase, revealed that PTN formation might be the cause of the reduced activity of aconitase under 0.5 mM ac. $NaNO_2$ stress. Tyrosine nitration generally contributes to the generation of additional negative charge to the protein and also adds comparatively bulky substituents to the protein which may lead to the alteration of local charge distribution as well as the configuration [16]. Thus, it can be deduced that 0.3 and 0.5 mM acidified sodium nitrite treatment induced PTN formation which triggered the alteration of configuration that might lead to the partial inhibition of aconitase. In addition to it, the gene expression study with 0.5 mM ac. $NaNO_2$, showed an interesting result. *ACO1* gene expression was found to be increased in presence of 0.5 mM acidified sodium nitrite. The major function of ACO1p is the conversion of citrate to isocitrate but this protein is also involved in different unrelated cellular processes, thus it acts as a moonlighting protein in yeast [17]. Among the different activities, maintaining of the mitochondrial DNA integrity is one of the important function of the ACO1p [17-19]. Hence, the higher expression of the *ACO1* indicated that the activity of ACO1p was required to maintain the mitochondrial DNA integrity in presence of 0.5 mM ac. $NaNO_2$ mediated nitrosative stress under the specified experimental condition. Unlike *ACO1*, the gene expression of *ACO2* was decreased by 50%, suggesting, 0.5 mM ac. $NaNO_2$ might affect the glucose metabolism via the TCA cycle. Altogether these results indicated that energy generation through the TCA cycle might be challenged under nitrosative stress. Because of the partial inhibition of aconitase, functioning of TCA cycle might be hampered. Thus, there was a possibility that cells might shift their metabolic flux towards formation of ethanol to increase reduced equivalent as the form of NADH inside the cell which may help to restore its cellular viability. Interestingly, increase in ethanol concentration was observed with higher glucose consumption under such condition that supports our hypothesis.

As ethanol production was increased significantly, hence, the activity of alcohol dehydrogenase (ADH) was estimated. Under nitrosative stress, the activity of ADH was increased significantly which supports the previous finding i.e. higher ethanol production. Further, the reason for this biochemical change was investigated. There were two possibilities of such modulations- either through higher expression of *ADH* genes (*ADH1*, *ADH2* and *ADH3*) or structural modification of ADH. To examine any structural modification, activity of ADH of GSNO or ac. $NaNO_2$ treated CFE was determined and compared with the activity of ADH of untreated CFE. Interestingly, CFE, treated with GSNO or ac. $NaNO_2$, showed no changes in ADH activity as compared to the ADH activity of untreated CFE. In addition, no impression of PTN was found in the presence of ac. $NaNO_2$, though Peroxynitrite, a potent nitrating agent, mediated inactivation of ADH was also reported earlier [20]. Again, no impression of *S*-nitrosylation formation was found in GSNO-treated ADH samples. Altogether these results suggest protein-level modification of ADH may not be possible in the presence of GSNO or ac. $NaNO_2$, probably due to the unavailability of suitable tyrosine and cysteine residue for nitration and *s*-nitrosylation respectively. Hence, next, the expression level of *ADH* genes (*ADH1*, *ADH2* and *ADH3*). were quantified.

In *S. cerevisiae*, ADH1 and ADH3 are mainly involved in ethanol production by using acetaldehyde as the substrate whereas ADH2 is involved in the reverse reaction i.e. production of acetaldehyde from ethanol [21]. Here, a significant increase in the expression level of *ADH3* in presence of 0.5 mM ac. $NaNO_2$ or 0.25 mM GSNO was found. A previous report showed higher ethanol production in *Dekkera bruxellensis* due to the overexpression of *ADH3* [21]. Thus, it can be concluded that ADH3 might have one of the most important role in ethanol production under nitrosative stress at least under the specified experimental condition. Interestingly, expression levels of *ADH1* and *ADH2* were only significantly increased in presence of 0.5 mM ac. $NaNO_2$. Unlike 0.5 mM ac. $NaNO_2$, almost no change in the expression of *ADH1* and *ADH2* were found in presence of 0.25 mM GSNO. The expression of *ADH2* was induced in presence of 0.5 mM ac. $NaNO_2$, which indicates that cells might be trying to utilize ethanol as a carbon source [22]. The activity of ADH2 might help to generate reducing equivalent in the form of NADH and maintain the redox status of the cell [23]. Overall, these results indicated probable metabolic reprogramming.

References:

1. Bartesaghi S, Radi R. (2018) Fundamentals on the biochemistry of peroxynitrite and protein tyrosine nitration. Redox Biol. 14:618-625.

2. Phaniendra A, Jestadi DB, Periyasamy L. (2015) Free radicals: properties, sources, targets, and their implication in various diseases. Indian J Clin Biochem. 30:11-26.

3. Coleman JW. (2001) Nitric oxide in immunity and inflammation. Int Immunopharmacol. 1:1397-406.

4. Abello N, Kerstjens HA, Postma DS, Bischoff R. (2009) Protein tyrosine nitration: selectivity, physicochemical and biological consequences, denitration, and proteomics methods for the identification of tyrosine-nitrated proteins. J Proteome Res. 8:3222-38.

5. Ying T, Jinsong G, Dong W, Kaile W, Jue Z, Jing F (2017) The potential regulatory effect of nitric oxide in plasma activated water on cell growth of *Saccharomyces cerevisiae*. J Appl Phys. 122:123302.

6. Sahoo R, Sengupta R, Ghosh S. (2003) Nitrosative stress on yeast: inhibition of glyoxalase-I and glyceraldehyde-3-phosphate dehydrogenase in the presence of GSNO. Biochem Biophys Res Commun. 302:665-70.

7. Radi R. (2018) Oxygen radicals, nitric oxide, and peroxynitrite: Redox pathways in molecular medicine. Proc Natl Acad Sci U S A. 115:5839-5848.

8. Lushchak OV, Inoue Y, Lushchak VI. (2010) Regulatory protein Yap1 is involved in response of yeast *Saccharomyces cerevisiae* to nitrosative stress. Biochemistry (Mosc). 75:629-64.

9. Lushchak OV, Piroddi M, Galli F, Lushchak VI. (2014) Aconitase post-translational modification as a key in linkage between Krebs cycle, iron homeostasis, redox signaling, and metabolism of reactive oxygen species. Redox Rep. 19:8-15.

10. Okuda T, Naruo M, Iijima O, Igarashi T, Katsuyama M, Maruyama M, Akimoto T, Ohno Y, Haseba T. (2018) The Contribution of Alcohol Dehydrogenase 3 to the Development of Alcoholic Osteoporosis in Mice. J Nippon Med Sch. 85:322-329.

11. Staab CA, Alander J, Brandt M, Lengqvist J, Morgenstern R, Grafström RC, Höög JO. (2008) Reduction of S-nitrosoglutathione by alcohol dehydrogenase 3 is facilitated by substrate alcohols via direct cofactor recycling and leads to GSH-controlled formation of glutathione transferase inhibitors. Biochem J. 413:493-504.

12. Corpas FJ, Chaki M, Leterrier M, Barroso JB. (2009) Protein tyrosine nitration: a new challenge in plants. Plant Signal Behav. 4:920-3.

13. Cipak Gasparovic A, Zarkovic N, Zarkovic K, Semen K, Kaminskyy D, Yelisyeyeva O, Bottari SP. (2017) Biomarkers of oxidative and nitro-oxidative stress: conventional and novel approaches. Br J Pharmacol. 174:1771-83.

14. Castro L, Tórtora V, Mansilla S, Radi R. (2019) Aconitases: Non-redox Iron-Sulfur Proteins Sensitive to Reactive Species. Acc Chem Res. 52:2609-19.

15. Han D, Canali R, Garcia J, Aguilera R, Gallaher TK, Cadenas E. (2005) Sites and mechanisms of aconitase inactivation by peroxynitrite: modulation by citrate and glutathione. Biochemistry. 44:11986-96.

16. Radi R. (2018) Oxygen radicals, nitric oxide, and peroxynitrite: Redox pathways in molecular medicine. Proc Natl Acad Sci U S A. 115:5839-5848.

17. Gancedo C, Flores CL, Gancedo JM. (2016) The Expanding Landscape of Moonlighting Proteins in Yeasts. Microbiol Mol Biol Rev. 80:765-77.

18. Chen XJ, Wang X, Butow RA. (2007) Yeast aconitase binds and provides metabolically coupled protection to mitochondrial DNA. Proc Natl Acad Sci U S A. 104:13738-43.

19. Yazgan O, Krebs JE. (2012) Mitochondrial and nuclear genomic integrity after oxidative damage in Saccharomyces cerevisiae. Front Biosci (Landmark Ed). 17:1079-93.

20. Crow JP, Beckman JS, McCord JM. (1995) Sensitivity of the essential zinc-thiolate moiety of yeast alcohol dehydrogenase to hypochlorite and peroxynitrite. Biochemistry. 34:3544-52.

21. Schifferdecker AJ, Siurkus J, Andersen MR, Joerck-Ramberg D, Ling Z, Zhou N, Blevins JE, Sibirny AA, Piškur J, Ishchuk OP. (2016) Alcohol dehydrogenase gene ADH3 activates glucose alcoholic fermentation in genetically engineered *Dekkera bruxellensis* yeast. Appl Microbiol Biotechnol. 100:3219-31.

22. Wasungu KM, Simard RE. (1982) Growth characteristics of bakers' yeast in ethanol. Biotechnol Bioeng. 24:1125-34.

23. Maestre O, García-Martínez T, Peinado RA, Mauricio JC. (2008) Effects of ADH2 overexpression in *Saccharomyces bayanus* during alcoholic fermentation. Appl Environ Microbiol. 74:702-7.

Chapter 4

Quantification and analysis of different key enzymes involved in glucose metabolism including ethanol fermentation under nitrosative stress

Introduction:

Saccharomyces cerevisiae cells have multiple and diversified mechanisms to regulate metabolic enzymes for adjusting metabolism under the different perturbations like genetic and environmental stresses, broadly termed as 'metabolic reprogramming' [1]. Several factors like transcriptional regulation, alteration in protein concentration, enzymatic activity, post translational modification, allosteric regulation etc. are mainly involved in metabolic reprogramming [1-4]. Complex interplay of genes expression under different internal and external stimuli or stress also contributes to the process [4].

In yeast cells, carbon metabolism is mainly facilitated via fermentation and TCA cycle. During fermentation, glucose first converts to pyruvate and then get reduced to ethanol, leading to the generation of energy and important intermediates which may act as growth factors. Though *S. cerevisiae* is a Crabtree positive (can generate energy via fermentation in presence of oxygen) yeast but TCA cycle is also very important for this organism to generate ATP, utilize non-fermented sugars, production of the precursors for different biosynthetic pathways and so on [1-3]. Under nitrosative stress, mainly TCA cycle enzymes are severely affected due to the protein modifications like protein tyrosine nitration, *s*-nitrosylation etc., thus, generation of energy under such condition may be hampered [5-8]. In contrast to this, different studies showed that cell viability of *S. cerevisiae* cells was not affected in the presence of sub-toxic dose or lower concentration of RNS [9-11]. But definitive studies regarding the characterization of glucose metabolism along with the metabolic reprogramming under nitrosative stress in *S. cerevisiae*, is not yet well-established.

Hence, in this study, activity of some key enzymes involved in different pathways (TCA cycle, glyoxylate pathway, PDH bypass pathway) of carbon metabolism were investigated under the specified experimental condition to delineate the glucose metabolism in the presence of acidified sodium nitrite. These data were also validated using a bioinformatics tool. This study may prove to be helpful to characterize the metabolic response of *S. cerevisiae* under acidified sodium nitrite mediated nitrosative stress.

Results:

To characterize the glucose metabolism under nitrosative stress, *S. cerevisiae* cells were first grown in YPD medium and then treated with either 0.5 mM ac. $NaNO_2$. Then, the cells were harvested, lysed and cell free-extract were prepared to investigate the activity of different key enzymes by performing enzymatic assays. All these results were compared with the control.

Effect of acidified sodium nitrite on citrate concentration and citrate synthase:

To study the citrate metabolism in the presence of 0.5 mM acidified sodium nitrite, the concentration of citrate and citrate synthase (CS) were assayed. CS is an important enzyme of the TCA cycle which catalyzes an irreversible reaction to form citrate from oxaloacetic acid (OAA) and acetyl-CoA [12]. Here, the concentration of citrate was found to be decreased by approximately 50% (both intracellular and extracellular), indicating that the synthesis of citrate might have decreased under stress condition **[Fig. 21A]**. Hence, the activity of CS was assayed. Here, the specific activity of CS was seen to be decreased by approximately 50% under the stress condition as compared to the control **[Fig. 21B]**, suggesting, the citrate metabolism as well as the TCA cycle might be hampered in the presence of 0.5 mM acidified sodium nitrite.

Effect of acidified sodium nitrite on key enzymes of glucose metabolism:

As the specific activity of CS was significantly affected in presence of 0.5 mM acidified sodium nitrite, thus next the utilization of pyruvate was checked via TCA cycle by assaying two important enzymes pyruvate dehydrogenase (PDH) [which catalyzes the conversion from pyruvate to acetyl-CoA] [12] and an anaplerotic enzyme pyruvate carboxylase (PC) [which catalyzes the formation of OAA from pyruvate] [12]. Interestingly, the specific activity of PDH and PC were observed to be decreased by approximately 50% and 15% respectively in the presence of 0.5 mM acidified sodium nitrite in comparison to the control **[Fig. 22A & B]**. Next, the fate of OAA in the TCA cycle was investigated. Therefore, the specific activity of malate dehydrogenase (MDH) which catalyzes the reversible conversion of OAA to malate, was assessed. Interestingly, it was found that the specific activity of MDH sharply increased by approximately 1.3 fold under the stress condition in comparison to the control **[Fig. 22C]**, indicating, TCA cycle was amortized under the stress condition but the higher

activity of MDH revealed that the conversion of oxaloacetic acid to malate might increase under 0.5 mM acidified sodium nitrite mediated nitrosative stress. On the other hand, ethanol production was also found to be increased under the same condition. These two phenomena jointly indicated towards a possibility of shifting of metabolic flux towards pyruvate under nitrosative stress. Hence, to check that, the activity of MDH (decarboxylating), that catalyzes the conversion of malate to pyruvate, was assayed. Here, ~1.3 fold increase in specific activity of MDH (decarboxylating) was observed in 0.5 mM ac. $NaNO_2$ treated cells **[Fig. 22D]**. Furthermore, specific activity of pyruvate decarboxylase (PDC) that catalyzes the conversion from pyruvate to acetaldehyde, was also determined. Here, a sharp 3.2 fold increase in the specific activity of PDC was found in the treated cells **[Fig. 22E]**, suggesting shifting of metabolic flux towards fermentation in presence of 0.5 mM ac. $NaNO_2$. In addition to it, a sharp decrease in the specific activity of isocitrate dehydrogenase (~50%) was observed in the treated cells. **[Fig. 22F]**. Isocitrate dehydrogenase (ICDH) is an important rate-limiting enzyme of TCA cycle [12]. Thus, it can be deduced from the obtained data that TCA cycle might be affected in presence of 0.5 mM ac. $NaNO_2$. Thus, next the activity of aldehyde dehydrogenase (ALDH), an important enzyme for the PDH-bypass pathway, was assessed [13]. Here, the activity of ALDH was found to be decreased by approximately 64% in the treated cell as compared to control **[Fig. 22G]**. Further, the activity of malate synthase (MS), an important enzyme of glyoxylate shunt (an anaplerotic variant of TCA cycle) [14], was also assessed and it was observed that the activity of malate synthase was decreased by approximately 40% under the stress condition **[Fig. 22H]**.

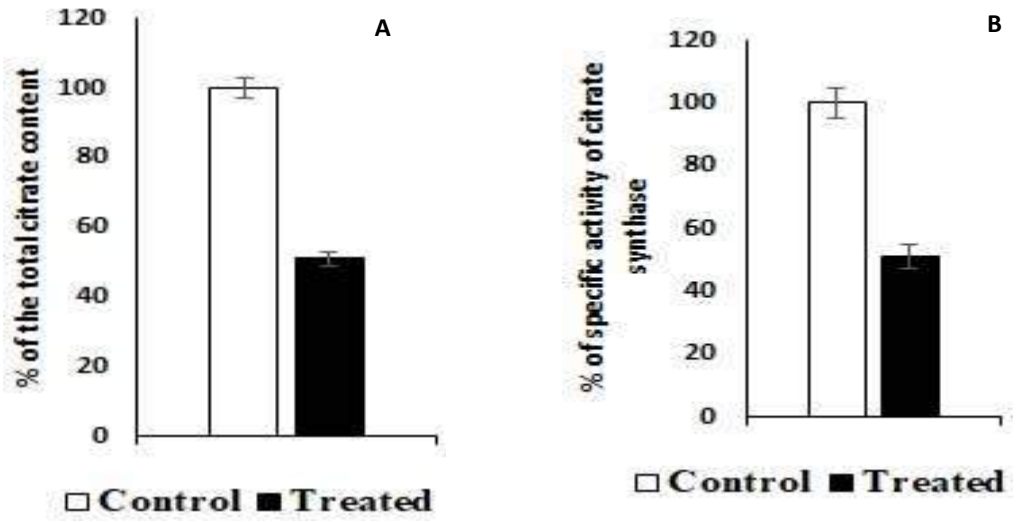

Fig. 21 Effect of 0.5 mM acidified sodium nitrite on **(A)** the total citrate content (Extracellular and Intracellular), and **(B)** specific activity of citrate synthase. Data are expressed as the change in the percentage of specific activity as compared to the control. Assays were performed in triplicate and expressed as the mean±SD. Supporting information regarding citrate content are mentioned in Table S9.

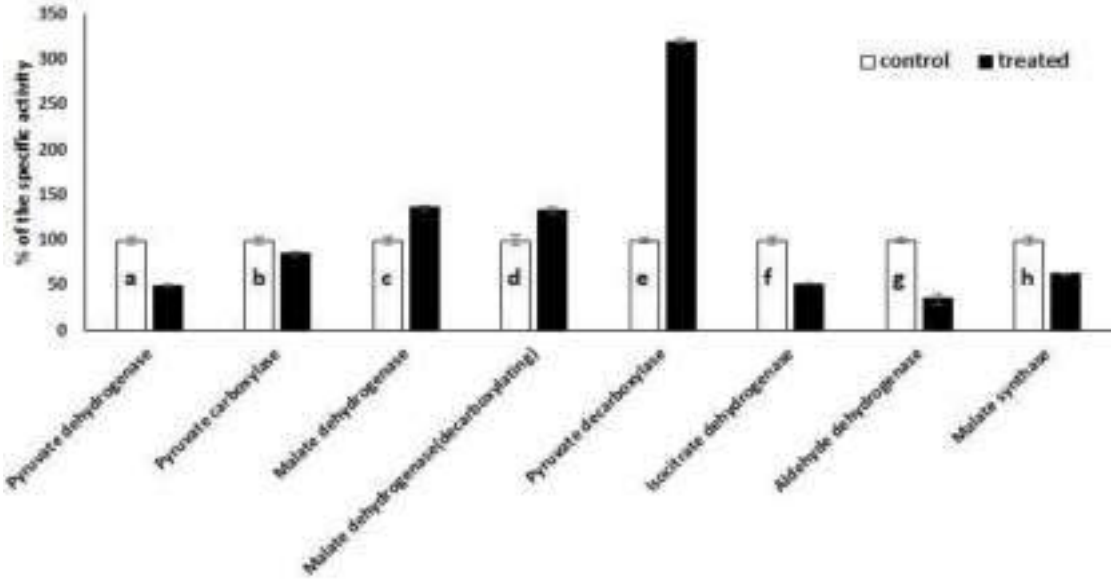

Fig. 22 Effect of 0.5 mM acidified sodium nitrite on the specific activity of **(A)** Pyruvate dehydrogenase **(B)** Pyruvate carboxylase, **(C)** Malate dehydrogenase, **(D)** Malate dehydrogenase (decarboxylating), **(E)** Pyruvate decarboxylase, **(F)** Isocitrate dehydrogenase, **(G)** Aldehyde dehydrogenase, **(H)** Malate synthase. Data are expressed as the change in the percentage of specific activity as compared to the control. Assays were done in triplicate and represented as mean±SD.

Network and functional annotation studies with the altered protein activities:

Network and functional annotation studies were performed to validate our findings that were obtained from different enzymatic assays. Under nitrosative stress, the enzymes with altered activity, were subjected for the analysis. It was found that malate dehydrogenase and pyruvate decarboxylase predominantly participated in the activated enzyme network with the highest number of connections **[Fig. 23A]**. Due to the higher activity of these two enzymes, it was predicted that yeast cellular system might be involved primarily in biological processes such as pyruvate metabolic process, malate metabolic process, and gluconeogenesis **[Table 7]** whereas the highest connectivity was found in citrate synthase, isocitrate lyase, pyruvate dehydrogenase and aconitase in the network generated by the enzymes with decreased activity under nitrosative stress **[Fig. 23B]**. In connection with the downregulated enzymes, TCA cycle, glyoxylate cycle, glutamate biosynthetic process, and acetate biosynthetic process were predicted to be negatively affected under the stress condition. From the point of view of cellular component, the enzymes at mitochondrial matrix or Mitochondrion, were predicted to be the most abundant. In addition to this, the activity of malate dehydrogenase activity and alcohol dehydrogenase (NAD) were predicted as the most enriched molecular functions in the treated yeast cells. On the other hand, molecular functions with the aldehyde dehydrogenase activity, transferase activity, transferring acyl groups, acyl groups converted into alkyl, and lyase activity, were predicted to be downregulated due to the decreased activity of these enzymes **[Table 7]**.

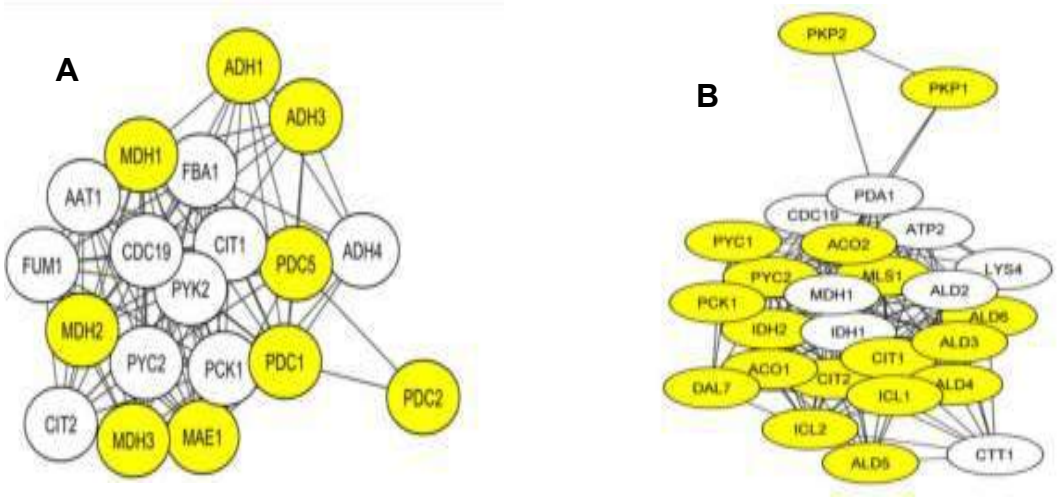

Fig. 23 Network representation of enzymes in the presence of 0.5 mM acidified sodium nitrite. **(A)** Network representation of enzymes with increased activities and **(B)** Network representation of enzymes with decreased activities. Highlighted colour denotes the enzymes with experimentally validated activities.

Table 7. Functional enrichment by activation/ deactivation of enzymes

	Term	% of genes	P-Value	Benjamini adjusted P-Value
Enrichment by activated enzymes due to stress				
Biological Process	pyruvate metabolic process	31.6	3.8E-10	8.7E-9
	malate metabolic process	26.3	3.8E-10	8.7E-9
	Fermentation	10.5	9.7E-3	4.0E-2
Cellular Components	mitochondrial matrix	31.6	3.1E-5	4.1E-4
	cytosol	42.1	2.1E-2	9.0E-2
Molecular Function	malate dehydrogenase activity	15.8	3.8E-5	6.1E-4
	alcohol dehydrogenase (NAD) activity	15.8	1.9E-4	2.3E-3
	Pyruvate kinase activity	26.3	3.6E-4	3.5E-3
Enrichment by deactivated enzymes due to stress				
Biological Process	tricarboxylic acid cycle	38.5	2.8E-15	1.5E-13
	glyoxylate cycle	19.2	6.6E-8	1.2E-6
	acetate biosynthetic process	11.5	1.2E-4	9.1E-4
Cellular Components	Peroxisomal matrix	42.3	4.3E-11	9.0E-10
	mitochondrial nucleoid	15.4	1.3E-4	9.2E-4
Molecular Function	aldehyde dehydrogenase activity	19.2	1.7E-7	9.3E-6
	transferase activity, transferring acyl groups, acyl groups converted into alkyl on transfer	15.4	9.8E-6	1.3E-4
	lyase activity	23.1	1.1E-4	9.7E-4

Discussion:

Under the sub-toxic dose of acidified sodium nitrite, the activity of some of the TCA cycle enzymes were found to be decreased significantly. Among the enzymes of the TCA cycle, CS is very important for mitochondrial functioning. Hence, the reduction

in the specific activity of CS in presence of 0.5 mM acidified sodium nitrite, indicated that the mitochondrion functioning was highly affected under nitrosative stress [15]. In addition to it, reduction in the activity of ICDH (catalyzes the conversion from isocitrate to α-ketoglutarate) [12], and PDH (catalyzes the conversion from pyruvate to acetyl CoA) [12], pointed towards depletion in citrate metabolism under nitrosative stress. Previous reports suggest that ICDH and PDH activity can be affected under redox stress i.e. oxidative and nitrosative stress [16, 17]. Formation of acetyl CoA is the vital factor for the shifting of glucose metabolic flux towards respiration [12]. The formation of acetyl-CoA can also occurr by a PDH-independent alternative pathway known as PDH-bypass pathway where the activity of PDC, ALDH are required among other enzymes [13]. Reduction in the activity of ALDH (oxidizes acetaldehyde to acetate [13]) might affect the acetyl-CoA production. In addition, lower availability of acetyl-CoA might also affect the activity of MS under stress condition. MS is an important enzyme of glyoxylate cycle, an anaplerotic variant of TCA cycle present in *S. cerevisiae* [14]. Hence, reduced activity of MS might also affect the glyoxylate cycle. Acetyl-CoA can also act as the positive allosteric modulator of PC, important anaplerotic enzyme [18]. It replenishes the intermediates of TCA cycle by catalyzing the reaction from pyruvate to oxaloacetic acid [12]. Thus, lower production of acetyl-CoA in presence of 0.5 mM acidified sodium nitrite, might interfere with the activity of PC [12, 18]. Hence, it can be concluded that the requirement for the replenishment of the intermediates of TCA cycle might be affected in presence of 0.5 mM acidified sodium nitrite, suggesting reduction in TCA cycle under nitrosative stress.

The elevated activity of MDH and MDH (decarboxylating) in presence of 0.5 mM acidified sodium nitrite suggested the possibility that OAA, formed by the activity of PC, might have been rerouted to pyruvate via malate formation. Hence, it can be understood that the flow of glucose metabolic flux towards the TCA cycle was reduced. Previous report also suggests that malate can cross the mitochondrial membrane but OAA cannot [12]. Thus, it can be understood that MDH activity was upregulated to form malate from OAA and subsequent conversion of malate to pyruvate by the activity of MDH (decarboxylating) under nitrosative stress. Though the affinity of MDH (decarboxylating) is very low (K_m= **50 mM),** but the activity of this enzyme can be induced in *S. cerevisiae* under adverse conditions like starvation [19]. This enzyme is also involved in accumulating the intracellular flux of NADPH [20], an important factor

of stress response [21], suggesting the role of MDH (decarboxylating) as a stress response enzyme. On the other hand, MDH can also participate in the generation of cytosolic NADH, an important factor of antioxidant system and energy metabolism [12, 22]. Therefore, it can be understood that in presence of 0.5 mM acidified sodium nitrite, when TCA cycle was heavily affected, higher activity of the MDH and MDH (decarboxylating) contributed for the generation of energy intermediates which in turn shifted the glucose metabolic flux towards fermentation. It has also been reported earlier that the activity of MDH (decarboxylating) can be upregulated during alcoholic fermentation in *S. cerevisiae* [23]. Report also suggest that the activity of MDH (decarboxylating) can be strongly induced at the time of switching of the metabolic flux from respiration to fermentation in *S. cerevisiae* [24]. In addition to it, the higher activity of PDC and ADH under stress condition also suggested the upregulation of ethanol fermentation. Thus, a metabolic reprogramming via shifting of metabolic flux from respiration to fermentation might have taken place in *S. cerevisiae* under acidified sodium nitrite mediated nitrosative stress. A model of metabolic reprogramming in *S. cerevisiae* in the presence of 0.5 mM acidified sodium nitrite mediated nitrosative stress, is proposed in **Fig. 24**.

To validate our findings, the wet lab data were also subjected for functional enrichment analyses and fermentation was predicted as one of the most activated biological processes under the experimental condition, clearly corroborating with the findings. In addition, malate metabolic process and pyruvate metabolic process were also predicted to be upregulated biological process whereas TCA cycle, glyoxylate shunt were predicted to be downregulated under such condition, clearly indicating towards higher ethanol production in *S. cerevisiae* under 0.5 mM acidified sodium nitrite mediated nitrosative stress. This metabolic reprogramming might not only be very important for the energy generation but it seemed like a part of the nitrosative stress response strategies. This reprogrammed glucose metabolism might be coupled with the cellular antioxidant machinery to overcome the stress condition. Hence, the cell viability was not significantly altered in 0.5 mM acidified sodium nitrite treated cells as compared to the control.

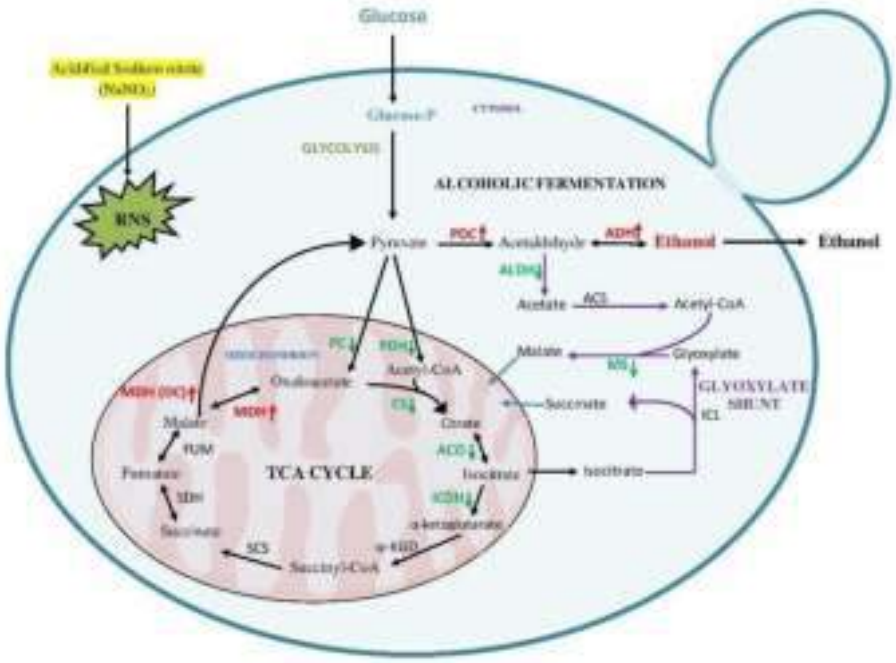

Fig. 24 Proposed switching of glucose metabolism in the presence of 0.5 mM acidified sodium nitrite. green arrows represent upregulated enzymes and red arrows represent downregulated enzymes in the presence of 0.5 mM acidified sodium nitrite. In this condition, energy generation through TCA cycle was compromised due to the lower activity of pyruvate dehydrogenase (PDH), citrate synthase (CS), aconitase (ACO), isocitrate dehydrogenase (ICDH), pyruvate carboxylase (PC) but the glucose metabolic flux was rerouted via higher activity of malate dehydrogenase (MDH) and malate dehydrogenase (decarboxylating) [MDH(DC)] towards pyruvate which was further metabolized via the fermentative pathway with the help of higher activity of pyruvate decarboxylase (PDC) and alcohol dehydrogenase (ADH) which resulted in higher production of ethanol. In addition to it, activity of malate synthase (MS) and aldehyde dehydrogenase (ALDH) were also reduced that might affect the glyoxylate shunt (an anaplerotic variant of TCA cycle) and PDH-bypass pathway (an alternative route of acetyl-CoA synthesis without the activity of PDH).

References:

1. Tripodi F, Nicastro R, Reghellin V, Coccetti P. (2015) Post-translational modifications on yeast carbon metabolism: Regulatory mechanisms beyond transcriptional control. Biochim Biophys Acta. 1850:620-7.

2. Turcotte B, Liang XB, Robert F, Soontorngun N. (2010) Transcriptional regulation of nonfermentable carbon utilization in budding yeast. FEMS Yeast Res. 10:2-13.

3. Schüller HJ. (2003) Transcriptional control of nonfermentative metabolism in the yeast Saccharomyces cerevisiae. Curr Genet. 43:139-60.

4. Winter G, Krömer JO. (2013) Fluxomics - connecting 'omics analysis and phenotypes. Environ Microbiol. 15:1901-16.

5. Phaniendra A, Jestadi DB, Periyasamy L. (2015) Free radicals: properties, sources, targets, and their implication in various diseases. Indian J Clin Biochem. 30:11-26.

6. Coleman JW. (2001) Nitric oxide in immunity and inflammation. Int Immunopharmacol. 1:1397-406.

7. Abello N, Kerstjens HA, Postma DS, Bischoff R. (2009) Protein tyrosine nitration: selectivity, physicochemical and biological consequences, denitration, and proteomics methods for the identification of tyrosine-nitrated proteins. J Proteome Res. 8:3222-38.

8. Corpas FJ, Palma JM, Del Río LA, Barroso JB. (2013) Protein tyrosine nitration in higher plants grown under natural and stress conditions. Front Plant Sci. 4:29.

9. Ying T, Jinsong G, Dong W, Kaile W, Jue Z, Jing F (2017) The potential regulatory effect of nitric oxide in plasma activated water on cell growth of *Saccharomyces cerevisiae*. J Appl Phys. 122:123302.

10. Nasuno R, Aitoku M, Manago Y, Nishimura A, Sasano Y, Takagi H. (2014) Nitric oxide-mediated antioxidative mechanism in yeast through the activation of the transcription factor Mac1. PLoS One. 9:e113788.

11. Peláez-Soto A, Roig P, Martínez-Culebras PV, Fernández-Espinar MT, Gil JV. (2020) Proteomic Analysis of *Saccharomyces cerevisiae* Response to Oxidative Stress Mediated by Cocoa Polyphenols Extract. Molecules. 25:452.

12. Voet D and Voet JG (1995) *Biochemistry*. 6th edn. J. Wiley & Sons, NY.

13. Remize F, Andrieu E, Dequin S. (2000) Engineering of the pyruvate dehydrogenase bypass in Saccharomyces cerevisiae: role of the cytosolic Mg(2+) and mitochondrial K(+) acetaldehyde dehydrogenases Ald6p and Ald4p in acetate formation during alcoholic fermentation. Appl Environ Microbiol. 66:3151-9.

14. Chew SY, Chee WJY, Than LTL. (2019) The glyoxylate cycle and alternative carbon metabolism as metabolic adaptation strategies of Candida glabrata: perspectives from Candida albicans and Saccharomyces cerevisiae. J Biomed Sci. 26:52.

15. Borys J, Maciejczyk M, Antonowicz B, Krętowski A, Sidun J, Domel E, Dąbrowski JR, Ładny JR, Morawska K, Zalewska A. (2019) Glutathione Metabolism, Mitochondria Activity, and Nitrosative Stress in Patients Treated for Mandible Fractures. J Clin Med. 8:127.

16. Auger C, Lemire J, Cecchini D, Bignucolo A, Appanna VD. (2011) The metabolic reprogramming evoked by nitrosative stress triggers the anaerobic utilization of citrate in Pseudomonas fluorescens. PLoS One. 6:e28469.

17. Ferrer-Sueta G, Campolo N, Trujillo M, Bartesaghi S, Carballal S, Romero N, Alvarez B, Radi R. (2018) Biochemistry of Peroxynitrite and Protein Tyrosine Nitration. Chem Rev. 118:1338-1408.

18. Adina-Zada A, Zeczycki TN, Attwood PV. (2012) Regulation of the structure and activity of pyruvate carboxylase by acetyl CoA. Arch Biochem Biophys. 519:118-30.

19. Redzepovic S, Orlic S, Majdak A, Kozina B, Volschenk H, Viljoen-Bloom M. (2003) Differential malic acid degradation by selected strains of Saccharomyces during alcoholic fermentation. Int J Food Microbiol. 83:49-61.

20. Knuf C, Nookaew I, Brown SH, McCulloch M, Berry A, Nielsen J. (2013) Investigation of malic acid production in Aspergillus oryzae under nitrogen starvation conditions. Appl Environ Microbiol. 79:6050-8.

21. Pollak N, Dölle C, Ziegler M. (2007) The power to reduce: pyridine nucleotides--small molecules with a multitude of functions. Biochem J. 402:205-18.

22. Miyagi H, Kawai S, Murata K. (2009) Two sources of mitochondrial NADPH in the yeast Saccharomyces cerevisiae. J Biol Chem. 284:7553-60.

23. Redzepovic S, Orlic S, Majdak A, Kozina B, Volschenk H, Viljoen-Bloom M. (2003) Differential malic acid degradation by selected strains of Saccharomyces during alcoholic fermentation. Int J Food Microbiol. 83:49-61.

24. Xiao W, Wang RS, Handy DE, Loscalzo J. (2018) NAD(H) and NADP(H) Redox Couples and Cellular Energy Metabolism. Antioxid Redox Signal. 28:251-272.

Chapter 5

Optimization of ethanol production using immobilized stressed *Saccharomyces* cells

Introduction:

The multifaceted application and utility of ethanol is increasing gradually. To meet this acing demands, fermentation technology for the production of ethanol is gaining sharp momentum globally. Though researchers are going on to check the suitability of different microorganisms for ethanol industry, but still yeast is the primary choice for ethanol fermentation [1]. Due to its high production rate, high ethanol tolerance, adaptive nature and ability of fermenting wide range of sugars, yeasts especially *Saccharomyces cerevisiae* is the most common microorganism used in ethanol fermentation industry [2]. Hence, different strains of *S. cerevisiae* were extensively studied to make it more suitable in terms of stress tolerance, ability to adapt, viability etc. for industrial ethanol production [3]. To make it suitable, different engineered strains of *S. cerevisiae* as well as other organisms have been developed [4]. Such metabolic or genetic engineering have some major disadvantages like complexity in developmental methods, high mutation rate, risk of contamination, human safety etc. Moreover, these processes are prohibitively expensive. Hence, there is a need to develop cost-effective, eco-friendly and easy processes for the industrial production of ethanol. On the other hand, immobilization of yeast cells is also gaining interest in ethanol production industry. This technique offers higher yield in less time and also the chance of contamination as well as mutation is very low [3]. Hence this work is mainly focused on developing a cost-effective, eco-friendly approach to improve the ethanol production by exposing *S. cerevisiae* cells to nitrosative stress. These yeast cells can adapt under the stress conditions as per the requirement. Therefore, not only the ability of stress tolerance but also the metabolism may be modified [6, 7] to counteract the stress condition.

Hence, the primary objective of the work was set to develop a cost-effective, non-hazardous, easy approach to improve the ethanol production by using nitrosative stress exposed immobilized *S. cerevisiae* cells.

Results:

To assess the applicability of the approach, 0.5 mM acidified sodium nitrite treated yeast cells were immobilized using calcium chloride and sodium alginate. Immobilized cells were transferred to the minimal medium containing different concentrations of molasses and ammonium sulphate. CCRD-based RSM was applied to find out the optimal condition of ethanol production under the specified experimental set up.

Optimization of ethanol production by central composite rotatable design based (CCRD) response surface methodology (RSM):

Here, concentration of molasses (A), concentration of ammonium sulfate (B), and incubation time (C) were selected as the independent variables and the influence of these independent variables were tested for ethanol production using CCRD based RSM technique. The optimal level for each of the independent variables was determined. 19 experimental runs were performed to optimize the ethanol production and the results are represented in **Table 8** containing both the actual and predicted responses. Analysis of variance (ANOVA) was performed for the above mentioned experimental set up and represented in **Table 9**. p value of the model is 0.003, suggesting, the model is highly significant and it can efficiently predict ethanol production as the actual response. The significant terms of the model are concentration of molasses (A) [$p = 0.0094$], incubation time (C) [$p = 0.0043$], molasses concentration^2 (A^2) [$p = 0.0010$] and incubation time^2 (C^2) [$p = 0.0045$]. By subjecting these results of the experimental set up, a second-order polynomial regression equation was generated by the respective software to estimate the concentration of ethanol that is represented in actual terms.

Table 8: Experimental design along with model predicted and actual ethanol yield response

Run	Factor 1A: C-source (%)	Factor 2B: N- source (%)	Factor 3C: Incubation time (h)	Ethanol Actual (g/L)	Ethanol Predicted (g/L)
1	12.50	1.02	15.00	21.73	21.66
2	5.00	0.05	24.00	7.24	8.79
3	20.00	2.00	6.00	20.26	17.22
4	20.00	2.00	24.00	34.74	34.24
5	12.50	1.02	30.14	28.24	25.11
6	20.00	0.05	6.00	11.52	11.36
7	12.50	2.66	15.00	14.02	18.27
8	5.00	2.00	24.00	11.52	10.19
9	5.00	2.00	30.14	8.68	4.03
10	25.11	1.02	6.00	27.50	27.79
11	12.50	1.02	15.00	21.70	21.66
12	5.00	0.05	6.00	3.15	2.17
13	-0.11	1.02	15.00	0	5.23
14	12.50	1.02	15.00	21.69	21.66
15	12.50	1.02	15.00	21.75	21.66
16	12.50	1.02	-0.14	0	1.80
17	12.50	1.02	15.00	21.75	21.66
18	20.00	0.05	24.00	23.34	26.51
19	12.50	-0.61	15.00	12.35	10.20

Table 9: CCRD based RSM model

Source	Sum of squares	df	Mean square	*F* value	P value prob> F
Model	890.41	9	98.93	7.52	0.0030
A: C-source	142.10	1	142.10	10.80	0.0094
B: N-source	9.99	1	9.99	0.76	0.4061
C: Incubation time	188.79	1	188.79	14.35	0.0043
AB	4.44	1	4.44	0.34	0.5756
AC	26.35	1	26.35	2.00	0.1907
BC	51.01	1	51.01	3.88	0.0805
A2	299.72	1	299.72	22.78	0.0010
B2	113.57	1	113.57	8.63	0.0165
C2	180.27	1	180.27	13.70	0.0045

R1 (Ethanol concentration), Actual = –10.30525+ 1.38894 x A + 5.61195 x B + 1.03751 x C + 0.17658 x AB + 0.035870 x AC + 0.020085 x BC – 0.04312 x A^2 – 2.76112 x B^2 – 0.028324 x C^2

The R^2 value (coefficient of determination) of 0.9377 signifies that the model could predict and explain 93% of the variability. The predicted and adjusted R^2 value were 0.5256 and 0.8817 respectively, presence in a reasonable agreement with each other. Adequate precision ratio of the model is 13.864, showing, high signal to noise ratio. Generally adequate precision ratio of 4 is desirable to judge the significance level of the model. Overall, R^2, adjusted R^2, predicted R^2, and adequate precision ratio were significantly higher which makes the model fit for the prediction of the optimized level of each of the variables used for the actual response i.e. ethanol production.

Comparison of model actual and predicted values for ethanol response (g/L) is presented in **Fig. 25**. The observed and actual values were spread by a line of 45^o (angle) in the plot, suggesting a reasonable aliment of predicted with the actual responses. The response surface plots and their contour plots showed the degree of interactions among three independent variables for ethanol production **[Fig. 26–28]**. The optimal levels of the independent variables were also determined from the second-order polynomial

regression equation, generated from the system. It was found that the ethanol production was significantly increased from 11.88 to 27.54 g/L with the enhanced concentration of molasses (A) ranging from 5 to 20% W/V **[Fig. 26]**, at the fixed concentration of nitrogen source (1.22% W/V). The significance of this factor for ethanol production under the specified experimental condition was also validated by ANOVA (*p* value of 0.0094).

The interaction between the concentration of molasses (A) and incubation time (C) showed a positive effect on ethanol production under the specified experimental condition with a *p* value of 0.0043 **[Fig. 27]**. When the concentration of carbon source was fixed at 20% W/V, ethanol production was significantly enhanced from 16.37 to 32.9 g/L with the gradual increase in incubation time ranging from 6 to 24 h.

In addition to it, The interaction between concentration of ammonium sulfate as the nitrogen source (B) and incubation time (C) didn't show a strong effect on ethanol production **[Fig. 28]** , suggesting, a non-significant (p value of 0.0805) interaction between these two independent variables for ethanol production under the specified experimental set up.

After the rigorous analysis of the interaction among these three independent variables, finally the model was employed to extract the optimized levels of the independent variables for ethanol production under the specified experimental set up. Model predicted that 34.24 g/L ethanol can be produced after 24 h of incubation using medium containing 20% W/V molasses and 1.74% W/V ammonium sulphate. This data mostly corroborated with the wet lab data, where 35.24 g/L ethanol was produced under the same condition.

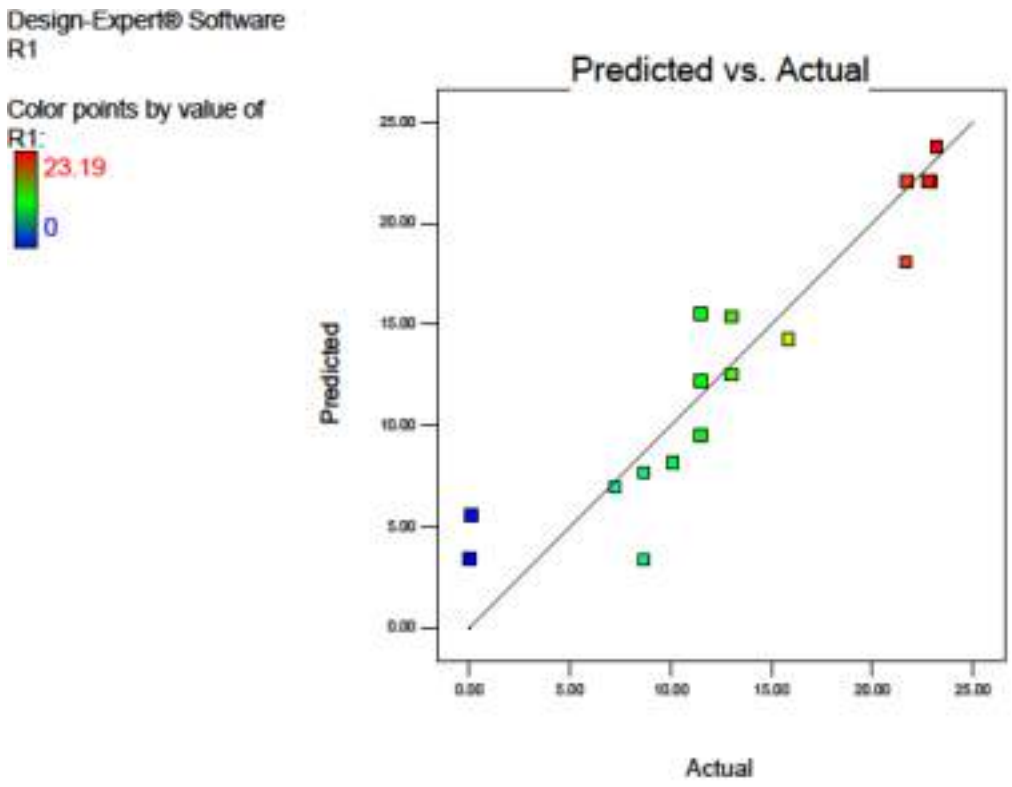

Fig. 25 Plot of actual values versus predicted values

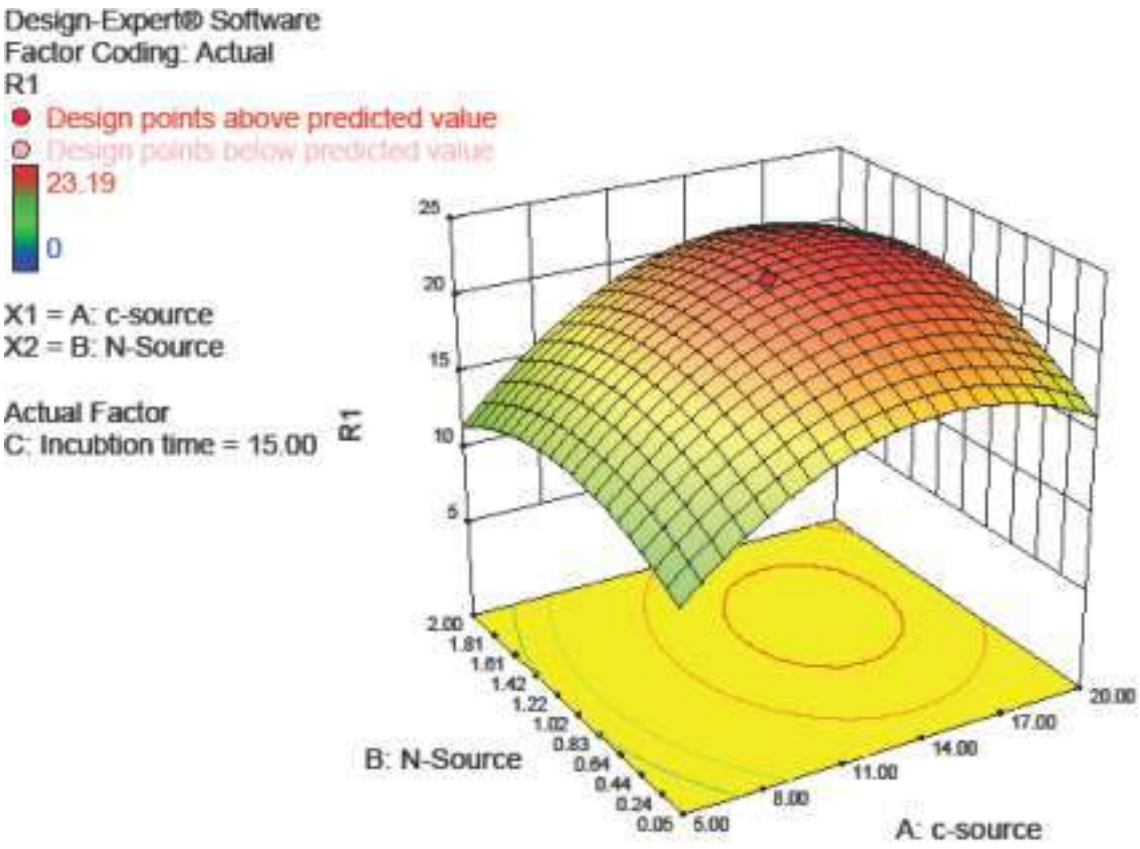

Fig. 26 Surface plot showing the effect of interaction between carbon source (Molasses) and nitrogen source (Ammonium sulfate)

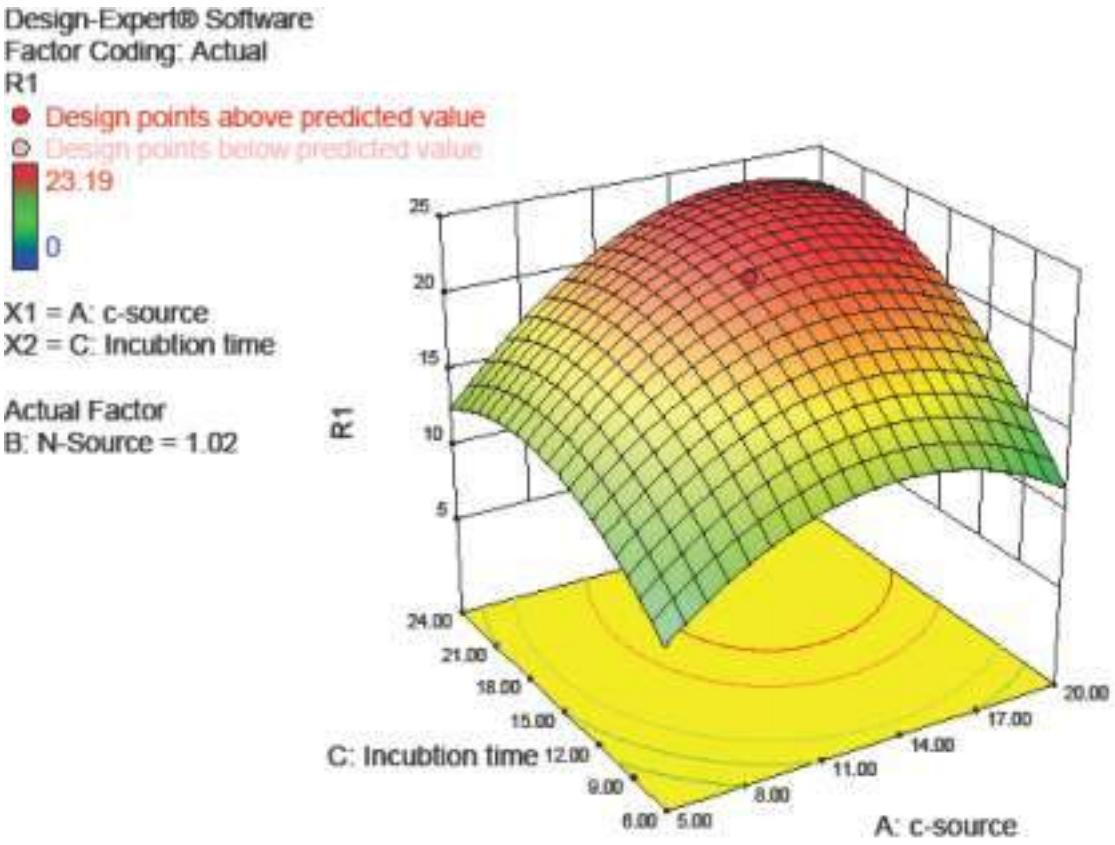

Fig. 27 Surface plot showing the effect of interaction between carbon source (Molasses) and incubation time

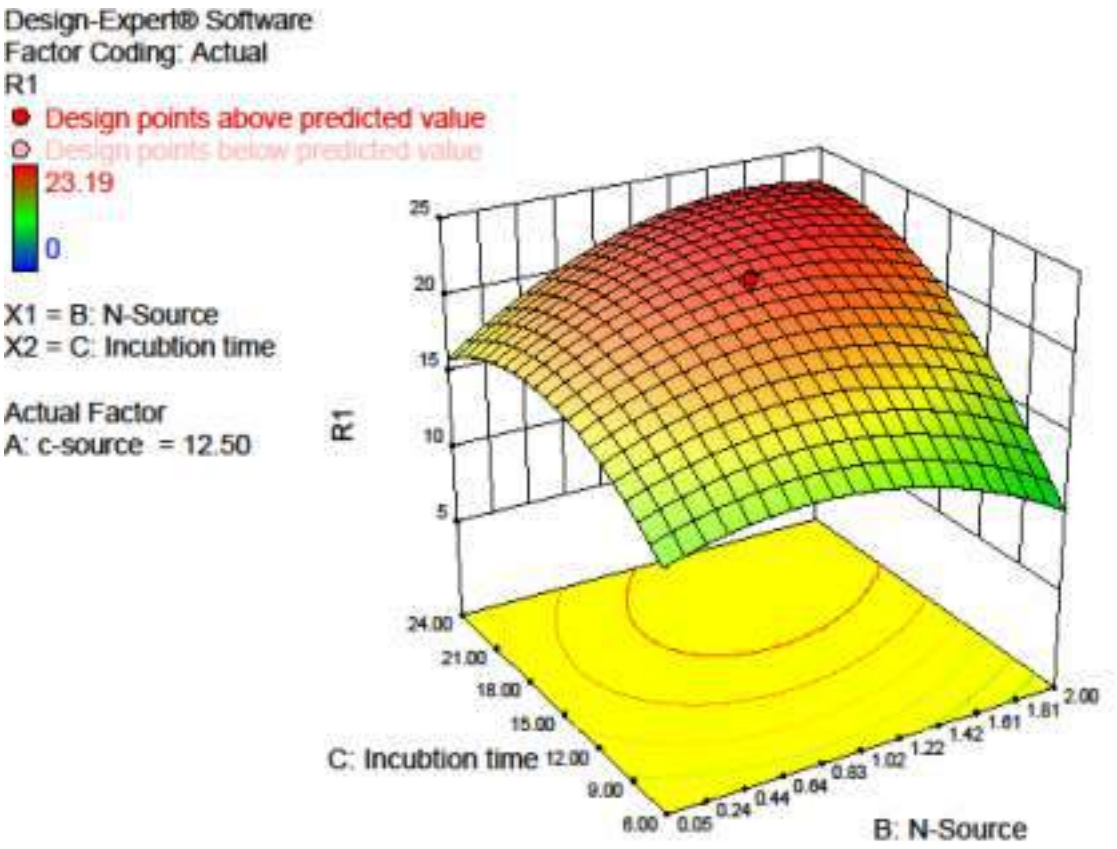

Fig. 28 Surface plot showing the effect of interaction between nitrogen source (Ammonium sulfate) and incubation time

Estimation of ethanol production by nitrosative stress exposed yeast cells grown in YPG and YPD Medium:

Yeast cells were first inoculated in YPD and YPG medium and after three hours 0.5 mM ac. Sodium nitrite was applied. Following an overnight incubation, nitrosative stress exposed cells were immobilized in calcium alginate beads and inoculated in RSM-optimized minimal medium to assess the ability of ethanol production of the nitrosative stress exposed yeast cells. It was found that nitrosative stress exposed

YPD grown yeast cells produced ethanol upto 2nd cycle without significant alteration in the production whereas the production was declined at the 3rd cycle **[Table 10]**. Interestingly, nitrosative stress exposed YPG grown yeast cells produced high concentration of ethanol upto 4th cycle and after that the production was declined significantly **[Table 11]**.

Table 10: Ethanol production by immobilized yeast cells grown in YPD medium

	Immobilization		
No. of cycle	1st	2nd	3rd
Ethanol production (g/L)	33±1	35±2	27±1

Table 11: Ethanol production by immobilized yeast cells grown in YPG medium

	Immobilization					
No. of cycle	1st	2nd	3rd	4th	5th	6th
Ethanol production (g/L)	31±1	36±2	39±1	35±1	24±1	19±1

Discussion:

In this study, to assess the applicability of the major finding of this work i.e. nitrosative stress induced yeast cells produce higher concentration of ethanol, was tried to assess. Hence, the experiments were designed with a view for future industrial application. Thus, minimal medium (containing ammonium sulphate and molasses) and immobilized yeast cells were used. CCRD-RSM software was also used in this work to find out the optimum condition under the specified experimental set up. From the obtained results, it was clear that factors i.e. concentration of molasses as the carbon source (A), concentration of ammonium sulfate as the nitrogen source (B) and incubation time (C) influenced ethanol production independently but their interaction had no significant effect on ethanol production. Moreover, R^2 value of the model was 0.9377 that indicates the excellent fitness of the model (93%). In addition to it, it was observed that nitrosative stress exposed YPG grown immobilized yeast cells produced ethanol more steadily as compared to nitrosative stress exposed YPD grown immobilized yeast cells. This was probably due to the production of higher concentration of ROS and subsequently high production of RNS in YPG medium [8]. Thus, it can be assumed that the altered physiology remained for a longer period of time in nitrosative stress exposed YPG grown immobilized yeast cells as compared to the nitrosative stress exposed YPD grown immobilized yeast cells. This resulted in enhanced ethanol production upto 4^{th} cycle by using nitrosative stress exposed YPG grown immobilized yeast cells.

References:

1. Willaert, RG. (2017) Yeast biotechnology. Fermentation 3:7–10.
2. Mohd Azhar SH, Abdulla R, Jambo SA, Marbawi H, Gansau JA, Mohd Faik AA, Rodrigues KF. (2017) Yeasts in sustainable bioethanol production: A review. Biochem Biophys Rep. 10:52-61.
3. Verbelen PJ, De Schutter DP, Delvaux F, Verstrepen KJ, Delvaux FR. (2006) Immobilized yeast cell systems for continuous fermentation applications. Biotechnol Lett. 28:1515-25.
4. Zaldivar J, Nielsen J, Olsson L. (2001) Fuel ethanol production from lignocellulose: a challenge for metabolic engineering and process integration. Appl Microbiol Biotechnol. 56:17-34.
5. Nevoigt E. (2008) Progress in metabolic engineering of Saccharomyces cerevisiae. Microbiol Mol Biol Rev. 72:379-412.
6. Matallana E, Aranda A. (2017) Biotechnological impact of stress response on wine yeast. Lett Appl Microbiol. 64:103-110.
7. Pretorius IS. (2000) Tailoring wine yeast for the new millennium: novel approaches to the ancient art of winemaking. Yeast. 16:675-729.
8. Macierzyńska E, Grzelak A, Bartosz G. (2007) The effect of growth medium on the antioxidant defense of Saccharomyces cerevisiae. Cell Mol Biol Lett. 12:448-56.

General conclusions...

1. **The sub-toxic doses of acidified sodium nitrite and *S*-nitrosoglutathione were different for *S. cerevisiae*.** Cell viability assay was revealed that the sub-toxic dose of acidified sodium nitrite or *S*-nitrosoglutathione were 0.5 mM and 0.25 mM respectively for *S. cerevisiae*.
2. **Alteration in redox homeostasis might give protection to overcome the nitrosative stress.** It was found that GSH/GSSG ratio was significantly higher in presence of acidified sodium nitrite or *S*-nitrosoglutathione.
3. **Activities of catalase, glutathione reductase, were required to overcome the nitrosative stress.** Biochemical assays revealed that the activity of catalase, glutathione reductase were found to be increased in presence of acidified sodium nitrite or *S*-nitrosoglutathione.
4. **TCA cycle as well as respiration in *S. cerevisiae* was significantly affected under nitrosative stress.** By performing enzymatic assays, it was found that the activity of different TCA cycle enzymes were decreased under nitrosative stress.
5. **Ethanol fermentation rate as well as alcohol dehydrogenase activity were found to be increased under nitrosative stress.** By using standard methods of alcohol estimation, it was observed that ethanol production and specific activity of ADH were increased in presence of acidified sodium nitrite or *S*-nitrosoglutathione.
6. **ADH3 might play an essential role under nitrosative stress.** qPCR analysis revealed that *ADH3* gene expression was found to be increased in the presence of acidified sodium nitrite and *S*-nitrosoglutathione.
7. **Aconitase activity was affected due to protein tyrosine nitration and *s*-nitrosylation whereas ADH was not prone to these.** Western blot analysis by using anti 3-nitrotyrosine antibody, the signal of PTN was found in 0.3 and 0.5 mM acidified sodium nitrite treated aconitase whereas the signal of PTN was not found in acidified sodium nitrite treated ADH. On the other hand, signal for *s*-nitrosylation was observed only in *s*-nitrosoglutathione treated aconitase.
8. **Variation in glucose metabolism might be an important part of the defence mechanism of *S. cerevisiae* to counteract the nitrosative stress.** In this study, it was observed that the activities of fermentative enzymes were increased whereas activities of TCA cycle enzymes were decreased. This altered metabolic strategy might be conjoined with the antioxidant system to overcome the nitrosative stress.
9. **Nitrosative stress exposed immobilized *S. cerevisiae* cells may be used in industrial ethanol production.** It was observed that nitrosative stress exposed immobilized *S. cerevisiae* cells produced ethanol efficiently for several cycles.

Supporting Information.....

Table S1: qPCR data analysis of *ACO1*

Average Experimental Ct Value TE	Average Experimental Ct Value HE	Average Contrl Ct Value TC	Average Contrl Ct Value HC
29.55	21.73	29.65	21.56

ΔCt Value (Experimental/ ΔCTE) = TE-HE = 7.82

ΔCt Value (Control/ ΔCTC) = TC-HC = 8.09

ΔΔCt value = ΔCTE- ΔCTC = -0.27

Fold change = $2^{-\Delta\Delta Ct}$ = 1.2

Gene being Tested Experimental (TE): *ACO1* Stress

Gene being Tested Control (TC): *ACO1* Control

Housekeeping Gene Experimental (HE): *GAPDH* Stress

Housekeeping Gene Control (HC): *GAPDH* Control

Table S2: qPCR data analysis of *ACO2*

Average Experimental Ct Value TE	Average Experimental Ct Value HE	Average Control Ct Value TC	Average Control Ct Value HC
29.42	21.58	28.55	21.87

ΔCt Value (Experimental/ ΔCTE) = TE-HE = 7.84

ΔCt Value (Control/ ΔCTC) = TC-HC = 6.68

ΔΔCt value = ΔCTE- ΔCTC = 1.16

Fold change = $2^{-\Delta\Delta Ct}$ = 0.45

Gene being Tested Experimental (TE): *ACO2* Stress

Gene being Tested Control (TC): *ACO2* Control

Housekeeping Gene Experimental (HE): *GAPDH* Stress

Housekeeping Gene Control (HC): *GAPDH* Control

Table S3: qPCR data analysis of *ADH1*

Average Experimental Ct Value TE	Average Experimental Ct Value HE	Average Contrl Ct Value TC	Average Contrl Ct Value HC
24.175	18.01	25.84	18.565

ΔCt Value (Experimental/ ΔCTE) = TE-HE = 6.165

ΔCt Value (Control/ ΔCTC) = TC-HC = 7.275

ΔΔCt value = ΔCTE- ΔCTC = -1.11

Fold change = 2 -ΔΔCt = 2.16

Gene being Tested Experimental (TE): *ADH1* Stress

Gene being Tested Control (TC): *ADH1* Control

Housekeeping Gene Experimental (HE): *GAPDH* Stress

Housekeeping Gene Control (HC): *GAPDH* Control

Table S4: qPCR data analysis of *ADH2*

Average Experimental Ct Value TE	Average Experimental Ct Value HE	Average Control Ct Value TC	Average Control Ct Value HC
24.53	18.01	26.355	18.565

ΔCt Value (Experimental/ ΔCTE) = TE-HE = 6.52

ΔCt Value (Control/ ΔCTC) = TC-HC = 7.79

ΔΔCt value = ΔCTE- ΔCTC = -1.27

Fold change = 2 -ΔΔCt = 2.41

Gene being Tested Experimental (TE): *ADH2* Stress

Gene being Tested Control (TC): *ADH2* Control

Housekeeping Gene Experimental (HE): *GAPDH* Stress

Housekeeping Gene Control (HC): *GAPDH* Control

Table S5: qPCR data analysis of *ADH3*

Average Experimental Ct Value TE	Average Experimental Ct Value HE	Average Control Ct Value TC	Average Control Ct Value HC
19.49	18.42	21.17	18.31

ΔCt Value (Experimental/ ΔCTE) = TE-HE = 1.07

ΔCt Value (Control/ ΔCTC) = TC-HC = 2.86

ΔΔCt value = ΔCTE- ΔCTC = -1.79

Fold change = 2 -ΔΔCt = 3.46

Gene being Tested Experimental (TE): *ADH3* Stress

Gene being Tested Control (TC): *ADH3* Control

Housekeeping Gene Experimental (HE): *GAPDH* Stress

Housekeeping Gene Control (HC): *GAPDH* Control

Table S6: qPCR data analysis of *ADH1*

Average Experimental Ct Value TE	Average Experimental Ct Value HE	Average Contrl Ct Value TC	Average Contrl Ct Value HC
21.65	18.2	22.04	18.47

ΔCt Value (Experimental/ ΔCTE) = TE-HE = 3.47

ΔCt Value (Control/ ΔCTC) = TC-HC = 3.57

ΔΔCt value = ΔCTE- ΔCTC = 0.1

Fold change = $2^{-\Delta\Delta Ct}$ = 1.07

Gene being Tested Experimental (TE): *ADH1* Stress

Gene being Tested Control (TC): *ADH1* Control

Housekeeping Gene Experimental (HE): *GAPDH* Stress

Housekeeping Gene Control (HC): *GAPDH* Control

Table S7: qPCR data analysis of *ADH2*

Average Experimental Ct Value TE	Average Experimental Ct Value HE	Average Contrl Ct Value TC	Average Contrl Ct Value HC
25.975	18.2	26.35	18.47

ΔCt Value (Experimental/ ΔCTE) = TE-HE = 7.775

ΔCt Value (Control/ ΔCTC) = TC-HC = 7.88

ΔΔCt value = ΔCTE- ΔCTC = -0.105

Fold change = $2^{-\Delta\Delta Ct}$ = 1.08

Gene being Tested Experimental (TE): *ADH2* Stress

Gene being Tested Control (TC): *ADH2* Control

Housekeeping Gene Experimental (HE): *GAPDH* Stress

Housekeeping Gene Control (HC): *GAPDH* Control

Table S8: qPCR data analysis of *ADH3*

Average Experimental Ct Value TE	Average Experimental Ct Value HE	Average Contrl Ct Value TC	Average Contrl Ct Value HC
21.935	23.43	24.135	23.595

ΔCt Value (Experimental/ ΔCTE) = TE-HE = -1.495

ΔCt Value (Control/ ΔCTC) = TC-HC = 0.54

ΔΔCt value = ΔCTE- ΔCTC = -2.035

Fold change = $2^{-\Delta\Delta Ct}$ = 4.098

Gene being Tested Experimental (TE): *ADH3* Stress

Gene being Tested Control (TC): *ADH3* Control

Housekeeping Gene Experimental (HE): *GAPDH* Stress

Housekeeping Gene Control (HC): *GAPDH* Control

Table S9: Citrate content in treated and control (untreated) culture of *S. cerevisiae*

Sample	Extracellular citrate content (ng/µL)	Intracellular citrate content (ng/µL)	Total citrate content (ng/µL)
Control	29±3	13±2	42±3
Treated	15±2	6±NA	21±2

Abbreviations...

ACO: Aconitase

AD: Alzheimer's disease

ADH: Alcohol dehydrogenase

$AgNO_3$: Silver nitrate

ALDH: Aldehyde dehydrogenase

ALS: Amyotrophic lateral sclerosis

ANOVA: Analysis of variance

Arg: Arginine

AsA: Ascorbate

Bax: Bcl-2-associated X *protein*

bcl-2: B-cell lymphoma 2

BH_4: Tetrahydrobiopterin

BK: Bradykinin

bNOS: bacterial NOS

BP: Biological process

BSA: *Bovine serum albumin*

Ca^{2+}: Calcium

CaM: Calmodulin

cAMP: cyclic adenosine monophosphate

Cav-1: Caveolin-1

CBF: Cerebral blood flow

CC: Cellular component

C*c*O: cytochrome *c* oxidase

CCRD-RSM: Central Composite Rotational Design- Response Surface Model

cDNA: Complementary DNA

CFE: Cell-free extract

cGMP: cyclic guanosine monophosphate

cIMP: cyclic inosine monophosphate

CLS: Chronological life span

CO_2: Carbondioxide

CS: Citrate synthase

CTAB: cetyltrimethylammonium bromide

Cys: Cysteine

DAF-FM:4-Amino-5-Methylamino-2',7'-Difluorofluorescein Diacetate

DAVID: Database for Annotation, Visualization and Integrated Discovery

DdH_2O: Double distilled water

DetaNONOate: Diethylenetriamine NONOate

DHLA: Dihydro lipoic acid

DNS: 3,5-Dinitrosalicylic acid

DR: Dietary restriction

DTNB: 5,5'-dithio-bis-(2-nitrobenzoic acid)

EDTA: Ethylenediaminetetraacetic acid

EDRF: Endothelium-derived relaxing factor

eNOS: Endothelial nitric oxide synthase

ERK: Extracellular signal-regulated kinases

ETC: Electron transport chain

FACS: Fluorescence-activated cell sorting

FAD: Flavin Adenine Dinucleotide

Fe: Iron

FITC: Fluorescein isothiocyanate

FMN: Flavin Mono-Nucleotide

GAPDH: Glyceraldehyde-3-phosphate dehydrogenase

GCL: γ-glutamylcysteine ligase

GO: Gene Ontology

GPCR: G-protein coupled receptor

GPx: Glutathione peroxidase

GR: Glutathione reductase

GRK2: G-protein coupled receptor kinase 2

GS-FDH: GSH-dependent formaldehyde dehydrogenase

GS: GSH synthetase

GSH: reduced glutathione

GSNO: *S*-nitrosoglutathione

GSNOR: GSNO reductase

GSSG: oxidized glutathione

h: Hour

$HCLO_4$: Perchloric acid

HD: Huntington's disease

HDAC2: Histone Deacetylase 2

H_2DCFDA: 2′,7′-Dichlorodihydrofluorescein diacetate

HEPES: 4-(2-hydroxyethyl)-1-piperazineethanesulfonic acid

Hmp1: Flavohemoprotein

HNE: 4-hydroxy-2-nonenal

H_2O_2: Hydrogen peroxide

H_2ONO^+: nitrous acidium ion

HRP: Horseradish peroxidase

H_2SO_4: Sulfuric acid

hsp90: Heat shock protein 90

ICDH: Isocitrate dehydrogenase

ICL: Isocitrate lyase

iNOS: Inducible nitric oxide synthase

InsP3RI: Inositol-1,4,5-trisphosphate receptor type I

iodoTMT: Iodoacetyl Tandem Mass Tags

IRAG: Inositol-1,4,5-triphosphate receptor associated cGMP kinase substrate

JNK: c-Jun N-terminal kinase

KCl: Potassium Chloride

$K_2Cr_2O_7$: Potassium dichromate

KMnO4: Potassium permanganate

KOH: Potassium hydroxide

LA: Lipoic acid

LDL: Low density lipoprotein

Leu: Leucine

L-NNA: NG-nitro-L-arginine

L-NAME: NG-Nitro- L-Arginine Methyl Ester

LOONO: Peroxynitrite intermediates

M: Molar

MAPK: Mitogen-activated protein kinase

MDA: Monodehydroascorbate

MDH: Malate dehydrogenase

MDH (DC): Malate dehydrogenase (decarboxylating)

MF: Molecular function

MLCK: Myosin light chain kinase

MLCP: Myosin light chain phosphatase

mM: milli-molar

MMTS: *S*- methyl methanethiosulfonate

MOPS: 3-(N-morpholino)propanesulfonic acid

MRC: mitochondrial respiratory chain complex

MRSA: methicillin resistance *Staphylococcus aureus*

mtDNA: Mitochondrial DNA

N: Nitrogen

NaCl: Sodium chloride

NAD: Nicotinamide adenine dinucleotide

NADH: Nicotinamide adenine dinucleotide hydrogen

NADPH: Nicotinamide adenine dinucleotide phosphate hydrogen

$NaNO_2$: acidified sodium nitrite

NHA: Nω-hydroxy-L-arginine

nNOS: Neuronal nitric oxide synthase

NO: Nitric oxide

NO^+: nitrosonium ion

NO_2: Nitrogen dioxide

NO_2^-: Nitrite

NO_3^-: Nitrate

NOS: Nitric oxide synthase

N_2O_3: dinitrogen trioxide

NOD: Nitric oxide dioxygenase

NOSIP: Nitric oxide synthase interacting protein

NOSTRIN: nitric oxide synthase trafficking inducer

O_2: Oxygen

O_2^-: Superoxide

OAA: Oxaloacetic acid

O.D.: Optical density

$ONOO^-$: Peroxynitrite

ORF: Open reading frame

PAGE*:* Polyacrylamide gel electrophoresis

PARP: Poly ADP-ribose polymerase

PBS: Phosphate-buffered saline

PC: Pyruvate carboxylase

PD: Parkinson's disease

PDC: Pyruvate decarboxylase

PDH: Pyruvate dehydrogenase

PDZ: post-synaptic density protein, discs-large, zona occludens -1

Phe: Phenylalanine

PKA: *Protein* kinase A

PKC: Protein kinase C

PM: Plasma membrane

PMSF: phenylmethylsulfonyl fluoride

polyQ: Polyglutamine

PTN: Protein tyrosine nitration

PTP: Permeability transition pore

PVDF: polyvinylidene difluoride

R^2: coefficient of determination

rDNA: Ribosomal DNA

RLS: Replicative life span

RNS: Reactive nitrogen species

ROS: Reactive oxygen species

$RS^{\bullet}$: Thiyl radical

RSNO: S-nitrosothiols

SD: Standard deviation

SDS: Sodium dodecyl sulphate

Ser: Serine

SERCA: Sarco/endoplasmic reticulum calcium ATPase

sGC: soluble guanylate cyclase

SR: sarcoplasmic reticulum

STRING: Search Tool for the Retrieval of Interacting Genes/Proteins

STREP: stress-starvation response element of *Schizosaccharomyces pombe*

TBST buffer: Tris buffered saline tween

TCA: tricarboxylic acid

Thr: Threonine

TRADD: TNF-receptor associated death domain protein

TRP: Transient receptor potential

Tyr: Tyrosine

VASP: Vasodilator sensitive phosphoprotein

VDCC: Voltage-dependent calcium channel

VLCAD: very long-chain acyl-CoA dehydrogenase

XOR: Xanthine oxidoreductase

Yhb1: Flavohemoglobin

YPD: yeast extract, peptone, dextrose

Zn: Zinc

Publications...

Cell Biochemistry and Biophysics (2020) 78:101–110
https://doi.org/10.1007/s12013-019-00897-y

ORIGINAL PAPER

Check for updates

Optimization of Ethanol Production using Nitrosative Stress Exposed *S.cerevisiae*

Swarnab Sengupta[1] · Minakshi Deb[1] · Rohan Nath[1] · Shyama Prasad Saha[1] · Arindam Bhattacharjee[1]

Received: 24 July 2019 / Accepted: 12 December 2019 / Published online: 24 December 2019

Abstract
S.cerevisiae is an industrially important organism known for its ability to produce ethanol as the demand for ethanol is increasing day by day all over the world, the need to find better and alternative ways to increase ethanol production is also rising. In this work we have proposed such alternative but effective method for producing ethanol by *S.cerevisiae*. Here, we are reporting for the first time the effect of nitrosative stress on ethanol production. Under in vivo condition, nitrosative stress is marked by the modification of macromolecules in the presence of reactive nitrogen species (RNS). Our result showed that treated cells were more capable for ethanol production compared with untreated cells. Our result also showed enhanced alcohol dehydrogenase activity under stressed condition. Further ethanol production was also optimized by using Response Surface Methodology (RSM) with stressed cells. Further, production of ethanol with immobilized beads of stress affected *Saccharomyces cerevisiae* was also determined. Overall, the obtained data showed that under nitrosative stress, the maximum ethanol production is 34.4 g/l after 24 h and such higher production was observed even after several cycles of fermentation. This is the first report of this kind showing the relation between nitrosative stress and ethanol production in *Saccharomyces cerevisiae* which may have important industrial application.

Keywords *Saccharomyces cerevisiae* · Nitrosative stress · Reactive nitrogen species (RNS) · Response surface methodology (RSM).

Introduction

Demand for ethanol is increasing day by day due to its versatile application and utility. To meet the acting demands, production of ethyl alcohol or ethanol through fermentation is gaining momentum globally. Despite the evolving trend of using bacteria for ethanol production, yeast is still the primary choice for fermentation [1]. Due to its high ethanol productivity, high ethanol tolerance and ability of fermenting wide range of sugars, yeasts especially *Saccharomyces cerevisiae* is the common microorganism employed in ethanol production [2]. In recent years, different strains of *Saccharomyces cerevisiae* were extensively studied to improve their ability for ethanol production. Industrially engineered yeast strains have to resist to the stress conditions rapidly and they have to adapt quickly by modifying their metabolic activities to avoid substantial viability loss. Ethanol production by using immobilized cells also has significant advances. Immobilized cells offer rapid fermentation rates with high productivity of ethanol. Immobilization enhances ethanol productivity and its yield while at the same time effectively eliminate the obstacles caused by high concentration of substrate and product in ethanol production. Hence the technique holds a great promise for the efficient production of fermented beverages, such as beer, wine as well as bioethanol [3].

Through metabolic engineering, bacterial and yeast strains have been constructed, which feature traits that are advantageous for ethanol production using lignocellulosic sugars [4]. But on the other hand, the inserted genes may have unexpected harmful effects. Another difficulty particular to the food and beverage industry is that containment of engineered yeast within the industrial plant cannot be guaranteed. Engineered yeast strains used in food and beverage production could be consumed by humans and may be released to the environment [5]. Moreover, metabolic and genetic engineering processes are highly

✉ Arindam Bhattacharjee
arbiochem@gmail.com

[1] Department of Microbiology, University of North Bengal, Siliguri, India

expensive, which is proving to be disadvantageous for the industries. To avoid such hurdles, new and cost effective alternative methods are needed. This work mainly focuses on proposing one such approach to increase ethanol production by applying nitrosative stress on yeast cells. Yeast cells can sense and adapt their physiology to the sequential stress conditions that they encounter. Therefore increasing stress tolerance is a suitable way to improve yeast industrial tolerance [6, 7].

In cell biology, "Stress" is a general term used to signify an event where under in vivo conditions the biochemical redox homeostasis of a cell is changed due to excessive production of different reactive species because of external stimuli, for e.g., the production of ROS (reactive oxygen species) and RNS (reactive nitrogen species). When a cell is challenged with RNS such as nitric oxide radical, peroxynitrite, nitrogen oxide radicals [8, 9], the hostile condition is known as "Nitrosative stress". In this stress condition an imbalance in the production and neutralization of reactive nitrogen and oxygen species, results in cellular damage [10]. RNS is formed due to the reaction of ROS and nitric oxide (NO). NO is a freely diffusible, short lived, and lipophilic molecule [11]. This agent acts as a key element of nitrosative stress in higher concentration. At this high concentration, it is actually toxic to cell as it can bind to heme, iron and copper containing protein [12, 13]. RNS can cause nitrosylation or nitration of different cellular components including metals, lipids, DNA, proteins which may inhibit or alter normal physiological functions [13]. It has been reported that several proteins of aerobic respiration e.g. aconitase, isocitrate dehydrogenase etc, can be nitrated that may result in the inhibition of TCA cycle in *Saccharomyces cerevisiae* [14]. It has been reported previously that the key enzyme of ethanol fermentation i.e. alcohol dehydrogenase of *Saccharomyces cerevisiae* can be affected during nitrosative stress [15]. Studies also suggest that when cells are exposed to nitrosative stress, intracellular redox homeostasis gets altered. This changed redox environment may lead to alteration in the physiochemical properties of the cell. Under such circumstances some proteins known as stress response enzymes, gets activated [16]. In this circumstance, it can be assumed that the metabolic pathway of *Saccharomyces cerevisiae* can be affected under nitrosative stress. Hence, the shifting of metabolic flux towards ethanol production becomes the study of interest. But there is almost no work in this field. On the other hand, it has also been reported that ethanol can be produced by *Saccharomyces cerevisiae* in both aerobic and anaerobic conditions [17].

Hence, the primary aim of this work was to study the effect of nitrosative stress on ethanol production by *Saccharomyces cerevisiae* in non-fermentative condition. The ethanol production by the immobilized nitrated yeast cells in a cheap medium containing molasses as the only carbon source was also an important objective of this study. This study will set up an approach that can be widely used in industry for higher alcohol production at low cost.

Materials and Methods

Yeast Culture and Growth Condition

Wild type haploid yeast cell *Saccharomyces cerevisiae* Y190 [ATCC 96400], a.payt from Prof. Sanjay Ghosh, CU, was used for all experimental purpose. To grow, yeast culture was maintained at 30 °C temperature in shaking condition (80 rpm) in YPD (2% W\V Yeast extract, 2% W\V peptone, and 2% W\V dextrose) medium and YPG medium (2% W\V yeast extract, 2% W\V peptone, and 3% V/V glycerol) for all our experimental conditions. Molasses and ammonium sulfate containing medium was used for the experiment based on CCRD-RSM. Acidified sodium nitrite was used as the stress agent for all the experiment.

Preparation of Acidified $NaNO_2$

Stock solution of 100 mM acidified $NaNO_2$ was prepared by mixing dissolved sodium nitrite (in H_2O) with concentrated HCl in a 1:1 ratio (V/V). Final concentration of this mixture was used as the nitrosative stress reagent at requisite amount to have effective concentration of 0.5 mM, 1 mM, and 3 mM acidified $NaNO_2$. pH value after addition of such mixture to the media was also checked and found to be between 6.8 to 7.0, which is in the optimal range for *Saccharomyces cerevisiae* Y190 growth.

Cell Viability Assay

Yeast cells were grown in YPD medium treated with different concentration of acidified $NaNO_2$ (0 mM, 0.5 mM, 1 mM, and 3 mM) and incubated in shaking condition. After overnight incubation, 1 ml of culture from each sample from both media were serially diluted and plated on YPD agar medium for viable cell count. Under same condition, growth curve of samples were assessed to spectrophotometrically at 600 nm.

Detection of ROS and RNS

Presence of ROS and RNS were detected as per the protocol of Invitrogen with slight modifications. In short, 2×10^6 cells were resuspended in PBS buffer pH 7.4 and fixed by absolute ethanol. After that dyes were added

(H_2DCFDA for ROS and DAM-FM for RNS) at the final concentration of 1 µM and incubated for 30 min in dark. For fluorescent microscopy (optika) excitation was fixed at 495 nm and emission at 515 nm. Micrographs (40 ×) were repeated for at least three independent experiments.

Estimation of Ethanol Production

Ethanol was estimated both by spectrophotometer and HPLC. Spectrophotometrically, ethanol estimation was done, using modified potassium dichromate method [18]. In short, overnight incubated treated and untreated yeast cells were centrifuged. One milliliter supernatants from each sample were added in the mixture of 0.25 M potassium dichromate ($K_2Cr_2O_7$), 0.1 M silver nitrate ($AgNO_3$), and 6 N sulfuric acid (H_2SO_4). After incubation samples were diluted and O.D. was recorded at 560 nm. Presence of ethanol was checked by HPLC model accordingly Zuky et al. [19] using Hi-Plex Hcolumn with the flow rate of 1 ml/min.

Preparation of Cell Free Extract (CFE)

Overnight grown treated and untreated cultures were taken and centrifuged under cold condition. Supernatants were discarded and pellets were suspended in lysis buffer [100 mM Tris-HCl at pH 7.6, 150 mM NaCl, 1 mM SDS, 1 mM DTT, 2 mM EDTA, protease inhibitor cocktail (Sigma-Aldrich, St. Louis, MO, USA), 1 mM PMSF] and were lysed using glass beads and vortexed until lysis. The soluble fractions were collected by centrifugation and the concentration of protein was determined via Bradford assay [20].

Alcohol Dehydrogenase Assay

Activity of alcohol dehydrogenase was determined as the protocol of Sigma. In short, cell lysate was taken for the alcohol dehydrogenase assay. Reaction mixture contains 50 mM sodium phosphate buffer at pH 8.8, 95% V/V ethanol and 50 mM β-NAD as the final concentration and diluted cell free extract. Time scan was performed for 6 min at 340 nm. Spectrophotometrically, the difference in initial and final O.D. was recorded.

Alcohol Dehydrogenase Inhibition Assay

Yeast cells were grown in YPD medium treated with acidified 0.5 mM $NaNO_2$ after 3 h of inoculation. At the same time 0.1 mM 2,2,2-trifluoroethanol was added in the sample and incubated. Ethanol production was estimated at 560 nm to check the inhibition of alcohol dehydrogenase. Untreated yeast cells were taken as the control [21].

Ethanol Production by Immobilization of Nitrated Yeast Cell

For the immobilization assay *S.cerevisiae* cells were first grown overnight in specified media in the presence of 0.5 mM sodium nitrite. Next, the culture was centrifuged and the cell pellet was resuspended in PBS buffer pH 7.0. 1 ml of such resuspended cell was then added slowly with 1% sodium alginate. After that cells were transferred to 0.5 M $CaCl_2$ solution drop wise with the help of a syringe with the formation of Ca-alginate beads having immobilized yeast cells. For, ethanol production 20 such beads was used to inoculate a broth media. Ethanol concentration was determined as stated earlier [22].

Optimization of Ethanol Production by Central Composite Rotatable Design based (CCRD) Response Surface Methodology (RSM)

Optimization of ethanol production was carried out using central composite rotatable design based (CCRD) response surface methodology (RSM) in order to study the interaction effect between three independent variables viz., molasses concentration (C-source) (A), ammonium sulfate concentration (N-source) (B) and Incubation time of yeast (C) in the fermentation broth. Due to the presence of "axial points" around the centre point in the CCRD design curvature of the model is allowed. As suggested by Saha et al. [23]. Three independent variables molasses concentration (A), ammonium sulfate concentration (B) and Incubation time of yeast (C) were used in five different coded levels ($-\alpha$, -1.0, $+1$, $+\alpha$). Table 1 represent the relationship between the coded level and actual values of each variables used in this study to optimize ethanol production.

The relation between the coded level of variables and actual values of the variables are explained by the following equation (Eq. 1):

$$X_a = (Z_a - Z_0)/\Delta Z \quad (1)$$

where, Xa is the coded value, Za is the actual value, Zo is the actual value at the centre point, and ΔZ is the step

Table 1 Coded and actual levels of variables used to construct the model

Factor	Unit	Coded Levels				
		$-\alpha$	−1	0	+1	$+\alpha$
A (Carbon source)	% W/V	0	5	12.50	20	25.11
B (Nitrogen source)	% W/V	0	0.05	1.02	2	2.66
C (Incubation time)	Hours	0	6	15	24	30.14

change of the variables. Total 20 experimental runs were conducted and the ethanol produced by the yeast was analyzed by the second order polynomial regression equation (2).

$$Y = a_0 + a_1x_1 + a_2x_2 + a_3x_3 + a_{11}x_1^2 + a_{22}x_2^2 + a_{33}x_3^2 + a_{12}x_1x_2 + a_{13}x_1x_3 + a_{23}x_2x_3 \quad (2)$$

where Y is the predicted ethanol production (g/l), a_0 is the intercept, X_i is the independent variables and a_i is the model coefficient parameters.

Statistical Analysis

All experiments were done in triplicate. Level of significance (p) was set at 0.05 for all experiments.

Results and Discussion

Effect on Cell Viability in the Presence of $NaNO_2$

Acidified sodium nitrite was used as a nitrosative stress agent in all our experiment to determine the sub-toxic dose of sodium nitrite, cellular viability was checked. After overnight stress in medium, it was observed that cellular viability was not significantly affected at 0.5 mM concentration of sodium nitrite (Fig. 1) as compared with the control set. Whereas in the presence of 1 mM and 3 mM sodium nitrite under the same experimental condition, cellular viability was seen to have decreased significantly. Growth curve experiment above same condition as above has also shown similar results with 0.5 mM concentration of sodium nitrite showing least effect as compared with 1 and 3 mM sodium nitrite (Fig. 2). Hence, the concentration of sodium nitrite was fixed to be at 0.5 mM for all our further experiments.

Effect of $NaNO_2$ on ROS and RNS Generation

Generation of ROS and RNS are important markers to study the redox homeostasis [24]. Thus, in this context, it was important to investigate the presence of the both ROS and RNS under our experimental condition. In both control and 0.5 mM acidified $NaNO_2$ treated yeast cells the generation of ROS and RNS were determined by fluorescent microscopy. Our result showed a significant change in RNS production in 0.5 mM acidified $NaNO_2$ treated yeast cells as compared with control set (Fig. 3). Whereas, we did not found any significant change in ROS generation in 0.5 mM acidified $NaNO_2$ treated yeast cells compared with control set (Fig. 4).

This result is very interesting it terms of our work. There was also no significant difference in the generation of ROS

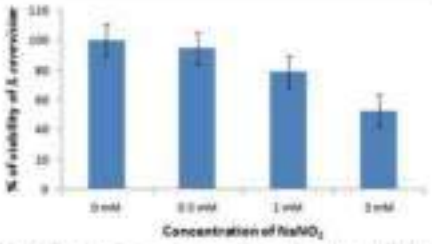

Fig. 1 Cell viability assay of untreated and treated (0.5, 1, 3 mM sodium nitrite) *S. cerevisiae*

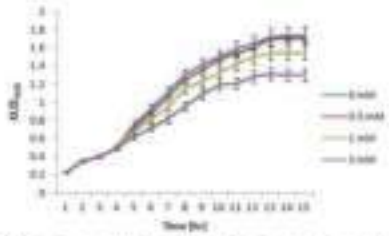

Fig. 2 Growth curve analysis: effect of nitrosative stress in untreated and treated (0.5, 1, 3 mM sodium nitrite) *S. cerevisiae*

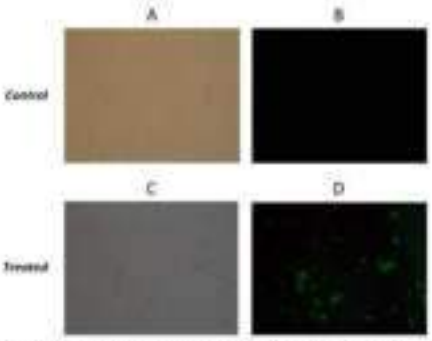

Fig. 3 Detection of RNS: the presence of RNS was visualized as green color. Fluorescence and corresponding phase contrast images of *S. cerevisiae* Y190 **a** and **b**. Control or untreated **c** and **d**. treated with 0.5 mM sodium nitrite

between both control and 0.5 mM acidified $NaNO_2$ treated yeast cells which indicates the presence of endogenous ROS in both control and treated yeast cells and 0.5 mM acidified $NaNO_2$ had no role in generation of ROS. Whereas, it is evident that 0.5 mM acidified $NaNO_2$ was responsible for

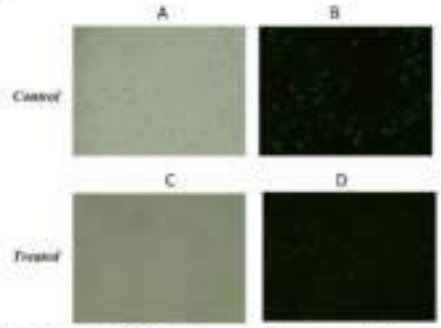

Fig. 4 Detection of ROS: the presence of ROS was visualized as green color. Fluorescence and corresponding phase contrast images of *S. cerevisiae* Y190 (a) and (b). Control or untreated (c) and (d) treated with 0.5 mM sodium nitrite

the generation of RNS. Thus, it can be concluded that the effect observed under our experimental condition was may be solely due to generation of RNS by of the 0.5 mM acidified $NaNO_2$.

Effect of $NaNO_2$ on Alcohol Production

As reported earlier, *S.cerevisiae* usually produces ethanol under aerobic condition [17], but this is much less as compared with fermentative condition. Under our experimental condition as mentioned in the materials and methods section ethanol production was found to be higher in the presence of 0.5 mM sodium nitrite stress as compared with the control. Our result suggests that in YPD medium ethanol production increased by 35% under nitrosative stress as compared with the control (Table 2). The result showed that under nitrosative stress the cellular metabolism flux and energy production has shifted significantly towards ethanol production, a major fermentative product. This may have happened due to alteration in biochemical pathways within the cell including modification of several important enzymes involved in cellular respiration and TCA cycle under nitrosative stress [10]. The presence of ethanol was also verified by HPLC (data not shown).

Effect of $NaNO_2$ on Alcohol Dehydrogenase Activity

In YPD medium, specific activity of alcohol dehydrogenase was significantly increased 34% when cells were treated with 0.5 mM $NaNO_2$ in comparison as compared with control (Table 3). To check that whether this alcohol production was solely due to the activity of ADH, an inhibitor assay was also performed. Addition of 2,2,2-trifluroethanol as a competitive inhibitor of ADH, ceased the activity resulting in complete inhibition of alcohol production. Both the control and the treated sample have shown similar results (Table 3).

Table 3 Ethanol production by treated and untreated *S. cerevisiae*

Sample	Ethanol (g/lit)
Control	21 ± 1
0.5 mM	28 ± 2

High amount of alcohol production in 0.5 mM $NaNO_2$ treated cells was due to the higher specific activity of alcohol dehydrogenase. Several studies reported that, aconitase, isocitrate dehydrogenase involved in TCA cycle can be nitrated in presence of NO or RNS resulting in inactivation of these enzymes [14]. So for the cell to survive, energy production via alteration biochemical pathways becomes essential. Therefore it is possible that, may be the cell was trying to reroute its metabolic flux toward fermentation. Alcohol dehydrogenase III, a mitochondrial protein is reported to be over expressed in nitrosative stress [25]. Glutathione dependent alcohol dehydrogenase also acts as a stress response enzyme, relieving the cell from nitrosative [25–28]. Altogether higher specific activity of ADH under experimental condition corroborates with the previous results and also suggests that it plays a vital role in energy production as well as stress reliever for a cell. This result clearly indicates that, alcohol dehydrogenase is the main enzyme responsible for the alcohol production at both stressed and unstressed condition in *Saccharomyces cerevisiae* [21].

Optimization of Ethanol Production by CCRD based RSM Technique

The effect of three independent variables molasses concentration (A), ammonium sulfate concentration (B), and incubation time (C) were tested for ethanol production by the yeast using CCRD based RSM technique. The optimal level for the each factor was determined. For optimization of ethanol production 19 experimental runs were performed and the results are represented in Table 4 with both the actual and model predicted responses.

Analysis of variance (ANOVA) was conducted for the above experimental design. The results are represented in Table 5. The results showed that the model is highly significant ($p < 0.003$) and can better predict the actual response i.e., ethanol production. Within the model molasses concentration (A) [$p = 0.0094$], incubation time (C) [$p = 0.0043$], molasses concentration^2 (A^2) [$p = 0.0030$] and incubation time^2 (C^2) [$p = 0.0045$] were the significant model terms. Using the result of this experimental design second-order polynomial regression equation is generated by software for ethanol concentration which is represented

Table 3 Specific activity of Alcohol Dehydrogenase of treated and untreated *S. cerevisiae*

SAMPLE	Specific activity of Alcohol Dehydrogenase (nM/min/mg)	Specific activity of Alcohol Dehydrogenase in the presence of 2,2,2-trifluoroethanol (nM/min/mg)
Control	10 ± 0.3	Not detected
0.3 mM	25 ± 0.4	Not detected

Table 4 Experimental design along with model predicted and actual ethanol yield response

Run	Factor 1A: C-source (%)	Factor 2B: N-source (%)	Factor 3C: Incubation (h)	Ethanol (g/l): Actual	Ethanol (g/l): Predicted
1	12.50	1.02	15.00	21.73	21.66
2	5.00	0.05	24.00	7.24	8.79
3	20.00	2.00	6.00	20.26	17.22
4	20.00	2.00	24.00	34.74	34.24
5	12.50	1.02	30.14	28.24	25.11
6	20.00	0.05	6.00	11.52	11.36
7	12.50	2.66	15.00	14.02	18.27
8	5.00	2.00	24.00	11.52	10.19
9	5.00	2.00	30.14	8.68	4.03
10	25.11	1.02	6.00	27.50	27.79
11	12.50	1.02	15.00	21.70	21.66
12	5.00	0.05	6.00	3.19	2.17
13	−0.11	1.02	15.00	0	5.23
14	12.50	1.02	15.00	21.69	21.66
15	12.50	1.02	15.00	21.75	21.66
16	12.50	1.02	−0.14	0	1.80
17	12.50	1.02	15.00	21.75	21.66
18	20.00	0.05	24.00	23.34	26.51
19	12.50	−0.61	15.00	12.35	10.20

in actual terms (Eq.3).

$$\text{R1(Ethanol concentration), Actual} = -10.30525 + 1.38894 \times A + 5.61195 \times B + 1.03751 \times C + 0.17658 \times AB + 0.035870 \times AC + 0.020085 \times BC - 0.043112 \times A^2 - 2.76112 \times B^2 - 0.028324 \times C^2 \quad (3)$$

The R^2 value (coefficient of determination) of 0.9577 indicates that the model could explain the 93% variability in the model response. The predicted and adjusted R^2 0.5256 and 0.8817, respectively, were in reasonable agreement with each other. The model high adequate precision ratio of 13.864 indicates that high signal to noise ratio. Generally adequate precision ratio of 4 is desirable to judge the significance level of the model. In overall sense the R^2, adjusted R^2, predicted R^2, and adequate precision all are significantly higher and thus the model could be employed for identification of optimized level of each of the variables used for ethanol response.

Table 5 CCRD based RSM model

Source	Sum of squares	df	Mean square	F value	p value Prob > F
Model	890.41	9	98.93	7.52	0.0030
A: C-source	142.10	1	142.10	10.80	0.0094
B: N-source	9.99	1	9.99	0.76	0.4061
C: Incubation time	188.79	1	188.79	14.35	0.0043
AB	4.44	1	4.44	0.34	0.5756
AC	26.35	1	26.35	2.00	0.1907
BC	51.01	1	51.01	3.88	0.0805
A2	299.72	1	299.72	22.78	0.0010
B2	113.57	1	113.57	8.63	0.0165
C2	180.27	1	180.27	13.70	0.0045

Comparison of model actual and predicted values for ethanol response (g/l) is presented in Fig. 5. The plot showed that the observed and actual values were spited by a line of angle of 45°, indicating a reasonable agreement of predicted response with the actual ones.

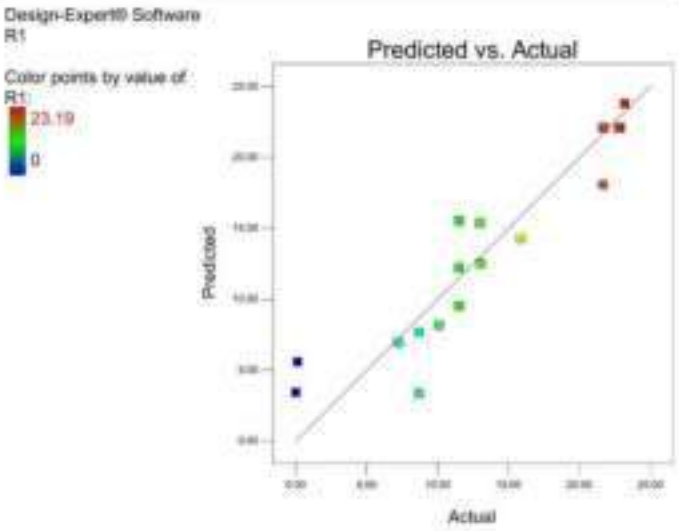

Fig. 5 Plot of actual values versus predicted values

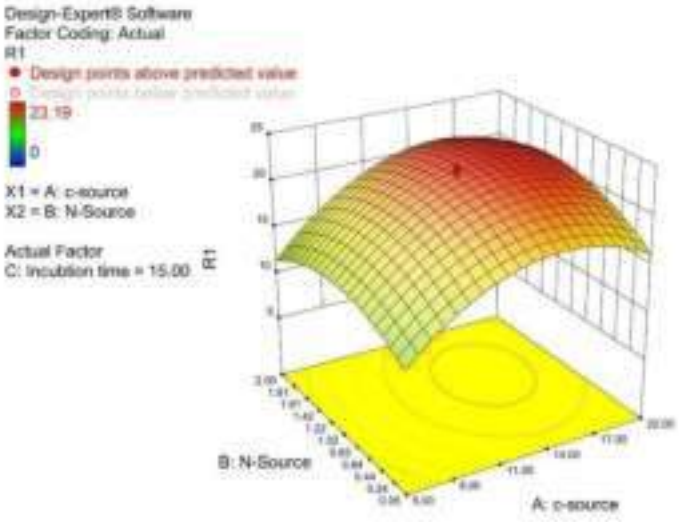

Fig. 6 Surface plot showing the effect of interaction between carbon source (Molasses) and nitrogen source (Ammonium sulfate)

The response surface plots and their contour plots described by second-order polynomial regression equation were generated in order to determine the interactions among variables and optimal level of variables for ethanol production (Figs. 6–8). It can be observed that the ethanol production was significantly varies with the molasses concentration (A) (Fig. 6). When the carbon source was enhanced from 5 to 20% W/V, keeping the nitrogen source fixed at 1.22% W/V, ethanol production was significantly enhanced from 11.88 to 27.54 g/l. The significance of the

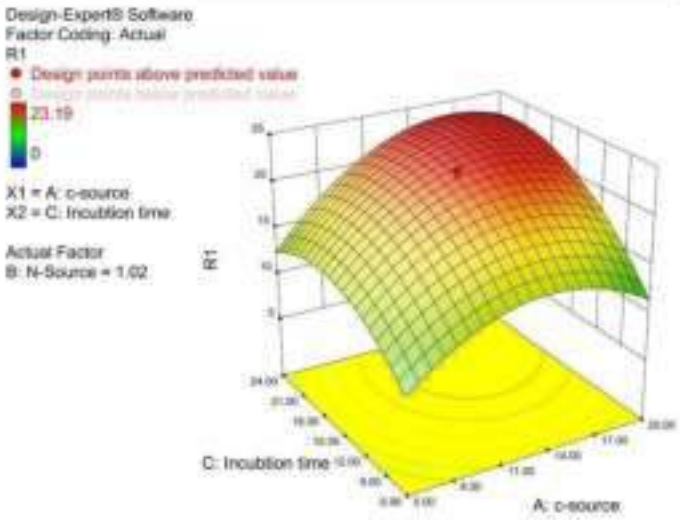

Fig. 7 Surface plot showing the effect of interaction between carbon source (Molasses) and incubation time

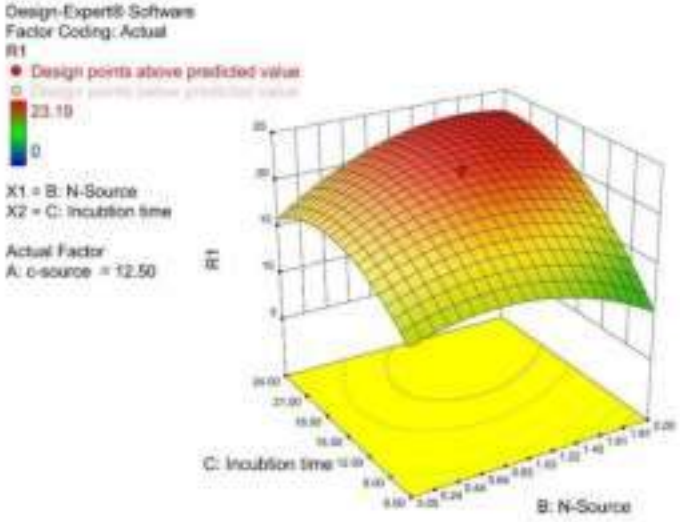

Fig. 8 Surface plot showing the effect of interaction between nitrogen source (Ammonium sulfate) and incubation time

carbon source was also confirmed from the ANOVA result which showed a p value of 0.0094.

The effect of interaction between the molasses concentration (A) and incubation time (C) is represented in Fig. 7 The result showed that along with carbon source, incubation time also significantly affect the ethanol production at a p value of 0.0043. Keeping the carbon source fixed at 20% W/V, when incubation time was gradually increased from 6 to 24 h, predicted ethanol production is also significantly enhanced from 16.37 to 32.90 g/l.

The effect of interaction between ammonium sulfate (B) and incubation time (C) is presented in Fig. 8 and it can be

Table 6 Ethanol production by immobilized yeast cells grown in YPD medium

	Immobilization		
No. of cycle	1st	2nd	3rd
Ethanol production (g/l)	33 ± 1	35 ± 2	27 ± 1

Table 7 Ethanol production by immobilized yeast cells grown in YPG medium

	Immobilization					
No. of cycle	1st	2nd	3rd	4th	5th	6th
Ethanol production (g/l)	31 ± 1	36 ± 2	39 ± 1	35 ± 1	24 ± 1	19 ± 1

observed from the plot that the ethanol production was not so much altered when either of the variables were increased or decreased. This result suggests, a non significant interaction between these two variables for ethanol production. This result is also supported by the ANOVA result where a p value of 0.0805 was obtained for these two variables. A mild increment of ethanol production was recorded from 20.24 to 25.18 g/l when nitrogen source concentration was increased from 0.05 to 2.00% W/V.

After careful analysis of the interaction between the variables for ethanol production, finally the model was employed to find out the optimized design space using the numerical optimization tool, where the response was asked for maximum level. It was obtained that carbon source concentration of 20.00% W/V, nitrogen source concentration of 1.74% W/V when used in the medium for 24 h of incubation time by the yeast, it will show 35.24 g/l of ethanol production which was very close to the model predicted response of 34.24 g/l.

Estimation of Ethanol Production by Yeast Cells under Nitrosative Stress Grown in YPG Medium

To assess the ability of nitrated yeast cells to produce ethanol over time, YPD grown stress exposed yeast cells were first immobilized in calcium alginate beads. The beads were then inoculated in fresh molasses containing medium to check for the production of ethanol. The process was repeated for several cycles using fresh molasses medium. Under our experimental condition it was observed that ethanol production with YPD grown stressed cells remains significantly unchanged for two cycles (Table 6). Whereas interestingly when YPG grown stressed yeast cells were used to repeat the same experiment, it was observed that ethanol production increased significantly upto 3rd cycles (Table 7). This may be due to the production of higher ROS and subsequently higher RNS by the yeast during their growth in respiratory proficient YPG media.

As ADH has a role in relieving the nitrosative stress [25], so with higher RNS accumulation, the expression of ADH might have significantly increased which eventually resulted in higher ethanol production. The gradual decrease in ethanol production with YPD and YPG grown immobilized yeast cells was may be due to cell death or changes in cellular physiology to relieve the effect of stress.

Conclusion

Under our experimental condition the present study showed that ethanol production by *Saccharomyces cerevisiae* increased, with the increase in ADH specific activity, when the cells were challenged with nitrosative stress. With the view to apply the process for industrial use, inexpensive nutrient sources were used during optimization. Moreover immobilization of yeast cells and its reuse for several cycles also helped in higher alcohol production and reduction of time and cost. This is the first report of this kind where an alternative method of ethanol production is explained with nitrated yeast cells. This approach is cost effective and productive. Therefore it holds a great promise for industrial production of fermented beverages, like beer, wine as well as bioethanol.

Acknowledgements The authors acknowledge the University of North Bengal for providing essential infrastructure and financial support to carry out this research.

Compliance with Ethical Standards

Conflict of Interest The authors declare that they have no conflict of interest.

References

1. Willaert, R. G. (2017). Yeast biotechnology. *Fermentation*, *3*, 7–10.
2. Mohd Azhar, S. H., Abdullah, R., & Jambo, S. A. et al. (2017). Yeasts in sustainable bioethanol production: a review. *Biochemistry and Biophysics Reports*, *10*, 52–61.
3. Verbelen, P. J., De Schutter, D. P., & Delvaux, F. et al. (2006). Immobilized yeast cell systems for continuous fermentation applications. *Biotechnology Letters*, *28*, 1515–1525.
4. Zaldivar, J., Nielsen, J., & Olsson, L. (2001). Fuel ethanol production from lignocellulose: a challenge for metabolic engineering and process integration. *Applied Microbiology and Biotechnology*, *56*, 17–34.
5. Nevoigt, E. (2008). Progress in metabolic engineering of *Saccharomyces cerevisiae*. *Microbiology and Molecular Biology Reviews*, *72*, 379–412.
6. Matallana, E., & Aranda, A. (2017). Biotechnological impact of stress response on wine yeast. *Letters in Applied Microbiology*, *64*, 103–110.

7. Pretorius, I. S. (2000). Tailoring wine yeast for the new millennium: novel approaches to the ancient art of winemaking. *Yeast, 16*, 675–729.
8. Forman, H., Fukuto, J. M., & Miller, T. (2008). The chemistry of cell signaling by reactive oxygen and nitrogen species and 4-hydroxynonenal. *Archives of Biochemistry and Biophysics, 477*, 183–195.
9. Palmer, R. M., Rees, D. D., & Ashton, D. S. (1988). L-arginine is the physiological precursor for the formation of nitric oxide in endothelium-dependent relaxation. *Biochemical and Biophysical Research Communications, 153*, 1251–1256.
10. Kurutas, E. B. (2016). The importance of antioxidants which play the role in cellular response against oxidative/nitrosative stress: current state. *Nutrition Journal, 15*, 71. https://doi.org/10.1186/s12937-016-0186-5.
11. Bhattacharjee, A., Majumdar, U., & Maity, D. et al. (2010). Characterizing the effect of nitrosative stress in *Saccharomyces cerevisiae*. *Archives of Biochemistry and Biophysics, 496*, 109–116.
12. Rogstam, A., Larsson, J. T., & Kjelgaard, P. (2007). Mechanisms of adaptation to nitrosative stress in *Bacillus subtilis*. *Journal of Bacteriology, 189*, 3063–3071.
13. Fang, F. C. (2004). Antimicrobial reactive oxygen and nitrogen species: concepts and controversies. *Nature Reviews Microbiology, 2*, 820–832.
14. Bhattacharjee, A., Majumdar, U., & Maity, D. et al. (2009). In vivo protein tyrosine nitration in *S. cerevisiae*: Identification of tyrosine-nitrated proteins in mitochondria. *Biochemical and Biophysical Research Communications, 388*, 612–617.
15. Crow, J. P., Beckman, J. S., & McCord, J. M. (1995). Sensitivity of the essential zinc-thiolate moiety of yeast alcohol dehydrogenase to hypochlorite and peroxynitrite. *Biochemistry, 34*, 3544–3552.
16. Claudia, L., Natallya, L., & Möller, A. (2013). Redox proteomics uncovers peroxynitrite-sensitive proteins that help *Escherichia coli* to overcome nitrosative stress. *The Journal of Biological Chemistry, 288*, 19698–19714.
17. Hagman, A., Säll, T., & Compagno, C., et al. (2013). Yeast 'make-accumulate-consume' life strategy evolved as a multi-step process that predates the whole-genome duplication. *PLoS ONE, 8*, e68734.
18. Sayyad, S. F., Chaudhuri, S. R., & Panda, B. P. (2015). Quantitative determination of ethanol in solids by using UV-visible spectrophotometer. *Pharmaceutical and Biological Evaluations, 2*, 204–207.
19. Zakya, A. S., Pennapa, N., & Andrade-Eiroa, Á. (2017). A new HPLC method for simultaneously measuring chloride, sugars, organic acids and alcohols in food samples. *Journal of Food Composition and Analysis, 56*, 25–33.
20. Bradford, M. M. (1976). A rapid and sensitive method for the quantitation of microgram quantities of protein utilizing the principle of protein-dye binding. *Analytical Biochemistry, 72*, 248–254.
21. Richard, L. T. (1998). The competitive inhibition of yeast alcohol dehydrogenase by 2,2,2-trifluoroethanol. *Biochemical Education, 26*, 239–242.
22. Pereira, A. P., Estevinho, L. M., & Mendes-Faia, A. (2014). Mead production: fermentative performance of yeasts entrapped in different concentrations of alginate. *Journal of the Institute Brewing, 120*, 575–580.
23. Saha, S. P., & Ghosh, S. (2014). Optimization of xylanase production by *Penicillium citrinum* xyn2 and application in saccharification of agro-residues. *Biocatalysis and Agricultural Biotechnology, 3*, 188–196.
24. Dhawan, V. (2014). Reactive oxygen and nitrogen species: general considerations. In N. K. Gangdy, S. K. Jindal, S. Biswal, P. J. Barnes & R. Pawankar Eds., *Studies on Respiratory Disorders* (pp. 27–47). New York, NY: Humana Press.
25. Staab, C. A., Alander, J., & Brandt, M. (2008). Reduction of S-nitrosoglutathione by alcohol dehydrogenase III is facilitated by substrate alcohols via direct cofactor recycling and leads to GSH-controlled formation of glutathione transferase inhibitors. *Biochemical Journal, 413*, 493–504.
26. Gow, A. J., & Stamler, J. S. (1998). Reaction between nitric oxide and haemoglobin under physiological conditions. *Nature, 391*, 169–173.
27. Saboo, R., Bhattacharjee, A., & Majumder, U. et al. (2009). A novel role of catalase in detoxification peroxinitrite in *Saccharomyces cerevisiae*. *Biochemical and Biophysical Research Communications, 38*, 5507–5511.
28. Liu, L., Hausladen, A., & Zeng, M., et al. (2001). A metabolic enzyme for S-nitrosothiol conserved from bacteria to humans. *Nature, 410*, 490–494.

Process Biochemistry 113 (2022) 62–70

Contents lists available at ScienceDirect

Process Biochemistry

journal homepage: www.elsevier.com/locate/procbio

Short communication

Characterizing the effect of *S*-nitrosoglutathione on *Saccharomyces cerevisiae*: Upregulation of alcohol dehydrogenase and inactivation of aconitase

Swarnab Sengupta, Rohan Nath, Arindam Bhattacharjee *

Department of Microbiology, University of North Bengal, India

ARTICLE INFO

Keywords:
Saccharomyces cerevisiae
Aconitase
Nitrosative stress
GSNO
adh3

ABSTRACT

When exposed to nitrosative stress, the redox status of *Saccharomyces cerevisiae* changes significantly in vivo. Under nitrosative stress, aconitase, which catalyzes the conversion of citrate to isocitrate in the tricarboxylic acid (TCA) cycle, is known to be vulnerable. In this study, aconitase was completely repressed in the presence of 0.25 mM *S*-nitrosoglutathione (GSNO) as the nitrosative stress agent. Furthermore, a ~1.5 fold increase in ethanol production and a 3.5 fold increase in alcohol dehydrogenase (ADH) activity were observed in the presence of 0.25 mM GSNO when compared to the control (untreated). Furthermore, we supported our findings with a gene expression study of the *adh3* gene, which showed a 4 fold increase in the presence of 0.25 mM GSNO. This is the first report of its kind to characterize ethanol production under GSNO stress. This study may prove to be industrially significant in ethanol production.

1. Introduction

GSNO is a well-known endogenous •NO donor that can play a significant role in the alteration of redox homeostasis *in vivo* [1]. A large body of research in stress biology indicates that GSNO can be used as a nitrosative stress agent [2–7]. Reactive nitrogen species (RNS), which form inside the cell during nitrosative stress, have the ability to modify biomolecules such as DNA and proteins [1–9]. The change in redox homeostasis *in vivo*, which may lead to changes in the physicochemical properties of the cell, is one of the most significant hallmarks of nitrosative stress [9]. RNS includes nitric oxide radicals (•NO), peroxynitrite ($ONOO^-$), and nitrogen oxide radicals(NO_2^-). These are formed when reactive oxygen species (ROS) react with nitric oxide [10]. Nitric oxide is a freely diffusible, short-lived, lipophilic molecule. At low concentration, •NO is involved in cell signaling, but at high concentrations, it binds to heme, iron, and copper-containing proteins [11–13] and becomes toxic to the cell. •NO and RNS both exhibit cytotoxic and cytostatic activities due to the inhibition of ATP production, altered iron metabolism, enzyme inhibition, DNA and DNA repair system damage [5, 11,14–20]. To counteract the hostile condition, various stress response enzymes such as catalase, glutathione reductase (GR), SOD, and others are activated [6,21,22].

S. cerevisiae is an excellent model for studying the effects of nitrosative stress. It has been reported that GSNO stress affects aconitase (aconitate hydratase; EC 4.2.1.3), an important enzyme of the TCA cycle in *S. cerevisiae* [2,23]. As a result, inhibiting aconitase activity may have an effect on the aerobic respiration of *S. cerevisiae*. Alcohol dehydrogenase (ADH3) has been reported to act as a stress-response enzyme during nitrosative stress using GSNO [24,25]. Thus, using GSNO under nitrosative stress may cause a change in cellular metabolism, which may eventually lead to increased ethanol production *via* the fermentative pathway. However, no such report exists that characterizes the effect of GSNO on ethanol production by *S. cerevisiae*. Although many studies on metabolic engineering in *S. cerevisiae* have been conducted [26–28], certain drawbacks such as complexity, mutation, human safety, costing, and time consumption remain [29–32]. Furthermore, such procedures are prohibitively expensive [29–33]. Thus, one of the major areas of interest is an alternative, cost-effective, and simple process for increasing ethanol production by *S. cerevisiae*.

As a result, the objectives of this study were to examine the effect of

Abbreviations: S. cerevisiae, *Saccharomyces cerevisiae*; SOD, super oxide dismutase; $HClO_4$, perchloric acid; KOH, potassium hydroxide; DTNB, 5,50-dithio-bis (2-nitrobenzoic acid); PBS, phosphate Buffer Solution; TCA, trichloroacetic acid; CTAB, hexadecyltrimethylammoniumbromide; $KMnO_4$, potassium permanganate; DNS, 3, 5-dinitrosalicylic acid; qPCR, Quantitative Real-time PCR; cDNA, complementary DNA; SD, standard deviation.

* Corresponding author at: Department of Microbiology, University of North Bengal, West Bengal, India.
E-mail address: arindam.bose@gmail.com (A. Bhattacharjee).

https://doi.org/10.1016/j.procbio.2021.12.001
Received 9 February 2021; Received in revised form 4 December 2021; Accepted 10 December 2021
Available online 11 December 2021

nitrosative stress by GSNO on ethanol production by *S. cerevisiae* and to look for any changes in metabolic activity from respiration to fermentation. This is the first report of its kind that directly correlates ethanol production with a simple, cost-effective, and ecofriendly process involving nitrosative stress.

2. Materials and methods

2.1. Yeast culture and growth

Wild type haploid *S. cerevisiae* Y190 [ATCC 96400], a gift from Prof. Sanjay Ghosh CU, was used for all experiments. Cells were grown in YPD (2 % W\V yeast extract, 2 % W\V peptone, and 2 % W\V dextrose) medium at 30 °C under shaking condition (80 RPM). The single colonies containing YPD agar plates were kept at 4 °C refrigerator and 50 % glycerol stocks were kept at − 20 °C freezer. The glycerol stock was used for the preparation of preinoculum. 200 µl. from the glycerol stock was inoculated in a fresh YPD broth and incubated overnight at 30 °C. After that, streak plating was done on YPD agar plate using the overnight grown culture and incubated overnight at 30 °C to isolate single colonies. Following that, the culture was checked for contamination by phase contrast microscopy. Then pre-inoculum was prepared by inoculating single isolated colony in YPD broth and again incubated overnight at 30 °C. The overnight grown *S. cerevisiae* cells were then used as inoculum for further experiments.

2.2. Preparation of S-nitrosoglutathione

GSNO was prepared according to the method of Hart with slight modifications [34]. In short, 0.5 M GSNO was obtained by mixing 1 M of $NaNO_2$ (Sigma-Aldrich) in double-distilled water and 1 M GSH (Himedia) in 1 N HCl in cold (1:1 V/V). The concentration of GSNO was measured spectrophotometrically (ThermoScientific MultiskanGO) at 335 nm. The above-mentioned instrument was used for all other spectrophotometric studies.

2.3. Cell viability assay

Mid-log phase yeast cells were grown in YPD medium treated with different concentrations of GSNO (0.25 mM, 0.5 mM, 1 easeumM) and incubated overnight in shaking condition. Following an overnight incubation, 1 ml of culture from each sample was serially diluted and plated on YPD agar medium for viable cell count. As a control, a culture with no GSNO was used. The growth curve was created by recording the O.D. at 600 nm for 11 h at 60 min intervals [35]. The growth curve was used to calculate the specific growth rate. Additionally, growth curve was also studied upto 48 h.

2.4. Preparation of cell-free extracts (CFE) and estimation of protein

Cell-free extract (CFE) of treated and untreated cultures were prepared for different enzymatic assays. Overnight grown cultures of treated and untreated samples were centrifuged, and the supernatants were discarded. The cell pellets were lysed by using glass beads and lysis buffer containing 100 mM Tris-HCl (pH 7.6), 150 mM NaCl, 1 mM SDS, 1 mM DTT, 2 mM EDTA, protease inhibitor cocktail (Sigma-Aldrich), and 1 mM PMSF [3]. The concentration of protein was estimated as per the Bradford protocol. The standard curve for estimation of protein concentration was prepared by using BSA [36].

3. Assay of redox homeostasis

3.1. Reduced to oxidized glutathione ratio

The concentrations of GSH (reduced glutathione) and GSSG (oxidized glutathione) were determined using the method described by Akerboom et al. [37]. CFEs (from both treated and untreated samples) were first deproteinized with 2 M $HClO_4$ (Merck), 2 M EDTA (Himedia), and then neutralized with 2 M KOH (Himedia), 0.3 M HEPES (Himedia) to pH 7. After centrifuging one portion of the neutralized samples at 5000 *g* for 5 min, the supernatants were collected to determine the total *in vivo* thiol concentration (GSH + GSSG) using Glutathione Reductase (GR) dependent DTNB (Himedia) reduction method. Another portion of the samples was treated with 2-vinylpyridine (50:1 V/V) for 60 min and used to determine GSSG. Time scan was done at 412 nm for 3 min. Both GSH and GSSG concentrations were expressed in nmol/mg of protein.

3.2. Glutathione reductase assay

The glutathione reductase assay was performed according to the protocol of Carlberg and Mannervik with slight modification [38]. In brief, 2 mM GSSG (Himedia), 3 mM DTNB, and 2 mM NADPH (Himedia) were mixed with an assay buffer containing 1 mM EDTA and CFE. Time scan was done at 412 nm for 3 min. Reaction mixture without CFE was taken as a baseline. Specific activity was expressed in mU/mg of protein.[1]

3.3. Catalase assay

Catalase activity was assayed according to the method of Aebi with slight modification [39]. In brief, H_2O_2 degradation was measured spectrophotometrically at 240 nm for 2 min. The reaction mixture contained 0.1 M potassium phosphate buffer at pH 7.5, 50 mM EDTA, H_2O_2 (Sigma-Aldrich), and CFE. Reaction mixture without CFE was taken as a baseline. Specific activity was expressed in mU/mg of protein[1].

3.4. S-nitrosoglutathione reductase (GSNOR) assay

GSNO Reductase assay was performed according to the protocol of Sahoo et al. with slight modifications [3]. In brief, 100 mM GSNO, 0.2 mM NADH (Himedia), and 0.5 mM EDTA were mixed in 20 mM Tris-Cl pH 8.0 with CFE. The conversion of NADH to NAD was recorded at 340 nm for 5 min. Reaction mixture without CFE was taken as a baseline. Specific activity was expressed in mU/mg of protein.

3.5. Confocal microscopy

Confocal microscopy (Leica TCS SP8) was used to detect nitric oxide (NO) and reactive oxygen species (ROS). NO and ROS were detected using the Invitrogen protocol, with some modifications. In brief, 2×10^6 cells were washed and resuspended in PBS pH 7.4 before being fixed with absolute ethanol. The dyes (H_2DCFDA [Invitrogen] specific for ROS and DAF-FM [Invitrogen] specific for NO) were then added at a final concentration of 1.5 µM and incubated in the dark for 20 min. Excitation was set to 495 nm for confocal microscopy and emission to 515 nm. The positive control for ROS analysis was prepared with 0.1 mM H_2O_2 treated *S. cerevisiae* cells. Experiments for NO and ROS were repeated independently at least three times and micrographs (45X) were taken. The intensity of fluorescence was quantified with at least 50 no. of cells for each sample assayed using the Leica LAS X software.

3.6. Aconitase assay

Aconitase assay was performed according to the protocol of Castro et al. [40] with slight modifications. In brief, the formation of isocitrate (Sigma-Aldrich) from cis-aconitate was determined

[1] mU/mg of protein is defined as 1 mg of protein that catalyzes the conversion of one nanomole of substrate per minute under the specified conditions of the assay method.

spectrophotometrically at 240 nm for 3 min. The reaction mixture contained 500 mM cis-aconitate, 100 mM Tris-Cl pH 8 with CFE. Reaction mixture without CFE was taken as a baseline. Specific activity was expressed in mU/mg of protein.

3.7. Estimation of ethanol and reducing sugar

Ethanol and reducing sugar concentrations were estimated as per the protocol of Zhang et al. with slight modifications [41]. In brief, overnight grown untreated and treated *S. cerevisiae* broth cultures were centrifuged at 5000 g, and supernatants were collected. After that supernatants were mixed with equal volume of 20 % TCA at room temperature for 5 min and then centrifuged at 10,000 g. The supernatants were then treated with 1/5 vol of 20 % CTAB at 65 °C for 10 min and again centrifuged at 10,000 g. These pretreated samples were then diluted 100 folds for ethanol estimation. Pretreated samples are mixed with $KMnO_4$ solution and incubated at 40 °C for 90 min. Initial and final O.D. were recorded at 526 nm. Standard curve for the ethanol estimation was prepared by using absolute ethanol (Merck). The 10-fold diluted pretreated sample was mixed with DNS solution for the estimation of sugar concentration. Standard curve for reducing sugar estimation was prepared by using glucose (Merck). Further, ethanol yield and productivity were determined as mentioned by Mithra et al. with slight modification [42].

3.8. Alcohol dehydrogenase assay

Alcohol dehydrogenase activity was determined as per the protocol of Walker with some modifications [43]. In brief, the reaction mixture contained 50 mM sodium phosphate buffer at pH 8.8, 95 % V/V acetaldehyde (Sigma-Aldrich), 50 mM β-NADH, and diluted CFE. The O.D. was recorded at 340 nm for 6 min to determine the formation of β-NAD from β-NADH. Reaction mixture without CFE was taken as a baseline. Specific activity was expressed in mU/mg of protein.

3.9. In vitro study of alcohol dehydrogenase

ADH was studied *in vitro* by directly adding GSNO to the CFE. Cells were first grown under the previously mentioned conditions, and CFE was prepared. The CFE was then treated directly with 0.25 mM GSNO for 60 min. Following that, the ADH activity of treated and untreated samples determined, as previously stated [43]. The experiment was repeated with pure ADH (Sigma-Aldrich).

4. Gene expression analysis of *adh1, adh2, adh3* by quantitative Real Time PCR

4.1. RNA isolation

RNA isolation was carried out in accordance with the protocol developed by Dr. KPC Life Sciences in India, using their developed kit containing columns. Overnight grown treated and untreated *S. cerevisiae* cultures were centrifuged at 5000g, and pellets were washed twice with 1X PBS. After adding buffers, the entire solution was transferred to the prelim column and centrifuged at 10,000 g. The column was discarded and isopropanol was added and transferred to a Chrome column and centrifuged at 10,000 *g*. The chrome column was then washed and centrifuged at 10,000 *g* for 10 min. Finally, RNA was eluted in 50 µl nuclease-free water and quantified using 1 % agarose TAE gel. For each set of experimental conditions, at least two biological replicates were used.

4.2. cDNA preparation

The template for cDNA synthesis was 500 ng of RNA from each sample. RNA was denatured at 65 °C for 5 min with 10 mM dNTP and 10 mM random hexamer. The mixture was then immediately chilled on ice. The reverse transcriptase (RT) enzyme (Thermo Scientific) was then mixed in 5X RT specific buffer and incubated at 42 °C for 60 min before being heat inactivated at 65 °C for 15 min.

Table 1
Primers used in this study.

Primers	Sequences (5′→3′)
adh1F	GTTGCCATCTCTGCTTGCTGC
adh1R	ACACCATGAGGGCCACCTTT
adh2F	GTTACACCCACCACCAGTTTCT
adh2R	ACGGTGGTACCCTTAGCTCT
adh3F	CTGTCCTCACGCTGACTTGT
adh3R	CAACAATACCGTTGGCCCTA
gapdhF	CGGTAGATTGGTCATGAGAAT
gapdhR	TGGTACAAGAAGGTTTGGAAA

4.3. Quantitative real time PCR set up

Quantitative Real-time PCR (Biorad CFX-96) reaction was performed with SUPERZyan qPCR mastermix (Dr. KPC Life sciences) in the desired reaction conditions. One reaction (+RT) was setup using synthesized cDNA as the template for qPCR. The diluted RNA sample was used as the template in another reaction (-RT). This is done to ensure that the isolated RNA is free of DNA contamination. Another negative control (NTC) with no template was set up. This was a two-step PCR with denaturation at 95 °C for 15 s, annealing, and extension at 60 °C for 30 s. For qPCR, the number of cycles was 40, followed by a melt curve. All + RT reactions were carried out in triplicate. Table 1 contains a list of primers.

4.4. Statistical analysis

All individual results are expressed as mean ± SD (Standard deviation) of at least three independent experiments for each biological sample, where applicable. To analyze the significant difference between control and treated samples, Student *t*-test was used at 0.05 level of significance (p).

5. Results

5.1. Effect of S-nitrosoglutathione on cellular viability of S. cerevisiae

To determine the sub-toxic dose, cell viability of *S. cerevisiae* Y190 was tested in the presence of various concentrations of GSNO (0 mM, 0.25 mM, 0.5 mM, 1 mM). After an overnight incubation under shaking conditions, it was discovered that the presence of 0.25 mM GSNO in the medium had no effect on cell viability when compared to the control (0 mM GSNO). In the presence of 0.5 mM and 1 mM GSNO, under the same experimental conditions, cellular viability was significantly affected by nearly 30 % and 60 %, respectively, as compared to control **[Fig. S1]**. In comparison to the control, the growth curve of *S. cerevisiae* was found to be unaltered in presence of 0.25 mM GSNO **[Fig. S2]**. Furthermore, specific growth rate was also estimated from the growth curve, and no difference was found between control and treated *S. cerevisiae* ($0.22 hr^{-1}$). As a result, the concentration of GSNO was set to 0.25 mM for all subsequent experiments.

5.2. Effect on redox homeostasis in the presence of S-nitrosoglutathione

To investigate the alteration in redox homeostasis *in vivo* under nitrosative stress, GSSG/GSH ratio, GR, GSNOR, and catalase activity, were assessed.

According to the results, the total content of oxidized glutathione (GSSG) was decreased by 2.4 fold and reduced glutathione (GSH) was increased by 1.6 fold in the 0.25 mM GSNO treated cells, resulting in a 3.9 fold increase in the GSH/GSSG ratio when compared to the control

Table 2
Estimation of total glutathione (GSH + GSSG), GSH/GSSG and activity of glutathione reductase (GR), Catalase and S-nitrosoglutathione reductase (GSNOR) in both treated and untreated (control) samples of *S. cerevisiae*.

Sample	(GSH + GSSG) nmol/mg of protein	GSH nmol/mg of protein	GSSG nmol/mg of protein	GSH/GSSG	GR Activity (nU)/mg protein)	Catalase Activity (nU)/mg protein)	GSNOR Activity (nU)/mg protein)
Control	92 ± 2	34 ± 0.5	46±NA	0.7	4 ± 0.5	4 ± 0.4	1 ± 0.02
0.25 mM GSNO	75 ± 2	55 ± 0.4	20±NA	2.75	14 ± 0.7	20 ± 0.5	4 ± 0.5

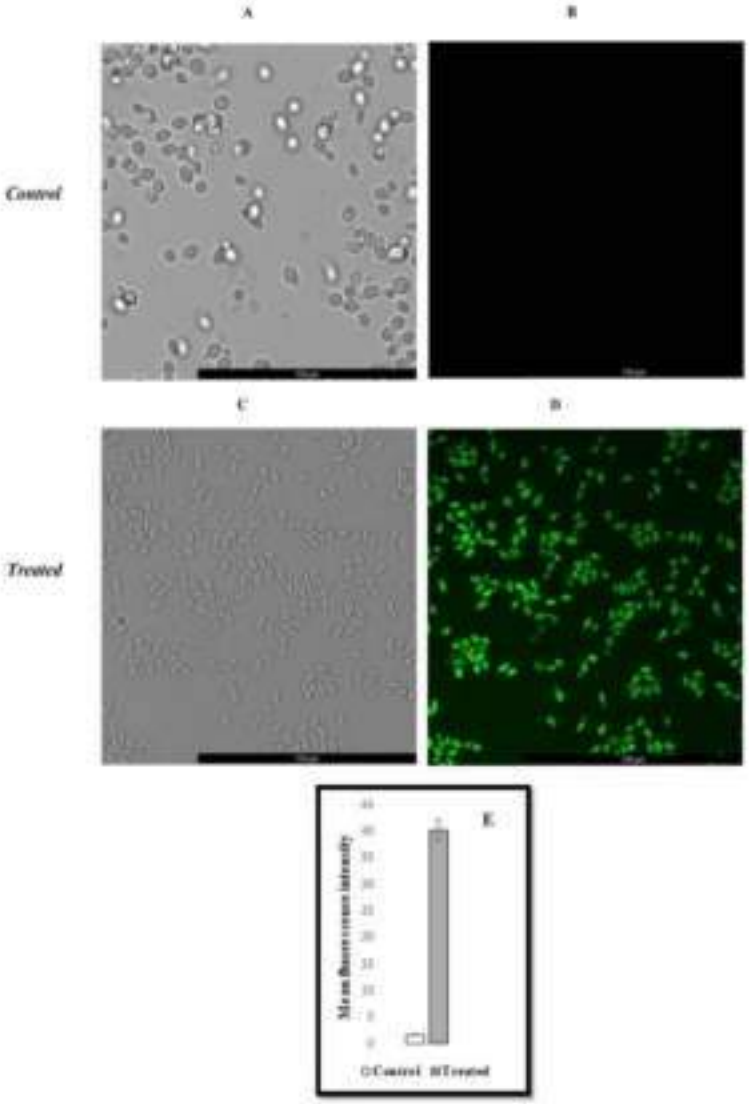

Fig. 1. Effect of S-nitrosoglutathione on nitric oxide (NO) generation: The presence of NO was visualized as green colour using DAF-FM (excitation at 495 nm and emission at 515 nm). Phase contrast and corresponding fluorescence images of *S. cerevisiae* control (A and B) and 0.25 mM GSNO treated (C and D). Micrographs were recorded at 45 × . Bar = 100 µm. The mean fluorescent intensity (E) was determined by using Leica LAS X software and represented as mean ± SD.

[Table 2]. The enzyme GR is responsible for catalyzing the conversion of GSSG to GSH [3]. As a result, we tested the GR activity of both treated and untreated samples. We discovered a 3.36fold increase in GR activity in the treated cells [Table 2]. This result supports the previous finding about the GSH/GSSG ratio. Furthermore, treated cells also showed 4.3 fold higher activity of GSNOR (GSNO reductase) as compared to control,

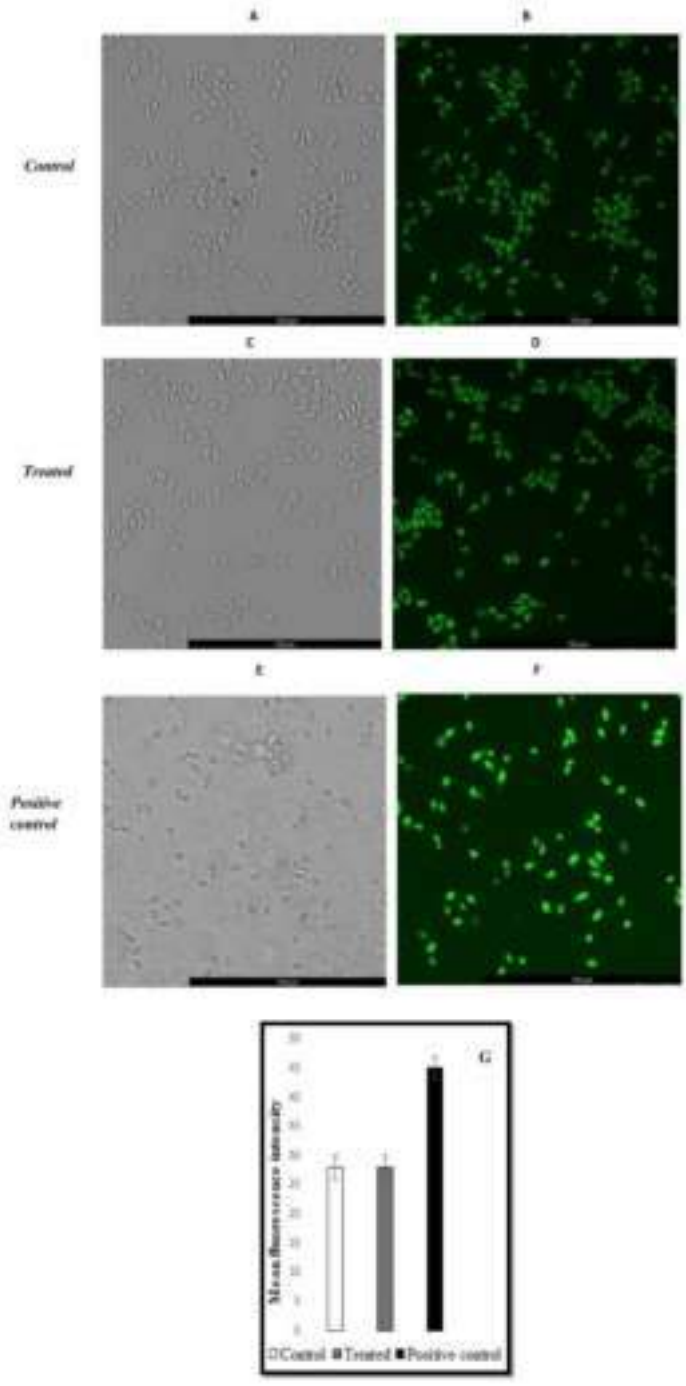

Fig. 2. Effect of S-nitrosoglutathione on reactive oxygen species (ROS) generation: The presence of ROS was visualized as green colour using H_2DCFDA (excitation at 495 nm and emission at 515 nm). Phase contrast and corresponding fluorescence images of *S. cerevisiae* control or untreated (A and B), 0.25 mM GSNO treated (C and D) and positive control [0.1 mM H_2O_2 treated] (E and F). Micrographs were recorded at 45 ×. Bar = 100 μm. The mean fluorescent intensity (G) was determined by using Leica LAS X software and represented as mean ± SD.

Table 3
Estimation of aconitase activity of treated and untreated (control) samples of *S. cerevisiae*.

Sample	Aconitase Activity (nU/mg protein)
Control	7 ± 0.25
0.25 mM GSNO	Not Detected

indicating that cells were expressing these enzymes to nullify the effect of GSNO [Table 2]. In the case of catalase, a general stress response enzyme, there was a 2.6 fold increase in specific activity in treated cells compared to controls [Table 2], implying that any ROS produced during the process was detoxified.

5.3. Effect of S-nitrosoglutathione on reactive oxygen species (ROS) and nitric oxide (NO) generation

To study redox homeostasis, it was critical to investigate the generation of ROS and NO [12]. The presence of ROS and NO was detected in our experimental conditions using confocal microscopy and mean fluorescence intensity. Surprisingly, NO was only detected in GSNO-treated cells [Fig. 1]. Untreated cells contained no NO. Whereas ROS was found in both the treated and untreated samples, there was no significant difference in ROS generation [Fig. 2]. As a result of the obtained data, it is possible to conclude that the effect observed under our experimental conditions is solely due to the generation of NO by 0.25 mM GSNO.

5.4. Effect of S-nitrosoglutathione on aconitase activity

It has previously been reported that nitrosative and oxidative stress can affect the activity of aconitase, a key enzyme in the TCA cycle [40, 44]. As a result, we used the aconitase assay in this study [Table 3]. Although aconitase activity was detected in untreated cells, it was not detected in cells treated with 0.25 mM GSNO. The result was particularly intriguing because it suggests that aconitase activity was suppressed under our experimental conditions.

5.5. Effect of S-nitrosoglutathione on ethanol production

When 0.25 mM GSNO was present, ethanol production increased significantly (~1.5 fold) when compared to the control [Table 4]. The ethanol yield was increased by approximately 1.3 fold and consumption of sugar was also 15 % higher under the stress condition. The volumetric productivity was also increased by approximately 1.5 fold in the presence of 0.25 mM GSNO. 76 % of the theoretical ethanol yield was found in the presence of 0.25 mM GSNO whereas only 59 % of the theoretical ethanol yield was found in untreated sample. Under our experimental conditions, these results suggest a possible shift in metabolic flux from respiration to fermentation.

5.6. Effect of S-nitrosoglutathione on alcohol dehydrogenase activity

Because ethanol production had increased, it was critical to investigate the activity of alcohol dehydrogenase. In this study, we discovered that ADH activity increased by 3.5 fold in the presence of 0.25 mM GSNO when compared to the control [Table 5]. Interestingly, no change in ADH activity was observed when an *in vitro* study was performed using CFE [Table 6], implying that GSNO may not be involved in ADH protein modification. ADH inhibition was also studied using 0.1 mM 2,2,2-trifluoroethanol. When the experiment was done with pure ADH, a similar type of result was obtained **[Fig. S3]**.

5.7. Effect of S-nitrosoglutathione on the expression of adh genes (adh1, adh2, adh3)

The expression levels of three important genes (*adh1*, *adh2*, *adh3*) were examined to determine the reason for the increased enzymatic activity of ADH in the presence of 0.25 mM GSNO. The expression of *adh1* **[Table S1A]** and *adh2* **[Table S1B]** were found to be increased by only 7 % and 5 %, respectively, whereas *adh3* expression **[Table S1C]** was found to be increased by 4 fold in the presence of 0.25 mM GSNO compared to the control [Fig. 3]. This result suggested that increased ADH enzyme activity in the presence of 0.25 mM GSNO was primarily due to an increase in *adh3* expression.

6. Discussion

We have reported for the first time in this study the relationship between GSNO stress and ethanol production by *S. cerevisiae*. Under subtoxic dose of GSNO stress, we found some significant changes in physicochemical properties of *S. cerevisiae* compared to control, indicating that the cells were attempting to combat the stress for survival. A significant 4.3 fold increase in GSNOR specific activity, for example, suggests that *S. cerevisiae* cells were attempting to counteract the stress imposed by GSNO by upregulating an enzyme that can reduce it to form GSSG. Again, the higher activity of GR converted GSSG to GSH, implying that an elevated level of reduced equivalents is required to maintain redox homeostasis *in vivo*. GSH is regarded as a stress response component that protects cells from reactive species-mediated cellular damage, metal toxicity, and so on [21,45]. Intracellular GSH plays an important role in the inhibition of NO activity [45,46]. When the GSH level decreases, NO activity induces DNA damage as well as protein modifications such as protein tyrosine nitration, *S*-nitrosylation and so on [47, 48]. According to some reports, GSNO acts as a reservoir of NO 'that can be transported outside the cell *via* a GSH transporter system [45,49]. As a result, the GSH can also maintain the cellular redox balance *via* the elimination of the nitrating agent. Catalase, which is known for its

Table 5
Estimation of alcohol dehydrogenase activity of treated and untreated (control) cells of *S. cerevisiae*.

Sample	Alcohol dehydrogenase Activity (nU/mg protein)
Control	10 ± 0.2
0.25 mM GSNO	35 ± 0.5

Table 6
Estimation of alcohol dehydrogenase activity of treated and untreated cell free extract (CFE) and treated CFE.

Conditions	ADH activity (nU/mg)
CFE	4 ± NA
0.25 mM GSNO treated CFE	4 ± NA
CFE + 2,2,2- trifluoroethanol	Not found
0.25 mM GSNO treated CFE + 2,2,2- trifluoroethanol	Not found

Table 4
Estimation of ethanol concentration, glucose consumption, ethanol yield, percentage of theoretical yield and volumetric productivity of treated and untreated (control) samples of *S. cerevisiae*.

Sample	Ethanol concentration (g/L)	Glucose consumed (g/L)	Ethanol yield (g/g of glucose)	% of theoretical yield	Volumetric Productivity (g/L/h)
Control	4.5 ± 0.3	15 ± 0.3	0.30	59	0.38
0.25 mM GSNO	7 ± 0.5	18 ± 0.4	0.39	76	0.56

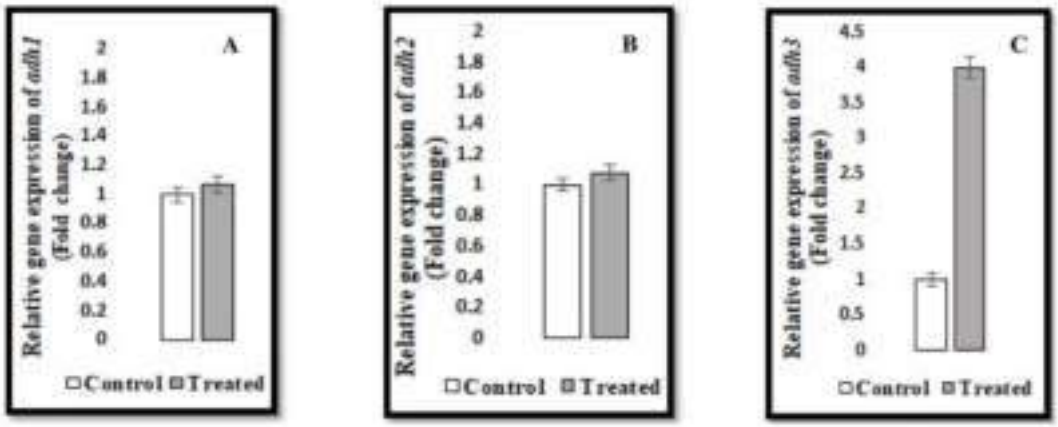

Fig. 3. Effect of S-nitrosoglutathione on adh genes expression: *qPCR analysis was done to determine the* **a.** *relative expression of adh1* **b.** *relative expression of adh2 and* **c.** *relative expression of adh3. The expression levels of adh genes (adh1, adh2 and adh3) were normalized with that of gapdh (glyceraldehyde-3-phosphate dehydrogenase) in each set and expressed as relative fold change taking the normalized expression level in respective untreated control as unity.*

catalytic detoxification of oxidants, was found to be upregulated by 2.5 fold in the presence of 0.25 mM GSNO in the same condition. Previous reports [8,30] also demonstrated that catalase help with the detoxification of nitrating agents such as peroxynitrite [31]. Confocal micrographs clearly demonstrated that NO was generated only in the presence of GSNO, and there was no significant change in ROS level after GSNO treatments, indicating that all the changes observed were due to the formation of NO or nitrosative stress.

Aconitase is an important enzyme in the TCA cycle [32]. The inactivation of this protein's $[4Fe\text{-}4S]^{2+}$ cluster *may* be responsible for the repression of aconitase activity in the presence of GSNO, according to our findings. According to the evidence, oxidation of the $[4Fe\text{-}4S]^{2+}$ cluster renders it inactive due to the formation of the $[3Fe\text{-}4S]^{1+}$ paramagnetic cluster, resulting in the inactivation of aconitase [33,34]. As a result, the TCA cycle in *S. cerevisiae* was severely affected, and metabolic flux was eventually switched from the respiratory to the fermentation pathway for generation of energy. This is evident from ethanol estimation in our experimental setup, where ~1.5 fold increase in ethanol production along with elevated yield (~1.3 fold) and volumetric productivity (~1.5 fold) were observed under 0.25 mM GSNO stress condition. From this, it can be concluded that, in the presence of GSNO-mediated nitrosative stress, the fermentation pathway may be activated in order to generate the energy required for cell survival. Then we looked into what was causing this stimulation.

A significant increase in the specific activity of ADH also supports our finding of increased ethanol production. Interestingly, it has been reported that ADH activity can be inhibited in *E. coli* in the presence of peroxynitrite, a potent nitrating agent [35]. It has also been reported that in the presence of GSNO, ADH3 can act as a stress response enzyme [24,25,36]. So we wanted to know how GSNO, as a nitrosative stress agent, modulates such biochemical changes whether through structural modification of ADH or increased expression of *adh* genes (*adh1*, *adh2* and *adh3*). To determine this, we first performed an *in vitro* assay of ADH to see if its activity changed. Interestingly, CFE treated with GSNO showed no changes in its ADH activity. This finding suggests that protein-level modification of ADH may not be possible in the presence of GSNO. As a result, we used qPCR to determine the quantitative expression levels of *adh1*, *adh2* and *adh3*. A significant 4 fold increase in *adh3* expression after GSNO treatment could be the main reason for higher enzymatic activity of ADH. However, there was no significant change in *adh1* and *adh2* expression in the presence of 0.25 mM GSNO compared to the control. This finding suggested that ADH3 activity was required to overcome the effect of GSNO stress in our experimental condition, which corroborated previous findings. According to reports, GSNO-mediated post-translational modifications such as *S*-nitrosylation of a protein can interfere with the protein-protein interactions by modulating phosphorylation, ubiquitination, acetylation, *etc.* [37,38]. Modulations of this type have the potential to influence cellular processes by altering the activity of various enzymes and proteins. As a result, there was a possibility that GSNO-mediated post-translational modifications of important transcription factor/s would result in increased *adh3* expression [39].

Overall, these findings indicate that sub-toxic concentrations of GSNO can induce the ethanol fermentation pathway without impairing cell viability. Because the primary goal of the fermentation industry is to achieve higher yield with fewer complexities, this process clearly has potential. This method will provide a simple, cost-effective (GSNO costs are very low), and non-hazardous approach. As a result, this GSNO-treated *S. cerevisiae* will be beneficial and novel for bioethanol production. Though many methods for increasing ethanol production have been developed, this strategy may gain traction in the future. However, because it is still a laboratory phenomenon, we believe that more research is required before it can be used in industry.

7. Conclusions

According to the findings of this study, aconitase activity was suppressed in the presence of 0.25 mN GSNO, which could result in inhibition of the TCA cycle. As a result, the metabolic flux of *S. cerevisiae* was switched from respiration to fermentation, and the *adh3* gene was overexpressed. As a result, the enzymatic activity of ADH was increased, resulting in increased ethanol production. This is the first report with a higher industrial significance on the relationship between GSNO stress and ethanol production. However, more detailed research is needed to understand the underlying molecular mechanism.

Data availability

Not applicable.

Declaration of Competing Interest

The authors declare that there is no conflict of interest.

Acknowledgment

This work was supported by the University of North Bengal, West Bengal, India [Ref. No. 1514/R-2020 Dated 01.06.2020]. Authors also acknowledge Bose institute, Kolkata and Dr. KPC Life sciences, Kolkata for providing services for confocal microscopy and qPCR respectively.

Appendix A. Supplementary data

Supplementary material related to this article can be found, in the online version, at doi:https://doi.org/10.1016/j.[illegible].

References

[illegible]

peroxynitrite reductase, J. Biol. Chem. 272 (1997) 27812–27817, https://doi.org/10.1074/jbc.272.44.27812.
[49] M.S. Choi, Pathophysiological role of S-nitrosylation and transnitrosylation depending on S-nitrosoglutathione levels regulated by S-nitrosoglutathione reductase, Biomol. Ther. 26 (2018) 533–538, https://doi.org/10.4062/biomolther.2018.179.
[50] R. Sahoo, A. Bhattacharjee, U. Majumdar, et al., A novel role of catalase in detoxification of peroxynitrite in S. cerevisiae, Biochem. Biophys. Res. Commun. 385 (2009) 507–511, https://doi.org/10.1016/j.bbrc.2009.05.062.
[51] L. Gebicka, J. Didik, Catalytic scavenging of peroxynitrite by catalase, J. Inorg. Biochem. 103 (2009) 1375–1379, https://doi.org/10.1016/j.jinorgbio.2009.07.011.
[52] C. Auger, J. Lemire, D. Cecchini, et al., The metabolic reprogramming evoked by nitrosative stress triggers the anaerobic utilization of citrate in *Pseudomonas fluorescens*, PLoS One 6 (2011), e28469, https://doi.org/10.1371/journal.pone.0028469.
[53] L. Castro, V. Tórtora, S. Mansilla, et al., Aconitases: non-redox iron-sulfur proteins sensitive to reactive species, Acc. Chem. Res. 52 (2019) 2609–2619, https://doi.org/10.1021/acs.accounts.9b00150.
[54] D. Han, R. Canali, J. Garcia, et al., Sites and mechanisms of aconitase inactivation by peroxynitrite: modulation by citrate and glutathione, Biochem. 44 (2005) 11986–11996, https://doi.org/10.1021/bi0509393.
[55] J.P. Crow, J.S. Beckman, J.M. McCord, Sensitivity of the essential zinc-thiolate moiety of yeast alcohol dehydrogenase to hypochlorite and peroxynitrite, Biochem. 34 (1995) 3544–3552, https://doi.org/10.1021/bi00011a008.
[56] N.H. Chen, K.Y. Djoko, F.J. Veyrier, et al., Formaldehyde stress responses in bacterial pathogens, Front. Microbiol. 7 (2016) 257, https://doi.org/10.3389/fmicb.2016.00257.
[57] M.V. Navarro, A. Chaves, D.G. Castilho, et al., Effect of nitrosative stress on the S-nitroso proteome of *Paracoccidioides brasiliensis*, Front. Microbiol. 11 (2020) 1184, https://doi.org/10.3389/fmicb.2020.01184.
[58] D.T. Hess, J.S. Stamler, Regulation by S-nitrosylation of protein post-translational modification, J. Biol. Chem. 287 (2012) 4411–4418, https://doi.org/10.1074/jbc.R111.285742.
[59] Y. Sha, H.E. Marshall, S-nitrosylation in the regulation of gene transcription, Biochim. Biophys. Acta 1820 (2012) 701–711, https://doi.org/10.1016/j.bbagen.2011.05.008.

BHATTACHARJEE ARINDAM (Orcid ID: 0000-0003-0853-9513)

Variation in glucose metabolism under acidified sodium nitrite mediated nitrosative stress in *Saccharomyces cerevisiae*

Running title: Nitrosative stress in *Saccharomyces cerevisiae*

Swarnab Sengupta[1], Rohan Nath[1], Rajabrata Bhuyan[2], Arindam Bhattacharjee[1#]

1 Department of Microbiology, University of North Bengal

Corresponding author: Department of Microbiology, University of North Bengal, West Bengal, India, pin-734013, Mobile no. +919674665722, Fax no. 0353-2776319, abmicrobio@nbu.ac.in

2 Department of Bio-Science and Biotechnology, Banasthali Vidyapith (Deemed) University, Banasthali, Rajasthan, India, Pin-304022

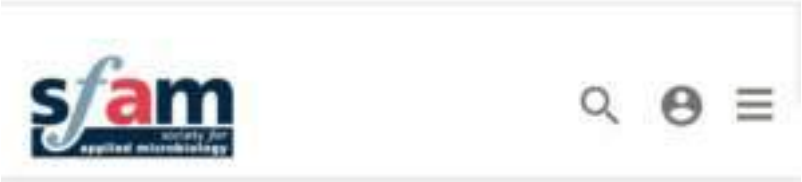

Journal of Applied Microbiology / Accepted Articles

ORIGINAL ARTICLE

Variation in glucose metabolism under acidified sodium nitrite mediated nitrosative stress in *Saccharomyces cerevisiae*

Swarnab Sengupta, Rohan Nath, Rajabrata Bhuyan, Arindam Bhattacharjee

First published: 15 June 2022

https://doi.org/10.1111/jam.15669

This article has been accepted for publication and undergone full peer review but has not been through the copyediting, typesetting, pagination and proofreading process which may lead to differences between this version and the Version of Record. Please cite this article as doi: 10.1111/jam.15669

Abstract

Aims

The work aimed to understand the important changes during glucose metabolism in *Saccharomyces cerevisiae* under acidified sodium nitrite (ac.$NaNO_2$) mediated nitrosative stress.

Methods and Results

Confocal microscopy and FACS analysis were performed to investigate the generation of reactive nitrogen and oxygen species and redox homeostasis under nitrosative stress was also characterized. qPCR analysis revealed that the expression of *ADH* genes were upregulated under such condition whereas the *ACO2* gene was downregulated. Some of the enzymes of tricarboxylic acid (TCA) cycle were partially inhibited whereas malate metabolism and alcoholic fermentation were increased under nitrosative stress. Kinetics of ethanol production was also characterized. Network analysis was conducted to validate our findings. In presence of ac.$NaNO_2$, *in vitro* protein tyrosine nitration (PTN) formation was checked by western blotting using pure alcohol dehydrogenase (ADH) and aconitase.

Conclusions

Alcoholic fermentation rate was increased under stress condition and this altered metabolism might be conjoined with the defense machinery to overcome the nitrosative stress.

Significance and impact of the study

This is the first work of this kind where the role of metabolism under nitrosative stress has been characterized in *S. cerevisiae* and it will provide a base to develop an alternative method of industrial ethanol production.

Keywords

Tricarboxylic acid (TCA) cycle, Malate metabolism, Alcoholic fermentation, Protein tyrosine nitration

Introduction

Nitrosative stress is an *in vivo* hostile condition which is created due to the "noxious" activity of reactive nitrogen species (RNS) **(Yoshikawa *et al.* 2016)**. RNS are formed during the reaction between reactive oxygen species (ROS) and nitric oxide (NO) **(Ridnour *et al.* 2004; Peluffo and Radi 2007)**. Alteration of the redox homeostasis along with the modification of macromolecules like DNA, proteins, lipids are considered to be the major consequences of nitrosative stress that leads to the modification of physicochemical properties of the cell **(Kurutas 2016; Patra *et al.* 2019; Patra *et al.* 2017; Carballal *et al.* 2014)**. Under nitrosative stress, this structural modification of proteins and enzymes by protein tyrosine nitration (PTN) and *S*-nitrosylation may result in the alteration of their activity. Hence, PTN and *S*-nitrosylation are considered as markers of nitrosative stress **(Bartesaghi and Radi 2018; Wang *et al.* 2014; Barbosa-Sicard *et al.* 2009)**. These modifications of the proteins may affect the 'normal' cellular functions like iron metabolism, aerobic respiration etc. **(Bartesaghi and Radi 2018; Wang *et al.* 2014; Barbosa-Sicard *et al.* 2009; Witkiewicz-Kucharczyk *et al.* 2020)**. To overcome such condition, cells have different defense strategies to detoxify the effect of RNS like stimulating stress response enzymes glutathione reductase (GR), catalase, superoxide dismutase (SOD) etc. as well as non-enzymatic (GSH, NADH etc.) responses. This induction of enzymatic and non-enzymatic response under stress conditions may cause alteration in the cellular responses for the survival of the organisms **(Bartesaghi and Radi 2018; Navarro *et al.* 2020; Lindemann C *et al.* 2013; Aquilano K *et al.* 2014; Pollak N *et al.* 2007)**.

Saccharomyces cerevisiae is one of the most extensively studied organism in the field of nitrosative stress **(Bhattacharjee *et al.* 2010; Liu L *et al.* 2000; Horan *et al.* 2006; Anam *et al.* 2020)**. Previous studies showed that the growth of *S. cerevisiae* was not significantly decreased in the presence of sub-toxic dose or lower concentration of RNS **(Ying *et al.* 2017; Nasuno R *et al.* 2014; Peláez-Soto *et al.* 2020)**. It has also been reported that the function of the respiratory chain in *S. cerevisiae* may get hampered under nitrosative stress due to the inactivation of several TCA cycle enzymes. One important enzyme of this cycle, aconitase, catalyzes the reaction from citrate to isocitrate, and is also a well-known marker of redox stress **(Lushchak *et al.* 2014)**. Previous reports suggest that it can be affected under nitrosative insult **(Radi 2018; Lushchak *et al.* 2010)**. Thus, ATP synthesis may get inhibited under such condition **(Ying *et al.* 2017; Sahoo *et al.* 2003)**. However, the exact mechanism of generation of energy as well as the citrate metabolism under such condition has not been well characterized. Earlier studies from our lab showed upregulation of ADH activity and higher

ethanol production under ac.$NaNO_2$ mediated nitrosative stress using *S. cerevisiae* **(Sengupta *et al.* 2020)**. A few reports also indicated towards an increase in alcohol dehydrogenase activity under nitrosative stress **(Liu L *et al.* 2000; Jahnová *et al.* 2019; Staab *et al.* 2008)**. Hence, all these reports imply that the glucose metabolic flux may get shifted from respiration towards fermentation pathway under nitrosative stress **(Ying *et al.* 2017; Fitzsimmons *et al.* 2018; Kitichantaropas *et al.* 2016; Tillmann *et al.* 2011)**. But, definitive studies regarding the characterization of glucose metabolism in *S. cerevisiae* under nitrosative stress condition was not yet well-established that can answer those questions.

Hence, the primary objective of our work was to characterize the glucose metabolism in *S. cerevisiae* under nitrosative stress by assaying different key enzymes of the TCA cycle, alcohol fermentation, malate metabolism and anaplerotic reactions. Further we investigated the alteration in redox homeostasis by estimating the reduced to oxidized glutathione (GSH/GSSG) ratio, catalase and GR. In addition to this, *in vitro* study of the protein modification in aconitase and ADH enzymes was also performed under stress condition. Here, we have tried to delineate the metabolic pathway in *S. cerevisiae* under nitrosative stress. This study has a huge potential as application for high ethanol production at industrial scale and at the same time serves as the base to characterize the metabolic responses of *S. cerevisiae* under nitrosative stress.

Materials and Methods

Yeast culture and growth

Wild type haploid *S. cerevisiae* Y190 [ATCC 96400] (a gift from Prof. Sanjay Ghosh, Calcutta University, India), was used for all the experiments. Cells were grown for overnight in YPD (2% w/v yeast extract [HiMedia], 2% w/v peptone [HiMedia] and 2% w/v dextrose [Merck] at 30°C at 80 RPM. The strain was preserved in 50% glycerol stocks at -20°C freezer. 200 µL from the glycerol stock was inoculated in a fresh YPD broth and incubated overnight at 30°C. Streak plating was performed on YPD agar to ensure purity and a single colony was cultured overnight in YPD broth at 30°C. These cultures were used as inoculum for further experiments at an $O.D._{600}$~0.05.

Preparation of acidified sodium nitrite and determination of cell viability

A 100 mM stock solution of ac.$NaNO_2$ was prepared by adding $NaNO_2$ to 0.2 N HCl. This was used as the 'NO donor' **(Regev-Shoshani *et al.* 2013)** and applied to the culture at the early log phase ($O.D._{600}$~0.3). After 12 hours, cell viability was determined using serial dilution and growth curves were also determined based on $O.D._{600}$ for 12 hours at 60-min intervals. For the control experiment, the yeast was cultured in absence of ac.$NaNO_2$.

Preparation of cell free extract (CFE) and estimation of protein concentration

Overnight (12 hours) grown cultures of treated and untreated samples ($O.D._{600}$ ~1.8) were centrifuged and cell pellets were mixed with lysis buffer containing 100 mM Tris-HCl pH 7.6, 150 mM NaCl, 2 mM EDTA, protease inhibitor cocktail (Sigma-Aldrich), and 1 mM PMSF and lysed by using glass beads. Concentration of protein was estimated as per the protocol of Bradford using BSA as the standard **(Bradford 1976)**.

Estimation of GSH:GSSG ratio

The GSH and GSSG concentration was determined according to the method of Akerboom et al. with slight modification **(Akerboom and Sies 1981)**. In brief, CFEs were first deproteinized with 2 M $HClO_4$, 2 mM EDTA and then neutralized with 2 M KOH containing 0.3 M HEPES pH 7.0. Half of the neutralized samples were taken to estimate the *in vivo* thiol concentration (GSH+GSSG) by GR [Sigma-Aldrich] dependent DTNB [5,5-dithio-bis(2-nitrobenzoic acid)] reduction. The other half was treated with 2-vinylpyridine (50:1 v/v) for 1 hour and used to determine the GSSG concentration by UV spectroscopy at 412 nm. Concentration of GSH and GSSG were expressed in nmol/mg of protein.

Detection of ROS and RNS

Confocal microscopy

RNS and ROS were detected by confocal microscopy (Leica TCS SP8) from Bose institute, Kolkata, as per the protocol of Invitrogen with some modifications. In brief, $2X10^6$ overnight grown cells were washed and resuspended in PBS pH 7.4 and fixed using absolute ethanol. Then, dyes (DAF-FM specific for NO and H2DCFDA specific for ROS) were added at a final concentration of 1.5 µM and incubated for 30 minutes in the dark. For confocal microscopy excitation was fixed at 495 nm and emission at 515 nm. Micrographs were captured at 45X magnification and the intensity of fluorescence was recorded using the Leica LAS X software.

FACS

FACS (BD LSRFortessa) analysis for ROS and RNS were done from IICB, Kolkata, as per the protocol of Invitrogen. Samples were prepared as mentioned above and dye-free cells were used as the blank. The photomultiplier tube voltage was kept at 190 mV for the FITC channel at a flow rate of 12 µl/min. 10000 events were recorded for each sample and histograms were prepared by plotting the cell counts against fluorescence in the FITC channel. Excitation and emission were set as above and data were analysed by using FACS Diva software.

Quantification of ethanol and reducing sugar

The concentrations of ethanol and reducing sugar were estimated as per the protocol of Zhang *et al.* with slight modifications **(Zhang P *et al.* 2019)**. In short, overnight grown untreated and

treated cultures were centrifuged at 5000 *g*, and supernatants were collected. These were mixed with an equal volume of 20% TCA at room temperature for 5 min. Following centrifugation at 10000 *g*, supernatants were treated with 1/5 volume of 20% CTAB at 65°C for 10 min and again centrifuged at 10000 *g*. Samples were diluted 100 fold and mixed with $KMnO_4$ solution and incubated at 40°C for 90 min. Initial and final O.D. were recorded at 526 nm. A standard curve for the ethanol estimation was prepared with absolute ethanol (Merck). For the reducing sugar estimation, the pretreated sample was diluted 10-fold and mixed with DNS solution, after which O.D. was recorded at 540 nm. A standard curve for reducing sugar estimation was prepared with glucose (Merck). The kinetics of ethanol production (yield and productivity) were also determined **(Mithra *et al.* 2018)**.

Enzymatic assays

All enzymatic assays were based on spectophotometric analysis. GR **(Carlberg and Mannervik 1975)** and malate synthase (MS) **(Chell *et al.* 1978)** were determined at 412 nm and catalase **(Aebi *et al.* 1984)** and aconitase **(Castro *et al.* 1994)** at 240 nm. Pyruvate carboxylase (PC) was measured after **Payne and Morris (1969)** and citrate synthase (CS) after **Srere 1971**. The other enzyme activities were determined by changes in NADH at 340 nm: pyruvate dehydrogenase (PDH), isocitrate dehydrogenase (ICDH) and malate dehydrogenase (MDH) **(Bergmeyer *et al.* 1974)**, MDH (decarboxylating) **(Geer *et al.* 1980)**, aldehyde dehydrogenase (ALDH) **(Bostian and Betts 1978)**, and pyruvate decarboxylase (PDC) **(Gounaris *et al.* 1971)**. In all cases specific activity was expressed in mU/mg of protein.

Estimation of the concentration of citrate

Intracellular and extracellular citrate concentration was determined by a citrate assay kit (Sigma-Aldrich) and expressed in ng/µL.

RNA isolation and qPCR

RNA isolation, cDNA preparation and qPCR was outsourced to Dr. KPC Life sciences, India. For this, treated and untreated samples were centrifuged at 5000 *g* and after two wash steps with PBS, RNA was isolated by use of standard affinity columns and eluted in nuclease-free water. 500 ng of RNA was used as the template for cDNA synthesis which was performed with 200 units of reverse transcriptase (RT) enzyme (Thermo Scientific) in RT buffer containing 10 mM dNTPs and 10 µM random hexamer. Following incubated at 42°C for 60 min and heat inactivation at 65°C for 15 min. The cDNA was used for +RT qPCR (Biorad CFX-96) using SUPERZym qPCR master mix (Dr. KPC Life sciences). The Diluted RNA sample was used as the template for (-RT) qPCR. A negative control (NTC) was set up without template. The two-step PCR was initiated with denaturation at 95°C for 15 sec and annealing and extension

was done at 60°C for 30 sec for 40 cycles, followed by a melt curve. The primers for the experimental and housekeeping genes were designed from NCBI and enlisted in **Table S1**.

Functional annotation and network analysis

The enzymes, with altered activity in presence of 0.5 mM ac.$NaNO_2$, were subjected for functional enrichment analysis. First, the STRING database was used to screen interactions followed by creating a functionally interacting network **(Szklarczyk *et al.* 2019)**. Few closely associated enzymes were added to the network to increase stability and obtain reliable predictions. The networks were analyzed and visualized using Cytoscape (Version 3.7) **(Shannon *et al.* 2003)**. Annotation of functionally activated and deactivated enzymes were analyzed using Gene Ontology (GO) analysis by DAVID (Database for Annotation, Visualization and Integrated Discovery) **(Dennis *et al.* 2003)**. Enzyme sets were taken from respective networks, and their annotations classified into biological process (BP), cellular component (CC) and molecular function (MF). For the GO analyses, Bonferroni correction method was used to identify significant terms associated with the genes and the error rates was reduced by removing the false discovery outcomes from any prediction.

Western blotting

Western blots were produced from 10% polyacrylamide gels **(Laemmli *et al.* 1970)** loaded with the pure enzymes aconitase (Sigma-Aldrich) and ADH (Sigma-Aldrich). Following transfer to PVDF membranes the blots were probed with anti 3-nitrotyrosine monoclonal antibody (Sigma-Aldrich) at 1:1000 dilution in TBST and following incubation with HRP conjugated goat anti-mouse IgG secondary antibody (Sigma-Aldrich) at 1:10000 dilution in TBST, bands were visualized by using chemiluminescence reagent (Abcam). Images were captured using DNR bio-imaging system miniBIS Pro (USA) with GelQuant Express Analysis Software.

Condition of stress and assays with pure aconitase and alcohol dehydrogenase

Pure protein (200 µg) was incubated for 30 min at room temperature in presence of different concentrations (0.1 mM, 0.3 mM, 0.5 mM) of ac.$NaNO_2$ and 0.1 mM peroxynitrite (positive control). An aliquot of 80 µg was used to determine PTN by western blotting as described above. The rest was used for specific activity determination described above.

Statistical analysis

Experimental data were statistically analyzed by using two tailed paired T-test and expressed as mean±SD. Level of significance (p) ≤ 0.01 was considered as significant. Most of the experiments were performed at least in triplicate.

Results

Effect of acidified sodium nitrite on redox homeostasis

The growth curves of *S. cerevisiae* (Fig. S1), were similar between control and 0.5 mM ac.$NaNO_2$ treated *S. cerevisiae* with a growth rate of 0.22 hr^{-1} for both, indicating that the used concentration of ac.$NaNO_2$ was not toxic to the cells. The redox homeostasis of treated and untreated cells was assessed by GSH/GSSG ratio, GR activity and catalase activity. The GSH/GSSG ratio was increased by 4.2 fold under the stress condition as compared to the control (Fig. 1A). There was no significant change in total glutathione concentration but the concentration of GSSG was decreased by 2.3 fold (Fig. S2A) whereas concentration of GSH was increased 1.8 fold (Fig. S2B) in treated cells. In addition, GR activity was increased by 4 fold under the stress condition (Fig. 1B). Activity of catalase was also increased, by approximately 2.4 fold under the stress condition as compared to the control (Fig. 1B). These findings suggest that the redox homeostasis of the cells were significantly altered under the stress condition and the cells were trying to compensate and adapt. To study the alteration of redox homeostasis, the generation and accumulation of ROS and RNS within the cell was investigated by confocal microscopy (Fig.2A-J) and FACS (Fig. 2K-N). The result showed that ROS was generated in both treated and untreated cells with no significant change, while, RNS generation was only observed in the 0.5 mM ac.$NaNO_2$ treated cells (79%), clearly suggesting that the changes observed in the treated cells were solely due to the generation of RNS. This data is corroborated with our previously published report **(Sengupta *et al.* 2020)**.

Effect of acidified sodium nitrite on kinetics of ethanol production

The effect of 0.5 mM ac.$NaNO_2$ on the ethanol yield and productivity was next determined. We found that ethanol yield was increased by 1.2 fold and consumption of sugar was ~14% higher under the stress condition. The volumetric productivity was increased, by approximately 1.3 fold in the presence of 0.5 mM ac.$NaNO_2$. 69% of the theoretical ethanol yield was achieved during treatment whereas only 59% of the theoretical ethanol yield was achieved in control (Table 1). These results clearly indicated that alcoholic fermentation rate was increased under ac.$NaNO_2$ mediated nitrosative stress. Next, we checked the effect of 0.5 mM ac.$NaNO_2$ on the TCA cycle and other biochemical pathways, for which activity of some of the key enzymes were determined.

Effect of acidified sodium nitrite on key enzymes of important biochemical pathways

The specific activity of aconitase was approximately 50% less in treated cells as compared to the control (Fig. 3A) and the combined concentration of intracellular and extracellular citrate

was also halved (Table S2), indicating that the synthesis of citrate was decreased under stress condition (Fig. 3B). Hence, we assayed the activity of CS and this was also found to be decreased by 50% (Fig. 3A), suggesting that the citrate metabolism as well as the TCA were affected. As the specific activity of CS was significantly reduced, the utilization of pyruvate was next assessed. Pyruvate is the end product of glycolysis and is an important secondary metabolite that is further utilized in the TCA cycle, either by formation of acetyl-CoA or OAA by the activity of PDH or PC, respectively **(Voet and Voet 1995)**. Interestingly, it was found that the specific activity of PDH and PC were lowered by approximately 50% and 15%, respectively, under the stress condition as compared to the control (Fig. 3A). The fate of OAA in TCA cycle needed to be established, for which we measured the activity of MDH as it catalyzes the reversible conversion from OAA to malate. Interestingly, activity of MDH was increased by approximately 1.3 fold under the stress condition (Fig. 3A). All these results indicated that the TCA cycle was amortized under the stress condition, but the higher activity of MDH implied that the concentration of malate might be increased in presence of 0.5 mM ac.$NaNO_2$. In combination with elevated ethanol production, this pointed towards increased pyruvate concentration within the cells under nitrosative stress. This was confirmed by measuring the activity of MDH (decarboxylating), that catalyzes the conversion from malate to pyruvate. Here, the activity of this enzyme was 1.3 fold increased in the treated cells (Fig. 3A). Furthermore, we assessed the specific activity of PDC and this was sharply increased by 3.2 fold (Fig. 3A). A drop of approximately 50% in the specific activity of ICDH was also observed under the stress condition (Fig. 3A). Based on these findings, we hypothesized that the TCA cycle was partially inhibited under the stress condition. Thus, we also determined the activity of ALDH, an important enzyme for the PDH-bypass pathway **(Remize *et al.* 2000)**. The activity of this enzyme was found to be decreased by 64% as compared to the control (Fig. 3A). Along with this, the activity of MS, an important enzyme of glyoxylate shunt (an anaplerotic variant of TCA cycle) **(Chew *et al.* 2019)**, was decreased by approximately 40 % in 0.5 mM ac.$NaNO_2$ treated *S. cerevisiae* cells (Fig. 3A).

Network and functional annotation studies with the altered protein activities

To validate our findings obtained from the biochemical enzymatic assays, we investigated the effect of nitrosative stress on different metabolic enzymes of *S. cerevisiae* using bioinformatics. Under nitrosative stress, the enzymes with altered activity were subjected to a network analysis and functional annotation studies. Of the activated enzymes, MDH and PDC predominantly participated in the network with a maximum number of connections (Fig. 4A). Due to the increased activity of these enzymes, the yeast cellular system was predicted to be involved

primarily in the biological processes of pyruvate and malate metabolism, and in gluconeogenesis (Table 2). The network formed by enzymes with decreased activity contained CS, isocitrate lyase, PDH, and aconitase with maximum connectivity (Fig. 4B). The terms for predicted biological processes with these enzymes were TCA cycle, glyoxylate cycle, and biosynthesis of glutamate and acetate. In terms of cellular location, most of the enzymes were predicted to be located in the mitochondria. Additionally, the most enriched molecular functions were predicted to be MDH activity and ADH (NAD) activity due to the activated enzymes in the treated yeast cells. On the other hand, the ALDH activity, transferase activity, transferring acyl groups, acyl groups converted into alkyl on transfer, and lyase activity might be reduced due to the decreased activity of enzymes participating in these functions (Table 2).

Effect of acidified sodium nitrite on *ADH* and *ACO* genes expression

As we found that ethanol production and ADH activity had increased and aconitase activity had decreased in the presence of 0.5 mM ac.$NaNO_2$, we assessed the expression of *ADH* and *ACO* genes. As Fig. 5 shows, expression of *ADH1*, *ADH2* and *ADH3* were increased by, ~2.1 fold, ~2.4 fold, and ~3.5 fold respectively, under the stress condition as compared to the control. Expression of *ACO2* was almost 50% lower in treated cells as compared to the control. Surprisingly, the expression of *ACO1* was found to be increased by 1.2 fold in treated cell in comparison to the control (Table S3-S7, Fig. 5).

***In vitro* Protein tyrosine nitration (PTN) study with pure aconitase and ADH**

As variation in glucose metabolism was observed with a significant upregulation of ADH and downregulation of aconitase, we assessed the protein tyrosine nitration (PTN) formation for these two enzymes. PTN formation was observed in aconitase following treatment with 0.3 mM and 0.5 mM ac.$NaNO_2$ but not with 0.1 mM ac.$NaNO_2$ treated aconitase or without treatment. The specific activity of aconitase was gradually reduced with the of higher concentrations of treatment of ac.$NaNO_2$. The reduction in aconitase activity was maximal for the positive control of 0.1 mM peroxynitrite treatment (Fig. 6A). Different results were obtained with pure ADH. PTN formation was only observed in 0.1 mM peroxynitrite treated ADH, while it was absent as a result of ac.$NaNO_2$ treatment. The specific activity of ADH remained unaltered in ac.$NaNO_2$ treated samples but drastically decreased in 0.1 mM peroxynitrite treated ADH as compared to the untreated ADH (Fig. 6B).

Discussion

In this present study, we demonstrate variation in glucose metabolism in *S. cerevisiae* under nitrosative stress that is mediated by 0.5 mM ac.$NaNO_2$. Results from FACS and confocal microscopy confirmed that ROS was equally produced in both treated and untreated cells, but

RNS was generated only in the presence of ac.$NaNO_2$. Hence, the observed phenomena were due to the nitrosative stress under our experimental condition. Changes in the redox homeostasis is a key marker of nitrosative stress **(Kurutas 2016; Maciejczyk *et al.* 2022)**. Under our experimental condition, an increased GSH/GSSG ratio, elevated concentration of GSH and reduced concentration of GSSG were observed, that in combination suggest that the treated cells responded by raising the intracellular reduced equivalent in the form of GSH **(Astuti *et al.* 2016)**. GSH is a well-known stress response component that helps to combat reactive-species mediated damage (**Aquilano K *et al.* 2014**). Previous reports have also suggested that the declined level of GSH may induce deleterious activity of NO in the form of DNA damage and protein modification **(Aquilano K *et al.* 2014; Kalinina and Novichkova 2021; Lei *et al.* 2016; Sies *et al.* 1997; Forman *et al.* 2009)**. This observation was corroborated with the higher activity of GR which catalyzes the conversion of GSSG to GSH under stress **(Forman *et al.* 2009)**. Though reported data suggests that GR activity can be inhibited in *Schizosaccharomyces pombe* under the peroxynitrite mediated nitrosative stress **(Sahoo *et al.* 2006)**, Navarro *et al.* recently reported that GR activity can be stimulated in the presence of NO **(Navarro *et al.* 2020)**. Here, we also found a sharp increase in GR activity in presence of 0.5 mM ac. $NaNO_2$. Thus, it can be concluded that GSSG was converted to GSH by the activity of GR to maintain the redox homeostasis under our experimental condition. In addition, activity of catalase, an important stress response enzyme **(Patra *et al.* 2019)**, was also increased in the treated cells, and this might be involved to detoxify reactive species that were generated by the action of ac.$NaNO_2$ **(Navarro *et al.* 2020; Bhattacharjee *et al.* 2010; Gebicka and Didik 2009; Sahoo *et al.* 2009)**.

In *S. cerevisiae* ADH1, ADH3, ADH4, and ADH5 produce ethanol from acetaldehyde whereas ADH2 is involved in the reverse reaction i.e. production of acetaldehyde from ethanol. It can be expected, that the elevated expression of *ADH1* and *ADH3* genes under the stress condition resulted in higher enzyme activity and this most likely contributed to higher ethanol production. That expression of *ADH2* was induced under stress condition might be due to the higher ethanol production. This enzyme can assist in generation of reducing equivalents in the form of NADH and maintain the redox status of the cell **(Maestre *et al.* 2008)**. Though *S. cerevisiae* is a crabtree-positive organism **(Pfeiffer *et al.* 2014)**, the increased percentages of theoretical ethanol yield, higher rate of sugar utilization indicated that the fermentation rate under the stress condition was upregulated. Overall, these results suggested a probable metabolic reprogramming towards fermentation. In addition, we found that the activity of PDH, CS, aconitase, ICDH were reduced in treated cells, clearly indicating a partial blocking of the

TCA cycle. These results are in line with earlier reports which showed the downregulation of mitochondrial proteins, mainly the TCA cycle enzymes, under nitrosative stress **(Auger *et al.* 2011; Abello *et al.* 2009)**. The activity of CS is considered as a marker of mitochondrial function, and the reduction in its specific activity suggested that the mitochondrion was highly affected in the presence of 0.5 mM ac.$NaNO_2$ **(Borys *et al.* 2019).** This was also supported by the higher expression of *ACO1*. The product of that gene not only catalyzes the conversion from citrate to isocitrate **(Staab *et al.* 2008)**, but is also involved in certain unrelated cellular processes, thus acting as a moonlighting protein **(Gancedo *et al.* 2016)**. One of the important functions of ACO1p is to maintain the integrity of mitochondrial DNA **(Gancedo *et al.* 2016; Chen *et al.* 2007; Yazgan and Krebs 2012)**. Hence, the higher expression of the *ACO1* indicated that the mitochondrial activity might be affected under the stress conditions we applied. Unlike *ACO1*, the gene expression of *ACO2* was reduced and overall specific activity of aconitase was dropped by 50%, suggesting that ac.$NaNO_2$ might affect transcription of aconitase. A model of glucose metabolism in *S. cerevisiae* in the presence of 0.5 mM ac.$NaNO_2$ is proposed in Fig. 7. The rate limiting enzyme of the TCA cycle is ICDH, which catalyzes the conversion from isocitrate to α-ketoglutarate **(Voet and Voet 1995)**, and this enzyme activity was decreased, together with that of PDH, which catalyzes the conversion from pyruvate to acetyl CoA **(Voet and Voet 1995).** This explains the observed reduction in citrate metabolism. Other reports have also suggested that the activity of PDH and ICDH can be affected under nitrosative and oxidative stress **(Auger *et al.* 2011; Ferrer-Sueta G *et al.* 2018)**. Formation of acetyl CoA from pyruvate is the key step for utilizing glucose via respiration pathway **(Voet and Voet 1995),** but acetyl-CoA can also be synthesized via the PDH-bypass pathway, a PDH-independent alternative route which requires the activity of PDC and ALDH among the other enzymes **(Remize *et al.* 2000)**. Though the activity of PDC [also a crucial enzyme of the fermentation pathway **(Voet and Voet 1995)**] was found to be increased, the activity of ALDH [oxidizes acetaldehyde to acetate **(Remize *et al.* 2000)**] was decreased under the stress condition. Reduction in ALDH activity might affect the acetyl-CoA production. In addition, activity of MS was decreased as a result of treatment, which might be due to the lower availability of acetyl-CoA. Reduced activity of MS might also affect the glyoxylate cycle, an anaplerotic variant of the TCA cycle present in *S. cerevisiae* **(Chew *et al.* 2019)**. Acetyl-CoA is also a positive allosteric modulator of PC, an important anaplerotic enzyme that replenishes the intermediates of TCA cycle by catalyzing the reaction from pyruvate to oxaloacetic acid **(Voet and Voet 1995, Adina-Zada *et al.* 2012)**. Any depletion in the production of acetyl-CoA under our experimental condition might be interfering with the activity of PC **(Voet and**

Voet 1995; Adina-Zada *et al.* 2012). Hence, all these results suggested that the requirement for replenishing the intermediates of the TCA cycle might be reduced in presence of ac.$NaNO_2$, indicating a partial blocking of the TCA cycle under the stress condition.

The detected elevated specific activity of MDH and MDH (decarboxylating) enzymes under the stress condition are very interesting as this observation suggests that, under the stress condition, OAA formed by PC was rerouted to pyruvate via formation of malate. It has been reported that OAA cannot cross the mitochondrial membrane but malate can **(Voet and Voet 1995)**. Reports suggest that the affinity of MDH (decarboxylating) is very low (K_m = 50 mM) but malate metabolism as well as activity of the MDH (decarboxylating) may be induced during the adverse conditions like starvation in *S. cerevisiae* **(Redzepovic *et al.* 2003)**. MDH (decarboxylating) also contributes to the generation of intracellular flux of NADPH **(Knuf *et al.* 2013)** that plays a major role in the protection against oxidative stress and also participates in different biological processes **(Pollak *et al.* 2007)**, suggesting a possible stress response activity of MDH (decarboxylating). On the other hand, activity of MDH is also very important to generate cytosolic NADH, an important component of energy metabolism and an antioxidant cofactor **(Voet and Voet 1995; Miyagi *et al.* 2009)**. Therefore, it is likely that under the stress condition, when the energy generation via TCA cycle was heavily compromised, upregulation of MDH and MDH (decarboxylating) helped to generate energy intermediates which in turn caused the rerouting of glucose metabolic flux towards fermentation. Again, higher activity of MDH (decarboxylating) has been also reported during alcoholic fermentation in *S. cerevisiae* **(Redzepovic *et al.* 2003)**. This enzyme can be strongly increased during the switching from respiration to fermentation in *S. cerevisiae* **(Xiao *et al.* 2018)**. We further observed increases in the activity of PDC and ADH, suggesting a higher rate of ethanol fermentation. Thus, a metabolic reprogramming towards fermentation might have taken place in the presence of ac.$NaNO_2$ in *S. cerevisiae*.

The experimental results were supported by bioinformatics analyses where fermentation was predicted as strongly activated, in combination with elevated malate metabolic metabolism. In contrast, the TCA cycle and glyoxylate shunt were predicted to be slowed down under the stress condition, confirming that variation in glucose metabolism in *S. cerevisiae* during nitrosative stress. The metabolic reprogramming might not only be involved in energy generation but also seemed to be a part of the stress response. This reprogrammed glucose metabolism was coupled with the antioxidant machinery of the cell, which in combination were able to maintain the cell viability to almost unaltered levels in 0.5 mM ac.$NaNO_2$ treated culture as compared to the control.

In vitro study of PTN was further carried out with pure aconitase and ADH. PTN is one of the important marker of redox stress **(Corpas *et al.* 2009; Cipak Gasparovic *et al*. 2017)**. As mentioned earlier, aconitase is very sensitive to redox stress **(Radi 2018; Lushchak *et al.* 2010)**. Aconitase contains a 4Fe-4S cluster in its active site **(Frick and Wittmann 2005)** and this is very prone to oxidation that leads to its inactivation **(Radi 2018; Wachnowsky *et al.* 2019; Fridovich 2003)**. Treatment with 0.3 and 0.5 mM ac.$NaNO_2$ produced a positive signal for PTN and reduced the specific activity of the treated enzyme. Tyrosine nitration increases the negative charge of the protein and also adds comparatively bulky substituents that in combination may alter local charge distribution as well as the protein configuration **(Radi 2018)**. This explains the partial inhibition of aconitase. However, ac.$NaNO_2$ treatment was not able to induce the formation of PTN in ADH. This enzyme remained unaltered without a change in western blots or specific activity, suggesting that ac.$NaNO_2$ could not affect the activity of the ADH via PTN formation.

In conclusion, our findings reveal that the nefarious activity of acidified sodium nitrite was substantially reduced by metabolic reprogramming towards fermentation, conjoined with the anti-oxidant defense system. This study provides insight into the variation in glucose metabolism in *S. cerevisiae* under acidified sodium nitrite mediated nitrosative stress and contributes to a better understanding of the mechanistics behind the process.

Acknowledgement

Authors acknowledge University of North Bengal for providing infrastructure and research project fund to carry out the research. Authors also acknowledge IICB, Kolkata, Bose institute, Kolkata and Dr. KPC Life sciences, Kolkata for providing the paid-services for FACS, confocal microscopy and qPCR respectively.

Conflict of interest

No conflict of interest declared.

Authors' contributions

AB & SS Designed the experiments SS & RN Performed the wet lab experiments and artwork preparation RB Designed and Performed the network analysis AB & SS analyzed the data and wrote the manuscript. All the authors read the manuscript and approved it for the submission.

Availability of data and material

Data available upon reasonable request.

References

Abello, N., Kerstjens, H.A., Postma, D.S., Bischoff, R. (2009) Protein tyrosine nitration: selectivity, physicochemical and biological consequences, denitration, and proteomics

methods for the identification of tyrosine-nitrated proteins. *J Proteome Res* **8**, 3222-38. https://doi.org/10.1021/pr900039c

Adina-Zada, A., Zeczycki, T.N., Attwood, P.V. (2012). Regulation of the structure and activity of pyruvate carboxylase by acetyl CoA. *Arch Biochem Biophys* **519**, 118-30. https://doi.org/10.1016/j.abb.2011.11.015

Aebi, H. (1984) Catalase in vitro. *Methods Enzymol* **105**, 121-6. https://doi.org/10.1016/s0076-6879(84)05016-3

Akerboom, T.P., Sies, H. (1981) Assay of glutathione, glutathione disulfide, and glutathione mixed disulfides in biological samples. *Methods Enzymol* **77**, 373-82. https://doi.org/10.1016/s0076-6879(81)77050-2

Anam, K., Nasuno, R., Takagi, H. (2020) A novel mechanism for nitrosative stress tolerance dependent on GTP cyclohydrolase II activity involved in riboflavin synthesis of yeast. *Sci Rep* **10**, 6015. https://doi.org/10.1038/s41598-020-62890-3

Aquilano, K., Baldelli, S., Ciriolo, M.R. (2014) Glutathione: new roles in redox signaling for an old antioxidant. Front Pharmacol **5**, 196. https://doi.org/10.3389/fphar.2014.00196

Astuti, R.I., Nasuno, R., Takagi, H. (2016) Nitric oxide signaling in yeast. *Appl Microbiol Biotechnol* **100**, 9483-9497. https://doi.org/10.1007/s00253-016-7827-7

Auger, C., Lemire, J., Cecchini, D., Bignucolo, A., Appanna, V.D. (2011) The metabolic reprogramming evoked by nitrosative stress triggers the anaerobic utilization of citrate in *Pseudomonas fluorescens*. *PLoS One* **6**, e28469. https://doi.org/10.1371/journal.pone.0028469

Barbosa-Sicard, E., Frömel, T., Keserü, B., Brandes, R.P., Morisseau, C., Hammock, B.D., Braun, T., Krüger, M., Fleming, I. (2009) Inhibition of the soluble epoxide hydrolase by tyrosine nitration. *J Biol Chem* **284**, 28156-28163. https://doi.org/10.1074/jbc.M109.054759

Bartesaghi, S., Radi, R. (2018) Fundamentals on the biochemistry of peroxynitrite and protein tyrosine nitration. *Redox Biol* **14**, 618-625. https://doi.org/10.1016/j.redox.2017.09.009

Bergmeyer, H.U., Gawehn, K., Grassl, M. (1974) Methods of enzymatic analysis. Weinheim: Verlag Chemie, Academic Press. New York.

Bhattacharjee, A., Majumdar, U., Maity, D., Sarkar, T.S., Goswami, A.M., Sahoo, R., Ghosh, S. (2010) Characterizing the effect of nitrosative stress in *Saccharomyces cerevisiae*. *Arch Biochem Biophys* **496**,109-16. https://doi.org/10.1016/j.abb.2010.02.003

Borys, J., Maciejczyk, M., Antonowicz, B., Krętowski, A., Sidun, J., Domel, E., Dąbrowski, J.R., Ładny, J.R., Morawska, K., Zalewska, A. (2019) Glutathione metabolism, mitochondria activity, and nitrosative stress in patients treated for mandible fractures. *J Clin Med* **8**, 127. https://doi.org/10.3390/jcm8010127

Bostian, K.A., Betts, G.F. (1978) Kinetics and reaction mechanism of potassium-activated aldehyde dehydrogenase from *Saccharomyces cerevisiae*. *Biochem J* **173**, 787-98. https://doi.org/10.1042/bj1730787

Bradford, M.M. (1976) A rapid and sensitive method for the quantitation of microgram quantities of protein utilizing the principle of protein-dye binding. *Anal Biochem* **72**, 248-54. https://doi.org/10.1006/abio.1976.9999

Carballal, S., Bartesaghi, S., Radi, R. (2014) Kinetic and mechanistic considerations to assess the biological fate of peroxynitrite. *Biochim Biophys Acta* **1840**, 768-80. https://doi.org/10.1016/j.bbagen.2013.07.005

Carlberg, I., Mannervik, B. (1975) Purification and characterization of the flavoenzyme glutathione reductase from rat liver. *J Biol Chem* **250**, 5475-80. https://doi.org/10.1016/S0021-9258(19)41206-4

Castro, L., Rodriguez, M., Radi, R. (1994) Aconitase is readily inactivated by peroxynitrite, but not by its precursor, nitric oxide. *J Biol Chem* **269**, 29409-15. https://doi.org/10.1016/S0021-9258(18)43894X

Chell, R.M., Sundaram, T.K., Wilkinson, A.E. (1978) Isolation and characterization of isocitratelyase from a thermophilic *Bacillus* sp. *Biochem J* **173**, 165-77. https://doi.org/10.1042/bj1730165

Chen, X.J., Wang, X., Butow, R.A. (2007) Yeast aconitase binds and provides metabolically coupled protection to mitochondrial DNA. *Proc Natl Acad Sci USA* **104**, 13738-43. https://doi.org/10.1073/pnas.0703078104

Chew, S.Y., Chee, W.J.Y., Than, L.T.L. (2019) The glyoxylate cycle and alternative carbon metabolism as metabolic adaptation strategies of *Candida glabrata*: perspectives from Candida albicans and Saccharomyces cerevisiae. *J Biomed Sci* **26**, 52. https://doi.org/10.1186/s12929-019-0546-5

Cipak Gasparovic, A., Zarkovic, N., Zarkovic, K., Semen, K., Kaminskyy, D., Yelisyeyeva, O., Bottari, S.P. (2017) Biomarkers of oxidative and nitro-oxidative stress: conventional and novel approaches. *Br J Pharmacol* **174**, 1771-1783. https://doi.org/10.1111/bph.13673

Corpas, F.J., Chaki, M., Leterrier, M., Barroso, J.B. (2009) Protein tyrosine nitration: a new challenge in plants. *Plant Signal Behav* **4**, 920-3. https://doi.org/10.4161/psb.4.10.9466

Dennis, G.Jr., Sherman, B.T., Hosack, D.A., Yang, J., Gao, W., Lane, H.C., Lempicki, R.A. (2003) DAVID: database for annotation, visualization, and integrated discovery. *Genome Biol* **4**, P3. https://doi.org/10.1186/gb-2003-4-9-r60

Ferrer-Sueta, G., Campolo, N., Trujillo, M., Bartesaghi, S., Carballal, S., Romero, N., Alvarez, B., Radi, R. (2018) Biochemistry of peroxynitrite and protein tyrosine nitration. *Chem Rev* **118**, 1338-1408. https://doi.org/10.1021/acs.chemrev.7b00568

Fitzsimmons, L., Liu, L., Porwollik, S., Chakraborty, S., Desai, P., Tapscott, T., Henard, C., McClelland, M., Vazquez-Torres, A. (2018) Zinc-dependent substrate-level phosphorylation powers Salmonella growth under nitrosative stress of the innate host response. *PLoS Pathog* **14**, e1007388. https://doi.org/10.1371/journal.ppat.1007388

Forman, H.J., Zhang, H., Rinna, A. (2009) Glutathione: overview of its protective roles, measurement, and biosynthesis. *Mol Aspects Med* **30**, 1-12. https://doi.org/10.1016/j.mam.2008.08.006

Frick, O., Wittmann, C. (2005) Characterization of the metabolic shift between oxidative and fermentative growth in *Saccharomyces cerevisiae* by comparative 13C flux analysis. *Microb Cell Fact* **4**, 30. https://doi.org/10.1186/1475-2859-4-30

Fridovich, I. (2003) With the help of giants. *Annu Rev Biochem* **72**, 1-18. https://doi.org/10.1146/annurev.biochem.72.081902.140918

Gancedo, C., Flores, C.L., Gancedo, J.M. (2016) The expanding landscape of moonlighting proteins in yeasts. *Microbiol Mol Biol Rev* **80**, 765-77. https://doi.org/10.1128/MMBR.00012-16

Gebicka, L., Didik, J. (2009) Catalytic scavenging of peroxynitrite by catalase. *J Inorg Biochem* **103**, 1375-9. https://doi.org/10.1016/j.jinorgbio.2009.07.011

Geer, B.W., Krochko, D., Oliver, M.J., Walker, V.K., Williamson, J.H. (1980) A comparative study of the NADP-malic enzymes from Drosophila and chick liver. *Comp Biochem Physiol* **65**, 25-34. https://doi.org/10.1016/0305-0491(80)90109-1

Gounaris, A.D., Turkenkopf, I., Buckwald, S., Young, A. (1971) Pyruvate decarboxylase. I. Protein dissociation into subunits under conditions in which thiamine pyrophosphate is released. *J Biol Chem* 246, 1302-9. https://doi.org/10.1016/S0021-9258(19)76974-9

Horan, S., Bourges, I., Meunier, B. (2006) Transcriptional response to nitrosative stress in *Saccharomyces cerevisiae*. *Yeast* **23**, 519-35. https://doi.org/10.1002/yea.1372

Jahnová, J., Luhová, L., Petřivalský, M. (2019) S-nitrosoglutathione reductase-the master regulator of protein s-nitrosation in plant NO signaling. *Plants (Basel)* **8**, 48. https://doi.org/10.3390/plants8020048

Kalinina, E., Novichkova, M. (2021) Glutathione in protein redox modulation through S-glutathionylation and S-Nitrosylation. *Molecules* **26**, 435. https://doi.org/10.3390/molecules26020435

Kitichantaropas, Y., Boonchird, C., Sugiyama, M., Kaneko, Y., Harashima, S., Auesukaree, C. (2016) Cellular mechanisms contributing to multiple stress tolerance in *Saccharomyces cerevisiae* strains with potential use in high-temperature ethanol fermentation. *AMB Express* **6**, 107. https://doi.org/10.1186/s13568-016-0285-x

Kruf, C., Nookaew, I., Brown, S.H., McCulloch, M., Berry, A., Nielsen, J. (2013) Investigation of malic acid production in *Aspergillus oryzae* under nitrogen starvation conditions. *Appl Environ Microbiol* **79**, 6050-8. https://doi.org/10.1128/AEM.01445-13

Kurutas, E.B. (2016) The importance of antioxidants which play the role in cellular response against oxidative/nitrosative stress: current state. *Nutr J* **15**, 71. https://doi.org/10.1186/s12937-016-0186-5

Laemmli, U.K. (1970) Cleavage of structural proteins during the assembly of the head of bacteriophage T4. *Nature* **227**, 680-5. https://doi.org/10.1038/227680a0

Lei, X.G., Zhu, J.H., Cheng, W.H., Bao, Y., Ho, Y.S., Reddi, A.R., Holmgren, A., Arnér, E.S. (2016) Paradoxical roles of antioxidant enzymes: basic mechanisms and health implications. *Physiol Rev* **96**, 307-64. https://doi.org/10.1152/physrev.00010.2014

Lindemann, C., Lupilova, N., Müller, A., Warscheid, B., Meyer, H.E., Kuhlmann, K., Eisenacher, M., Leichert, L.I. (2013) Redox proteomics uncovers peroxynitrite-sensitive proteins that help *Escherichia coli* to overcome nitrosative stress. *J Biol Chem* **288**, 19698-714. https://doi.org/10.1074/jbc.M113.457556

Liu, L., Zeng, M., Hausladen, A., Heitman, J., Stamler, J.S. (2000) Protection from nitrosative stress by yeast flavohemoglobin. *Proc Natl Acad Sci USA* **97**, 4672-6. https://doi.org/10.1073/pnas.090083597

Lushchak, O.V., Inoue, Y., Lushchak, V.I. (2010) Regulatory protein Yap1 is involved in response of yeast *Saccharomyces cerevisiae* to nitrosative stress. *Biochem (Mosc)* **75**, 629-64. https://doi.org/10.1134/s0006297910050135

Lushchak, O.V., Piroddi, M., Galli, F., Lushchak, V.I. (2014) Aconitase post-translational modification as a key in linkage between Krebs cycle, iron homeostasis, redox signaling, and metabolism of reactive oxygen species. *Redox Rep* **19**, 8-15. https://doi.org/10.1179/1351000213Y.0000000073

Maciejczyk, M., Zalewska, A., Gryciuk, M., Hodun, K., Czuba, M., Ploszczyca, K., Charmas, M., Sadowski, J., Baranowski, M. (2022) Effect of Normobaric Hypoxia on Alterations in Redox Homeostasis, Nitrosative Stress, Inflammation, and Lysosomal Function following Acute Physical Exercise. *Oxid Med Cell Longev* **2022**, 4048543. https://doi.org/10.1155/2022/4048543

Maestre, O., García-Martínez, T., Peinado, R.A., Mauricio, J.C. (2008) Effects of *ADH2* overexpression in *Saccharomyces bayanus* during alcoholic fermentation. Appl Environ Microbiol. **74,** 702-7. https://doi.org/10.1128/AEM.01805-07

Mithra, M.G., Jeeva, M.L., Sajeev, M.S., Padmaja, G. (2018) Comparison of ethanol yield from pretreated lignocellulo-starch biomass under fed-batch SHF or SSF modes. *Heliyon* **4,** e00885. https://doi.org/10.1016/j.heliyon.2018.e00885

Miyagi, H., Kawai, S., Murata, K. (2009) Two sources of mitochondrial NADPH in the yeast Saccharomyces cerevisiae. *J Biol Chem* **284**, 7553-60. https://doi.org/10.1074/jbc.M804100200

Nasuno, R., Aitoku, M., Manago, Y., Nishimura, A., Sasano, Y., Takagi, H. (2014) Nitric oxide-mediated antioxidative mechanism in yeast through the activation of the transcription factor Mac1. *PLoS One* **9**, e113788. https://doi.org/10.1371/journal.pone.0113788

Navarro, M.V., Chaves, A.F.A., Castilho, D.G., Casula, L., Calado, J.C.P., Conceição, P.M., Iwai, L.K., de Castro, B.F., Batista, W.L. (2020) Effect of nitrosative stress on the *s*-nitroso-proteome of *Paracoccidioides brasiliensis*. *Front Microbiol* **11**, 1184. https://doi.org/10.3389/fmicb.2020.01184

Patra, S.K., Bag, P.K., Ghosh, S. (2017) Nitrosative Stress Response in *Vibrio cholerae*: Role of S-Nitrosoglutathione Reductase. *Appl Biochem Biotechnol* **182**, 871-884. https://doi.org/10.1007/s12010-016-2367-2

Patra, S.K., Samaddar, S., Sinha, N., Ghosh, S. (2019) Reactive nitrogen species induced catalases promote a novel nitrosative stress tolerance mechanism in *Vibrio cholerae*. *Nitric Oxide* **88**, 35-44. https://doi.org/10.1016/j.niox.2019.04.002

Payne, J., Morris, J.G. (1969) Pyruvate carboxylase in *Rhodopseudomonas spheroides*. *J Gen Microbiol* **59**, 97-101. https://doi.org/10.1099/00221287-59-1-97

Peláez-Soto A, Roig P, Martínez-Culebras PV, Fernández-Espinar MT, Gil JV (2020) Proteomic analysis of *Saccharomyces cerevisiae* response to oxidative stress mediated by cocoa polyphenols extract. *Molecules* **25**, 452. https://doi.org/10.3390/molecules25030452

Peluffo, G., Radi, R. (2007) Biochemistry of protein tyrosine nitration in cardiovascular pathology. *Cardiovasc Res* **75**, 291-302. https://doi.org/10.1016/j.cardiores.2007.04.024

Pfeiffer, T., Morley, A. (2014) An evolutionary perspective on the Crabtree effect. *Front Mol Biosci* **1**, 17. https://doi.org/10.3389/fmolb.2014.00017

Pollak, N., Dölle, C., Ziegler, M. (2007) The power to reduce: pyridine nucleotides--small molecules with a multitude of functions. *Biochem J* **402**, 205-18. https://doi.org/10.1042/BJ20061638

Radi, R. (2018) Oxygen radicals, nitric oxide, and peroxynitrite: Redox pathways in molecular medicine. *Proc Natl Acad Sci USA* **115**, 5839-5848. https://doi.org/10.1073/pnas.1804932115

Redzepovic, S., Orlic, S., Majdak, A., Kozina, B., Volschenk, H., Viljoen-Bloom, M. (2003) Differential malic acid degradation by selected strains of Saccharomyces during alcoholic fermentation. *Int J Food Microbiol* **83**, 49-61. https://doi.org/10.1016/s0168-1605(02)00320-3

Regev-Shoshani, G., Crowe, A., Miller, C.C. (2013) A nitric oxide-releasing solution as a potential treatment for fungi associated with tinea pedis. *J Appl Microbiol* **114**, 536-44. https://doi.org/10.1111/jam.12047

Remize, F., Andrieu, E., Dequin, S. (2000) Engineering of the pyruvate dehydrogenase bypass in Saccharomyces cerevisiae: role of the cytosolic Mg(2+) and mitochondrial K(+) acetaldehyde dehydrogenases Ald6p and Ald4p in acetate formation during alcoholic fermentation. *Appl Environ Microbiol* **66**, 3151-9. https://doi.org/10.1128/AEM.66.8.3151-3159.2000

Ridnour, L.A., Thomas, D.D., Mancardi, D., Espey, M.G., Miranda, K.M., Paolocci, N., Feelisch, M., Fukuto, J., Wink, D.A. (2004) The chemistry of nitrosative stress induced by nitric oxide and reactive nitrogen oxide species. Putting perspective on stressful biological situations. *Biol Chem* **385**, 1-10. https://doi.org/10.1515/BC.2004.001

Saboo, R., Bhattacharjee, A., Majumdar, U., Ray, S.S., Dutta, T., Ghosh, S. (2009) A novel role of catalase in detoxification of peroxynitrite in *S. cerevisiae*. *Biochem Biophys Res Commun* **385**, 507-11. https://doi.org/10.1016/j.bbrc.2009.05.062

Saboo, R., Dutta, T., Das, A., Sinha Ray, S., Sengupta, R., Ghosh, S. (2006) Effect of nitrosative stress on Schizosaccharomyces pombe: inactivation of glutathione reductase by peroxynitrite. Free Radic Biol Med **40,** 625–631. https://doi.org/10.1016/j.freeradbiomed.2005.09.029

Saboo, R., Sengupta, R., Ghosh, S. (2003) Nitrosative stress on yeast: inhibition of glyoxalase-I and glyceraldehyde-3-phosphate dehydrogenase in the presence of GSNO. *Biochem Biophys Res Commun* **302**, 665-70. https://doi.org/10.1016/s0006-291x(03)00251-1

Sengupta, S., Deb, M., Nath, R., Saha S.P., Bhattacharjee, A. (2020) Optimization of ethanol production using nitrosative stress exposed *S. cerevisiae*. *Cell Biochem Biophys* **78,** 101-110. https://doi.org/10.1007/s12013-019-00897-y

Shannon, P., Markiel, A., Ozie,r O., Baliga, N.S., Wang, J.T., Ramage, D., Amin, N., Schwikowski, B., Ideker, T. (2003) Cytoscape: a software environment for integrated models of biomolecular interaction networks. *Genome Res* **13**, 2498-504. https://doi.org/10.1101/gr.1239303

Sies, H., Sharov, V.S., Klotz, L.O., Briviba, K. (1997) Glutathione peroxidase protects against peroxynitrite-mediated oxidations. A new function for selenoproteins as peroxynitrite reductase. *J Biol Chem* **272**, 27812-7. https://doi.org/10.1074/jbc.272.44.27812

Srere, P.A. (1969) Citrate synthase: [EC 4.1.3.7. Citrate oxaloacetate-lyase (CoA-acetylating)]. *Methods Enzymol* **13**, 3-11. https://doi.org/10.1016/0076-6879(69)13005-0

Staab, C.A., Alander, J., Brandt, M., Lengqvist, J., Morgenstern, R., Grafström, R.C., Höög, J.O. (2008) Reduction of S-nitrosoglutathione by alcohol dehydrogenase 3 is facilitated by substrate alcohols via direct cofactor recycling and leads to GSH-controlled formation of glutathione transferase inhibitors. *Biochem J* **413**, 493-504. https://doi.org/10.1042/BJ20071666

Szklarczyk, D., Gable, A.L., Lyon, D., Junge, A., Wyder, S., Huerta-Cepas, J., Simonovic, M., Doncheva, N.T., Morris, J.H., Bork, P., Jensen, L.J., Mering, C.V. (2019) STRING v11: protein-protein association networks with increased coverage, supporting functional discovery in genome-wide experimental datasets. *Nucleic Acids Res* **47**, D607-D613. https://doi.org/10.1093/nar/gky1131

Tillmann, A., Gow, N.A., Brown, A.J. (2011) Nitric oxide and nitrosative stress tolerance in yeast. *Biochem Soc Trans* **39**, 219-23. https://doi.org/10.1042/BST0390219

Voet, D. and Voet, J.G. (1995) Biochemistry. J. Wiley & Sons, New York

Wachnowsky, C., Hendricks, A.L., Wesley, N.A., Ferguson, C., Fidai, I., Cowan, J.A. (2019) Understanding the mechanism of [4Fe-4S] cluster assembly on eukaryotic mitochondrial and cytosolic aconitase. *Inorg Chem* **58**, 13686-95. https://doi.org/10.1021/acs.inorgchem.9b01278

Wang, Y.T., Piyankarage, S.C., Williams, D.L., Thatcher, G.R. (2014) Proteomic profiling of nitrosative stress: protein S-oxidation accompanies S-nitrosylation. *ACS Chem Biol* **9**, 821-30. https://doi.org/10.1021/cb400547u

Witkiewicz-Kucharczyk, A., Goch, W., Olędzki, J., Hartwig, A., Bal, W. (2020) The reactions of H_2O_2 and GSNO with the zinc finger motif of XPA. Not a regulatory mechanism, but no synergy with cadmium toxicity. *Molecules* **25**, 4177. https://doi.org/10.3390/molecules25184177

Xiao, W., Wang, R.S., Handy, D.E., Loscalzo, J. (2018) NAD(H) and NADP(H) redox couples and cellular energy metabolism. *Antioxid Redox Signal* **28**, 251-272. https://doi.org/10.1089/ars.2017.7216

Yazgan, O., Krebs, J.E. (2012) Mitochondrial and nuclear genomic integrity after oxidative damage in Saccharomyces cerevisiae. *Front Biosci (Landmark Ed)* **17**, 1079-93. https://doi.org/10.2741/3974

Ying, T., Jinsong, G., Dong, W., Kaile, W., Jue, Z., Jing, F. (2017) The potential regulatory effect of nitric oxide in plasma activated water on cell growth of *Saccharomyces cerevisiae*. *J Appl Phys* **122**, 123302. https://doi.org/10.1063/1.4989501

Yoshikawa, Y., Nasuno, R., Kawahara, N., Nishimura, A., Watanabe, D., Takagi, H. (2016) Regulatory mechanism of the flavoprotein Tah18-dependent nitric oxide synthesis and cell death in yeast. *Nitric Oxide* **57**, 85-91. https://doi.org/10.1016/j.niox.2016.04.003

Zhang, P., Hai, H., Su, D., Yuan, W., Lia, W., Ding, R., Teng, M., Ma, L., Tian, J., Chen, C. (2019) A high throughput method for total alcohol determination in fermentation broths. *BMC biotechnol* **19**, 30. https://doi.org/10.1186/s12896-019-0525-7

Figure captions

Fig. 1 Effect of 0.5 mM acidified sodium nitrite on **(A)** GSH/GSSG ratio, **(B)** specific activity of glutathione reductase, and catalase. Data are expressed as the change in the percentage of specific activity as compared to the control. Assays were performed in triplicate for each biological sample and expressed as mean±SD. White and black bars represent control and ac.$NaNO_2$-treated cells, respectively.

Fig. 2 Effect of 0.5 mM acidified sodium nitrite on reactive nitrogen species and reactive oxygen species generation. Confocal microscopy analysis for the generation of reactive nitrogen species **(A-D)** and reactive oxygen species **(F-I)**. Micrographs were recorded at 45X magnification. Bar=100 µm. The mean fluorescent intensity for reactive nitrogen species **(E)** and reactive oxygen species **(J)** were determined by using Leica LAS X software and represented as mean±SD. FACS analysis for the reactive nitrogen species **(K, L)** and reactive oxygen species **(M, N)**. FACS analysis was done by using FACS Diva software.

Fig. 3 Effect of 0.5 mM acidified sodium nitrite on **(A)** the specific activity of various relevant enzymes. Data are expressed as the change in the percentage of specific activity as compared to the control. **(B)** Citrate content of extracellular and intracellular fractions combined. Assays were done in triplicate and represented as mean±SD. White and black bars represent control and ac.$NaNO_2$-treated cells, respectively.

Fig. 4 Network representation of enzymes in the presence of 0.5 mM acidified sodium nitrite. Network representation of **(A)** enzymes with increased activities and **(B)** enzymes with decreased activities. Highlighted colour denotes the enzymes with experimentally validated activities.

Fig. 5 Effect of 0.5 mM acidified sodium nitrite on three *ADH* and two *ACO* genes. The expression level of the genes was normalized with that of *GAPDH* (glyceraldehyde-3-phosphate dehydrogenase) in each set and expressed as the relative fold change as compared to the control. White and black bars represent control and ac.$NaNO_2$-treated cells, respectively.

Fig. 6 Effect of different concentrations of acidified sodium nitrite (0.1, 0.3, 0.5 mM) and 0.1 mM peroxynitrite on the specific activity of pure proteins (aconitase and alcohol dehydrogenase) along with the protein tyrosine nitration (PTN) formation. Western blotting for PTN and specific activity of **(A)** aconitase, **(B)** alcohol dehydrogenase. Data are expressed in A and B as the change in the percentage of specific activity as compared to the control. The assays were performed in triplicate and expressed as mean±SD.

Fig. 7 Proposed switching of glucose metabolism in the presence of 0.5 mM acidified sodium nitrite. Green downward arrows represent upregulated enzymes and red upward arrows represent downregulated enzymes in the presence of 0.5 mM acidified sodium nitrite. In this condition, energy generation through TCA cycle was compromised due to the lower activity of pyruvate dehydrogenase (PDH), citrate synthase (CS), aconitase (ACO), isocitrate dehydrogenase (ICDH), pyruvate carboxylase (PC) but the glucose metabolic flux was rerouted via higher activity of malate dehydrogenase (MDH) and malate dehydrogenase (decarboxylating) [MDH(DC)] towards pyruvate which was further metabolized via the fermentative pathway with the help of higher activity of pyruvate decarboxylase (PDC) and alcohol dehydrogenase (ADH) which resulted in higher production of ethanol. In addition, activity of malate synthase (MS) and aldehyde dehydrogenase (ALDH) were reduced that might affect the glyoxylate shunt (an anaplerotic variant of TCA cycle) and PDH-bypass pathway (an alternative route of acetyl-CoA synthesis without the activity of PDH).

Table 1 Estimation of ethanol concentration, glucose consumption, ethanol yield, percentage of theoretical yield and volumetric productivity of treated and untreated (control) samples of *S. cerevisiae*

Sample	Ethanol concentration (g/L)	Glucose consumed (g/L)	Ethanol yield (g/g of glucose)	% of theoretical yield	Volumetric Productivity (g/L/h)
Control	4.5±0.3	15±0.3	0.30	59	0.38
Treated	6±0.5	17±0.4	0.35	69	0.50

Table 2 Functional enrichment by activation/ deactivation of enzymes

	Term	% of genes	P-Value	Benjamini adjusted P-Value
Enrichment by activated enzymes due to stress				
Biological Process	pyruvate metabolic process	31.6	3.8E-10	8.7E-9
	malate metabolic process	26.3	3.8E-10	8.7E-9
	Fermentation	10.5	9.7E-3	4.0E-2
Cellular Components	mitochondrial matrix	31.6	3.1E-5	4.1E-4
	cytosol	42.1	2.1E-2	9.0E-2
Molecular Function	malate dehydrogenase activity	15.8	3.8E-5	6.1E-4
	alcohol dehydrogenase (NAD) activity	15.8	1.9E-4	2.3E-3
	Pyruvate kinase activity	26.3	3.6E-4	3.5E-3
Enrichment by deactivated enzymes due to stress				
Biological Process	tricarboxylic acid cycle	38.5	2.8E-15	1.5E-13
	glyoxylate cycle	19.2	6.6E-8	1.2E-6
	acetate biosynthetic process	11.5	1.2E-4	9.1E-4
Cellular Components	Peroxisomal matrix	42.3	4.3E-11	9.0E-10
	mitochondrial nucleoid	15.4	1.3E-4	9.2E-4
Molecular Function	aldehyde dehydrogenaseactivity	19.2	1.7E-7	9.3E-6
	transferase activity, transferring acyl groups, acyl groups converted into alkyl on transfer	15.4	9.8E-6	1.3E-4
	lyase activity	23.1	1.1E-4	9.7E-4

Figure 1

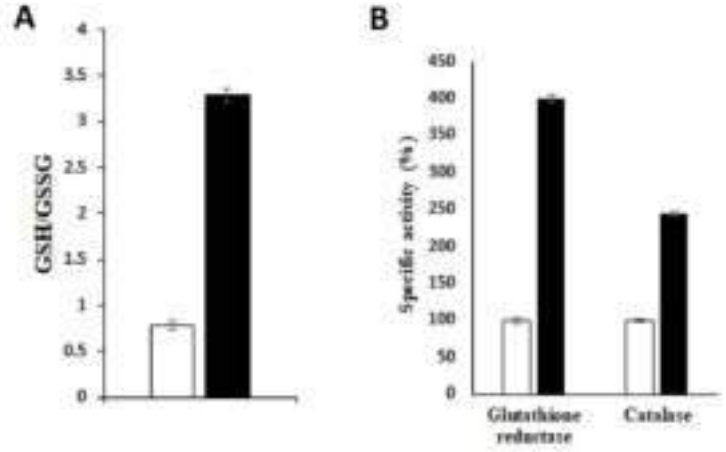

Figure 2

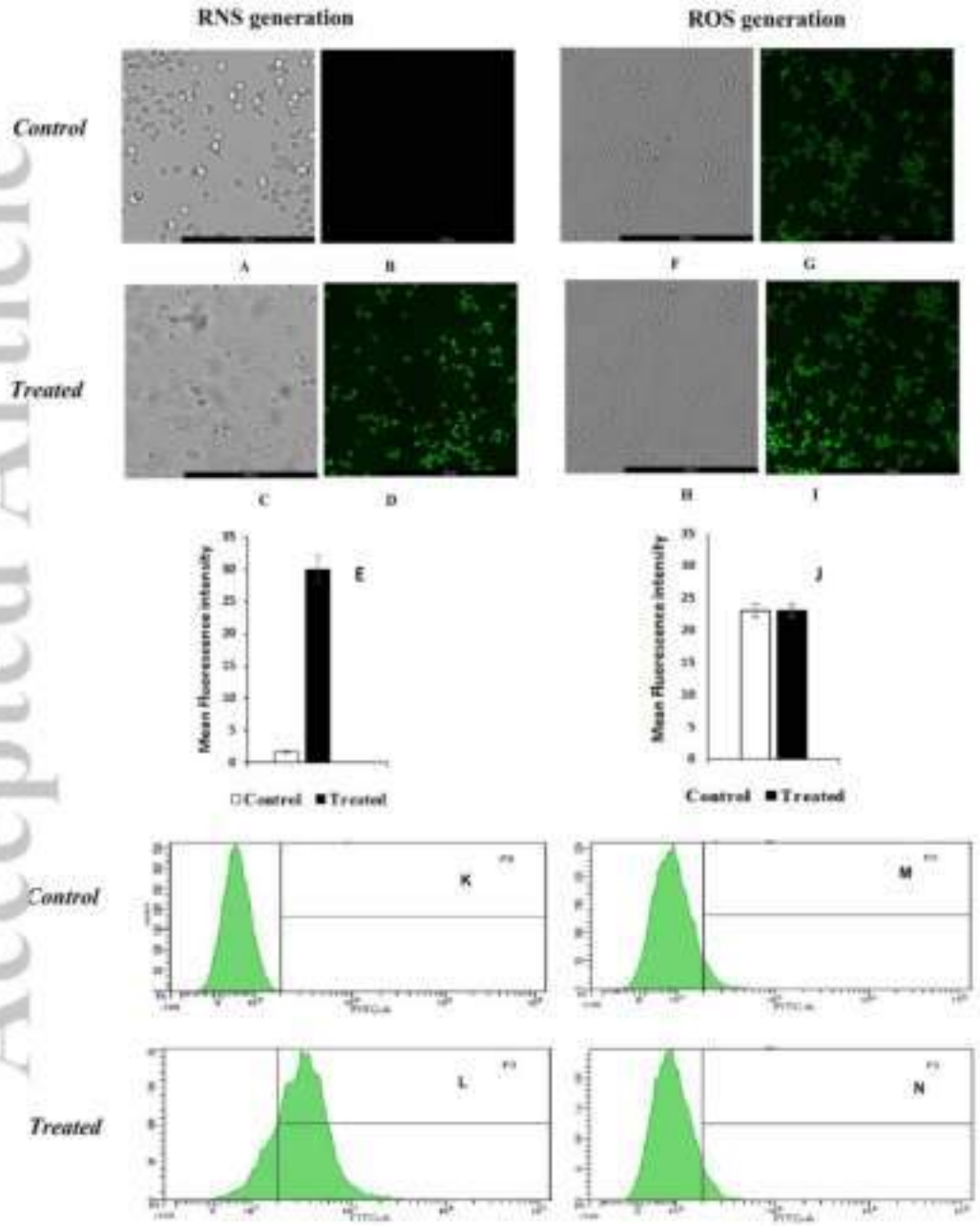

Figure 3

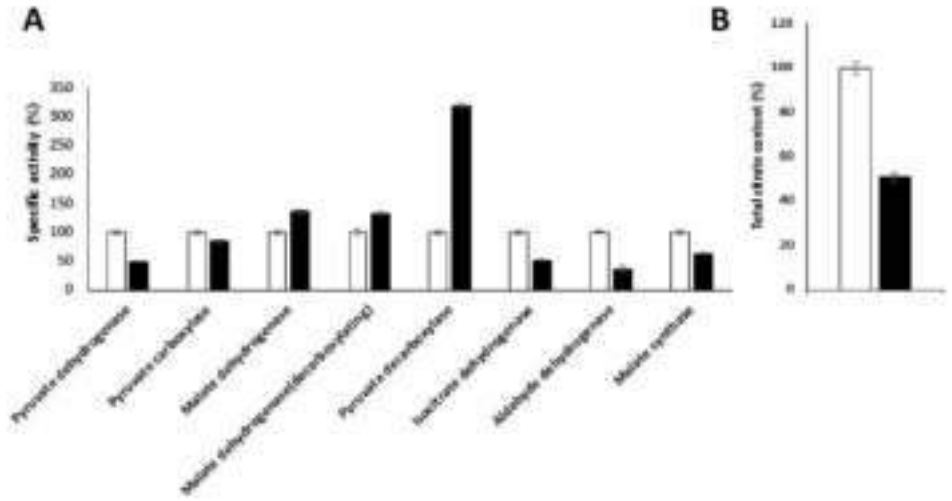

Figure 4

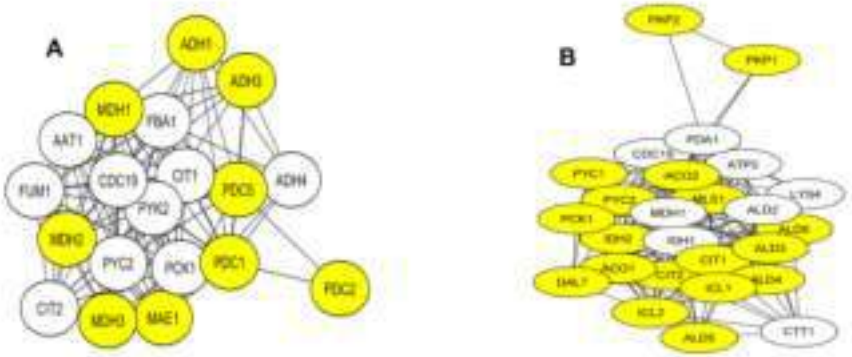

Figure 5

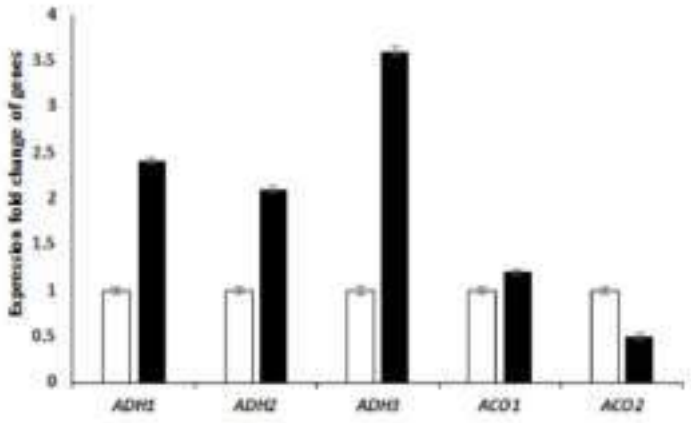

Figure 6

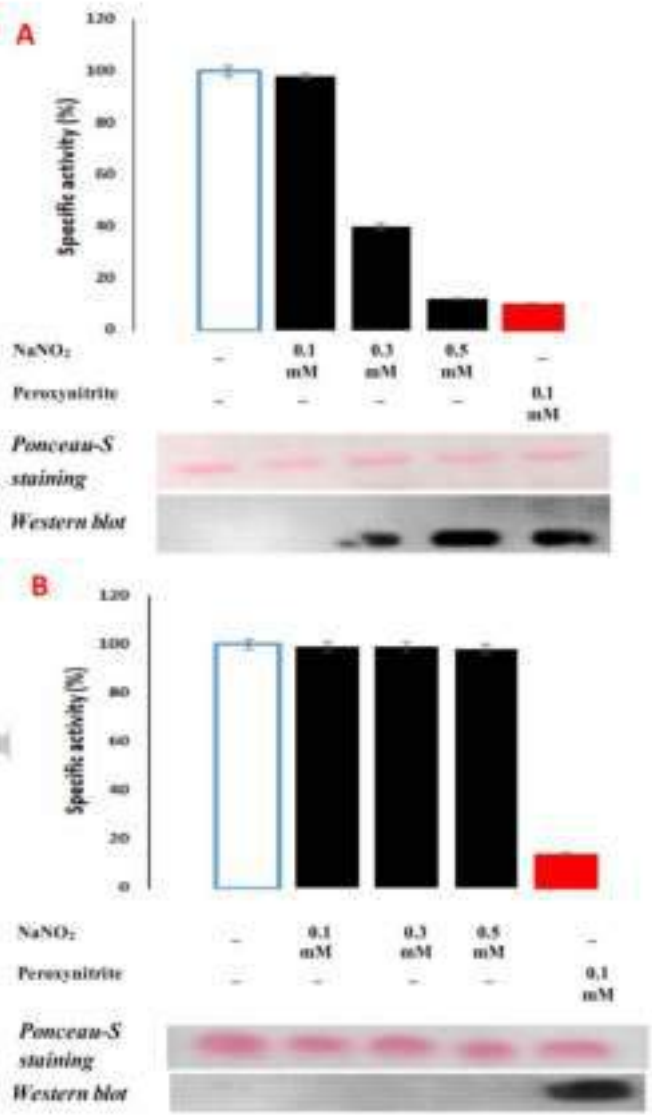

Figure 7

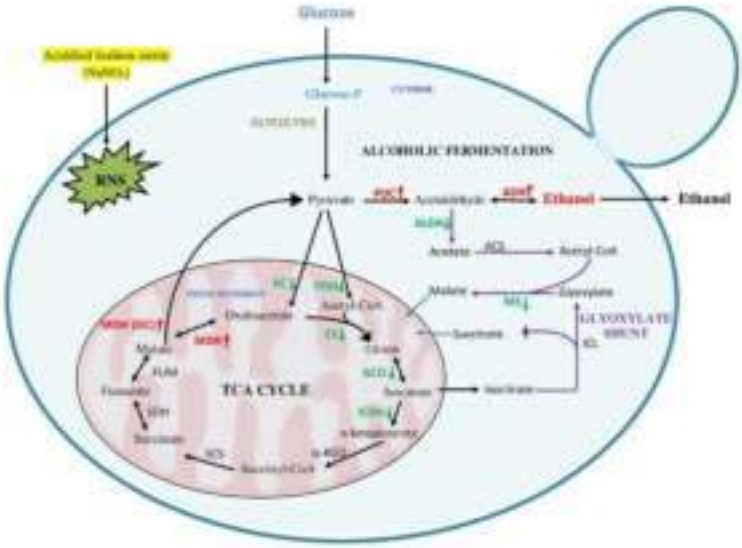

Seminars...

1st Regional Science and Technology Congress-2016
Jalpaiguri Division, West Bengal

Organized by

Department of Science & Technology, Government of West Bengal

&

Ananda Chandra College, Jalpaiguri

Outstanding Paper Award

is presented to

Swarnab Sengupta

for the paper co-authored with

Arindam Bhattacharjee

titled

Characterizing the effect of nitrosative stress on ethanol production by Saccharomyces cerevisiae

presented at

Ananda Chandra College, Jalpaiguri on November 7-8, 2016

Sonam Yogel Bhutia
Nodal Officer
1st Regional Science and
Technology Congress-2016
Jalpaiguri Division, West Bengal

Dr. Dhiraj Kumar Basak
Principal
Ananda Chandra College
Jalpaiguri

Arvind Kumar Mina, IAS
Joint Secretary
Department of Science and Technology
Government of West Bengal

International Conference on Nanotechnology: Ideas, Innovations and Initiatives – 2017 (ICN:3I-2017)

Organized by

Dept. of Mechanical & Industrial Engineering and Centre of Nanotechnology

Certificate of Appreciation

ICN:3I-2017 is pleased to award this certificate to

Prof./Dr./Ms./Mr. Suvarnali Sengupta

from University of North Bengal, Siliguri, India

for presenting ~~Plenary~~ / ~~Invited~~ / Oral / ~~Poster~~ / ~~Participation~~ in this International Conference held at Indian Institute of Technology, Roorkee, India during 06-08 December 2017.

Dr. Kaushik Pal	Prof. Sumeer K. Nath	Prof. Dinesh Kumar
Convener, ICN:3I-2017	Chairman, ICN:3I-2017	Chairman, ICN:3I-2017

An interdisciplinary National Seminar

Vistas in Life Science Research

March 29, 2019

Organized by

Department of Biotechnology, Department of Microbiology,
Department of Tea Science & Department of Bioinformatics

University of North Bengal

Accredited by NAAC with grade A

CERTIFICATE OF PARTICIPATION

Prof/Dr/Mr/Ms. SWARNAB SENGUPTA *participated as a registered delegate in the seminar. He / She presented paper on* 'BEST ORAL PRESENTATION' *in the invited/oral/poster session and chaired the session* TECHNICAL SESSION

Dipanwita Saha

Dr. Dipanwita Saha
Organizing Secretary

Prof. Pranab Ghosh
Chairman